SIMMS, Jr., Frederick Eugene, 1937-
THE IGNEOUS PETROLOGY, GEOCHEMISTRY AND STRUCTURAL GEOLOGY OF PART OF THE NORTHERN CRAZY MOUNTAINS, MONTANA.

University of Cincinnati, Ph.D., 1966
Geology

University Microfilms, Inc., Ann Arbor, Michigan

THE IGNEOUS PETROLOGY, GEOCHEMISTRY AND STRUCTURAL GEOLOGY OF PART OF THE NORTHERN CRAZY MOUNTAINS MONTANA

A dissertation submitted to
The Graduate School of
the University of Cincinnati in
partial fulfillment of the re-
quirements for the degree of

DOCTOR OF PHILOSOPHY

1966

by

Frederick Eugene Simms, Jr.
B.A. Rutgers University 1958
M.S. West Virginia University 1960

UNIVERSITY OF CINCINNATI

June 3 19 66

I hereby recommend that the thesis prepared under my supervision by Frederick Eugene Simms Jr.

entitled The Igneous Petrology, Geochemistry and Structural Geology of Part of the Northern Crazy Mountains, Montana

be accepted as fulfilling this part of the requirements for the degree of Doctor of Philosophy

Approved by:

Leonard H. Larsen

Frank L. Koucky

William F. Jenks

Form 668—Grad. School—1M—8-64

Frederick Simms

ABSTRACT

This thesis is primarily concerned with the igneous petrology, geochemistry and structural geology of part of the Crazy Mountains, Montana. These mountains consist of Cretaceous-Paleocene sandstones and shales that are intruded and metamorphosed by two complex diorite stocks and by countless outlying dikes, sills and other hypabysal bodies of Eocene Age. These intrusives consist of a wide variety of types that have been subdivided into a main alkali-calcic and a main alkaline series. In the northern Crazy Mountains 55-square-mile map area they are malignites (mafic feldspathoid syenites), feldspathoid syenites, trachytes, mafic trachytes, latites, quartz latites, rhyolites and minor amounts of andesite, basalt and lamprophyres as well as variants. These intrusives transect and conform to a series of folds and a monocline in the map area.

Pre-intrusive differentiation predominated in the development of these compositionally simple to complex intrusives. The less striking and more complicated development of possible (?) insitu differentiation phenomena in intrusives (as compared to Shonkin Sag laccolith) may be due to the tectonic situation. Minor irregular leucocratic segregations, vague geometric mineral segregations and pegmatite pods occur in the alkalic types.

The main objective has been to define the relationship between the two groups, with emphasis on the alkaline group. There is strong evidence for two main separate magma series. The latite-mafic trachyte group falls in both series and complicates the pattern. The

overlapping time of intrusion of the two series, the redetermined primary magma of the alkaline series (by Larsen's 1940 method) and the placing of the quartz latites and rhyolite porphyries with the alkali-calcic series conflict with Larsen's (1940) observations.

The main variations of these series can be explained in terms of the composition of the primary magma and fractional crystallization differentiation in the systems diopside-forsterite-anorthite and SiO_2-$NaAlSiO_4$-$KAlSiO_4$ with the former mafic (petrogeny's primitive) system predominating in the early stages of evolution and the latter system (petrogeny's residua) predominating in the later stages.

LIST OF FIGURES

FIGURE PAGE

FIGURE PAGE

FIGURE PAGE

INTRODUCTION

General statement

The Crazy Mountains are an isolated range located in a westward prolongation of the south central Montana plains. The range is one of eleven separate mountainous areas which compose the central Montana petrographic province that extends along the Rocky Mountain front from the Canadian border southward to northern Wyoming (E. Larsen, 1940). Each of these mountain masses consists in large part of Cretaceous-Tertiary extrusives, sills, laccoliths, dikes and stocks. A wide range of compositions occur with alkalic types often predominating.

The Crazy Mountains are located near the focus of a number of structural trends. A series of shallow intrusions occurs in this area that is structurally and compositionally diverse. These intrusions have altered and deformed a thick sequence of Cretaceous to early Tertiary sandstones and shales.

Although surface exploration has been accomplished throughout the Crazy Mountains by oil companies relatively few published studies have appeared in this century. John Wolff (1938) did not publish his complete findings until 30 years after he completed field studies in the Crazy Mountains. His geologic map was of reconnaissance nature (scale 1:250,000), as were those of Iddings and Weed (1894) and Weed (1899). In general, these early studies were excellent for their time. Wolff's and E. Larsen's work indicates that two different igneous series are associated in the Crazy Mountains.

In 1962 it appeared to Prof. L. H. Larsen that a new study of the area might contribute to the solution of a number of important geologic problems, especially the possible consanguineous relationship of these two rock series. With emphasis on this latter problem, a program of detailed field and laboratory study was initiated at the University of Cincinnati. Under this program, the writer has studied an area in the northern Crazy Mountains in which alkaline rocks predominate, while John Tappe has studied the dioritic stock of the southern Crazy Mountains. More recently, John D. Sims has begun stratigraphic studies of the Cretaceous to Paleocene Livingston-Fort Union Sequence in the northern Crazy Mountains.

Previous work

In 1882, A.D. Wilson, chief topographer for the Northern Transcontinental Survey, mapped the Crazy Mountains on a scale of 1:250,000. A year later J. E. Wolff made the first geological exploration of the Crazy Mountains for the same survey. He returned for further study in 1889 and 1907. Wolff wrote short notes in 1885, 1890, 1893, and 1898, but did not publish his completed research until 1938 when he wrote:

> "The geographical position and height of the Crazy Mountains, near natural lines of travel crossing the plains to enter the mountains of eastern (western ?) Montana, made them conspicuous landmarks and attracted the attention of the early explorers, without inducing a closer examination; thus, Lewis and Clark passed the southern foot of the mountains in 1806 and named the Shield's River. F. V. Hayden in 1872 speaks of the distant range (he called them the 'Crazy Woman Mountains') and Captain Ludlow's expedition in 1873 passed down the south fork of the Musselshell River, at their north end, where E. Dana (Dana and Grinnel, 1876) the accompanying geologist noted the theralite sills of Comb Creek."

In 1879 the 45th Congress, following recommendations of the National Academy of Sciences, created the United States Geological Survey and President Hayes signed an Act which simultaneously abolished the four surveys led by Clarence King, F. V. Hayden, John Wesley Powell and George Wheeler.

Under J. W. Powell, the young survey began its well known atlas folio series in 1894. Folio One is the Livingston Folio which includes the southern half of the southern Crazy Mountains. With Arnold Hague as Geologist in Charge, the geology of this 60 minute quadrangle

(1:250,000) was mapped by J. P. Iddings and W. H. Weed in 1890-1891. The remainder of the Crazy Mountains was studied from 1892-1894 by Weed assisted by L. V. Pirsson and described in the Little Belt Mountains Folio (Folio 56, 1899).

Pirsson (1905) and E. S. Larsen (1940) related the igneous petrology to that of similar rock sites elsewhere in Montana and defined the central Montana petrographic province. Rosenbusch (1887, 1896, 1898, 1907, 1910 and elsewhere), Rosenbusch and Osann (1922) and Johannsen (1938) have described the petrography of the theralites.

L. R. Mansfield (1909) reported on the glaciation, having accompanied Wolff on his 1907 trip. In 1918, C. F. Bowen described the geology in the northeast along the Upper Musselshell valley. Tanner (1949) discussed the general geology directly to the north in the Castle Mountains. Alden (1932) considered the terrace deposits on the flanks of the Crazy Mountains.

Numerous workers have studied the stratigraphy and the structure of the lowlands surrounding the Crazy Mountains. On this subject, Thom (1957) has presented a general discussion. The two most recent papers on stratigraphic and sedimentary relations are by Roberts (1964) and McMannis (1965).

Methods of study

The writer, accompanied by Mr. Rodney Eigenberger, undertook a general reconnaissance of the Crazy Mountains and studied regional geological relations during a ten-week period in the summer of 1962. For three and a half months during the following summer, the writer, accompanied by Mr. John D. Sims, mapped in detail a 55 square mile east-west strip north of the Upper Shields River. Mr. Sims, (University of Cincinnati, M. S. Thesis, 1964) also studied the stratigraphy of the Fort Union formation in the area during this period. During July, 1964, the writer, his wife Moira, and Mr. Richard Scheper spent ten days in the Crazy Mountains completing the field work.

The mapping was accomplished on United States Department of Agriculture 1954-55 air photos at a scale of approximately 1:20,000. The data were transferred to United States Forest Service 1957 Class C planimetric maps which have been compiled from these air photos. More recent air photos show the present location of roads. Elevations were approximated by Taylor and Paulin altimeters. More than 1000 rock and mineral samples, many oriented, were collected for laboratory studies. In addition to the usual field methods, a number of specific gravity measurements were determined using a Beckman Air Comparison Pycnometer and triple beam balance.

The laboratory studies involved petrographic model analyses, mineral identification by optics, X-ray diffraction and fluorescence, staining and other qualitative chemical tests, the measurement of rock magnetism, specific gravity and the compilation of norms and other geochemical parameters.

The various materials and data for these studies are on file at the Geology Department of the University of Cincinnati.

Acknowledgements

The writer is indebted to a number of organizations and individuals for their assistance, advice and encouragement in preparation for this dissertation.

The study was initiated through the aid of a 1962 National Science Foundation Summer Fellowship Grant for which the writer is extremely grateful. The field study was continued in 1963 and 1964 with partial support from the Fenneman Fund of the University of Cincinnati. The writer is especially thankful to the United States Forest Service District Ranger Philip G. Schlamp and Ranger George Forman for advice and the privilege of using Forest Service cabins. Acknowledgement is given to the Yellowstone-Bighorn Research Association for the use of their library and other facilities at Red Lodge, Montana. The computer work was supported by N.S.F. grant G 19281 to the University of Cincinnati.

The writer is grateful to his thesis advisors, Professors L. H. Larsen, F. J. Koucky and W. F. Jenks for their advice and assistance in the field and laboratory and for many helpful suggestions during

preparation of this report. Thanks are due to the late Professor Arie Poldervaart and to Dr. Vincent Manson of Columbia University for providing a computer program for calculating C.I.P.W. norms, to Professor Peter Lessing of Syracuse University for determining K/Rb ratios of five rock samples, to Professor C. S. Hurlburt, Jr. and the Harvard Museum for the use of J. E. Wolff's thin sections of the Crazy Mountain igneous rocks, to Messers Rodney Eigenberger, John D. Sims, Richard Scheper, David Rife and Moira Simms, for their assistance in the field and laboratory, to Richard Scheurer for his advice and assistance in the computer work.

The writer especially wants to thank the Fred Williams family of Livingston, Montana for their warm hospitality and constant advice and encouragement in the field.

Last but not least, the writer acknowledges his parents, Mr. and Mrs. F. E. Simms, Sr., his grandfather Herman Gardner, his uncle, Rand Gardner, his brothers Bob, Steve, and Dick, and his mother-in-law, Mrs. Martha Kennedy for their constant encouragement, advice and financial support.

GENERAL GEOGRAPHY AND GEOLOGY

Location and accessibility

The Crazy Mountains are a northerly trending cluster of rugged peaks which rise abruptly above the southwestern corner of the central Montana plains (p. 28). Situated between 110° 15' and 110° 45' West longitude and 45° 45' and 46° 30' north latitude and extending 20 miles east-west and 45 miles north-south, they are located between the towns of Livingston, Harlowtown and Ringling (Fig. 1).

The map area of the present study is in the northwestern part of the Crazy Mountains extending 10 miles east-west and 5 to 7 miles north-south on the boundary between Meagher and Park counties (Fig. 2). The area is limited on the south by the Upper Shields River, on the west by Smith Creek, on the north by the Musselshell River lowlands and on the west by the Big Elk Creek and American Fork-Shields River drainage divide (plate 1). The area covers sections between and including T6N, R10E Section 30; T5N, R10E section 19; T6N, R11E Section 33; T5N, R11E Section 14. Sections arranged in a checkerboard pattern are in the Gallatin and the Lewis and Clark National Forests.

The area is accessible by means of unpaved Forest Service roads which enter from the west along the Shields River Valley and from the north along Cottonwood Creek. The Shields River road is graveled from the western map boundary to Serrett Creek. The remaining non-graveled roads are treacherous after rains. Depending upon lumbering conditions various areas are accessible by logging roads. Most of these are not

shown on the map, but appear on the most recent aerial photographs. Information as to trail conditions may be obtained at the Forest Service Office in Livingston, Montana.

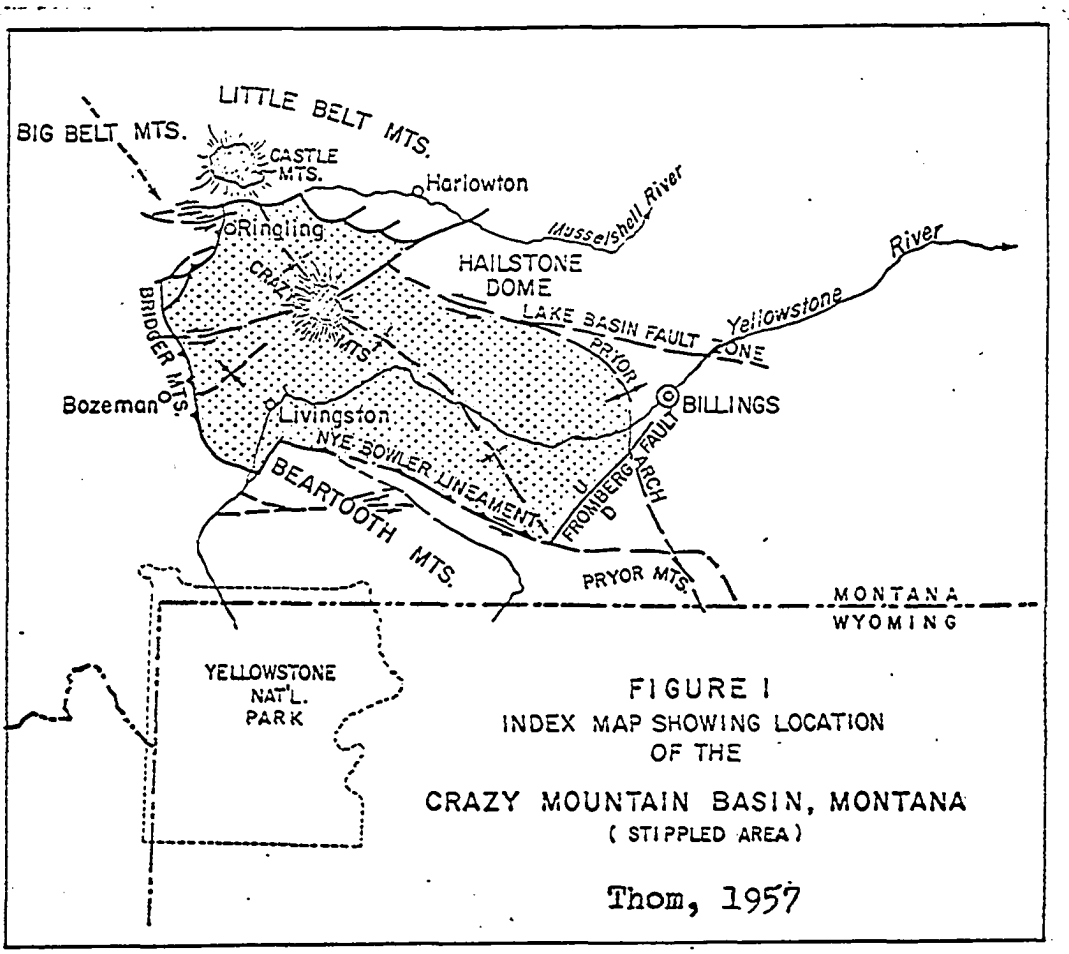

FIGURE 1
INDEX MAP SHOWING LOCATION OF THE
CRAZY MOUNTAIN BASIN, MONTANA
(STIPPLED AREA)

Thom, 1957

Fig. 2

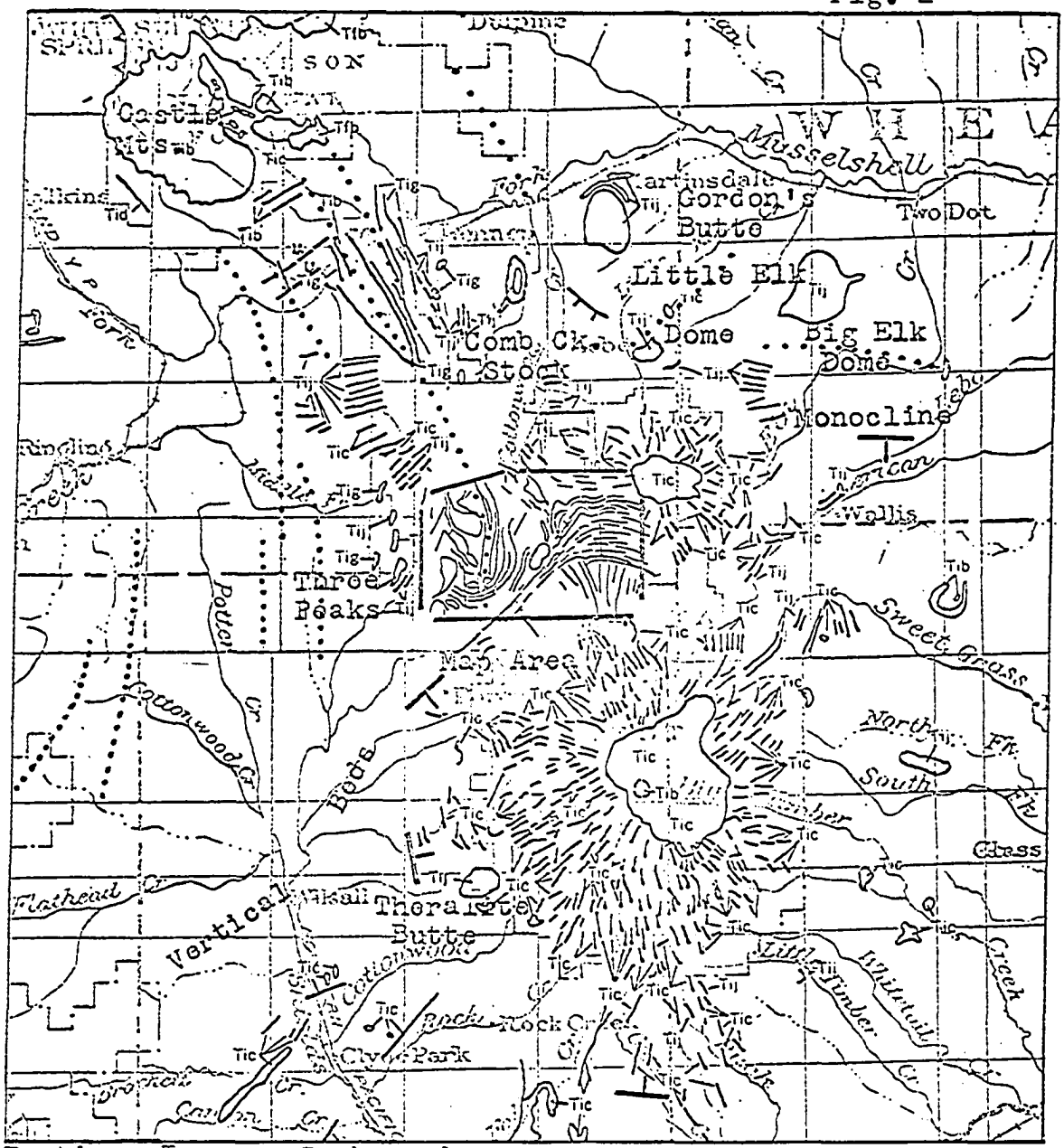

Tertiary Igneous Rocks and some Structural Features of the Crazy Mountains and Castle Mountains, Montana
Modified from Merewether, 1960, Scale 1:500,000

Rocks with essential minerals of quartz, alkali feldspar and/or plagioclase

- Tib - intrusive, felsic, quartz
- Tfb - flow, felsic, quartz
- Tic - intrusive intermediate
- Tid - intrusive, mafic

Rocks with essential minerals of feldspathoids and/or, in mafic and ultramafic rocks, alkali feldspar

- Tij - intrusive, mafic
- Tig - intrusive felsic, containing foldspathoids

Thrust fault — reverse fault — normal fault

General dip of beds

..... Anticlinal and or domal axis (domes are specified)

Topography

The Crazy Mountains rise abruptly 5,000' above a western elongation of the Missouri Plateau into the northern Rocky Mountain Front (Fenneman, 1931, p. 62). They are separated from the Big Snowy Mountains to the northeast, the Castle Mountains to the north, the Bridger Mountains to the west and the Beartooth Mountains to the south.

In the northwestern part of the mountains, which includes the present study area, the terrain is exceptionally varied because of the differing degrees of mountain glaciation superimposed on tilted edges of soft strata and more resistant sills, dikes and laccoliths (Figs. 2, 3, 4, 5). The maximum relief is 3250', with the highest elevation, the 9,000' ridge, in the northeast part of the map area and lowest elevation, 5,750', on the Shields River in the southwest.

The upper Shields River Valley at the southern edge of the map area partly transects geologic structures and separates the northern Crazy Mountains from the southern peaks (Plate 1, Fig. 4). This valley appears to cut across resistant sills and some workers (Wolff, 1938) have searched for the faults which localized it. It may be that the valley is an incompletely adjusted stream course caused by superposition from the earlier graded surfaces similar to Indian Creek and other streams in the Castle Mountains.

The Smith River synclinal valley, which is the western map boundary, is narrower and shorter than the upper Shields Valley. To the east of the Smith River, Billie Butte rises abruptly almost 1,900' above the valley floor. It is a synclinal phacolith with a measured thickness of at least 360' (the cross section Plate 1 indicates it is thicker).

and up to one mile across.

East of Billie Butte is a 2,800' north-trending, rugged mountain on which Davey Butte and Virginia Peak stand out prominently. On the top and flanks of this mountain are a series of ridges and cliffs reflecting sills and laccoliths exposed on a southward-plunging, breached anticline. The only obvious sign of glaciation in the western part of the map area is the cirque on the west central side of this mountainous area (Fig. 6,7).

In the middle of the map area is a rolling saddle, 1,300' above the Shields River valley floor, which separates the north-flowing Cottonwood Creek-Musselshell River drainage from the Shields River drainage. Rising sharply at least 200' above this col is northerly-trending Target Peak.

The summit of the eastern half of the area is an irregular ridge more than 3,100' above the Shields Valley. The ridge separates two north-facing cirques from a south-facing cirque and is the westward extension of the rolling summit area around Loco Peak. Frost polygons are developed on this summit (Fig. 8). As can be seen in the panorama (Fig. 3), this eastern area displays the early to early-intermediate stage of alpine glaciation (Fenneman, 1931, p. 180).

Alden (1932) writes that Mansfield (1907) apparently connected the development of the northern summit surface with the surrounding terraces which stand from 7,000' to 5,800' elevation. Alden indicates that the terraces may be of a later origin, and that smoothing of the summit surface dates possibly to the Cypress Plain (Oligocene and Miocene), (see section on superficial deposits). The reader is referred to

Fenneman (1931, pp. 75-76) and Bevan (1925, p. 586) for the details on this problem. These dates may set an upper limit for the time of intrusion as the surface transects many igneous rock types. Eocene ages are cited for some of the other alkaline intrusives of the Central Montana province (Gillully, 1965). It is not impossible for some of the intrusives to be Oligocene.

Near the juncture of Mill Creek with the Shields River, a malignite dike forms a ridge which projects above the alluvium. Apparently the gravel was deposited around the ridge. Similar situations appear on a generalized map of the Crazy Mountains (Graves, 1957).

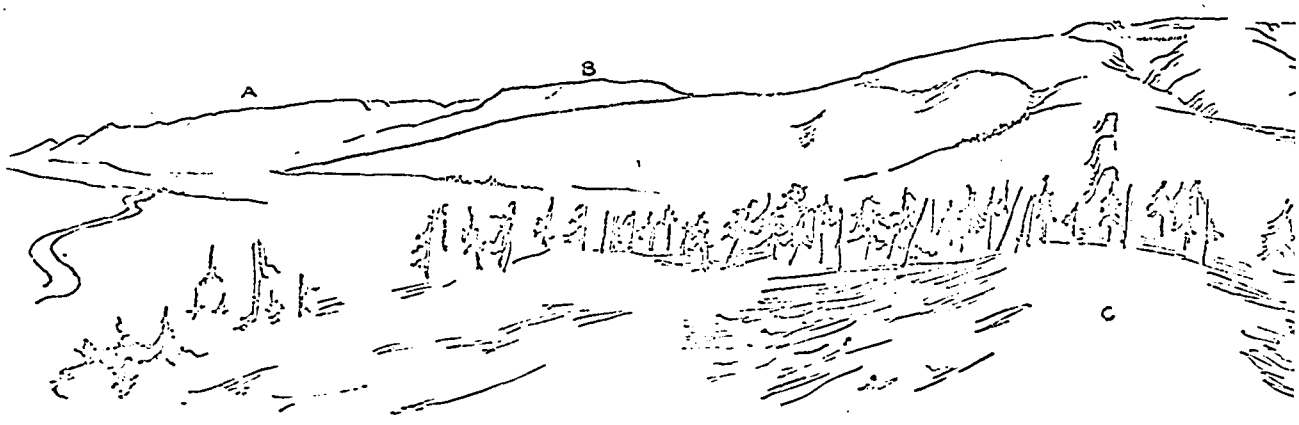

A. Malignite sills and phacolith on breached southward plunging Robinson Anticline (5 miles distant)

B. Target Peak feldspathoid syenite laccolith (3.5 miles distant)

D. Cirque
southe
felsic

C. Northward trending 20' thick andesite porphyry dike (foreground) 6715'

FIG. NORTHWARD PANORAMA FROM NEAR FOREST
SCOFIELD CREEK AND THE UPPER SHIELDS RIVER I
SKETCH

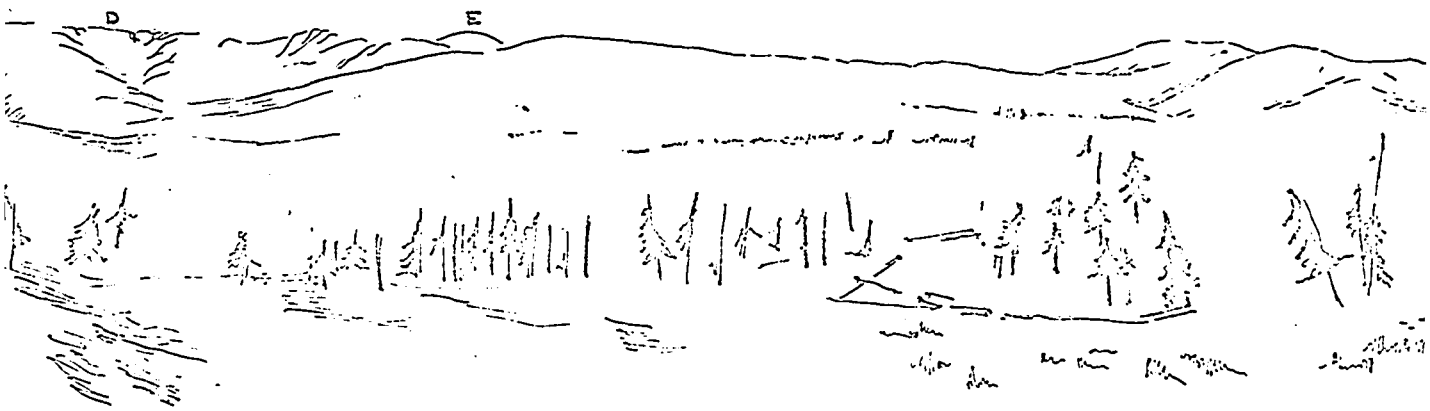

E. Loco Mountain Stock 9187'
(4 miles distant)

Lebo Peak (3 miles distant

Cirqued Ridge developed on
southeast to south dipping
felsic sills (3 miles distant)

FOREST SERVICE ROAD SOUTHEAST OF THE JUNCTION OF
ER IN THE SOUTHEAST PART OF THE MAP AREA
ETCH FROM PHOTOGRAPHS

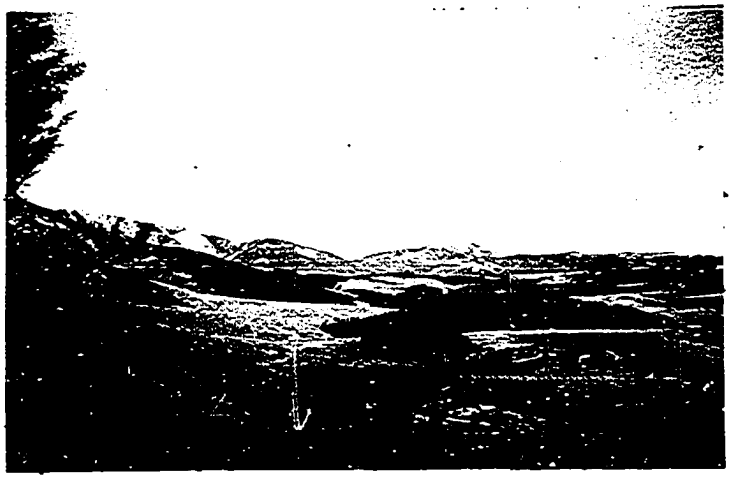

Fig. 4 View east from the nose of the Robinson anticline. The Upper Shields River Valley is in the foreground. In the middle background is the Shields River-Big Elk Creek drainage divide at the southeast corner of the map area. Loco peak is in the middle background and is covered with pink igneous talus. In the left background are several northeast to east trending ridges underlain by a southerly dipping sill set.

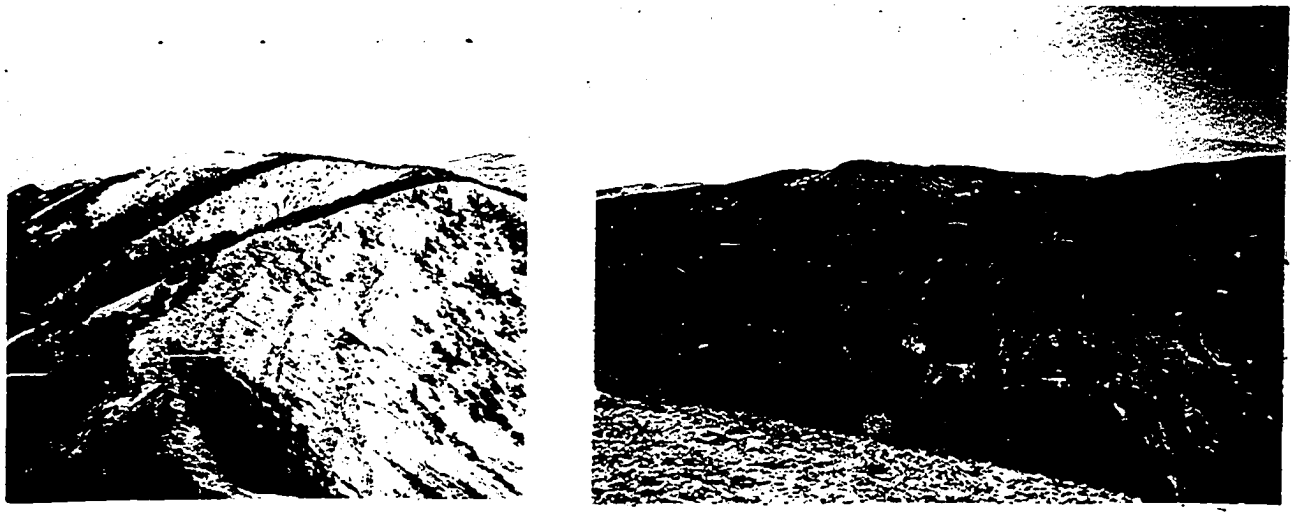

Fig. 5 Views from the different positions on the arete ridge near Lebo Peak towards the west and southwest respectively, showing the southwestward striking, interbedded sills, sandstones and shales. The country rock is often dark and the more resistant units especially where the strata septa are thin. Contrast the right picture where the resistant sills are separated by thick strata sequences and the left picture where the sills are nearly in contact.

Fig. 6 View southwest from the Smith Creek Valley into the Great Cliffs, with the 110 foot thick stratigraphically lowest malignite sill. The purple sandstones and shales appear to be offset by an eastward trending fault, though Wolff (1938, p. 1598) concludes that it is a joint which has controlled the configuration of the base of the intrusive. Wolff does state that this joint is on line with an eastward trending fault which extends to the west base of Virginia Peak.

Fig. 7 View from the north side of the Great Cliffs of the same feature as described above. The maturely glaciated Southern Crazy Mountains are in the background. The Shields River Valley is in The left background.

General geology of the Crazy Mountains

At the level of exposure, the Crazy Mountain intrusions transect the Cretaceous to Paleocene Livingston-Fort Union sandstones and shales (p. 22). Around the southern Crazy Mountains these beds dip generally toward a stock (Fig. 2) although near the stock the dip is centrifugal.

This central intrusive (4 miles by 6 miles in horizontal dimension) is composed chiefly of diorite and minor amounts of gabbro, picrite and granodiorite. A smaller stock ten miles to the north consists of diorite and quartz diorite. A zone of hornfels up to two miles wide is developed around each of these two larger bodies. The two stocks and the surrounding country rocks are cut by innumerable dikes and sills of aplite, granite porphyry, diorite porphyry, basalt and lamprophyres.

In the northern mountains, besides the above mentioned smaller stock, a series of north trending folds and an eastward trending monocline are intruded by countless sills, laccoliths and various discordant bodies of rhyolite and quartz latite porphyry, syenite, feldspathoidal syenite, latite, mafic trachyte, andesite porphyry, malignite, basalt, lamprophyres and related rock types. Malignite intrusives occur along the west side of the southern mountains as well.

Unconsolidated alluvial and terrace deposits and slide rock deposits are most common in the southwest part of the map area.

STRATIGRAPHY

Fort Union sandstones and shales

The upper and middle parts of the consolidated sedimentary sequence exposed in the map area are equivalent to the Melville Formation (late Paleocene) of the Fort Union group. This is indicated by lithologic similarities with the type section on the east side of the Crazy Mountains, and fossil plants and teeth remains of the vertebrate Gidleyina Silberlingii (?) according to Sims (1964) and Simpson (1937). Sims (p. 15) describes the sequence as follows:

> "The series is drab, mostly thin-bedded, silty sandstones. Occasional limestone nodules are present in lenticular bands. Upon weathering these nodules have an orange brown color.
>
> An average sandstone is medium to fine-grained, subangular to subrounded, calcareous, has very little clay size material or clay minerals, moderate amounts of lithic material, and some carbonaceous material. Mudstones are generally very silty with only moderate amounts of clay minerals. Bedding fissility is almost totally lacking. The best bedding fissility is observed when large amounts of carbonaceous material is present in mudstones. Some soft coaly shale layers were noted in the middle one third of the measured sequence...
>
> One of the most striking features of the sandstones is the ubiquitous nature of the calcite cement present in large quantities and its apparent corrosive nature on the quartz and feldspar grains."

Not yet described in detail is a thin sequence which is characterized by purple, thin-bedded sandstones and siltstones including contorted beds. This section occurs at the lowest part of the stratigraphic section along the axis of the Robinson Anticline and in the Great Theralite Cliffs. McMannis (1955) has tentatively placed the entire section of the map area in the Fort Union group. The total

thickness of this stratigraphic section has not been measured there. Simpson (1937), (p. 14), describes about 7,000 feet of Fort Union on the eastern side of the Crazy Mountains.

Surficial deposits

Thick deposits of coarse gravels occur along the Shields River in the southwest part of the map area. Their extent is shown by a dash-dot-dot line on the map (Plate 1). The thickest exposure of gravels is nearly 100', occuring on the south side of the Shields River halfway between Bennett and Lodgepole Creeks.

Several benches occur in the upper Shields River Valley. These terminate at steep bluffs which rise 100' above the valley floor. The benches are partly composed of morainic material, (Mansfield, 1909). The 100' section of gravels underlies this bench level which stands at 6,150' near the junction of the Forest Lake road and Shields River road.

Alden (1932) states that these benches are equivalent to the Number One bench (Flaxville Plain) of Miocene to Pliocene age in eastern Montana and adjacent areas (see discussion p. 13). He notes that the pebbles which range from a fraction of an inch to three feet in diameter, are mostly of igneous rock and show no evidence of glacial action. The benches are probably also equivalent in elevation to gravel veneered pediments found on the Smith River vasin (see Wolf, 1964, p. 500), (Tanner, 1948, pp. 150,152). Wolf regards these latter terraces as Pliocene and early Pleistocene and connects them with a rolling subsummit level at 7,000' to 8,000' in the Big Belt and Little Belt Mountains.

There are three localities of recent large earth movements in the area. These are shown on the geologic map. The largest is the rock

slide that occurs in the north above Forest Lake. Rock debris from a 40' latite sill extends across the Cottonwood Creek Valley and forms the dam for Forest Lake. A slumped area is located one-half mile south of Forest Lake along the east side of Cottonwood Creek. A large rock slide also occurs on the east side of Target Peak. It may include the lower bench of nepheline syenite to the east and 200' below Target Peak.

Numerous recent landslides have been described and mapped in the surrounding mountains such as the Little Belt and the Gallatin Mountains (Wolf, 1964: Roberts, 1964).

Fig. 8 Frost polygons on the gently rolling surface near Lebo Peak east of the map area looking east toward Beverly Peak.

STRUCTURE

General statement

A discussion of the structure of the Crazy Mountains is presented in the following sequences: (1) Tectonic characteristics of the Crazy Mountains Basin and surrounding uplifts; (2) Previously proposed tectonic sequence and controls; (3) Detailed structural characteristics of the writer's map area and the relations to surrounding structures. The first two headings concern a review of the literature and may be omitted by the reader.

Tectonic characteristics of the Crazy Mountains Basin and surrounding uplifts

The mountains lie in a complex northwest-trending structural depression termed the Crazy Mountains Basin or Syncline (Fig. 1). It is adjacent to the northern margin of the Middle Rocky Mountains-Colorado Plateau "Range and Basin" province, (Fig. 9), which contains more than 20 intermountain basins of various sizes and shapes, all of which were produced by similar orogenic forces during Laramide time. According to Thom (1957, p. 10), the Crazy Mountain Basin is of special geological interest and importance because it is situated at the junction of three tectonic provinces of second order magnitude into which the North American tectonic zone has been divided. The basin, covering approximately 8,000 square miles, is considered to be a third order magnitude tectonic unit (Fig. 10). The structures surrounding the Crazy Mountain Basin are depicted in Fig. 11 and 13, and have been discussed by many writers (Thom, 1923; Spencer, 1959; Eardley, 1961).

Briefly, the southeast side of the Crazy Mountains Basin is separated from the Bighorn Basin by the Nye-Bowler structural lineament and the Pryor Mountain monoclinal flexure and fault zone. The southern margin is the uplifted northern edge of the Beartooth Mountains. This boundary zone is complicated by thrust faults, folds and laccolithic intrusions. The basin is defined on the southwest and west by the Bridger and Big Belt block uplifts and related thrusts. The Crazy Mountains Basin possibly has two structural axes which intersect at the locus of the Crazy Mountain main intrusives that form the mountainous part of the basin (Thom, 1957).

The northern edge of the basin is characterized by a series of north-trending folds. These folds are northwest around the southeast end of the Big Belt block uplift, where they are complicated by thrust faults. The eastern folds abutt against the Castle Mountain stocks and are intruded by laccolithic and other related hypabyssal intrusives.

Toward the east and northeast, the central Montana plains are characterized by nearly rectangular areas of shallow dip which are bounded on one side by sharp monoclinal flexures and often small domes and laccolithic intrusions. The Lake Basin and Cat Creek en-echelon fault zones are located along such monoclinal flexures.

Tectonic sequence and controls

At this point it may be useful to summarize the tectonic development of the region according to previous workers.

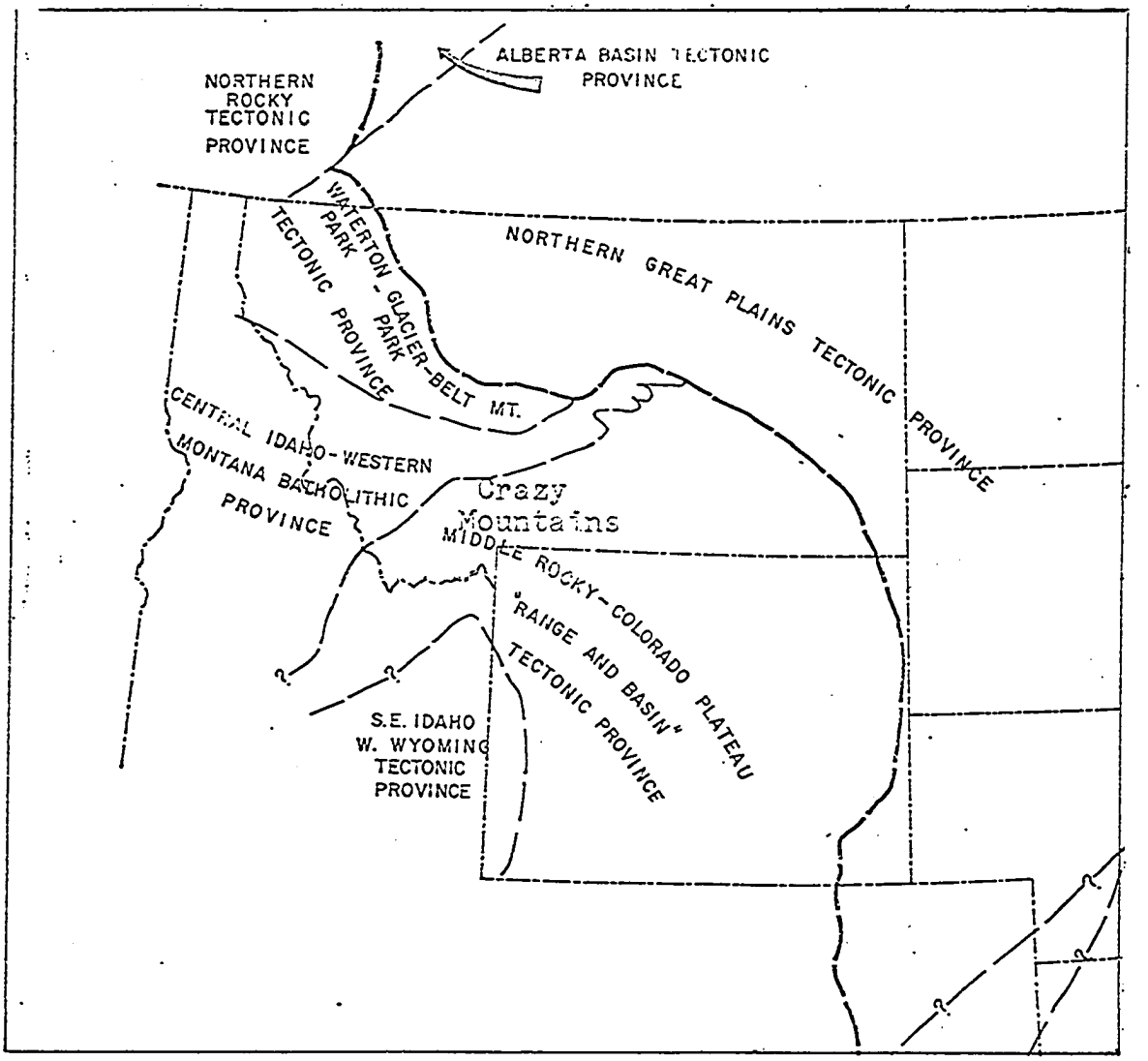

Fig. 9 Sketch map showing segmentation of first order tectonic features (Cordilleran orogenic belt and continental shield) - into second-order tectonic provinces. Thom, 1957

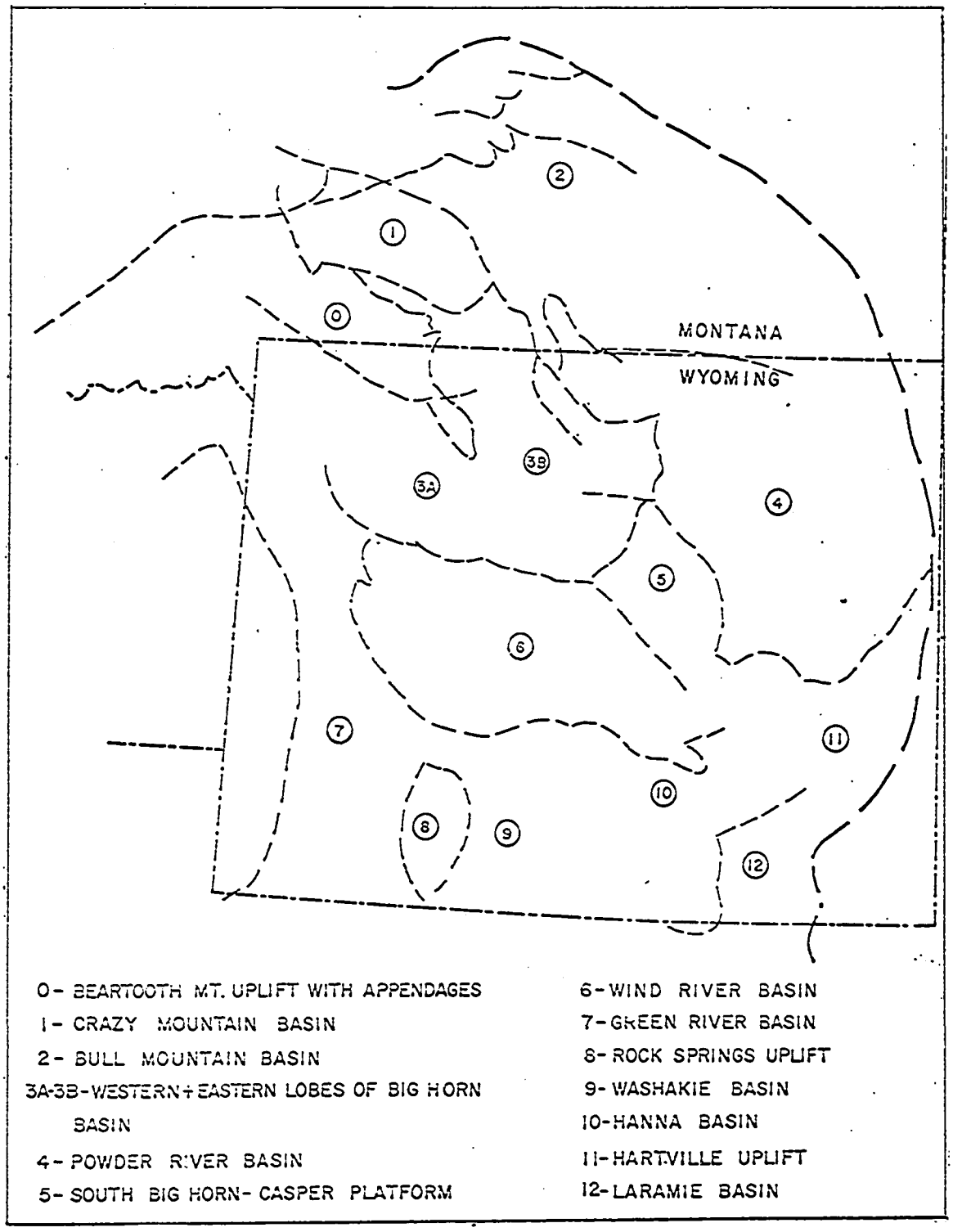

Fig. 10 Sketch map showing segmentation of middle Rocky-Colorado plateau second order tectonic province into third-order tectonic units. Thom, 1957.

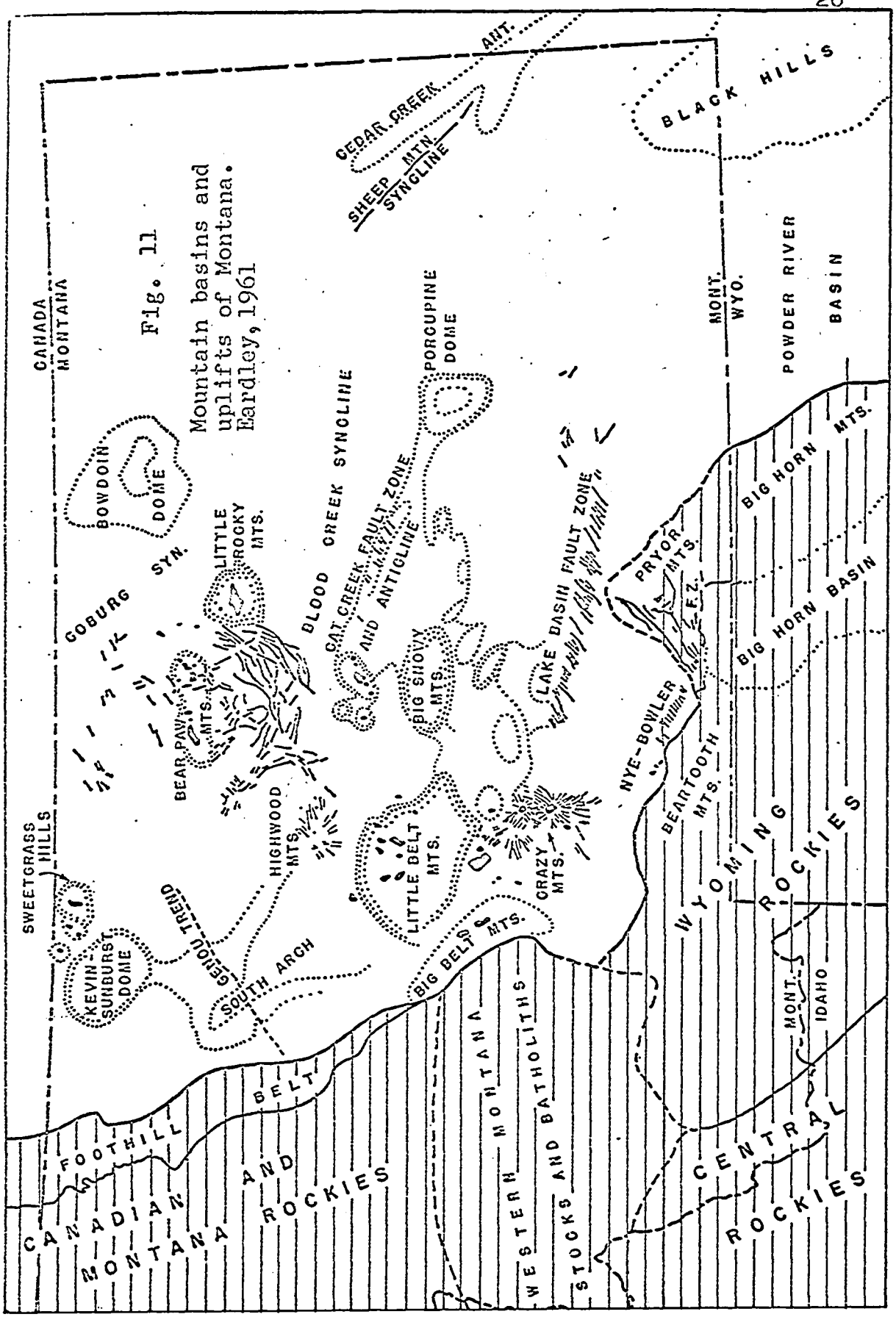

Fig. 11

Mountain basins and uplifts of Montana. Eardley, 1961

Thom (1957, p. 10) writes that two major diastrophic cycles have occurred in that part of the Cordilleran region in which the Crazy Mountains Basin is situated. The first occurred within Early Precambrian time and the second from Late Precambrian (Beltian) time to the present. Thom divides each cycle into four main phases: (1) geosynclinal subsidence and sedimentation; (2) orogenic compression and folding accompanied by eruptive and intrusive activity; (3) notable regional (vertical) uparching; (4) erosional planation of the previously built mountain system.

Thom believes that zones of weakness formed during the compressional phase of the first cycle significantly affected sedimentary and structural development of the second cycle (Fig. 12). Perry (1950), Thom (1957) and others consider that a major crustal rift controlled the extent of the southern shore of the Beltian embayment, (Fig. 13). This southern limitation to Beltian deposition extended from the Rochester Mining District in western Montana through the Crazy Mountains intrusive center according to these authors.

The orogenic phase of the second diastrophic cycle began in the Upper Jurassic on the Pacific coast (Ransome 1913 and Lindgren, 1913 and Thom, 1957) A series of deformations and intrusions progressively affected areas further to the east. The various phases of the Boulder Bathylith were emplaced over a period of 77.8±1.6 to 70.2±1.5 million years ago (Knopf, 1965). Thom (1957, p. 14) writes that by early Eagle (Cretaceous) time the present western Montana ranges and basins had been effectively defined and Eagle coastal plain deposits spread across the Crazy Mountains Basin. By Judith River time (Upper Cretaceous), volcanic vents were supplying great amounts of material to

the basin.

According to Thom (1957) the second diastrophic cycle orogenic phase reached maximum intensity in eastern Cordilleran areas at the beginning of Wasatch (lower Eocene) time and resulted in large scale thrust faulting and folding accompanied by the emplacement of major bathyliths and satellitic stocks in the root zones of several major overthrusts. The Crazy Mountains intrusives were emplaced along the major Beltian "shoreline" rift at about the same time. The various radiometric age dates on the alkaline rocks of the Bearpaw Mountains indicate that they were emplaced from 68 to 40 million years ago (Pecora, W, personal communication in Gilluly, 1965, and Pecora et al, 1957). Middle to late (?) Eocene fossil plants and fish have also been recovered in the main volcanic sequence of the Bearpaw Mountains. The oldest date indicates that the volcanism of the Central Montana Petrographic Province closely follows emplacement of the major bathyliths and stocks farther west. McMannis (1965) concludes that deformation began much later (Post Fort Union), did not last as long and was much weaker in the Plains Province. Some intense folding and thrusting postdates the main deformation (Bathylithic intrusion etc.) but it is reasonably certain that Laramide compressional deformation had ceased before Middle Eocene time in western Montana.

The Crazy Mountains are located near the intersection of the "shoreline fault" and the projection of the Lake Basin fault zone, two of the proposed basement weakness zones (Fig. 13). As on many of

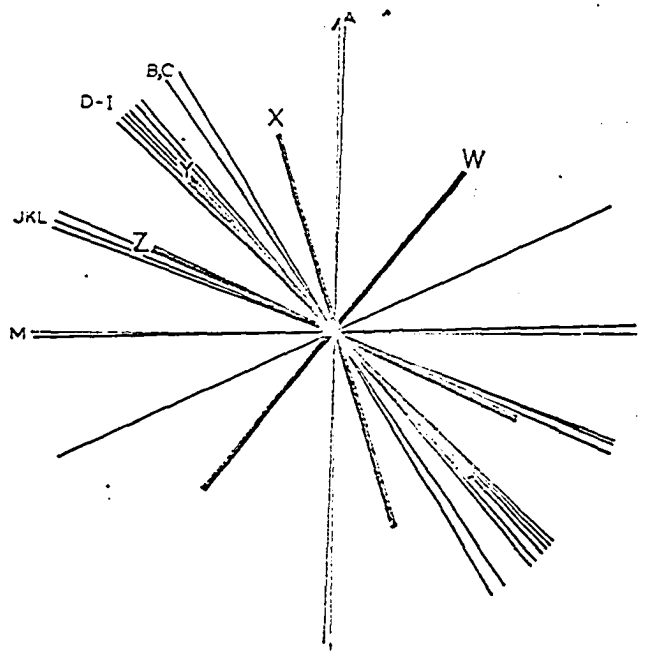

Comparison of Regional Trends with Patterns in Beartooth Core.

The heavy short lines are fracture trends in the core of the Beartooth Range. The lighter longer lines are the axes of major structures in the shelf region. A and M are the fault that border the Pryor Mountains, B and C are the axes of Cedar Creek anticline and Bighorn Mountains, D-1 are the axes of Bighorn Basin, Wind River Range, Crazy Mountain syncline, folds and thrusts in the Gros Ventre Mountains, trend of the northern Rockies, J, K, and L are the trends of the Cat Creek fault zone, the Lake Basin zone, and the Nye-Bowler Lineament, and M is one prominent trend in the Owl Creek Mountains.

Fig. 12 Spencer, 1958, p. 21

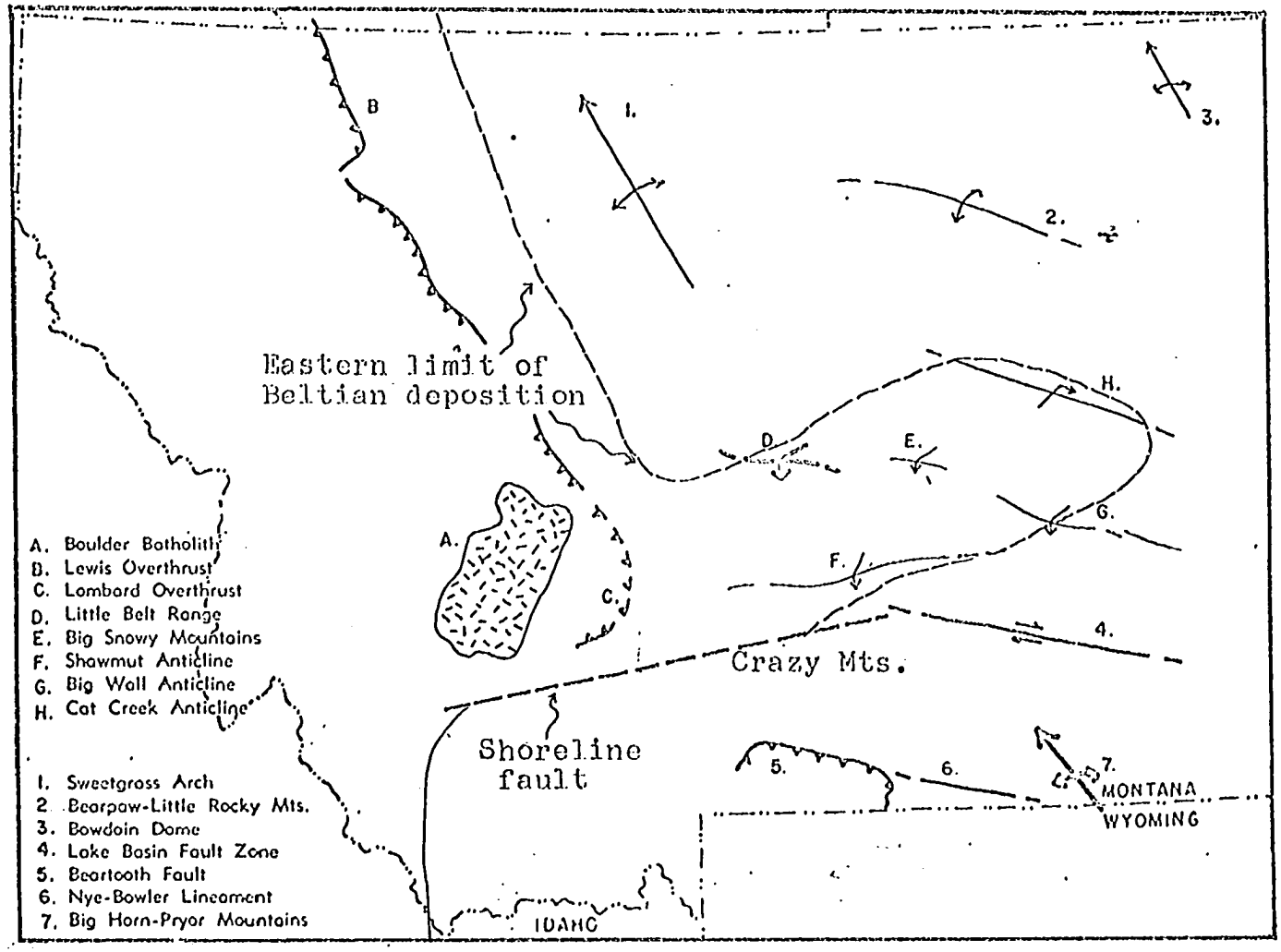

Fig. 13 Tectonic features of western Montana including the shoreline fault and eastern limit of Beltian deposition. Harris,1957.

the other central Montana structures, the deep fractures are not prominently expressed. This lack of expression of the faults seems to point to their development over several periods of movement (Harris, 1957). Fuller (1964) from a United States wide, north-south magnetic profile study concludes:

> "Continental magnetic anomaly patterns are interrupted by east-west features similar to, though less obvious than, those found in the east Pacific... By analogy with the east Pacific studies, the magnetic features are interpreted as the expression of a pattern of fractures. However, there is no evidence of consistent offset comparable with that found in the east Pacific. The fractures are considered to be deep and partly decoupled from the upper reaches of the crust so that they are clearly recognized in the thin oceanic crust but are partly masked by local shallow complexities in the continental crust."

In addition, the Bouguer Gravity Map (Steinhart, Meyer, 1961, p. 306) indicates that a distinct negative anomaly occurs in the Crazy Mountains. This anomaly is elongate eastward, thus including the Lake Basin Fault zone (Fig. 14).

Harris (1957) argues that an incompetent asymmetrical wedge formed from the Beltian embayment sediments had important control on the structural development (Fig. 13, 11). He thinks that the incompetent wedge was not able to transmit compressive forces to the east, therefore more folds and faults occurred to the north of the "shoreline fault" in the Beltian embayment than to the south in the Crazy Mountains Basin. Spencer (1959) states that a related tectonic control was important with respect to the Beartooth Uplift where a competent block was able to transmit forces to the east and was less

deformed itself. In addition, he writes that:

> "Thom (1955) places more emphasis on the shape of the uplifted blocks. The larger wedge uplifts occur at several orders of magnitude and apparently are essentially coincident in size and outline with granitoid bathylitic masses which have "headed" as they approach the surface, thus giving upon cooling massive rock units with the shape of a downward pointing wedge. Under compression, the more yielding country rock is forced beneath the sloping flanks of these wedges, causing them to be elevated straight up, if the slope of the sides be the same, or a tilted wedge uplift if the sides of the plutons have different dips."

Berg (196), also discusses the development of these foreland uplifts. Thom considers that the west-northwest trending asymmetrical anticlines of central Montana represent tilted blocks at depth with faulted sides. He believes that the faults die out upward and are the sites of intrusions (Fig. 17). Thom writes that the anticlinal trends may be due to refraction of the westward forces off of the northeastern "shoreline fault". Eardley (1961) downplays the idea that these structural zones control sites of intrusives.

Smith (1965) following Chamberlain and others considers that sinistral transcurrent movements have played an important role in the tectonic development of the Northern Rocky Mountains.

> "Transcurrent movements were concentrated along a series of deep-seated, fundamental shear zones that trend west-northwestward from central Montana and cut obliquely beneath the more northerly trends of the main Cordilleran mobile belt. The shear zones (megashears), which also accomodated considerable vertical movements, are expressed at the surface as a series of outstanding structural and topographic lineaments

Fig. 14

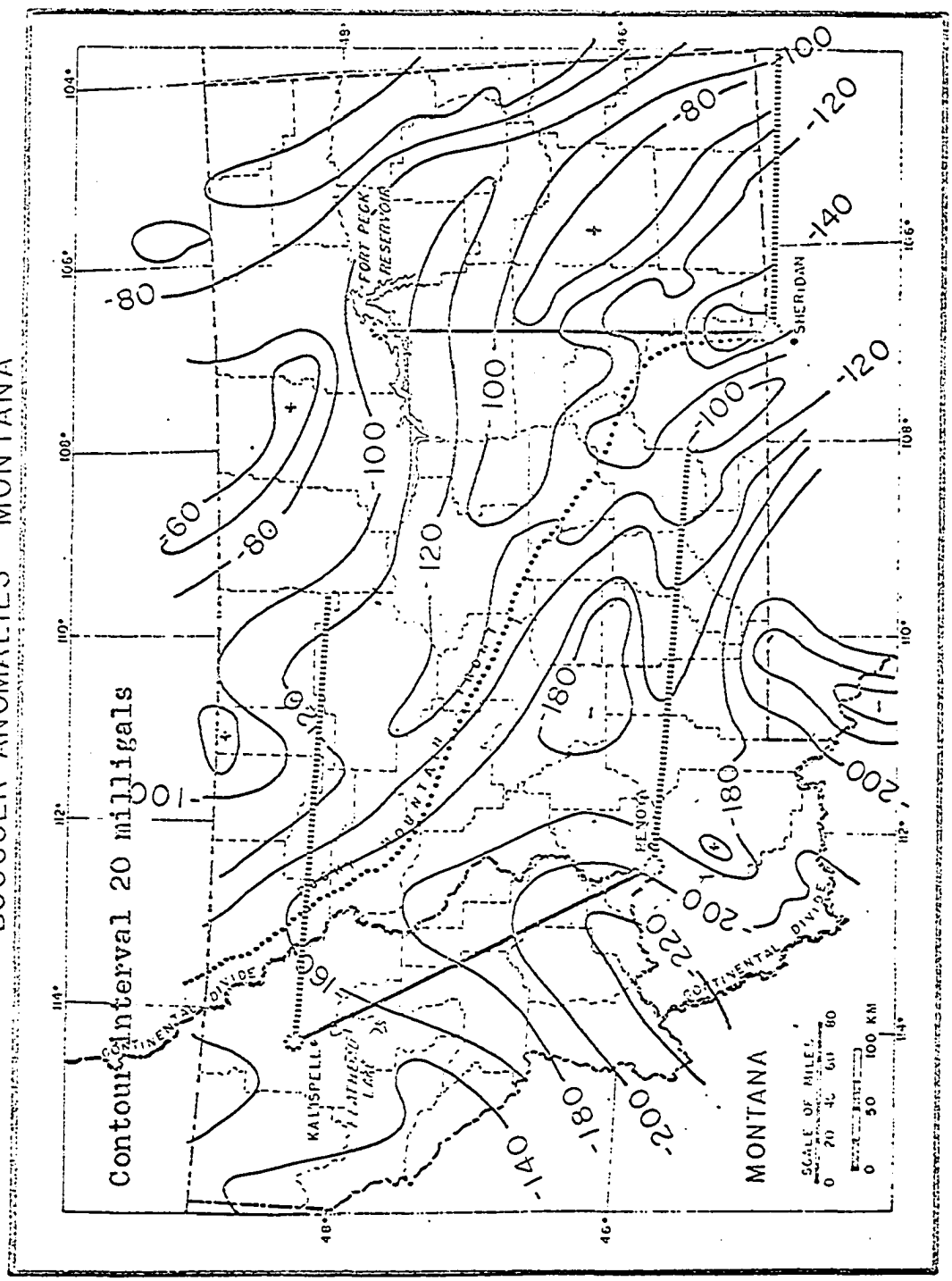

that are called the Lewis and Clark Lineaments."

Other tectonic controls have been considered: Thom (1923) writes that the basin formation could be due to depletion of a magma chamber beneath the Crazy Mountains Basin. Bowen (1918) concluded that the Little Elk-Shawmut domal complex in the northeast Crazy Mountains was due to igneous intrusions. Rouse (1937) states that laccoliths have controlled the dip of later thrusts along the Beartooth front on the south side of the basin.

Likewise, Tanner (1949) writes that early orogenic dioritic stocks of the Castle Mountains controlled later folding and thrust faulting. Reeves (1924, 1927, 1927) has shown considerable evidence for large scale thrust faulting around the Highwood and Bearpaw Mountains. The slippery bentonitic Cretaceous formations were zones along which movement occurred.

DeSitter (1956) considers that the shape of a basin with respect to the direction of the deforming forces influences the shapes of the folds within the basin. If the deforming forces are at oblique angles to the edge of the basin, then a series of short echelon folds results parallel to the basin border, such as the Kettleman Hills domal complex. The Kettleman Hills domal complex is analagous to the Little Elk-Shawmut domal complex.

In summary, a number of tectonic controls have been proposed as being important with respect to Cretaceous-early Tertiary orogeny in central Montana. They are: (1) the basement fracture pattern, shape of the separate crustal blocks and relative vertical and lateral movement along these blocks; (2) configuration of the incompetant Beltian wedge of sediments; (3) refraction of applied forces off the

basement structural highs; (4) shape of the basin with respect to the direction of applied forces; (5) subsidence due to depletion of magma chambers; (6) the position of previously intruded igneous bodies and the position of sedimentary formations which might act as greased low angle fault zones.

In the following chapters, manifestations of some of these tectonic features are reported.

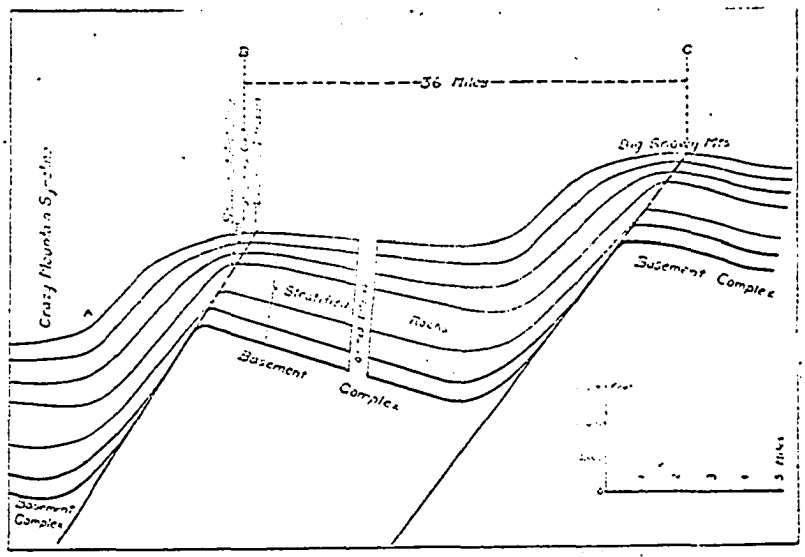

Fig. 15 Section showing assumed relation of surface structural features and subsurface faults in the Musselshell Valley, Montana (Thom, 1923).

General structure and igneous intrusives of the map area

General statement

The western part of the map area consists of the south plunging Hensley Syncline and the south plunging asymmetrical Robinson Anticline with a steep eastern flank. These folds are part of a series of northwestward curving folds which extend northward into the Castle Mountain area (Fig. 2). Eastward the east flank of the Robinson Anticline passes into a southeast to south dipping monocline, the strike of which curves from northeast to almost due east in the eastern part of the area (Plate 1). This monocline flattens out to the southeast and, farther to the south toward the southern stock, the dips are northerly and westerly. In the north central part of the map area, the beds flatten out with a few small folds forming over minor intrusions. Several minor faults transect and parallel fold axes and are described along with the joint patterns on the following pages. The configuration and distribution of the dikes, sills and laccoliths and their relations to the previously mentioned structures are discussed. In general, concordant intrusives predominate in high dip areas while discordant intrusives predominate in low dip areas, at least on the surface.

Hensley (Smith Creek) Syncline

The southward plunging Smith Creek Syncline is located along the western margin of the map area and is on line with the Hensley Syncline to the north, but it does not appear to be continuous with it

according to early mapping (Weed, 1897; Wolff, 1938). Yet Tanner (1949) indicates they are the same fold. The fold axis passes near the juncture of the Smith Creek and Shields River roads, trends N. 15 W. up Smith Creek three miles to the north where it passes out of the mapped area. A secondary trough occurs beneath Billie Butte laccolith as shown in the cross section (Plate 1). The secondary trough extends to the southeast as is indicated by the folded malignite sill just north of the Upper Shields River. This secondary axis is not an apparent shift in the fold axis due to topography superimposed on a non-vertical axial plane.

On the eastern limb of the syncline, in section 6, T. 5 N, R. 10 E. and section 31, T. 6 N, R. 10 E., changes of dip and strike are numerous and abrupt. Numerous anomalous steep dips are on line with a north trending malignite porphyry dike located on the northwest edge of the map. The dike exposure is stratigraphically lower than the strata to the south which contains these variable dips. The intrusion may have forcefully folded and/or fractured the sediments on line with the dike, or the dike was controlled by a previous fracture.

Robinson anticline and associated fractures

Eastward, the eastern flank of the Hensley (Smith Creek) Syncline passes into the Robinson Upfold. The axis of this southward plunging anticline trends north-south in the southern part of the map area. At the north edge of the map area the axis arcs to a N. 9° W. trend, parallel with the Smith Creek Syncline. This anticline continues to the north into the Castle Mountains where a minor fold on a slight angle to the main axis forms the subsidary Coral Creek Anticline (Tanner, 1949, Fig. 2).

The generalized cross section B-B' (Plate 1) across the nose of the anticline indicates that the fold has a slightly steeper eastern limb. The asymmetry becomes greater and more apparent to the north in cross section A-A'. The nose is gently rounded just north of the Shields River as is indicated by the outcrop pattern.

Dikes and steeply dipping sills are numerous along the anticlinal axis. Reversal of dip is abrupt across the axis. Wolff (1938), but not Weed (1909) proposed a fault along the fold axis. No fault or slickensides are exposed in the zone, but fractures could be made less obvious by multiple dike intrusion. Here one vertical intrusive contact is highly discordant with the strata but not well exposed.

The above observations do not particularly disagree with those of Tanner (1949), (p. 113) who writes, "The folds within the Crazy Mountain Basin are typical chevron folds...dip on the limbs of the folds being practically constant from anticlinal crest to synclinal trough. In the immediate vicinity of the fold axis however, the strata are

strongly contorted: tight folding, shearing and overthrusting on the scale of a few inches occur in an axial zone a few tens of feet wide. It is obvious from folding of this type that the Cretaceous strata were incompetent to transmit compressive stress during folding, and it is probable that they die out at depth". "It has been mentioned that the fault planes are tight, there is no evidence of fault-breccia or fault plane mineralization" (Tanner, 1949, p. 126). Red shales and sandstones (see Stone and Calvert, 1916, and McMannis, 1958) appear on both limbs in equivalent structural positions indicating negligible displacement if such a fault occurs. This should be substantiated by stratigraphic studies.

If the fault occurs it apparently terminates to the south on the anticlinal nose overlooking the Shields River. There is the possibility that post-fault sill intrusion could hide the fault zone on the nose. This faulted axis is directly on line with the Ibex laccolith 10 miles to the south (Fig. 2). Like most of the anticlinal sills, the Ibex laccolith is composed of malignite, but is associated with dioritic intrusives (pp. 114,115).

Many of the features described by Tanner and the writer are very similar to those associated with thrust faults around the Highwood Mountains and Bearpaw Mountains (Reeves, 1924, 1927). Some of these features are:

(1) Anticline-like structures which have curving axes and sometimes are chevron and flat-topped.

(2) Associated parallel faults usually have minor surface. expression, usually a zone of vertical beds, and are mainly recognized

by stratigraphic offset. "The faults are not accompanied by minor joints or vein material..."

(3) "The dip of the fault planes is commonly between 25°-45°, actually about the same as the dip of the strata along the upthrown side of the faults. Along strike the fault commonly persists for several miles terminating in a sharp plunging fold". (Reeves, 1927, p. 101).

Reeves believes that these faults with associated folds pass into shallow dipping thrust faults. This is based on the lowest strata exposed along faults, curvature of the fault planes and well data.

The surface expression of the faults depends to great extent on the depth of erosion according to Reeves. Gwinn (1964) has described a similar situation in the Appalachians. He believes that apparent difference between central and southern Appalachian folds and related faults is in part due to depth of erosion. Hoskins (1965) explains a plunging fold of the Pennsylvania Appalachians as follows:

> "The relationship of the Henrietta axial fault to the plunging fold provides additional evidence to support Gwinn's hypothesis (1964) that plunges of major anticlines are controlled by decreasing displacement along the thrust responsible for major anticlinal folds of the Appalachian Mountains."

Likewise, Roberts (1965) proposes shallow seated deformation for the Livingston, Montana area in the southwest corner of the Crazy Mountains Basin upon the basis of the field relations of faults which

are often associated with northwest trending arcuate folds. Yet detailed stratigraphic and geophysical studies are necessary in the study area for better interpretation of structure at depth.

To the north, the Robinson Anticline (Fig. 2), is terminated by the Castle Mountain intrusives. Implacement of the western granitic stock may have been controled by a thrust fault which extends northeast and north of White Sulphur Springs (Tanner, 1949, p. 133).

In the Great Cliffs on the west side of the anticline trending at right angles to the Robinson fold is possibly a minor reverse fault or joint that dips 65° north. In these cliffs this fracture controlled the emplacement of a malignite sill (Fig. 6,7).

A thin dike follows the fault zone for about 5'. Less than a mile to the east the fracture is indicated by the abrupt bend in the west side of Virginia Peak syenite laccolith (Plate 1). Slickensided Virginia Peak syenite talus occurs $\frac{1}{4}$ to $\frac{1}{2}$ mile south of the abrupt bend which could be related to this fault zone. This is parallel to the South Fork zone of en echelon faults along the Musselshell River (Fig. 2). They are vertical faults with down thrown sides also to the south (Tanner, 1949, p. 104?).

The monocline

East of the Robinson Anticline, the strike curves from northeast to east in the easternmost part of the area. The southward tilted beds dip up to 70°. South of the southernmost sill (highest stratigraphically) the dip reverses from 20° south to 20° north, (Plate 1). Locally in this southeast area, near the dikes, the shallow dips are to the

east or west. These anomalous dips may be related to a few minor north trending normal faults with displacements of less than ten feet which also occur near the dikes.

To the east the monocline is directly on line with a flexure which is the southern limb of the Little Elk-Shawmut anticline domal complex (Fig. 2). East of the map area the beds, including sills, wrap northerly to the northeast side of the northern stock. Here the beds bend abruptly to the east. To the southwest of the map area the monocline is on line with the vertical beds near Wil..sall. They trend southwest to Bridger Pass like Thom's shore line fault or the "Perry" line. (Perry, 1950; Thom, 1957).

Target Rock laccolith dominates the topography of the monocline. A Minor down-fold. . : occurs below it. Its relation to the structure is similar to that of Billie Butte in that it's axis is located on the flank of a fold. The downfold below Target Rock is less pronounced than that associated with Billie Butte, probably due to the difference in size of the bodies. To the north of the monocline is a small area in which dips are shallow. In this area, minor elongate flexures occur over small intrusions (Plate 1).

Dikes

Distribution

Several sets of dikes occur with different strike trends. These trends have distinct relations to the directions of the folds (Plate 1). In addition, the dikes predominate in areas of low strata dip.

In the western part of the area, a set of parallel dikes occur near and parallel with the north-trending anticlinal (Fig. 15). On the western flank of the anticline is a set of parallel dikes trending N. 20 E. and diagonal to the fold axis.

In the southeast corner of the map area, a fanning dike set trending perpendicular to the strike of the monocline occurs with a north-south symmetry plane. To the north, some of these dikes curve in map view (Plate 1). Nearly on line with this set, to the northwest is a dike set with a N. 55 W. trend. Weed's (1899) map displays a number of dikes to the east of the present map area with a northeast trend which might prove to be a mirror image of the last mentioned set of the curving dike pattern. To the south as is indicated by Weed's and Wolff's maps, and John Tappe (personal communication 1964), the radiating pattern of the dikes around the southern stock may have a north south symmetry line. A larger number of dikes appear to trend north-south (Fig. 2). A similar curving, bilaterally symmetrical dike pattern associated with two stocks is the well known Spanish Peaks, Colorado, igneous complex (Knopf, 1936). After mapping of the surrounding areas has been accomplished, a mechanical analyses of the stress pattern might be inferred for the Crazy Mountains similar to that developed by Ode (1957) for Spanish Peaks area.

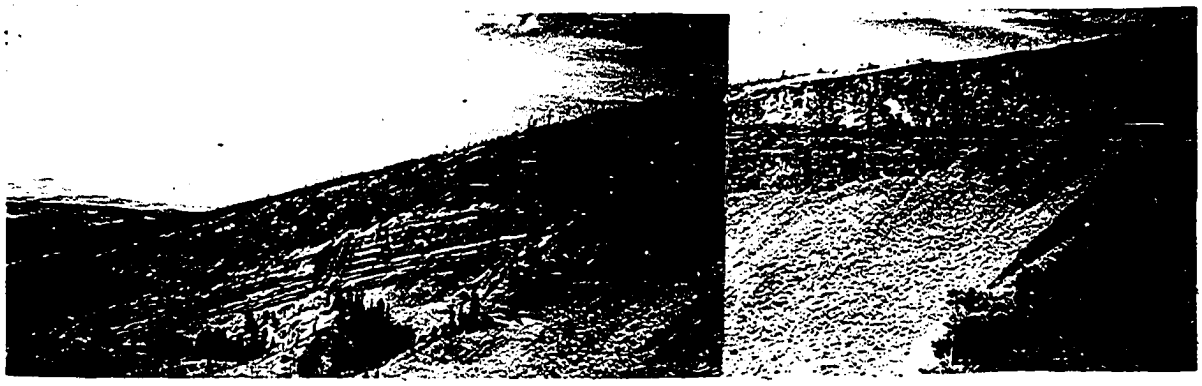

Fig. 16 View of the north face of the Great Cliffs displaying the groups of northward trending dikes transecting the reddish sandstones and shales and sometimes the malignite sill on the west flank of the Robinson Anticline.

Fig. 17 View of the north face of the Great Cliffs showing several dikes transecting two 10' akeritic sills and sandstones and shales. The dikes are trachytes and malignites. In the center, a malignite dike bluntly terminates downward.

Size and concentration

Single dikes are usually less than 25 feet thick. Complex dikes (compound or multiple) are usually less than 100' thick. The few quartz latite dikes such as the north trending dike at the head of the Upper Shields River Valley are 200' thick. The dikes vary in thickness horizontally and vertically but no definite [illegible] trends could be ascertained because of scarcity of exposures and topographic data. These thicknesses contrast with the 1 to 20' thick dikes in the Highwood Mountains, Montana or the 20 to 60' thick dikes of Spanish Peaks, Colorado.

Some dikes are up to two miles in length and are probably longer as many have not been traced to the south or north. In surrounding areas much longer dikes occur such as the malignite dike in Ibex Quadrangle to the south of the map area. In the Highwood Mountains they are up to 2 miles in length but at Spanish Peaks some are over 15 miles long.

In the southeast part of the map area, there are over fifty dikes with an aggregate thickness of over 1,100' in four miles representing four to five per cent of the territory. This same per cent of dike width of invaded territory is found across the island of Mull. Concentration of dikes varies greatly in dike swarms. In case of the northern Britain Caldonian Etive swarm, dikes make up about thirty per cent of the surface of the country (Anderson, 1951).

Complex dikes

Three types of complex dikes are recognized, especially in the

southwestern fanning dike set:

(1) Along the Upper Shield's River is a multiple dike composed of a medium grained basalt with a fine-grained inner phase of basalt.

(2) Composite dikes with multiple relationships are commonest of complex dikes (phases of different composition, one chilled against the other of either basalt, andesite porphyry and latite). In one dike along the Upper Shields River both phases appear to be finer grained at their mutual contact. One explanation is that the later phase was intruded at the chilled country rock contact of the previously intruded dike.

The later phase can be margined on both sides by the earlier phase, on one side or both sides of the earlier phase. These physical relations between the two phases may vary along the dike. Often a sedimentary septa up to 5 feet thick occurs between the two phases.

(3) Not as numerous as the last group are composite basalt-porphyritic feldspar basalt dikes with contacts between phases gradational over a few inches. Some of the mineralogical variations across dikes is post-magmatic.

These different dike types are found in a similar abundance in the Highwood Mountains (Buie, 1941).

Composite dikes indicate a change in the magma being intruded or lateral differentiation occurred with intrusion. According to Bhattachargi and Smith (1964), composite dikes can be formed by a

flow process as a result of one injection of a homogenous magma. The first idea is preferred because the porphyritic feldspar basalt phase (?) is chilled against the basalt (multiple relations ip) in other dikes and because of the occurence of sedimentary septa between these phases.

In the Great cliffs a fanning set of basic dikes occurs (Fig. 18). A large carbonate vein is found in the center of this dike group. Apparently later carbonate bearing solutions were controlled by these previously intruded dikes.

More definite conclusions about the nature of these complex dikes should come from areas of more complete exposure such as around the southern stock.

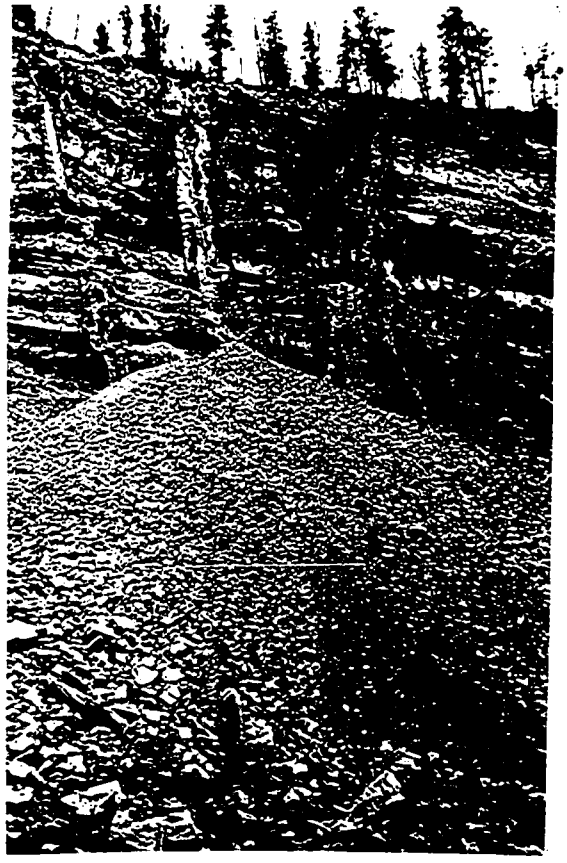

Fig. 18 View of the north face of the Great Cliffs showing a set of fanning lamprophyric dikes with an irregular white, calcite vein in the middle of the set.

Concordant and miscellaneous intrusives

General statement

Except in the southeast and northcentral part of the map area igneous intrusives that are interlayered with sedimentary strata predominate. These hypabyssal intrusives include mainly sills and at least two phacoliths and one laccolith.

The basic alkaline rocks (malignites) predominate on the Robinson Anticline at the lower stratigraphic interval,as felsic rocks (quartz latites, latites, trachytes) predominate, stratigraphically higher, on the eastward trending monocline (see section on petrology).

It was difficult to determine the lateral continuation of each body because of the large number of sills, their thinness and the thinness of the sedimentary septa, paucity of exposure, and similarity of igneous rock types.

Sills

Distribution and size

Along the axis of the Robinson Anticline and near the northeast edge of the map area the largest number of concordant intrusives are exposed. In these areas a total thickness of about 1,600' of concordant intrusives occur (including one phacolith). At least 72 separate intrusives occur with a mean thickness of about 23' (addition data besides section above). The malignites, mafic trachytes - latites and quartz latites have a median thickness of about 15', 10' and 30' respectively. Interestingly, 21 malignite intrusives, 27 mafic trachyte-latite intrusives and 27 quartz latite intrusives

occur in above mentioned area. They vary from 1' simple sills to 300' complex sills in the northeast part of the map area. Some of these intrusives have been traced along strike for three miles.

The felsic sills increase in number to the northeast toward the northern stock (Fig. 5), as the malignites are concentrated on the anticlinal nose.

Structural features

Discordant contacts, thinner sedimentary septa, and more sills in contact are most prevalent to the northeast. Asymmetrical undulating contacts and pressure ridges (flow wrinkles, Fig. 19) are seen occasionally. Sill terminations are also rarely exposed. One sill termination below Target Peak is irregular with two bulging noses, while another exposed in the Great cliffs has uplifted the strata (Fig. 20). This sill has split off another sill exposed higher in the Great Cliffs, (Fig. 21). Weed noted that thinner felsic sills being finer grained are generally darker than the thicker felsic sills.

The Great Anticlinal phacolith

The thickest intrusive on the Robinson Anticline is the 140' phacolith that occurs at the southernmost peak of the anticlinal ridge. In section view at right angles to the anticlinal axis the phacolith base is apparently concordant while the top is not exposed (Fig. 86). In a section parallel to the axis the base is concordant and discordant in various places (Fig. 22, 23). In this section large intrusive

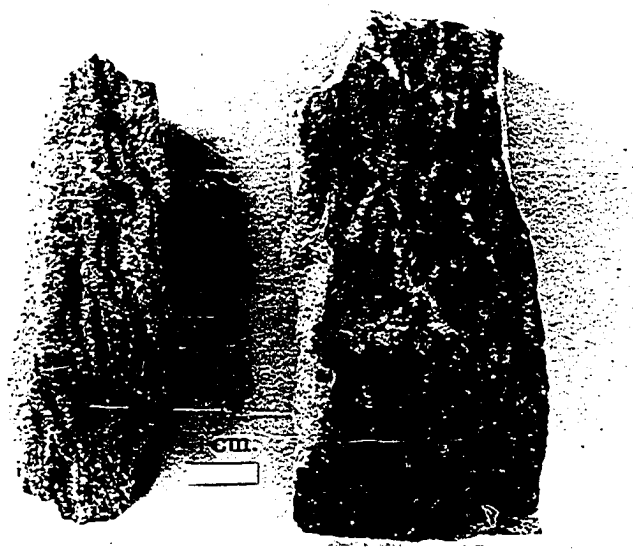

Fig. 19 Flow wrinkles from the vertical east contact of concordant intrusive 578 of quartz latite. The wrinkles on the right are asymmetric with the steep side upward in the field. Apparently the magma direction of movement was mainly vertical. Similar asymmetrical flow wrinkles are developed between steeply dipping concordant intrusive 410 and 411. These latter wrinkles have a wavelength of 3.2 cm. and an amplitude of .6 cm. and are oriented with their crests horizontal. 411 has a sheared border 5-10 mm. thick which contains deformed plagioclase phenocrysts.

asymmetrical undulations on the phacolith base and overturned country rock protrusions indicate the intrusion was from the northwest (the protrusion is overturned in the direction of flow probably). This body appears to terminate abruptly on the western flank of the anticline at the contact with a north trending malignite dike. The contact between the two bodies is not exposed. Chemical analysis of the samples from the dike and the coarse grained upper part of the phacolith are similar. These features indicate that the dike could have been the feeder for the phacolith. The dike also extends to a higher stratigraphic level than the sill.

A phacolith shape is usually taken to be the consequence of folding. Folding occurred contemporaneously with or previous to intrusion, (Hunt, 1953, p. 149).

Billie Butte phacolith and Target Peak laccolith

Only Billie Butte phacolith and Target Peak laccolithic intrusives are exposed well enough to estimate sizes. The top is eroded from Target Peak, (Fig. 24), but its summit must be near the upper contact as is indicated by boat shaped country rock inclusions. The upper contact of Billie Butte laccolith is not exposed, but nearness to the top is indicated by structural projections. The bases of these two intrusives are concordant. Target Peak is eliptical in cross section while Billie Butte may have a concave upward top, as is indicated by the topographic saddle on its summit and the downfold in the malignite above on strike to the south. Beneath the bodies

Fig. 20 Terminated sill displayed in Fig. 21. Thin-bedded sandstones and shales are deformed by the sill. The termination has influenced the basal configuration of the upper sill. Trees at top for scale.

Fig. 21 Eastward view of the Great Cliffs displaying the terminated lower split sill as well as other features described in Fig. 20, 6 and 7.

Fig. 22 Eastward view of the north-south cliff of the anticlinal phacolith. Top of the body has been eroded. The left side of the body is concordant with the strata below. In the center, covered by the trees, two asymmetrical contact undulations are developed at the base. To the right, the base is sharply discordant with the underlying strata. In the right background is the head of the Upper Shields River Valley.

Fig. 23 Close-up of the base of the phacolith described in Fig. 22, shows one of the two asymmetrical contact undulations (in both, the side which forms the largest angle with the general structural dip is on the up-dip side; the undulation pictured is 15' long and 6' high with a 6 inch-long protrusion of country rock which is recumbent to the southeast, P on diagram).

shallow downfolds occur. The axis of the minor folds beneath are on the flanks of the major anticline. As phacoliths are usually taken to owe their shape to folding - the intrusion occurring with or after folding, the non-concordance of the Hensley Synclinal axis and the phacolith axis indicates a complicating factor is involved. The feeder for the laccolith may have controlled the site of the body. Possibly a post intrusive period of folding occurred.

The maximum thickness of Target Peak laccolith is 100'. It has a plan view area of 0.18 square miles. Billie Butte laccolith is at least 360' thick and has a plan view area of 0.7 square miles. As a comparison, Cowboy Creek differentiated (?) laccolith, one of the smaller laccoliths of the Highwood Mountains, Montana, has an estimated thickness of 200' and 0.8 square miles ground plan.

Other shaped bodies

In the northcentral part of the map area are several unusual igneous intrusives in the shape of roof tops and trap doors (Fig. 26). These are composed of akerite. Their emplacement may have been controlled by fault zones. These exposures display the local deforming ability of these intrusives. In the upper example either magmatic stoping or differential lateral slippage of strata occurred in order to make room for the intrusive. The minor contact effects indicate the latter is the case. There are other small domes just to the east of the above intrusives which probably overlie bodies similar to these figured intrusives.

Fig. 24 View to the northwest from the Upper Shields River Valley. In the background are Target Peak feldspathoid syenite laccolith (right), Virginia Peak aegerine syenite laccolith (center) and Davie Butte trachyte sill (left).

Fig. 25 View to the southeast along the upper Cottonwood Creek ravine of a northwest trending lamprophyre dike which is offset into four segments. On the opposite side of the ravine, 50 feet away, it is one simple dike.

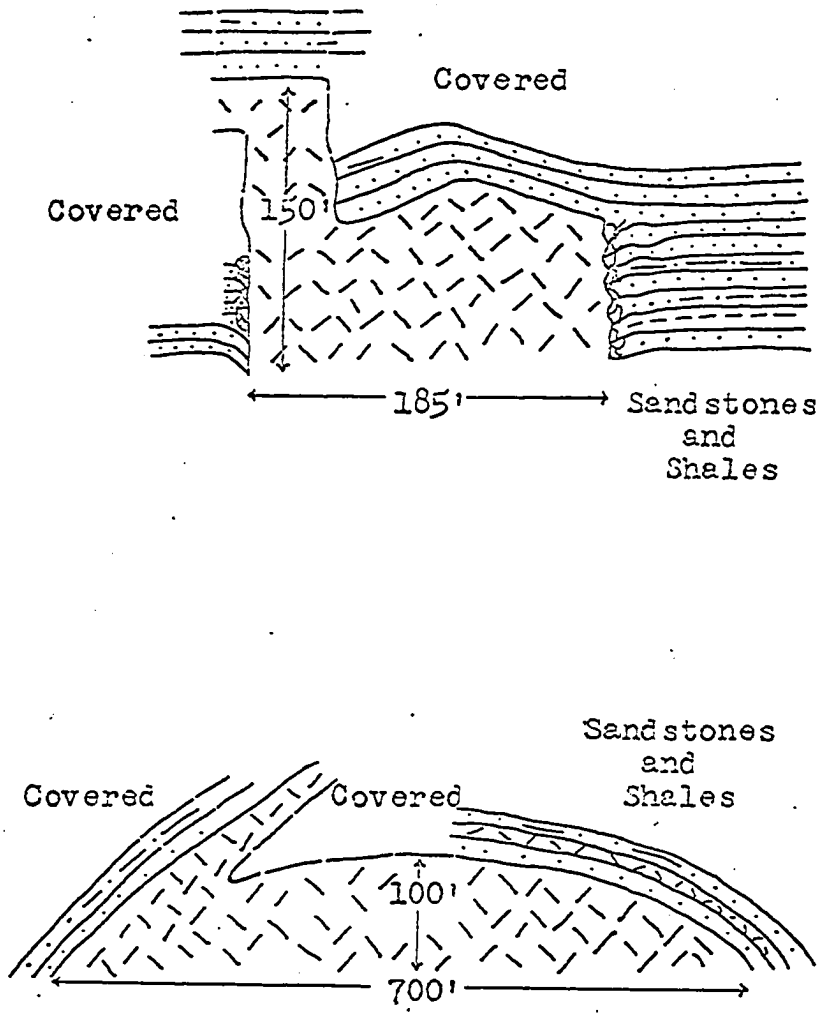

Fig. 26 Cross sections of hypabyssal akeritic intrusions that have locally deformed the surrounding strata. These bodies are linear in plan view and on line with each other. The left hand side (west) of these intrusives may be controlled by a fault which would explain the trap door structure of the lower body and the bowed down and intensely fractured left contact of the upper body.

Relationships between intrusives

Several types of discordant intrusives occur that may occupy the conduits for transferring magma to concordant high level intrusives. These include stocks, pipes and dikes.

In many areas, such as the Highwood Mountains, it is a moot question as to the exact nature of feeders of laccoliths but because a greater stratigraphic section is exposed in the Crazy Mountains than is usual, exposures allow the determination of relations between concordant and discordant intrusives. Besides stocks and pipes, there are several lines of evidence that indicate that dikes fed many laccoliths and sills.

Three pipes and the small Comb Creek stock occur to the west and north of the map area and probably acted as magma conduits. These are discussed in some detail by Wolff (1938). The northeast trending sill set thickens and the sedimentary septa become thinner and more metamorphosed to the northeast. In the northeast corner of the map area and beyond, many of the sills are in contact forming composite bodies more than 300' thick. The quartz latite dikes at the head of the Upper Shields River thicken rapidly in short distances. Evidently many of these intrusives had a major conduit in association with the northern stock, to the northeast of the map area. This latter relationship needs to be studied further.

Some evidence for dike conduits is as follows:

(1) Some dikes are connected to sills. Examples are two malignite

dikes on the nose of the Robinson Anticline. In east center of Section 21 T. 5 N. R. 10 E. a thin malignite dike is connected to thin local sill (Plate 1). A similar occurrence to the south 0.5 miles can be seen from the Shields River road. In the cliff north of Forest Lake numerous thin dikes occur that pass into sills.

(2) A number of concordant bodies terminate near a dike outcrop, both intrusives having similar compositions. The Great Anticlinal phacolith has a surficial expression which terminates on the western flank of the anticline near a north trending malignite dike (Plate 1). Northeast of Forest Lake sills terminate near and on line with dike trends of similar mineralogical composition (Plate 1). In the fanning dike set complex dike outcrops occur near exposure of thin sills of similar composition.

The termination of sills near dikes could be due to "damming" effect on the sill by a previously intruded dike. In fact, on the nose of the Robinson Anticline (west center of Section 15 T. 5 N. R. 10 E) a thin lamprophyre sill terminates near a latite dike. The sill, turns sharply upward into a thin short dike. In all other cases the dike and sill are of similar composition. The similar compositions must be accepted as coincidence for this "damming" effect to be caused and is considered to be a highly unlikely coincidence.

(3) The overall distribution of dikes and sills of similar composition indicates the dikes are connected. For almost every concordant body a dike is found nearby of similar composition, except the

middle of the northeast trending sill set as well as Target Rock feldspathoid syenite and Virginia Peak Syenite. This relation is observable in the middle of the map area where malignite sills terminate in the vicinity of malignite dikes, the possible connections being destroyed by erosion. The exceptions will be considered later.

Even though concordant bodies are connected to dikes this does not necessarily prove that the dikes are conduits. It can be argued that these were just part of the inter-connected network of openings and potential openings that were developed during folding, that they were filled almost passively either upward or downward.

Several lines of evidence indicate that the dikes were more than simple fracture fillings (1) the dikes are often complex; several pulses of magma had used the unique channels. (2) the dike rock usually has a different texture than the analagous sill even though they have similar thickness, indicating different geologic conditions in the dike and sills (needs to be substantiated). (3) several dikes and other related discordant bodies show evidence of forceful injection at their upward termination as do the few exposed sill terminations.

Also the laccoliths that are well exposed are elongate, but not elongate in the direction of the major stocks as in the Henry Mountains. Hunt (1953, p. 1) uses this latter fact as evidence that the laccoliths there were fed laterally from the stocks. (Concordant bodies mapped by Wolff, 1938 on the margin of the southern stock were no doubt fed from that stock).

The general relationship that dikes predominate in low dip areas while concordant bodies predominate in high dip areas indicates that the type of intrusive developed depends on the dip of the beds in which case comformable bodies would feed dikes in certain cases. This is difficult to demonstrate in the field because of topography.

Joints

The attitudes of joints in the map area were recorded with regard to type of rock structure (sedimentary rocks, discordant or concordant intrusive (Fig. 27). The joints were subdivided on the basis of areas with different structural dip, plotted on Wolff nets and rotated so that the bedding was horizontal (Fig. 29., 30). Unfortunately 60 per cent of the recorded joints occur in the southwest section of the map where the northwest trending set of dikes occur. In fact, joint concentrations increase towards the dikes, joints being less than a foot apart in sills and strata near the dikes. It was not possible to observe other joints due to poor exposures.

The only generalization that is possible is that the major joint direction is N. 30° W and vertical, parallel to many of the dikes in the map area (Fig. 12.). Regionally, the N. 30° W. trend parallels the Bighorn Mountains axis, the Cedar Creek Anticline axis and faults in the Beartooth Mountains core in the Livingston Peak area. Also a number of joints trend northeast in the southeast part of the map area parallel many dikes there.

Fig. 27 Prominent jointing developed parallel to contacts in an eastward dipping malignite sill. Exposed along the Upper Shields River Road. Entire exposure is malignite.

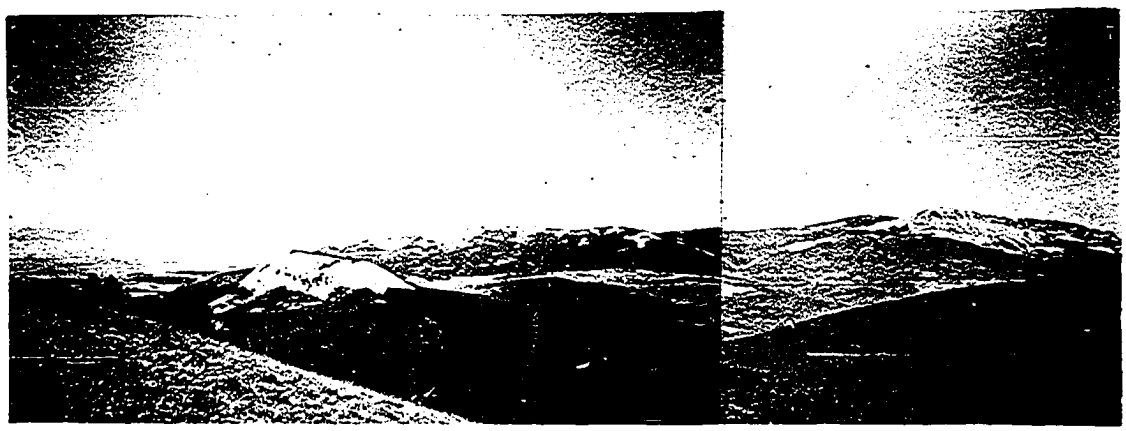

Fig. 28 Westward view from near the summit of Beverly Peak, Virginia Peak (right) and Davey Butte (center) are ridges on the east flank of the Robinson Anticline. The axis of the anticline coincides with wooded ridge in the right background. To the left, (southwest) is Target Peak laccolith, the Shields River Valley and Bridger Range in the background.

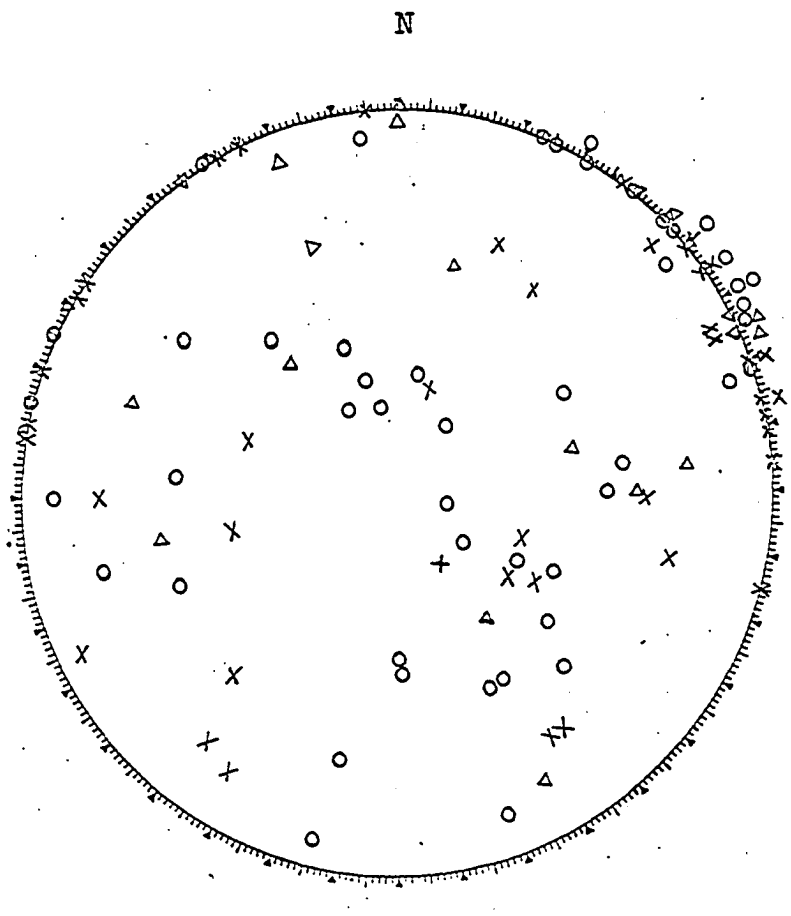

Fig. 29 Poles to joint planes from the map area plotted on the lower hemisphere of a Wulff net. Joint Sandstones and shales (crosses), concordant intrusives, (triangles) and discordant intrusives (circles).

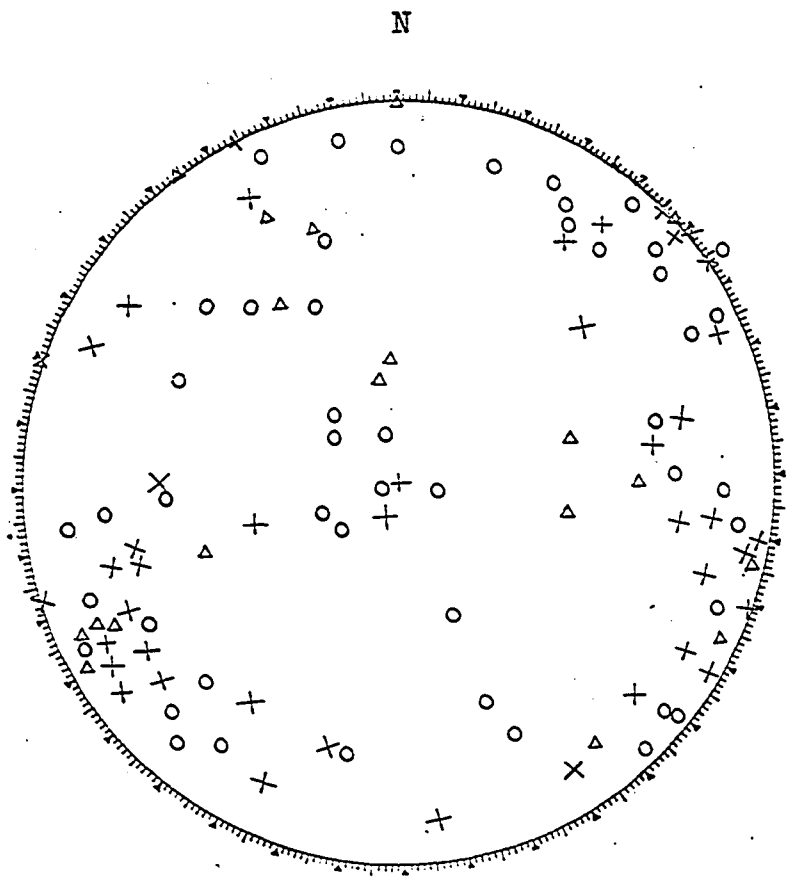

Fig. 30 Poles to joint planes from the map area. Corrected for tilt of strata. Poles plotted on the lower hemisphere of a Wulff net. Sandstones and shales (crosses) concordant intrusives (triangles), discordant intrusives (circles).

Concluding statement on the relationship of general structure and intrusion

A full understanding of the relationship of the tectonics and intrusion will have to await the study of the northern quartz diorite stock. A few further remarks are proper here.

As the previous chapters have indicated, the northern Crazy Mountains intrusives are coincident with a number of important regional structural features. This, to a certain extent, negates Eardley, (1961) who has stated that the igneous complexes of the central Montana plains are not concentrated along structural trends.

The fold-intrusive pattern is not quite as simple as that found by Tanner (1949, p. 133).

He has observed the following:

> "The dike swarm which extends into the Castle Mountain area from a center in the Crazy Mountains was injected into folded strata before faulting occurred. In field relationship to the sedimentary rocks, the dikes resemble sills in that they closely parallel the bedding and have very sharp borders without regard to any apparent cross cutting or development of apophyses. They are restricted, however, to steeply dipping flanks of folds and do not extend across fold axis. It is highly probable that the magma was injected laterally from a central stock while the sedimentary rocks were being folded."

Indeed, concordant bodies do appear to predominate in areas of high dip as dikes predominate in areas of low dip, but there are many exceptions such as the Great Cliff malignite sills and Billie Butte phacolith which occur along the axis of folds in the map area.

PETROGRAPHY

Introduction

The Shields River area was chosen for study because it contains a broad spectrum of the alkalic rock types known to occur in the Crazy Mountains. Diversity of igneous rocks is one of the prime characters of the area - it contains most of the alkaline types plus some that appear to be alkali-calcic (p. 162).

The rocks have been subdivided into seven groups which are easily recognized in the field (Plate 1). They are (1) rhyolite and quartz latite porphyries, (2) mafic trachytes and latites, (3) basalts, (4) andesite porphyries, (5) lamprophyres, (6) feldspathoid syenites-syenites, and (7) malignites as shown schematically in Fig. 31. The relationship between the various groups indicated by this diagram is derived from the simplest megascopic petrography, and is similar to that relationship indicated by geochemical considerations (SiO_2 vs. C. I. diagram, p. 179). On the following pages these groups are discussed in separate sections except for the andesite porphyries, basalts and lamprophyres which are discussed together for convenience. The reader is referred to the summary (156, 157) for the essential characters of the various rock groups and Plate 2 as well as the thin section descriptions in the appendix.

The A.G.I. modal classification of igneous rocks (Peterson, 1961) has been followed in most cases.

	Abundant Feldspathoids, Zeolites	Minor Quartz or Zeolite, usually	Abundant Quartz most in matrix
Felsic	Feldspathoidal Syenites	Syenites	Rhyolite Quartz latite porphyries
Intermediate		Akerites Mafic trachytes, latites	
	Malignite	Andesite porphyries	
		Lamprophyres	
Mafic		Basalt	
	Olivine, Augite, Aegerine	Augite Hornblende	Hornblende

The complete mineralogy summarized on pp 155, 156.

Fig. 31 Igneous Rock Groups recognized in part of the northern Crazy Mountains (mainly the Shields River Map Area).

Rhyolite and quartz latite porphyries

Nomenclature

Wolff (1938) termed this rock group granite or quartz latite porphyries and sometimes white porphyries. In the map area and generally elsewhere in the northern Crazy Mountains they are rhyolite and quartz latite porphyries. Chemically, on the basis of the differentiation index vs. SiO2 diagram, (p. 199), these rocks range from near the average dellenite (rhyolite transitional to quartz latite) to near the average rhyodacite (fine-grained equivalent of granodiorite). Yet they are granodioritic according to normative orthoclase-albite-anorthite ratios of the Jones and Pratt classification (see Witkind, 1964, based on Nockold's data for the calc-alkaline series).

Location

The rhyolites and quartz latites have three main occurrences in and around the Shields River area: (1) in the central part of the sill set which trends northeast from Target Peak, (2) as an unusually thick north-trending dike at the head of the Shields River and (3) as sills and dikes on Mount Elmo, northwest of Forest lake beyond the map area.

In the northeast trending sill set, a few intrusive contacts indicate that intrusion of these sills was not simultaneous and that the direction of intrusion may have been paralles to the dip (vertical), (p. 52). These bodies are transected by a few north trending basalt-andesite porphyry dikes which are also reported by

Wolff (1938, p. 1595) to transect the northern stock and contact zone (Weed, 1899) probably called these latter rocks camptonites.

Mineralogy

The following description is based on ten samples. The specific gravities of four of these range from 2.68 to 2.59 as the color index varies from 10.1 to 5.5. They are white, gray and pink. The textures are porphyritic with fine-grained microgranitic to felsic groundmass.

COMMON HORNBLENDE (maximum 7 per cent) is pleochroic light brown to yellow and various colors of green; darker green rims sometimes occur. The maximum c:Z' angle ranges from 17 to 29 degrees. Chlorite pseudomorphic after hornblende is common.

BIOTITE (maximum 9 per cent) is pleochroic black, deep red, dark brown to light yellow. It is associated and intergrown with chlorite and hornblende. Sphene and sometimes apatite are inclusions. Rare calcite interlayers occur. Biotite appears to alter to a different colored chlorite from that formed from hornblende in section S-31.

CHLORITE (maximum 5 per cent) is pleochroic light green to light brown and some appears to be penninite on the basis of color and interference color. The chlorite is formed from the alteration of hornblende and biotite as is indicated by pseudomorphism and sphene inclusions (sphene inclusions occur in all three minerals). Calcite and less often magnetite occur in these pseudomorphs. In

pseudomorphs chlorite tends to occur near rims with calcite near centers. In amygdules, other calcite-chlorite relations occur (Fig. 32, 33). Lehmann (1965, p. 31, etc.) has described similar occurrences in basic dike rocks of southern England.

PLAGIOCLASE occurs mainly as phenocrysts (20 to 39 per cent). Zoning is common but usually not prominent (Fig. 34 is an exception). Anorthite content varies from 33 to 20, less commonly to 5. Lath-like inclusions in the potassium feldspar are andesine (An. 45) in sample 578. The phenocrysts range from 0.5 mm. to 2 mm. in length, seldom up to 4 mm. Rare narrow potassic rims and antiperthite occur in one sample. Albite and Carlsbad and rare Pericline (?) twinning are developed in the phenocrysts. The plagioclase is usually turbid (Fig. 35). Alteration products are sericite and epidote.

POTASSIUM FELDSPAR (0 to 11 percent) occurs in several relations with plagioclase (Figs. 36, 37, 38). Lath perthite occurs with the plagioclase component sometimes extending into the matrix. Elsewhere the potash phase is surrounded partly or wholly by soda feldspar. Aggregates of potash feldspar occur near plagioclase feldspar aggregate edges. The potassium phase is perfectly rectangular to irregular in shape and has a low 2V (20 to 30 degrees) indicating sanidine. However, Wolff (p. 1613) reports orthoclase enclosing oligoclase laths and bordered by oligoclase (Ab 73) in parallel growth (Sample 149.89). In length they range from about 0.5 mm. to 2 mm., sometimes up to 1 cm. Thus they are generally larger than the plagioclase.

QUARTZ occurs as distinctive rounded, amoeboid, sutured, polycrystalline phenocrysts (Figs. 39, 40) and in the fine-grained

groundmass as elongate, irregular individuals in rows (Fig. 41), and as fine intergrowths with alkali feldspar. Usually only about 5 per cent is coarse enough to be definitely identified, although Wolff determined 24 per cent modal quartz (19 per cent quartz in the norm) in one example. One phenocryst contains a transecting vein of finer grained quartz, indicating that the grain may be xenocrystic.

Several other features indicate these quartz phenocrysts may be xenocrystic in nature. (1) They occur in polycrystalline aggregates. (2) They are sometimes fractured with abundant submicroscopic inclusions that are absent along fractures and borders as if the inclusions were removed by the affect of magma. (These inclusions must be studied further before more definite conclusions can be made). (3) Some of the rounded grains have sharp angular broken-like edges indicating a mechanical break-up of the grain (Fig. 39).

The FELSIC MATRIX ranges in grain size from .1 to .01 mm. and is composed of an intergrowth of alkali and feldspar and quartz (Fig. 42). The felsic matrix varies from 41 to 71 per cent of these rocks. Compositions have been computed using modal and chemical data for 479A assuming no potassium is in the plagioclase phenocrysts. The result is reasonable and indicates that the matrix has a composition of Or. 31, QUARTZ 37, Ab. 32, and negligible An. This composition lies just below the cotectic for 1000 bars pressure in the system QZ-Ab-Or. and at the average granite composition (p. 207).

ACCESSORY MINERALS are MAGNETITE with LIMONITIC alteration, APATITE and SPHENE. CALCITE and EPIDOTE and ZIRCON and a trace of colorless anhedral PYROXENE has occasionally been recognized.

Wolff (1938, p. 1614) states that these rocks grade into hornblende akerites. Based on mineralogy and chemistry in the present study (p. 82 and Fig. 94) there appears to be a discontinuity between the two groups. However, southeast of Target Peak one intrusive may contain both rock types.

Fig. 32 Calcite amygdule (upper right) surrounded by anhedral to hexagonal quartz crystals and includes light green chlorite. The mass is in a felsic matrix containing bent plagioclase (P), biotite (B) with sphene inclusions, and apatite, plane light, 30X, acid porphyry sill S-31.

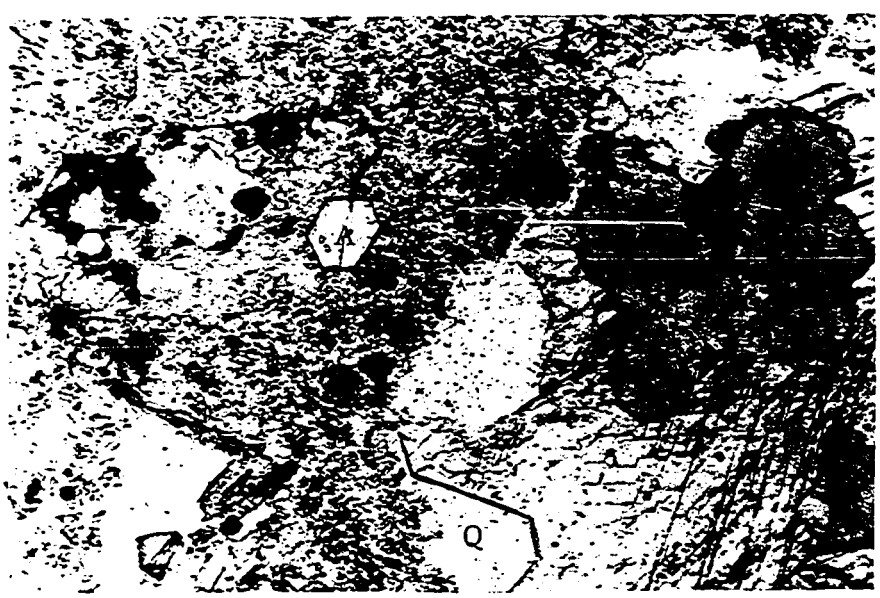

Fig. 33 Edge of amygdule shown above, apatite (A) in matrix, quartz (Q), calcite (Ca), chlorite (Ch), sphene in pseudomorph of hornblende, 120X, acid porphyry sill S-31.

Fig. 34 Zoned plagioclase (P), albite-oligoclase ?, in turbid brown felsic matrix with other altered plagioclase phenocrysts; X-nicols, 40X, acid porphyry sill S-126.

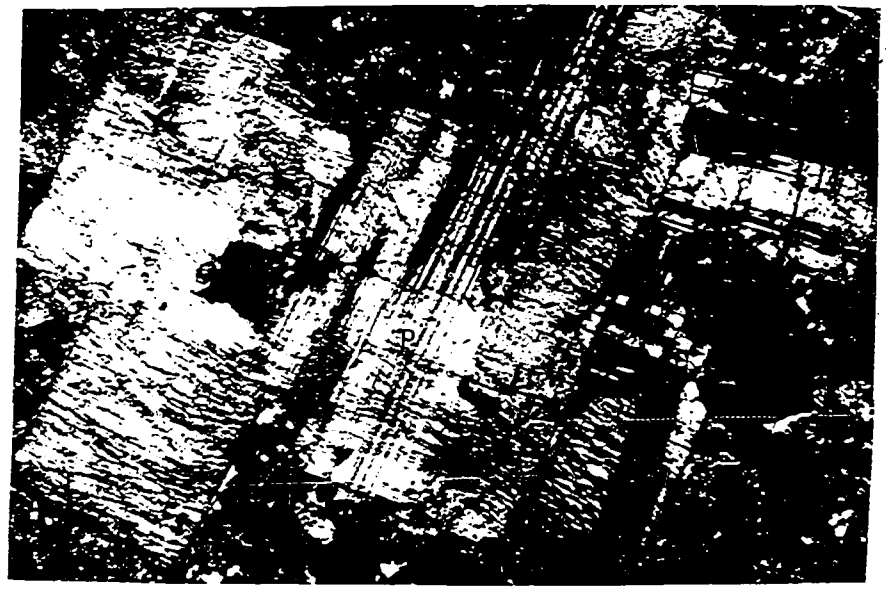

Fig. 35 Altered plagioclase (P) in aggregates in turbid brown felsic matrix; X-nicols, 40X, acid porphyry sill S-126.

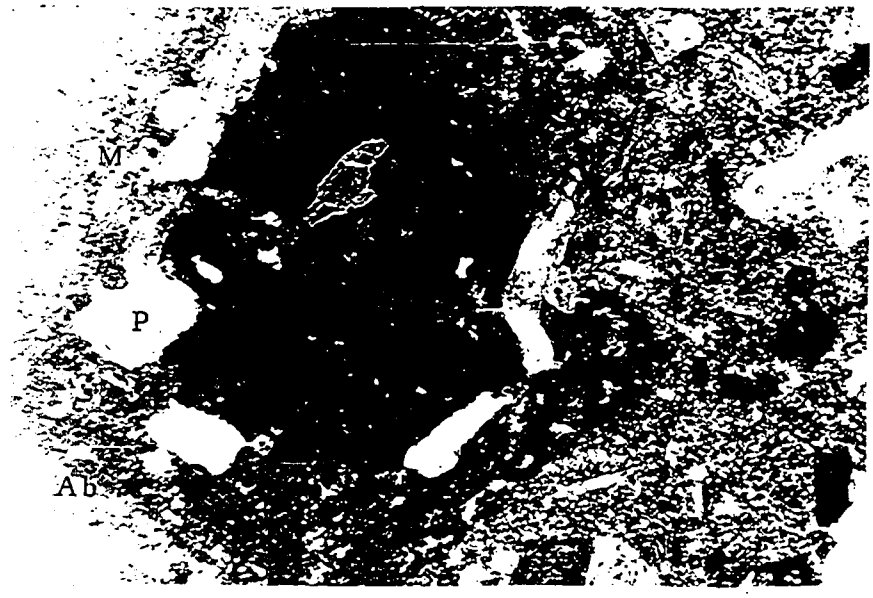

Fig. 36 Feldspar phenocrysts with potassium feldspar core (K), plagioclase (P), inclusions near edge; albite (Ab) rim is gradational in places with matrix (M), X-nicols, 30X, quartz latite porphyry 578.

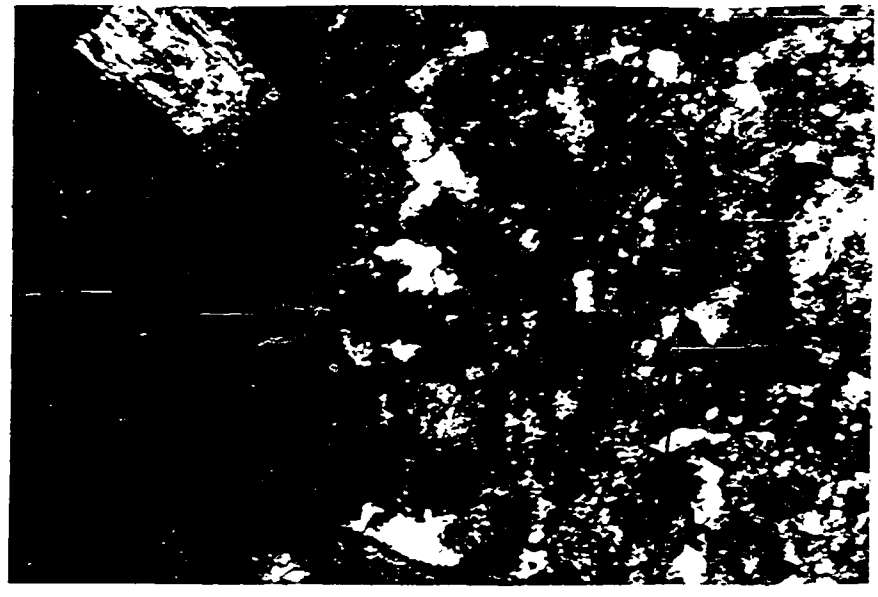

Fig. 37 Zone across complex feldspar phenocryst shown in Fig. 36; X-nicols 120X, quartz latite porphyry 578.

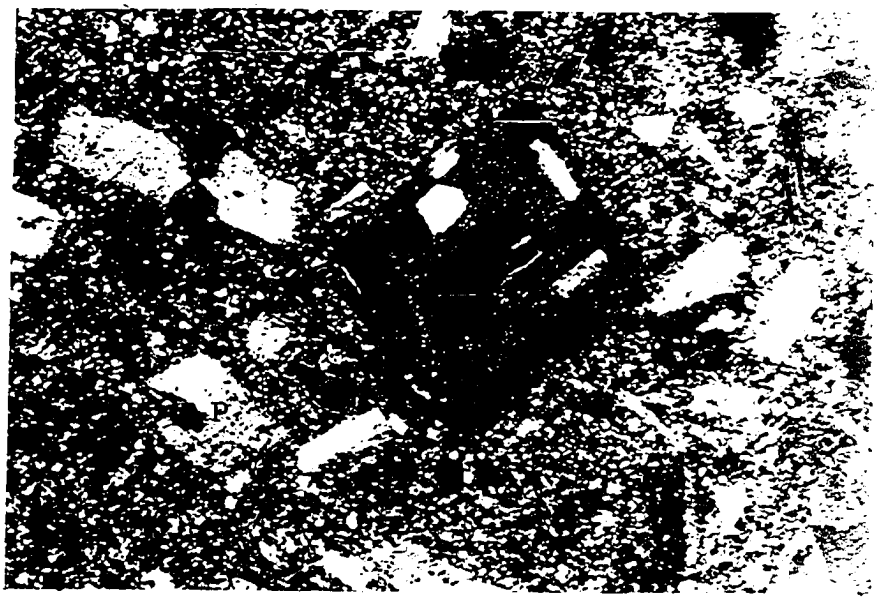

Fig. 38 Euhedral Microperthite (Mp), plagioclase (P), biotite phenocrysts in matrix of alkali feldspar, quartz; X-nicols, 30X, rhyolite porphyry S-70.

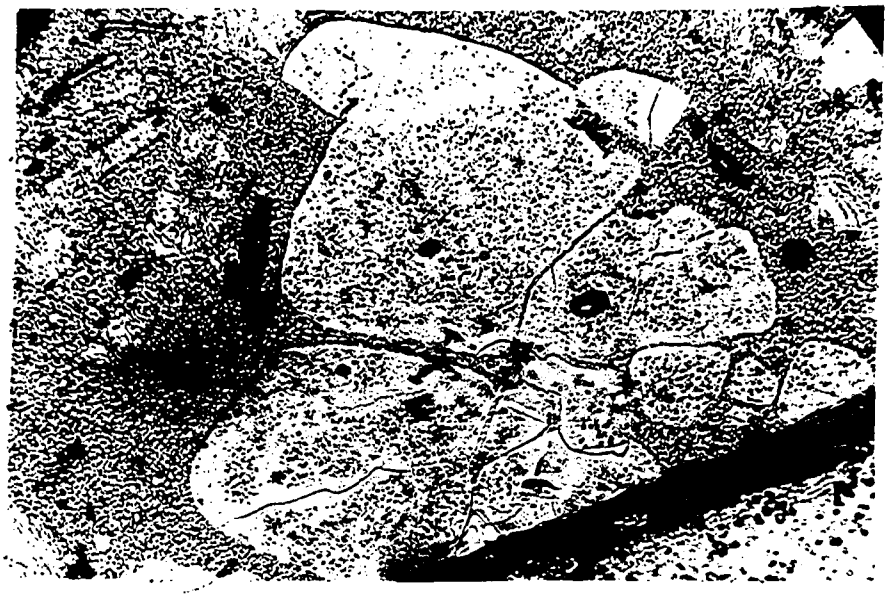

Fig. 39 Rounded, fractured quartz xenocryst in felsic matrix. with plagioclase laths and biotite. Submicroscopic inclusions in quartz are absent from rim and fractured zones; plane light, 120X, rhyolite porphyry sill S-70.

Fig. 40 Rounded polycrystalline quartz aggregate, with amphibole (?) and other inclusions in felsic matrix with plagioclase, biotite and opaques; X-nicols, 30X, rhyolite porphyry sill S-70.

Fig. 41 Quartz in elongate row, hornblende pseudomorphed by calcite (C) and opaques, also plagioclase and hornblende in felsic matrix, plane light, 30X, acid porphyry sill S-31.

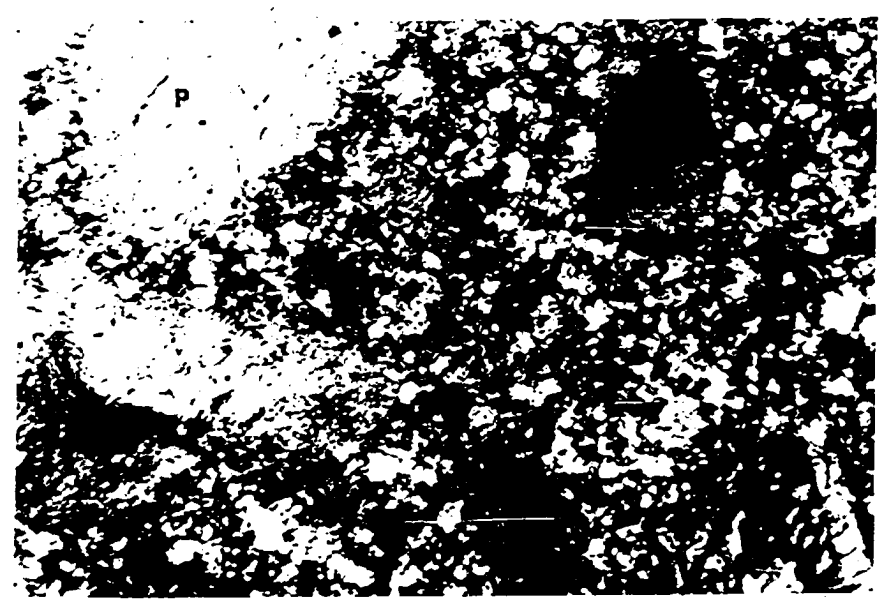

Fig. 42 Plagioclase (P), biotite in felsic matrix of alkali feldspar and quartz (grain size .1 mm. to .01 mm.); X-nicols 120X, rhyolite porphyry sill S-70.

Mafic trachytes, latites and other intermediate types

Nomenclature

This rock group includes these intermediate rocks which are called white porphyries or akerites (mildly alkalic latitic rocks) by Wolff (1938, p. 1612). He also calls the more acid types (p. 70) white porphyries. Weed (1899) termed them andesite porphyries, syenites and trachyte porphyries. In the map area they range from mafic trachytes to latites. The color index of the latites is about the same as the mafic trachytes. In thick intrusives such as Billie Butte phacolith, the rocks are mafic microsyenitic to micromonzonitic. Some unstudied samples may be andesitic.

Location

Within the map area these rocks are found as the upper and lower series of sills of the southwest trending sill--set, northwest-trending dikes and sills around Forest Lake, the lowest sills on the Robinson Anticline and Billie Butte laccolith. In the entire mountain range, according to Wolff, (p. 1013), these rocks and the quartz latites and granite (rhyolite) porphyries are common in a large area extending from the head of American Fork to the north end of the range, and from the eastern foot of the range around Big Elk Creek westward to the north-sloping summit. (North west of map area?)

Mineralogy

Megascopically they range from various shades of brown to light green and pink, nearly always with green pyrobole phenocrysts and greater or lesser amounts of cream to white feldspar phenocrysts. It is more common for the pyroxene-rich examples to have a pinkish matrix. The texture is usually fine-grained porphytic with a trachyitic groundmass. Many of these rocks are glomeroporphyritic.

The color index ranges from 17 to 29 for 16 examples, although near contacts the color index is as low as 11, due in part to replacement of pyrobole by chlorite and calcite. On the basis of the color index, this group appears to be distinct from the quartz latites and rhyolite porphyries. Other mineralogical differences are described below.

These intermediate rocks can be subdivided into two sub-groups on the basis of the predominating pyrobole and type of feldspar phenocryst. Though, on the basis of the normative Ab/An ratio and the Peacock variation diagrams (Fig. 96) this subdivision is not apparent.

The PYROXENE rich types are mainly mafic trachytes. These contain from 8 to 16 per cent AUGITE, usually zoned to AEGERINE-AUGITE rims and sometimes with some DIOPSIDIC cores. In the HORNBLENDE rich types (usually latitic), colorless to light green augite, occasionally with aegerine-augite rims, ranges from 0 to 8 per cent. Some is diopsidic (?). The pyroxenes are usually colorless to medium green and occasionally occur in aggregates. The

maximum c:Z' ranges from 45 to 58 degrees. In some examples augite has been converted to biotite, chlorite, magnetite and/or hornblende (Fig. 43,44). Schiller structure is sometimes developed. Wolff (pp. 1619, 1620) has given the detailed optical properties of these pyroxene. The pyroxene: hornblende ratios from 16 samples indicate a break between pyroxene and hornblende dominating subgroups.

The HORNBLENDE rich subgroup contains from 8 to 18 per cent hornblende, while the pyroxene rich type contains from 0 to 3 per cent hornblende. The hornblende has various shades of green to light brown pleochroism and is often zoned (Fig. 43,44). It occurs in aggregates and the maximum c:Z' ranges from 11 to 34 degrees. Wolff (p. 1621) cites a chemical analysis of the hornblende from akerite 31 07' as well as optical properties.

BIOTITE (0 to 8 per cent) occurs in various shades of brown to rare black or light green. It is sometimes zoned, and may contain apatite and sphene inclusions. The biotite is often associated with other mafics.

CHLORITE is usually a minor constituent, although in one phase of a composite sill it occurs as 9 per cent of a rock (587B). Near the contact of some sills (S 76A) complete replacement of the amphibole by chlorite and some calcite has occurred. The chlorite is light green to various shades of brown and is rarely colorless. Some of the chlorite has been identified as penninite. Occasionally sphene occurs as inclusions.

PYROXENE is in various states of conversion to hornblende, biotite and chlorite and reactions between hornblende; biotite and chlorite are evident by textural relations (Fig. 45,46). Magnetite and sphene are associated with the above reactions.

The PLAGIOCLASE and ALKALI FELDSPAR PHENOCRYSTS range from a trace to 25 per cent, generally less than in the quartz latites and rhyolite porphyries. There are some examples of coarser, less distinctive porphyritic types such as altered 587B. The plagioclase phenocrysts in the hornblende rich types are generally oligoclase-andesine (An 29 to An 49). The pyroxene types generally contain albite-oligoclase. Microperthite and anorthoclase (?) occur as phenocrysts in the pyroxene types (Fig. 47). Various twins, rims and other parts of phenocrysts take a light potassium stain, indicating significant potassium content. The stained part is often the altered part of the phenocryst, and the above test may not be a reliable indication of potassium content. More determinative work needs to be done on these feldspars, but it is difficult because of the alteration whose products include sericite, epidote, sometimes calcite and zeolite and rarely analcite.

The TRACHYTIC MATRIX consists of alkali feldspar and usually minor quartz. The entire matrix feldspars will usually stain for potassium but this test is not reliable on such fine and altered materials. In some samples such as S-112, with few phenocrysts, the matrix also contains calcic plagioclase (An 46). Albite, sodic oligoclase, orthoclase and microperthite, in various proportions, in the

matrix have been previously described by Wolff. The groundmass crystals range to a maximum of .6 mm. in length, but are usually much smaller. The matrix is usually turbid from alteration which makes mineral identification difficult.

OPAQUES are magnetite and oxidized products and range from over 1 to 8 per cent. They are usually anhedral, sometimes bimodal in size distribution and are often associated with other mafics and apatite. As much as 5 per cent QUARTZ occurs in the matrix of many samples except those with analcite.

A maximum of 5 per cent ANALCITE occurs in the lower part of Billie Butte syenite laccolith as clear, triangular interstitial patches and larger anhedral masses. In some cases the interstitial analcite has been zeolitized. Some of the analcite may be zoned (according to changes in relief) and clear interstitial analcite between turbid brown feldspar laths is striking. Analcite occurs also as a network replacement of feldspar phenocrysts on occasion.

The following minerals are fairly common as minor constituents. CALCITE occurs in several situations (Figs. 48,49,50). APATITE occurs rarely as aggregates near mafics or in calcite masses. SPHENE occurs as inclusions in biotite and chlorite, is sometimes associated with calcite and magnetite and occurs near pseudomorphs mentioned previously.

Wolff pointed out that these rocks have notable xenoliths of all sizes which contain various proportions of colorless and light green augite, green and brown hornblende, altered plagioclase, magnetite, apatite and biotite. Conversion of the pyroxene to hornblende and

biotite in these inclusions is similar to that which occurs to individual pyroxene grains in the host rock. Nockolds (1934) and Deer (1935, 1937) discuss the series monoclinic pyroxene to hornblende to biotite and modification of basic inclusions in intermediate rocks and acid rocks.

Tentatively, on the basis of a spot check on one dike and one sill, the mineralogical variation along these bodies is minor (compare S-78 and S-76, which are about 400' apart along strike). Quartz latite and latite (94 a, b) occur in one intrusive below Target Rock.

The composite southward dipping laccolith north of Beverley Peak has not been studies in detail but it appears to be composed of several phases of hornblende latite (?) and a highly altered (chloritized) pyroxene rich trachyte (587B). Other nearby sills rich in pyroxene are altered also while the hornblende latite phases are relatively unaltered (megascopically at least). It may be that the chloritization accompanied intrusion of the later (?) hornblende phases.

Intermediate types of the radiating dike set

In the radiating dike set intermediate rock types occur which are similar to those just described but they also have a number of differences. They are generally brown to gray, have negligible feldspar phenocrysts and contain noticeable zeolite and calcite amygdules (Fig. 51). Anhedral and euhedral hornblende xenocrysts and dioritic inclusions occur.

The hornblende types are similar to the hornblende latites previously described (p. 84) except for the brown color of the hornblende (should be verified on other samples besides 445c), abundance of chlorite, commoness of amygdules and less common feldspar phenocrysts in the presently discussed samples. The pyroxene rich types differ from the mafic pyroxene trachytes in that they are more equigranular, and sometimes contain more calcic feldspar (latitic to trachytic on the basis of plagioclase type and color index; examples 266, 297). They also have the same differences as listed between the hornblende kinds.

The chemical analysis of 445c indicates a close similarity to the other intermediate kinds. The significance of the similarity with respect to sequence of intrusion will be discussed (p. 143).

In addition, two or three thin blue and gray, fine-grained dikes occur in the Upper Shields River. They contain no phenocrysts and are grouped with intermediate types on the basis of general color and geographical association.

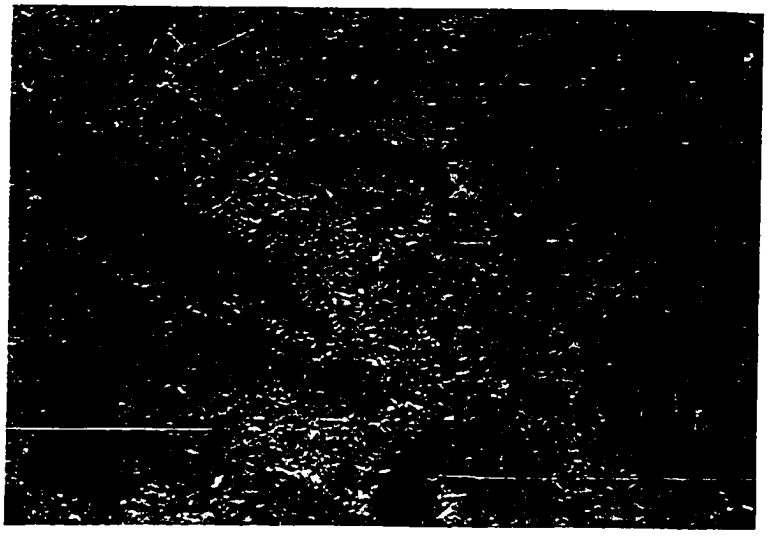

Fig. 43 Brown hornblende, biotite, colorless pyroxene (Px), magnetite, in a feldspar matrix; plane light, 30X, hornblende latite 112.

Fig. 44 Same as Fig. 43 above; X-nicols, 30X.

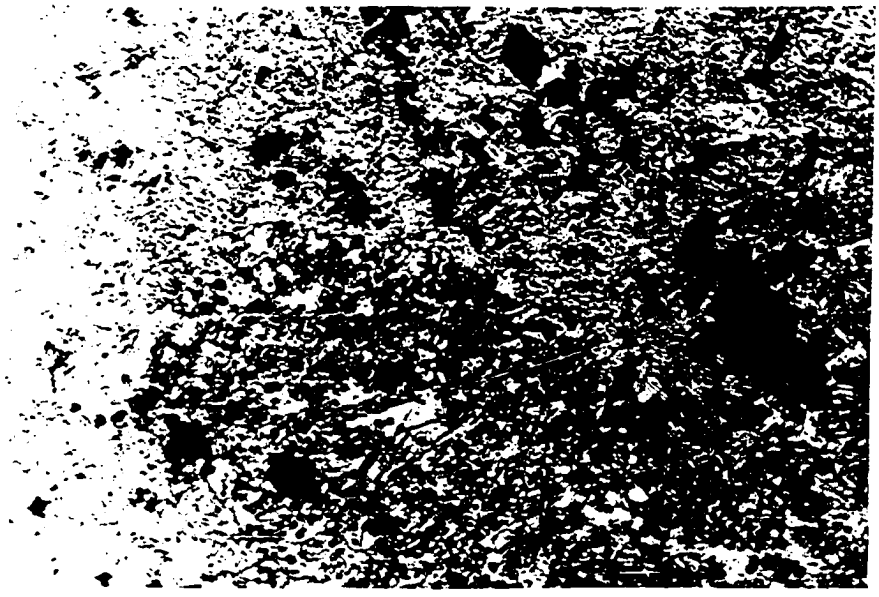

Fig. 45 Augite phenocryst replaced by chlorite, magnetite, biotite, calcite and feldspar; in matrix is hornblende, opaques and altered andesine-oligoclase; plane light, 30X hornblende latite 112.

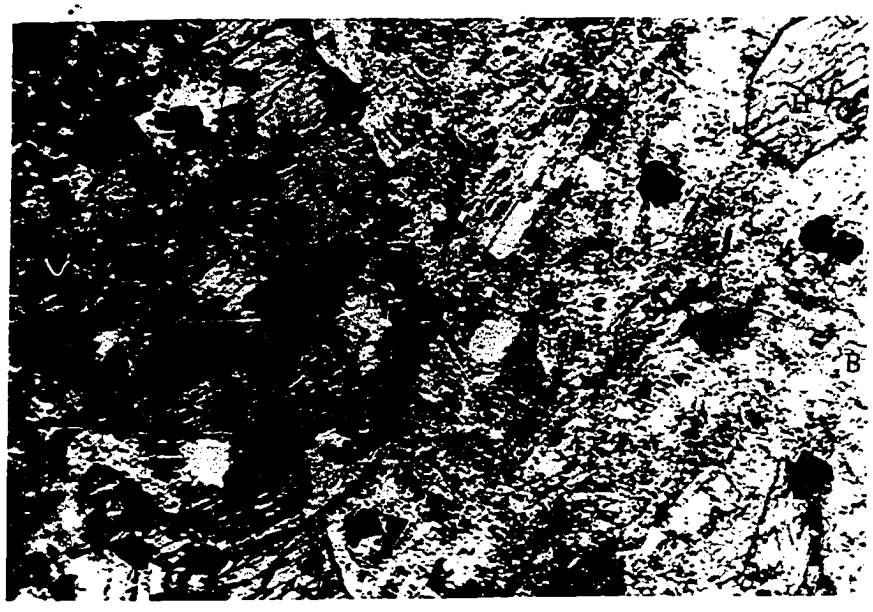

Fig. 46 Same as Fig. 45 above; at edge of pyroxene phenocryst (Px), partly replaced by green brown chlorite (Ch?), biotite (B) and magnetite; clear light brown hornblende (H), feldspar (F), calcite and biotite in groundmass; plane light, 120X.

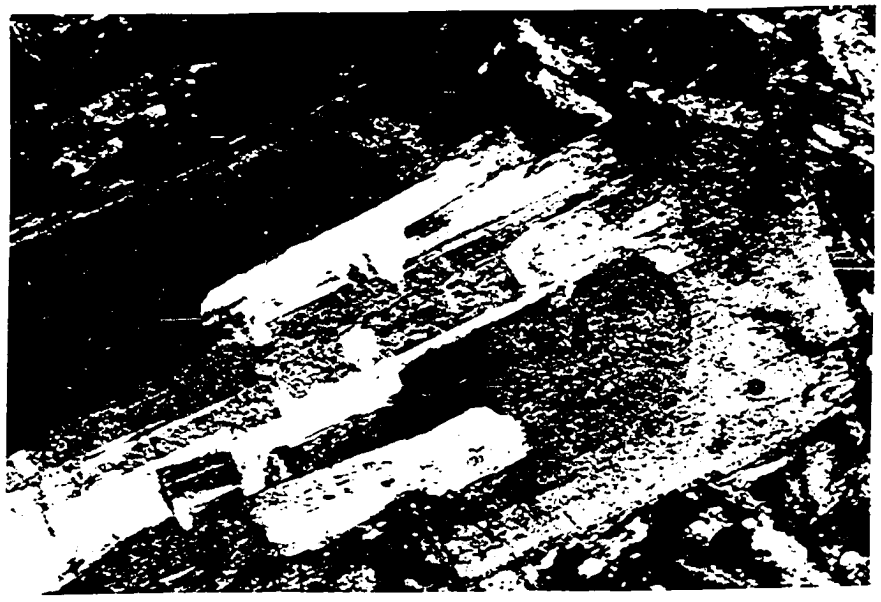

Fig. 47 Plagioclase phenocryst enveloped by zoned alkali feldspar which nicely stained for potassium. Degree of staining is slightly less intense toward rim but not definite enough to indicate that the potassium phase contains less potassium near rim. Replacement of the calcic plagioclase by the alkali phase indicated by texture; X-nicols, 30X mafic trachyte 383.

Fig. 48 Calcite amygdule rimmed with euhedral and anhedral quartz; amygdule is surrounded by biotite; X-nicols, 30X, hornblende latite 482.

Fig. 49 Calcite (C) partly pseudomorphing green hornblende, turbid feldspar laths, biotite with sphene inclusions; plane light, 190X, mafic trachyte, 515.

Fig. 50 Calcite selectively replacing altered alkali feldspar; X-nicols, 190X, mafic trachyte, 515.

Fig. 51 Calcite - zeolite (Z) amygdule in trachytic matrix, some holes in slide; X-nicols, 30X, hornblende latite 445c.

Basalt, andesite porphyry and lamporphyres

General statement

Three main mafic types occur in the map area besides the malignites, usually as dikes. They are basalts, andesite porphyries and lamprophyres. Only a few examples of these have been studied in thin section. Megascopically there appear to be a number of variants, and they will not be discussed in detail here. The reader is referred to the summary (p. 150), plate 2, and appendix on thin section descriptions for their essential description. As the intermediate dikes of the fanning dike set, all of these have been strongly propylitized (Figs. 52, 53, 54). Their field relations are complex and that aspect is emphasized in the following discussion.

Chloritized basalt

The basaltic types are black to brown porphyrites. The finer ones are distinguished by plagioclase and pyroxene phenocrysts (712b, Fig. 55) or only pyroxene phenocrysts (259). The latter appear lamprophyric megascopically. Some of the lighter colored examples may actually be andesitic (254). They contain labordorite-andesine, augite, biotite, chlorite and opaques, essentially. A few examples display abundant amygdules of calcite rimmed by chlorite (362, 365). Sample 366 contains a two inch quartzite inclusion. In 369 a multiple intrusive relationship is indicated between two basaltic phases. Samples 712a and 712b, taken respectively from the center and one foot from the contact of a 10-foot-thick bluntly terminated dike indicate

an increase in chlorite and biotite toward the contact. Some of the basaltic phases of the complex dikes contain one-inch felsic veins which trend parallel and perpendicular to the dike contacts (260b).

Wolff did not describe any rocks as being basaltic, though some of his thin sections have basaltic written on them. Although chloritized, the chemical analysis of 445b compares closely to some tholeiite basalts.

Andesite porphyries

The megascopic appearance of white to cream plagioclase laths in a gray to green matrix distinguishes the andesite porphyries. Rarely, these dikes can be traced along strike for two miles without any apparent change in composition. The essential characters of this type is indicated by description by 652a and 338a in the appendix. Essentially, they contain andesine - oligoclase, hornblende, augite, chlorite and opaques.

The finer contacts (260b) of the andesite porphyries resemble the basaltic contacts. A few intrusive contacts are chilled against basaltic phases, tentatively affording a time relationship. The contact of both phases appears chilled in 368, possibly indicating that the later phase was intruded at the sediment contact of the previous phase. A detailed study of these complex dikes in places of more complete exposure, along with a more complete microscopic study, may add important petrological information.

The uppermost-stratigraphic thin, propylitic basic sill 339,

terminates near the contact with andesite porphyry dike 343. These two bodies have similar petrologic features and probably are connected.

Lamprophyres

No doubt some of the lamprophyre dikes would be included in Wolff's discussion of dikes of camptonitic habit on the basis of location and prophylitization. Specifically, he termed one of these dikes an alkalic syenite and Sample 4507' as a camptonite. If anything the latter is closer to a minette-kersantite on the basis of Wolff's mode and chemical analysis. (Compare the chemical analysis to p. 352, Hatch, Wells and Wells, 1952). Other biotite lamprophyres occur occasionally throughout the map area, (see 442 and 547 in appendix). These contain augite, biotite, alkali feldspar, magnetite and calcite and zeolite. Sample 442 (Fig. 56) of the fanning dike set is transected by a latite sill. Sample 574 is an inclined lamprophyre dike transecting a malignite sill on the nose of the Robinson Anticline (Fig. 57). The dike contains a quartzite (?) inclusion. Quartz xenoliths in biotite lamprophyres are common and according to many workers give evidence of their origin (Turner and Verhoogan, 1960, p. 255). The latter workers suggest that these rocks could be derived by selective fusion of potassic minerals of granite and mica schist during reaction with the basic magma. Sample 459 represents an inclined lamprophyre dike which occurs just northwest of Forest Lake. The fact that most of the known lamprophyre dikes are inclined with respect to the vertical may have structural implications.

Fig. 52 Intersertal, replacement texture of chlorite, selective replacement of plagioclase, by chlorite (Ch) and opaques, biotite also in matrix; plane light, 120X, basalt 445B.

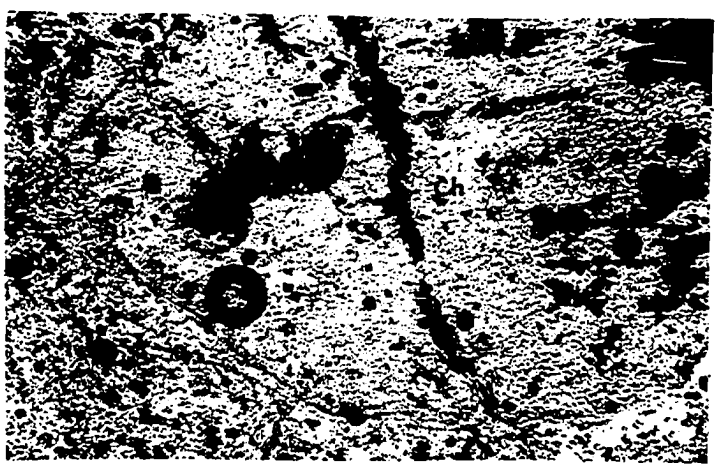

Fig. 53 Pseudomorph of chlorite (Ch) and opaques after pyroxene, plane light 30X, andesite porphyry 652A.

Fig. 54 Chlorite pseudomorphs after pyroxene and parallel chlorite veins in plagioclase; X-nicols, 30X, basalt porphyry 445B.

Fig. 55 Augites (Ag) and plagioclase phenocrysts with inclusions of biotite and fine opaques, matrix of plagioclase, opaques; plane light, 30X, porphyritic basalt 712A.

Fig. 56 Calcite which has been emplaced along the basal cleavage of biotite, no signs of replacement. The biotite layers are slightly bent to make room for the calcite, in matrix is alkali feldspar, zeolites, opaques and calcite (Ca); plane light, 120X, biotite lamprophyre, 442.

Fig. 57 Left side is edge of a biotite aggregate (aggregate has general outline of pyrobole), also some pyroxene in the aggregate, in matrix is potassium feldspar, calcite, opaques, apatite, also partly chloritized pyroxene phenocrysts; plane light, 120X, biotite lamprophyre 574.

Feldspathoid syenite, trachytes and textural variants

Nomenclature

The rocks discussed in this section are among the most felsic and are undersaturated to slightly oversaturated in silica. They include rocks that were termed by Wolff (1938) as nepheline syenite, soelvsbergite, bostonite, alkali syenite and syenite porphyry. The chemical similarity of these types is indicated by Fig. 111. In this map area they consist of feldspathoidal syenite, trachyte and variants including rare rhomb porphyries. Pegmatite pods that occur in the feldspathoidal syenites are discussed separately in this section.

Location

These rocks occur in the Crazy Mountains as a number of separate intrusions in an area that extends westward from the Lebo Mountain Stock to west of Three Peaks and from the Upper Shields River to the Musselshell River on the north (Fig. 2). They are described by Wolff under sections on the laurvikite of Comb Creek (the laurvikite itself is more equivalent to the mafic syenites), nepheline syenite, soelvsbergite and bostonite.

Within the map area, the group is represented by the feldspathoidal aegerine-augite syenite of Target Peak laccolith, the aegerine-augite syenite of Virginia Peak laccolith, a thin aegerine-augite trachyte porphyry dike nearly concordant with the axis of the Robinson anticline and three thin rhomb porphyry intrusives, one of which occurs along the axis of the Robinson anticline and the other two just at the north edge of the map area.

Mineralogy

These rocks range from gray and light green to medium green with conspicuous pink alkali feldspar phenocrysts where finer grained. They are fine-to medium-grained porphyritic, with a trachytic groundmass of feldspar and aegerine-augite. A wavy foliation occurs, in 680A, at a vertical contact between two igneous bodies near the axis of the Robinson anticline.

The color index ranges from 6 to 17. Ferromagnesian minerals consist almost entirely of acicular, colorless to brown-green to green pleochroic AEGERINE-AUGITE with AEGERINE rims or aegerine, (Fig. 58). Sometimes the pyroxenes occur in loose aggregates and they are rarely chloritized. A rare OLIVINE aggregate occurs in S-135. The olivine is colorless and is successively surrounded by MAGNETITE, SERPENTINE, BIOTITE and numerous aegerine-augite crystals similar to occurrences in the malignites (see later discussion of this feature in relation to the malignites). One or two other biotite grains occur nearby and are also rimmed by numerous aegerine-augite crystals. The texture indicates that in the above two cases the pyroxene is not a reaction product of the biotite but is an accumulation due to another process. Minor OPAQUES, including their oxidation products, occur.

ALKALI FELDSPAR makes up to 53 to 94 per cent of these rocks, the wide range being due to zeolitization. A maximum of 38 per cent is phenocrysts. The feldspar consists mainly of microperthite (100u-5u in size), and albite (Fig. 59). Wolff (p. 1618) cites a chemical

analysis of one of the phenocrysts and discusses the feldspar optical properties. He describes the feldspars as "anorthoclase", which are sometimes mottled by albite patches or zoned and which commonly have a periphery of albite. In a classification based on optical properties and chemistry (Tuttle, 1952b), the feldspar is of the orthoclase-low albite series. Near intrusive contacts where the rock is more distinctly porphyritic, the phenocrysts are optically homogenous (although they may stain irregularly) with distinct Carlsbad twinning. (Many anorthoclases are cryptoperthitic; Deer, Howie and Zussman, Vol. 4, 1963, p. 61). A vague grid twinning is rarely developed in parts of phenocrysts. In optically homogenous parts of phenocrysts, the estimated 2V varies from 60 to 70 degrees. A turbid brown alteration occurs, similar to that in the Pilansburg foyaites (Figs. 60,66). Alteration and potassium stain often conform to twin boundaries indicating compositional difference. As Wolff observed, the albite phase is usually concentrated near the rim of phenocryst. The rim of the albite failed to take the sodium rhodizonate stain for calcium, indicating less than 3 per cent anorthite molecule (Bailey, Stevens, 1960, p. 1020). Using Wolff's analysis of the feldspars mentioned above and the mode of 459, a computed chemical analysis compares favorably with the chemical analysis of the rock (Table 1).

In Target Peak laccolith, usually less than 4 per cent NEPHELINE occurs. It is clear, anhedral and invariably rimmed by sodalite alteration (Fig. 61, 62). Both of these minerals are more common in the associated pegmatites (p. 108), although a more com-

plicated alteration product occurs there. The sodalite is nearly always isotropic and is light yellow, but is sometimes turbid pink in thin sections. As in the pegmatites, the sodalite was confirmed by the HNO_3 test, producing NaCl crystals on the sodalite surface. Square and six-sided polycrystalline pseudomorphs of zeolite (?) after analcite-leucite (?) are usually associated with the nepheline (Figs. 61, 62,63).

ANALCITE is more common than nepheline, comprising up to 6 per cent by volume of many samples. It is most often clear and interstitial (secondary?). Near the contacts, primary six-sided and four-sided outlines of primary analcite (?) are prominent. These are replaced by calcite, less often by zeolite and rarely by chlorite at the intrusive contact (Fig. 64). Elsewhere they are usually replaced by a polycrystalline mosaic of zeolite (?) which ranges in size from .1 to .01 mm. (negative potassium stain) and sericite (?). In the finer grained examples, aegerine needles parallel the cleavage direction in the analcite and light brown and dusty purple sodalite partly replaces the analcite (Fig. 65). Occasionally in the clear analcite, a complex twinning is developed and is reminiscent of that which occurs in analcite in the pegmatites.

Often the feldspars are highly zeolitized, zeolitic feldspar accounting for 20 per cent of the rock in some cases. APATITE, CALCITE and SERICITE are common in minor amounts, while SPHENE and CANCRINITE are rare. Wolff (p. 1611) also reports NATROLITE, BROWN HORNBLENDE (rare), NOSELITE and in one of the sills "considerable primary quartz".

Table 1

	Chemical Analysis of 499	Computed Composition of 499
SiO2	62.77	59.76
TiO2	.24	
Al2O3	18.22	19.83 + Fe
FeO	.35	
MnO	.03	
MgO	.21	
CaO	1.09	.55
Na2O	8.43	8.04
K2O	4.91	4.17
H2O+	1.10	
H2O-	.29	
P2O5	.43	

Used an average composition of aegerine in these computations (Deer Howie and Zussman, 1963) and Wolff's (1938) analysis of "anorthoclase". See Plate 2 for the mode.

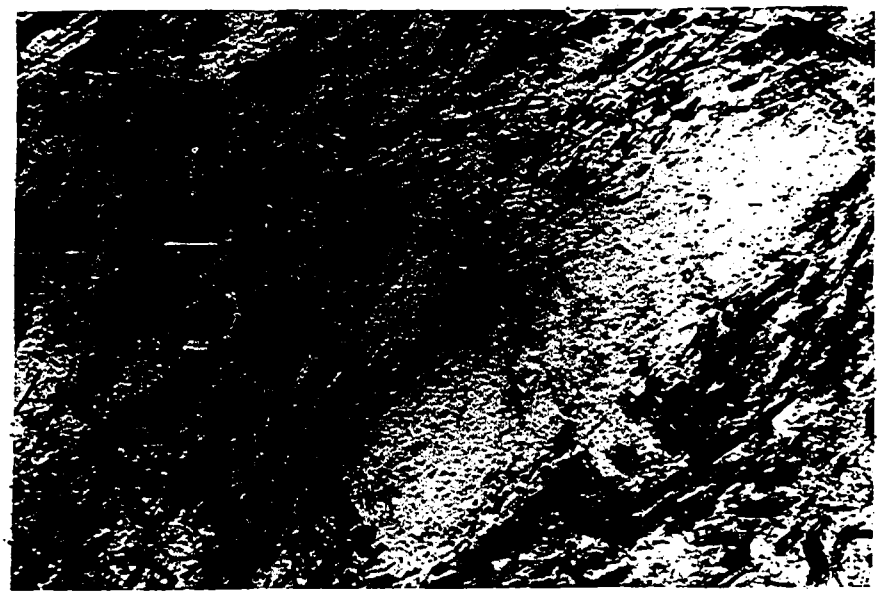

Fig. 58 Alkali feldspar phenocrysts and matrix, aegerine needles; plane light, 30X, aegerine trachyte porphyry 498.

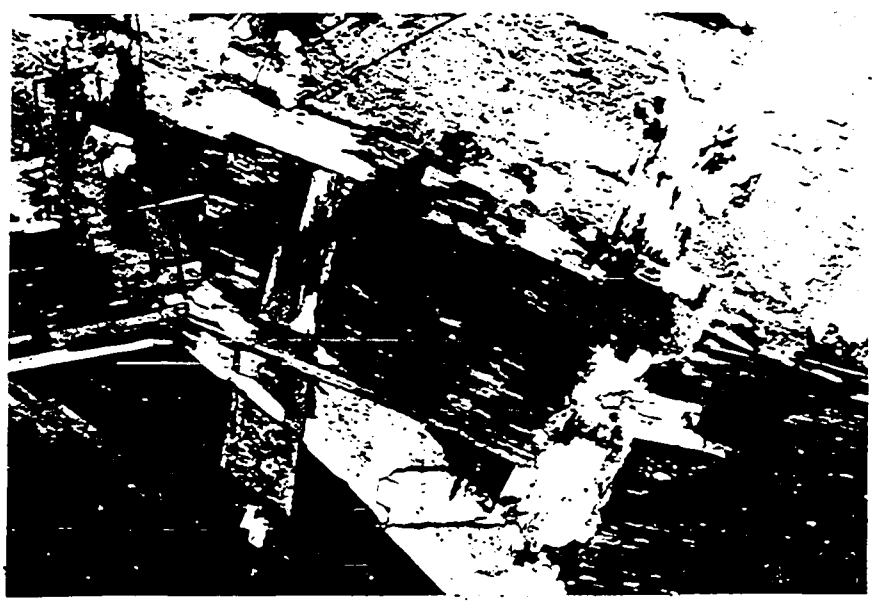

Fig. 59 Microperthite texture, black interstitial areas are clear analcite. Compare with the texture of the white foyaite of the Pilanesberg Complex (Retief, 1964, p. 502) feldspathoid syenite S-116.

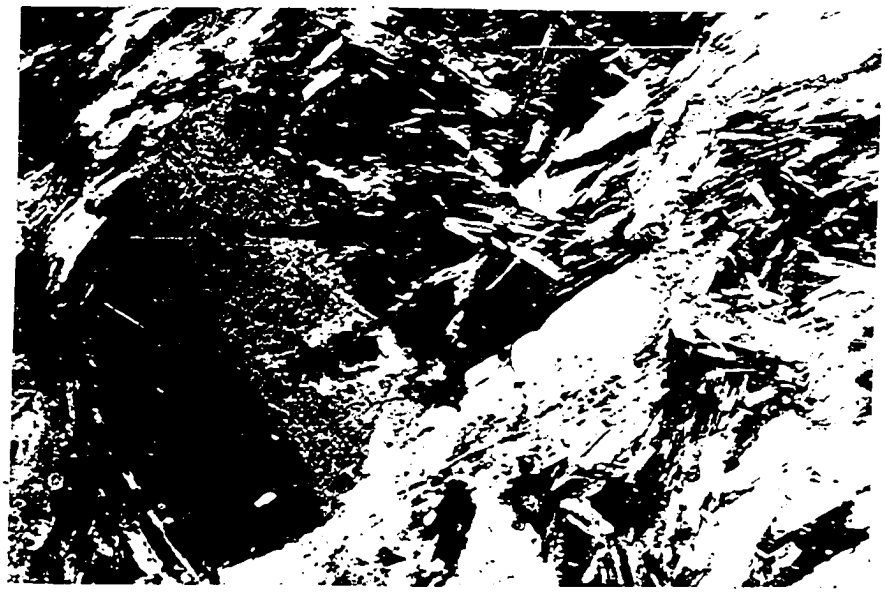

Fig. 60 Alkali feldspar; X-nicols, 30X, aegerine trachyte porphyry S-15.

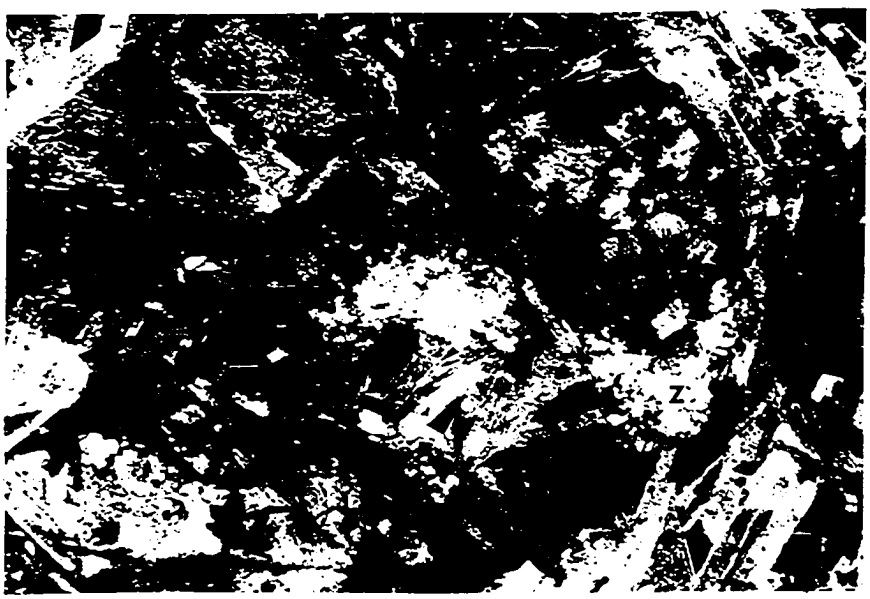

Fig. 61 Aggregate of subhedral nepheline (N) and polycrystalline zeolite (?Z) which are pseudomorphs after analcite or leucite (?) nepheline is altered on rims to brown (megascopically pink) isotropic sodalite; aegerine and alkali feldspar are also in aggregate, alkali feldspar surrounds the aggregate; X-nicols, 30X, Target Peak feldspathoid syenite S-142.

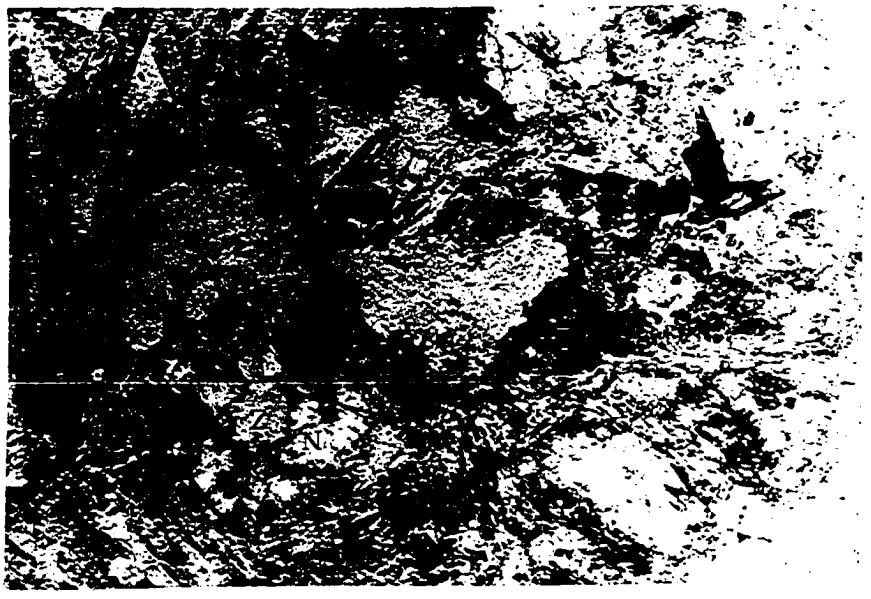

Fig. 62 Same as Fig. 61, feldspar is turbid, the nepheline (N) is clear with dark edges and the zeolite (?Z) is clear.

Fig. 63 Polycrystalline zeolite (?Z) pseudomorph after analcite (?) or leucite in contact with sodalite (S), alteration of nepheline (N), aegerine and turbid perthite (F); plane light, 30X, Target Peak feldspathoid syenite S-142.

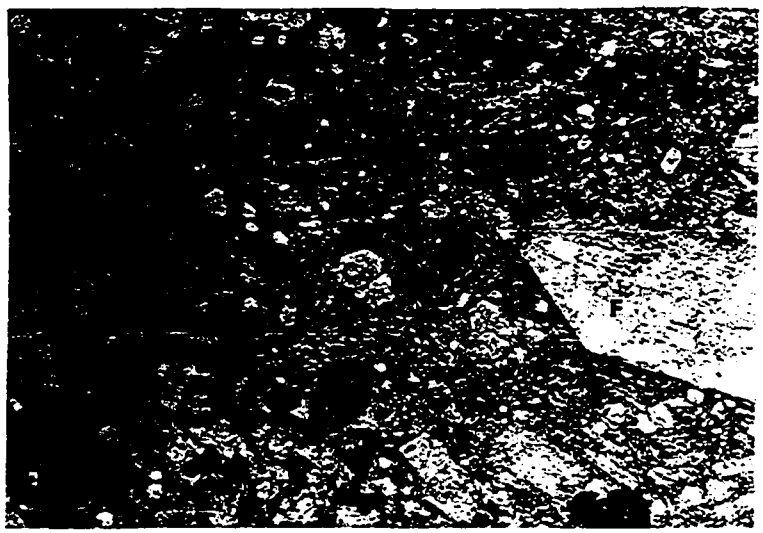

Fig. 64 Pyroxene replaced by chlorite (Ch); nepheline and analcite replaced by calcite (Ca); zeolitized feldspar(F) phenocryst; plane light, 30X, at lower contact of Target Peak feldspathoid syenite S-61.

Fig. 65 Edge of analcite (An) phenocryst, aegerine microlites parallel the cleavage, turbid alteration in analcite, alkali feldspar (F) and aegerine matrix; plane light, 30X, trachyte porphyry 705.

Pegmatite pods of Target Peak feldspathoid syenite

Four or five coarse grained pegmatite pods have been found near the top of two benches of Target Peak laccolith. In some respects these pods are similar to those which occur in the Bearpaw Mountains nepheline syenites and related rocks (Pecora, 1942). Sometimes they are 1 foot to 3 feet in cross-section with feldspar and aegerine often elongate at right angles to an abrupt border. In general, they contain the same minerals as the feldspathoid syenites, however the nepheline, sodalite and analcite are often more abundant in the pegmatites.

AEGERINE occurs as prisms and radiating fibrous aggregates, and is pleochroic brown-green to green, sometimes only slightly zoned, elsewhere it contains aegerine-augite cores. The radiating fibrous aggregates are usually surrounded by analcite. Nearly submicroscopic light green and colorless aegerine prisms occur in most altered minerals.

ALKALI FELDSPAR is the predominant mineral and occurs as laths about one centimeter long. It is altered to a microperthitic intergrowth of zeolite and feldspar, according to a composite diffractogram (Fig. 67). Alternating laminae take the potassium stain. Feldspars are usually turbid, often due to very fine aegerine and other replacement products including numerous minute apatites. One interference figure (low 2V) has been obtained in the homogeneous center of one of these feldspars which is perthitic toward terminations, but the high

2V nature of the feldspars from the syenite and one unaltered pegmatite pod from the talus indicate that the low 2V figure may have been from zeolitized material.

Euhedral to subhedral clear NEPHELINE occurs in the pegmatites. The nepheline has two directions of imperfect cleavage (Fig. 68). Invariably the nepheline is marginally converted to a zoned light yellow to orange, rarely dusty (deep red to pink megascopically) alteration product.

Edgar (1965) concluded from diffraction studies that many of the alterations (those mostly pink) of nepheline are mainly natrolite. Less commonly, it is mainly analcite or chlorite or mica, or plagioclase and/or nepheline. A different situation occurs in the Target Peak pegmatites therefore some detail on the alteration product is given below.

The lighter yellow part of the alteration product appears to be isotropic in a few places (SODALITE?) and is gradational or in sharp contact with light orange to brown birefringent parts which are uniaxial positive and negative in various areas. A slab treated with HNO_3 until dry produced NaCl cubes regularly distributed across the colored material. In addition, minor prismatic $CaSo_4H_2O$(?) crystals formed rarely in vein-like areas in the material in radiating groups of fibers. These tests indicate a Cl and SO_4(?) bearing substance such as sodalite or cancrinite. This contrasts with the fine-grained nepheline syenite in which the usually isotropic sodalite was only covered by

NaCl crystals only (in single test). Aegerine-augite microlites also occur in the material. The index of refraction of the more common birefringent material is about 1.51-1.49, a little above common sodalite and natrolite but similar to cancrinite. A methyl blue stain test was negative on the anisotropic part but distinctly positive on the isotropic parts. This latter test negates nepheline, sodalite, analcite and natrolite for the anisotropic part. It is probably not cancrinite (see appendix). This leaves the main alteration product unidentified though the isotropic part may be sodalite. The anisotropic part is probably not natrolite such as Edgar has described though, natrolite (colorless) is a common nepheline replacement product in the malignites.

ANALCITE occurs as triangular clear areas between feldspar laths. It displays various intensities of complex twinning and birefringence and probably includes other zeolites. Some of it may actually be non-cubic analcite. Two determinations of very slightly birefringent material indicates a constant 1.490 ± .002 index of refraction. Two cleavages at right angles are developed. The zeolitized parts contain very fine aegerine, causing a megascopic green cast in the mineral.

SERICITIC alteration, CALCITE and OPAQUES, including MAGNETITE and oxidized products, are minor. Two other unidentified minerals occur rarely (see appendix for some properties).

Fig. 66 Microperthite phenocrysts with turbid brown rims in matrix of fine grained microperthite and aegerine-augite prisms; plane light, 30X, Virginia Peak aegerine trachyte porphyry (459) 499.

Fig. 67 Perthite-like zeolization of alkali feldspar; alternating laminae take stain for potassium; zeolitized analcite between lath outlines in lower right hand corner; plane light, 30X, Target Peak nepheline syenite pegmatite S-118.

Fig. 68 Nepheline alteration controlled by two directions of cleavage; unidentified alteration product and light sodalite (?So), alteration; aggregates of fibrous aegerine; plane light, 30X, Target Peak nepheline syenite pegmatite S-118.

Fig. 69 Slightly altered alkali feldspar and plagioclase phenocrysts in trachytic matrix; chloritized biotite also in matrix; X-nicols, 30X rhomb porphyry, S-26.

Mineralogy of rhomb porphyries

The few rhomb porphyries consist of altered POTASSIUM FELDSPAR and PLAGIOCLASE (?) phenocrysts 5 cm. long in a trachytic groundmass of altered ALKALI FELDSPAR, AUGITE, BIOTITE, OPAQUES and CHLORITE (Fig. 69, 70). Sample 578 is the only example studied in detail. Tentatively they appear to be somewhat similar to some samples of rhomb porphyries from Oslo, Norway, the type area. If so they are the only plagioclase containing rhomb porphyries reported outside the Oslo area (Oftedahl, 1946).

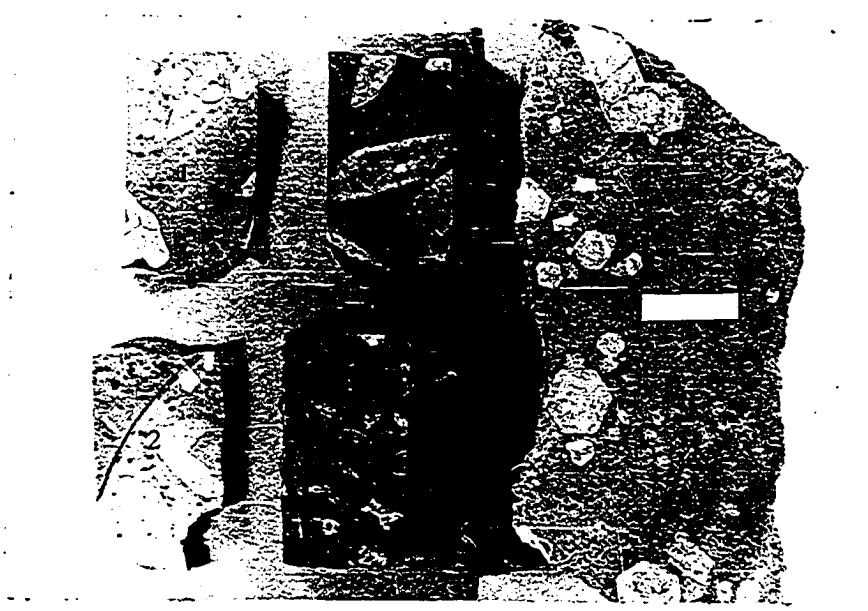

Fig. 70 Rock slabs 1, 2, 5 are respectively rhomb porphyries 188, 188b, and 678 from the northern Crazy Mountains. Rock slabs 2 and 3 are rhomb porphyries from the Oslo, Norway Petrographic Province.

Mafic and intermediate alkaline rocks-malignites

Nomenclature

This group includes those mafic and intermediate alkaline rocks that consist mainly of variable amounts of clinopyroxene, alkali feldspar, nepheline, olivine, biotite, and zeolite. They have been called theralites by Wolff (1938), soda-shonkinites by Larsen (1940), malignites by Hatch, Wells and Wells (1952) and classified tentatively with the nepheline syenites by Johannsen (1938). Johannsen (1938, vol. 4, pp. 1605) has also given a short and inaccurate review of the petrographic nomenclature of these rocks.

The writer prefers the designation malignite because the present usage of the term theralite does not fit these rocks mineralogically, and does not correspond with shonkinites either chemically or mineralogically. Theralite usually contains significant plagioclase, and shonkinites usually have orthoclase as the predominating leucocratic mineral and more potassium than sodium. This group of rocks from the northern Crazy Mountains have none of these characteristics. They correspond best to malignites mineralogically and chemically, in fact Wolff described one sample as malignose on the basis of the C.I.P.W. norm classification. Essentially a malignite is composed of about half aegerine-augite and varying proportions of nepheline and orthoclase, usually about equal amounts.

Location

With few exceptions, those rocks occur only in the northern Crazy Mountains, from the Upper Shields River northward to the Musselshell

River where they occur as about six large laccoliths and numerous sills and dikes (Wolff, p. 1606). Twelve miles to the south of the map area the thick Theralite Butte laccolith occurs (Fig. 2). Within the map area (Plate 1) these rocks predominate on the Robinson Anticline in a phacolith, laccolith and numerous sills and dikes. To the east, several dikes occur in the northwest trending dike set, near Forest Lake.

MINERALOGY

These rocks are dark green to gray-green, with large prisms of pyroxene which often weather out in relief. A pink sodalitic alteration product of nepheline sometimes is megascopically visible. The texture ranges from fine to medium-grained hypidiomorphic to fine-grained porphyritic near intrusive contacts and in thinner dikes and sills. The clinopyroxenes have subparallel orientation especially near intrusive contacts (Fig. 71).

The malignites have a wide compositional range as is evidenced by the range of specific gravities from 3.03 to 2.65 (most commonly from 3.03 to 2.81), and the range of the volume of mafic minerals from 85 to 23 (more commonly 85 to 47).

The PYROXENE consists of (diopsidic) augite zoned toward rims of aegerine-augite and aegerine (Fig. 72). These crystals are up to 6 mm. long but usually less than 3 mm. This mineral is pleochroic, colorless, mainly light and medium green but also yellow-green and brown. The compositional zoning usually is indicated by greener

rims, but in rarer cases zoning can only be recognized under crossed nicols. Color zoning appears to be gradual generally, but also abrupt in many cases. Perfect euhedral outlines of aegerine-augite, surrounded by aegerine, is observable (627D). In some instances a crystal will appear to have gradational zoning in one crystalographic direction and abrupt zoning in another. Zoning is often abrupt on terminations. The thickness of the aegerine rims varies significantly on various parts of crystals. Dike 645 has augites with extremely narrow green rims and the matrix contains abundant aegerine needles. In some samples (577) fibrous radiating aggregates are very common (Fig. 73,74). This aegerine is colorless to medium green to brown, gray translucent and opaque.

Rarely, a thin zone of biotite occurs between the augite and aegerine-rich rims, and augites surrounded by large biotite plates are without aegerine rims. In 627D, a biotite edge conforms to the boundary between augite and aegerine-augite (Fig. 72) indicating that the biotite and aegerine crystallized at about the same time. In the Great Cliffs laccolith and the Great Anticlinal phacolith, the aegerine-augite and aegerine are intergrown with katophorite (Fig. 75). Inclusions are biotite, magnetite and less often apatite and zeolite. Multiple and simple twinning is common in the pyroxene. In 643, where a particular augite grain and an olivine grain are in contact, there is no aegerine developed on the augite and no biotite on the olivine. Elsewhere biotite surrounds the same olivine and aegerine surrounds the same augite. In the base and top of the Great Anticlinal laccolith, aggregates (about 1.2 cm. across) of smaller (5 mm.) pyroxene crystals occur. These are without aegerine-augite rims. Occasional

green centers occur. Green zones also occur around inclusions of zeolite and along cracks in pyroxenes (Fig. 76). Wolff (p. 1619) cites a chemical analysis and optical properties of a nearly homogenous augite from his sample 101 07'. Pyroxene varies from 60 to 14 per cent within these intrusives. In the almost leucocratic of these rocks (577), the pyroxene, is almost entirely aegerine-augite and aegerine.

OLIVINE and pyroxene are concentrated in the middle concordant bodies of the Robinson anticline. Olivine content ranges from a trace to 20 per cent from body to body. Within the Great Anticlinal laccolith olivine ranges from a trace to 9 per cent, increasing toward the upper and eastern parts of the body. The olivine is colorless, often elongate and up to 3 mm. across. It is altered initially along cracks, and peripherally. Rare serpentine and magnetite occur in these cracks and marginally. These in turn are surrounded by biotite (Fig. 76,77). The olivine occurs within various stages of complete replacement within one sample such as Dike 643. Minor clinopyroxene was noted by Yagi (personal communication, 1965) to rarely rim the olivine in 704F. Magnetite and sometimes aegerine are inclusions. Olivine 643 has BETA equal to 1.670 ± .002 and GAMMA equal to 1.686 ± .002, (10 per cent Fa), and d_{130} equal to 2.7775 (13.5± 4 per cent Fa). This Fa content is typical for picrites and olivine nodules; Fa content for THERALITE rocks is usually in the range of Fa 80 to Fa 58 (Deer, Howie and Zussman, p. 25, 1962).

BIOTITE varies from 4 to 21 per cent in these rocks. It ranges from sometimes colorless centers to light brown, to yellow-brown, to red-brown, to black. The rims are usually zoned darker (Fig. 78). These darker borders on occasion extend irregularly into the centers and fan-shaped zones of darker colors occur rarely. Sometimes two or three dark zones occur within a phenocryst. Apatite and a rare red and green unidentified mineral occur as inclusions. In 224 the biotite contains zeolite, pseudomorphic after nepheline (?) (Fig. 78). Spikes of aegerine rarely outlines the biotite margin. More often biotite is intergrown with green and brown aegerine-augite and hastingsite. In 577 biotite is euhedral with sanidine (Fig. 79, 80). Red-brown biotite pseudomorphs replace augite (Fig. 82). X-ray fluorescence indicates high barium (confirming Wolff's barium test, 1938, p. 1623) and significant titanium in the biotite. Mineral association and colorless centers indicate the biotite is phlogopitic.

Magnesium HASTINGSITE occurs only in two thick concordant intrusives (1 to 9 per cent in the Great Anticlinal phacolith and at least 1 per cent in the Great Cliffs sill), (Fig. 75). It occurs as prisms usually intergrown with aegerine and biotite, and as radiating fibrous aggregates. It is pleochroic including various shades of brown, including liver-brown to light blue-green, and contains inclusions of apatite and zeolite and curious, radiating, fibrous, colorless needles next to an augite border in 704E. In 627F, hastingsite occurs in channels in olivine. Wolff (p. 1620) cites a

chemical analysis and detailed optical properties of this amphibole. Deer, Howie and Zussman (1962, vol. 2) following Miyashiro (1957) have reclassified this amphibole as magnesio-kataphorite.

Unzeolitized ALKALI FELDSPAR occurs as up to 13 per cent of the rock (577) or up to 20 per cent including slightly zeolitized feldspar (598). Usually much less unzeolitized feldspar occurs. Tentatively three types of feldspar are present including sanidine and other two types of alkali feldspar.

SANIDINE occurs in some thinner dikes and sills and in leucocratic segregations. It has a 2V of about 10 degrees (estimated) with BETA equal to 1.530 $\pm$ .0002 and ALPHA equal to 1.528$\pm$ .002. It is euhedral to anhedral, (especially euhedral in the segregations) clear but often with turbid brown streaks, and displays poor to good cleavage (Fig. 80, 83, 84). The sanidine often contains natrolite pseudomorphs after nepheline. A diffractogram indicates either zeolite contamination or a triclinic phase in this feldspar separation. The first suggestion is preferred as thin zeolite veins transect the freshest feldspar making perfect separations difficult.

An alkali feldspar with a 2V of less than 60 degrees occurs occasionally in several sills and laccoliths. (That of 598 has a slight grid twinning and is perthitic). This feldspar may correspond to the "orthoclase" (2V=54°) of Gordon's Butte which Wolff analyzed chemically and optically (p. 1617). In order to classify the feldspar according to modern terminology the chemical analysis and optic properties have been compared to Tuttle's (1952 and 1952b) diagrams

comparing the ratio Or/An +Ab versus 2V and versus indices of refraction. In the comparison Ce 8 was ignored and recalculation to 100 per cent was made giving Or 73 Ab 15 An 10. These data compared favorably to Tuttle's two diagrams. Gamma is .002 high and is the only real inconsistency. This comparison placed the feldspar in the orthoclase - low albite series with the microperthite of the feldspathoid syenites (p. 101).

Comparison was also made with Oftedahl's (1948) diagram relating the ratio Ab:An:Or to $\frac{1}{2}(\alpha+\gamma)$ and A angle X. A angle X is reasonable but the indices of refraction are too low. This poor comparison may be due to contaminating elements (Ba, Fe, Rb, Sr) (Deer, Howie and Zussman, 1963, p. 61) or because the feldspar is a partially unmixed cryptoperthite. The last season is preferred because the contaminating elements if anything would increase the index of refraction.

In addition an alkali feldspar with a 2V larger than 60° also occurs in minor amounts in many intrusives.

NEPHELINE occurs as euhedral and subhedral, clear to turbid crystals with moderate cleavage. In some fresh appearing samples (577) nepheline has been completely replaced by zeolites although other minerals are not altered except some augite. Seven mineral separations displayed no nepheline according to diffractograms (in 577). Elsewhere in more altered samples (598) the nepheline is marginally replaced by pink sodalite similar to that which occurs in the aegerine syenites. The nepheline occurs poikilitically

enclosing augite or euhedral with augite. Nepheline (pseudomorphed by zeolite ?) is often enclosed in sanidine and biotite. The writer observed 11 percent nepheline as a maximum in these rocks, but usually there is much less. Wolff observed 15 per cent nepheline in unzeolitized samples from the Great Anticlinal laccolith and 25 per cent from a body in the Shields River Basin. He cites optical properties of the nepheline (barium containing), (p. 1622) and noted up to 21 per cent of a primary sodalite group mineral occurring poikilitically in feldspar. These high concentrations occur in intrusives west and north of the present map area.

Rosenbush (1887, p. 250) noted that in a sample from the Three Peaks area all of the nepheline and orthoclase has been completely transformed to zeolites (Fig. 84,85). The nepheline is more completely zeolitized than the feldspar and usually the coarser grained samples are least zeolitized. The zeolite is mainly natrolite (X-ray, D.T.A.).

In 577 NATROLITE occurs as 56 per cent of the rock. Here it displays a multiple twinning unusual for natrolite. The twinning may allow for less volume change in zeolitization of nepheline. A diffractogram indicates a single phase and compares well with the diffractogram of 2" and 2" zeolite veins that cut the malignite sills.

ANALCITE occurs as a primary (?) and secondary mineral. It appears interstitially and in leucocratic segregations (p. 123).

Accessory minerals are APATITE, SERICITE, SODALITE, CALCITE,

SPHENE, SERPENTINE, IDDINGSITE, (CANCRINITE ?) and an unidentified red translucent anhedral mineral. Apatite occurs in most samples. An almost submicroscopic, micaceous, moderately birefringent mineral has been tentatively identified as sericite. Cancrinite was searched for but not positively identified. Zeolitized pink and blue speckled sodalite occur occasionally. Some represents altered nepheline. A moderately birefringent zeolite may indicate Thomsonite (?). Another replacing zeolite (?) has an index of refraction higher than 1.56 (unusual for a zeolite). Calcite is more common than sphene. A red translucent anhedral alteration product occurs in many samples. In 1/3 of the slides studied in detail narrow rims and veins of serpentine occur on the olivine. The serpentine is yellowish brown to greenish brown. Orange to red-brown iddingsite is rare.

Opaques include MAGNETITE and oxidized products and PYRITE replaced by LIMONITE. These are anhedral to euhedral. The magnetite is often associated with olivine, biotite and pyroxene. Opaques occur up to a maximum of 3 per cent.

The remnant magnetization of these rocks is moderately strong. The magnetic vectors are strongly scattered in analyzed samples. A.C. demagnetization did not improve the scatter. The magnetite scatter is in part due to alteration.

Leucocratic segragations in malignites

In several malignite sills and dikes (655, 666, x-25, 707), irregular, medium-grained, leucocratic segregations are very common. They have a maximum width of 3 mm. and usually are less than 5 mm. long. Some are very irregular while others are lensoid and spherical. They are usually elongate parallel to intrusive contacts. The segregations are composed mainly of zeolites, (including ANALCITE and SANIDINE. AEGERINE, BIOTITE, rare OPAQUES, CANCRINITE (?) and CALCITE also are present (Fig. 86).

Some of the zeolite may be NATROLITE. Megascopically pink CHABAZITE -GMELINITE occurs. Analcite is euhedral to anhedral, with aegerine inclusions. The sanidine is euhedral, tabular, and is altered to zeolite. It has parallel extinction in many cases, turbid brown inclusions and moderate cleavage. The biotite is zoned from various shades of brown to black. Opaques are rare and anhedral. Lath cancrinite (?) may be the best example of cancrinite occurrence in all of these rocks. The dark green aegerine occurs in fibrous aggregates.

At 223, a one-foot segregation or vein of natrolite with books of biotite occurs. In malignite sill 219, one-inch zeolite veins are parallel to a nearby transecting lamprophyre dike.

These examples probably represent late-stage magmatic differentiates; though the sanidine in some may indicate rather high temperatures. The irregular segregations could be cognate xenoliths, while the veins may represent late-stage accumulation along cooling

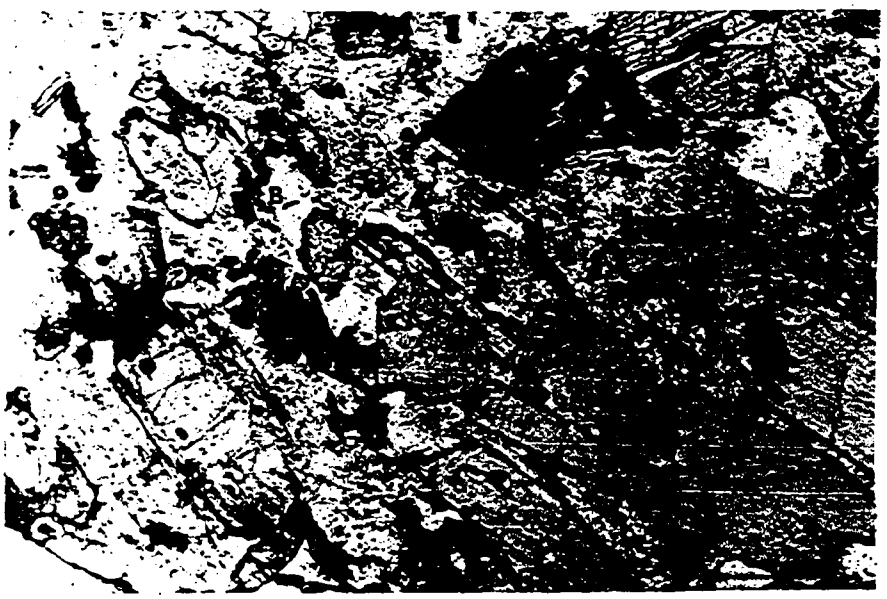

Fig. 71 Subparallel pyroxene and biotite (B), rare iddingsite (?)(I) with relict cleavages (?) of olivine; plane light, 30X, malignite 390A.

Fig. 72 Augite (Ag) rimmed by aegerine-augite, biotite (B), aegerine (Ae), zeolite groundmass; X-nicols, 120X, malignite, 704B.

Fig. 73 Fibrous, translucent aegerite, intergrown with clear zeolite; broken aegerine-augite prism healed with zeolite; in the lower left-hand corner is feldspar (F) which has no intergrown aegerine; minor biotite; plane light, 30X leucomalignite 577.

Fig. 74 Aegerine aggregate intergrown with interstitial zeolite, zoned biotite (B), turbid sanidine (Sa); augite; plane light, 30X, leucomalignite 577.

Fig. 75 Intergrown aegerine-augite, biotite (B) and magnesio-katophorite (M); zeolitized leucocratics; plane light, 30X, malignite 704F.

Fig. 76 Olivine surrounded by biotite and opaques; augite with a green zone around a zeolite inclusion; zeolitized leucocratic matrix; plane light, 30X, malignite 217.

Fig. 77 Olivine phenocrysts replaced along thin veins by serpentine and surrounded by biotite; also augite phenocrysts in matrix of aegerine-augite, biotite and zeolite; plane light, 30X, porphyritic malignite 643.

Fig. 78 Zoned biotite enclosing euhedral zeolite pseudomorph after nepheline; aegerine needles extend into zeolite; zeolite and sericite alteration of nepheline; interstitial zeolite after analcite (?); X-nicols, 30X, malignite 224.

Fig. 79 Zeolite pseudomorphs after nepheline (Z); zoned biotite (B) turbid brown, stained, anhedral sanidine (Sa); aegerine-augite (Ag); X-nicols, 30X, leucomalignite 577. Indicated crystallization sequence is below:

Augite ——→ Aegerine-augite ——→ Aegerine ——→
Nepheline ——→ ——→ Sanidine→
——→ Biotite more Fe rich ——→

Fig. 80 Same as above, plane light.

Fig. 81 Partial and complete red-brown biotite pseudomorphs of augite; light brown phlogopitic biotite; turbid sanidine (Sa); zeolite with minute opaque inclusions; plane light, 30X, leucomalignite 577.

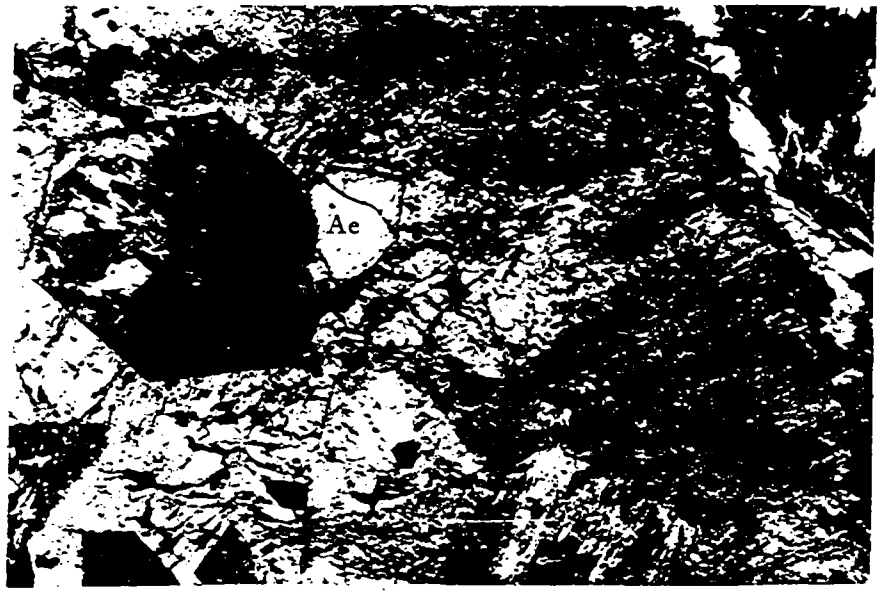

Fig. 82 Natrolite (N), pseudomorph after nepheline in turbid brown anhedral sanidine (Sa), zeolite veins transecting most minerals; augite(Ae); X-nicols, 30X, leucomalignite 577.

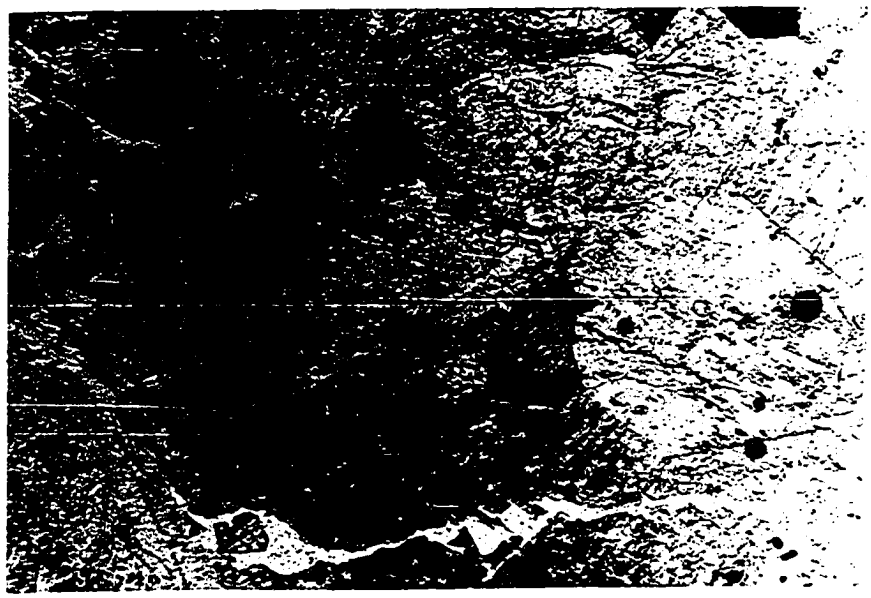

Fig. 83 Same as Fig. 82; notice the numerous inclusions in the zeolite in upper right corner; plane light.

Fig. 84 Euhedral laths of natrolite (N) pseudomorphic after nepheline; biotite (B); anhedral turbid sanidine (Sa); X-nicols, 30X, leucomalignite 577.

Fig. 85 Partially zeolitized nepheline (Ne); also augite (Ae) and opaques; plane light, 30X, malignite.

Fig. 86 Edge of leucocratic segregation; euhedral lath sanidine (Sa); zeolite, sericite and biotite in segregation; augite (Ae) and zoned biotite surround the segregation; X-nicols, 30X, malignite 665.

or tectonic joints. Leucocratic segregations such as these are common in basic alkaline sills. (Turner and Verhoogen, 1960, p. 390).

Petrologic variations within concordant intrusives

Compositional variations within the concordant hypabyssal intrusives are not dramatic. Billie Butte and the Great Anticlinal phacolith, two of the thickest intrusives, have been studied in some detail. In brief, the vertical variations (nearly perpendicular to basal contacts) is similar to that of the lower shonkinite layer of Shonkin Sag, Montana as shown in Fig. 87. The variations in densities and volume of heavy minerals for two sections from the Great Anticlinal phacolith and the densities from two sections of Billie Butte phacolith are indicated in Fig. 87.

Billie Butte phacolith

This body is at least 360 feet thick. From the base to 165 feet above a small increase in density occurs. Densities in a full 360 foot section have not been measured but probably would not be much different than in the two measured sections according to several hand specimens. Two samples, 634B from 19 feet above the base and 634E from 85 feet above the base respectively, have 19 per cent and 29 percent mafics. The lower sample also contains 5 percent analcite while the upper sample contains none. From 45 feet to about 75 feet above the base the rock is nonporphyritic as the

upper and lower part are distinctly porphyritic. The gradation from one textural type to another is abrupt and occurs in about a foot and includes one to two inch porphyritic layers interbedded with non-porphyritic layers. These interlayers of the two textural types probably indicate that this body is a composite intrusion of two magmas of similar composition though slightly more mafic above. It has been mentioned that in the western part of the map area a number of the steeply dipping concordant bodies have chilled contact with each other and make up composite bodies with small differences in composition.

Great Anticlinal phacolith

The variation of densities in the east section (Fig. 87,88) of the Great Anticlinal phacolith is similar to that of the shonkinite layer of Shonkin Sag though slightly greater. The top of the phacolith at this section has been eroded. With the upward increase in density is an increase of heavy minerals along with an increase in olivine from 2-5 per cent to 9 per cent. This differs from Gordon's Butte where there is an increase in olivine and augite downward (Wolff, p. 1603). The middle section of the phacolith is somewhat different in that it has a lighter layer with zeolite veins near the top (Fig. 87). The top of the latter section is probably not far from the original top of the body as is indicated by structural projections and the small pyroxene aggregates (p116) which occur at the bottom and at the top of the body.

It is difficult to correlate these two sections as the base of the middle section is about 60 feet in elevation below the eastern section (Fig. 87,88). It is possible the lighter zone near the base

of the eastern section is the continuation of the lighter zone at the top of the middle section as they are approximately at the same elevation.

The cause of the variations in this last described body will have to await further study. Crystal settling such as described by Hurlbut for Shonkin Sag (1940) cannot be ruled out as is indicated by Fig. 87. But the 300 to 350 foot Gordon's Butte malignite laccolith increases in olivine and augite toward the base and has interlayered shale bands. It is difficult to see a consistent composition variation pattern as contrasted with the differentiated bodies of the Highwood and Bearpaw Mountains, Montana.

In conclusion, the increase in densities upward or a lighter layer at the top in some sections (and mineralogy) in some of the Crazy Mountain concordant bodies is reminiscent of differentiated (by gravity mainly, supposedly) bodies of the Highwood Mountains. If gravity settling has occurred in the Crazy Mountains concordant bodies the development of lighter syenitic layers near the tops is much less striking than the Highwood Mountains. This is difficult to reconcile with the fact that the eastern section of the Great Anticlinal phacolith has a greater though similar variation of specific gravities to the shonkinite layer of Shonkin Sag. This implies that more crystal settling occurred in this body than in Shonkin Sag and a well-developed syenite layer should have formed. One could argue that such a syenite layer could have been squeezed off to other positions after differentiation during some phase of folding.

These other positions might be Virginia Peak syenite laccolith at the same stratigraphic level as well as Target Peak laccolith which is slightly higher stratigraphically. One might be inclined to eliminate this as an explanation since separate volumes of these bodies are probably too great to have differentiated from the exposed source phacolith. Also their rather consistent leucocratic composition would indicate a very efficient separation process. One would think that it would be possible to find some melanocratic fractions in these bodies. (more than the occasional olivine surrounded by biotite) if they separated directly from the melanocratic malignite of the phacolith. A slow passive ejection due to slow folding might be possible.

Another possibility is that the missing leucocratic fraction of the phacolith might be some higher body now long eroded away. Preintrusive differentiation from the malignite magna at a greater depth is a more plausible source for Target Peak and Virginia Peak laccoliths. This differentiation would occur in gradual steps as is indicated by the sill variation from malignite to leucomalignite to feldspathoidal syenite.

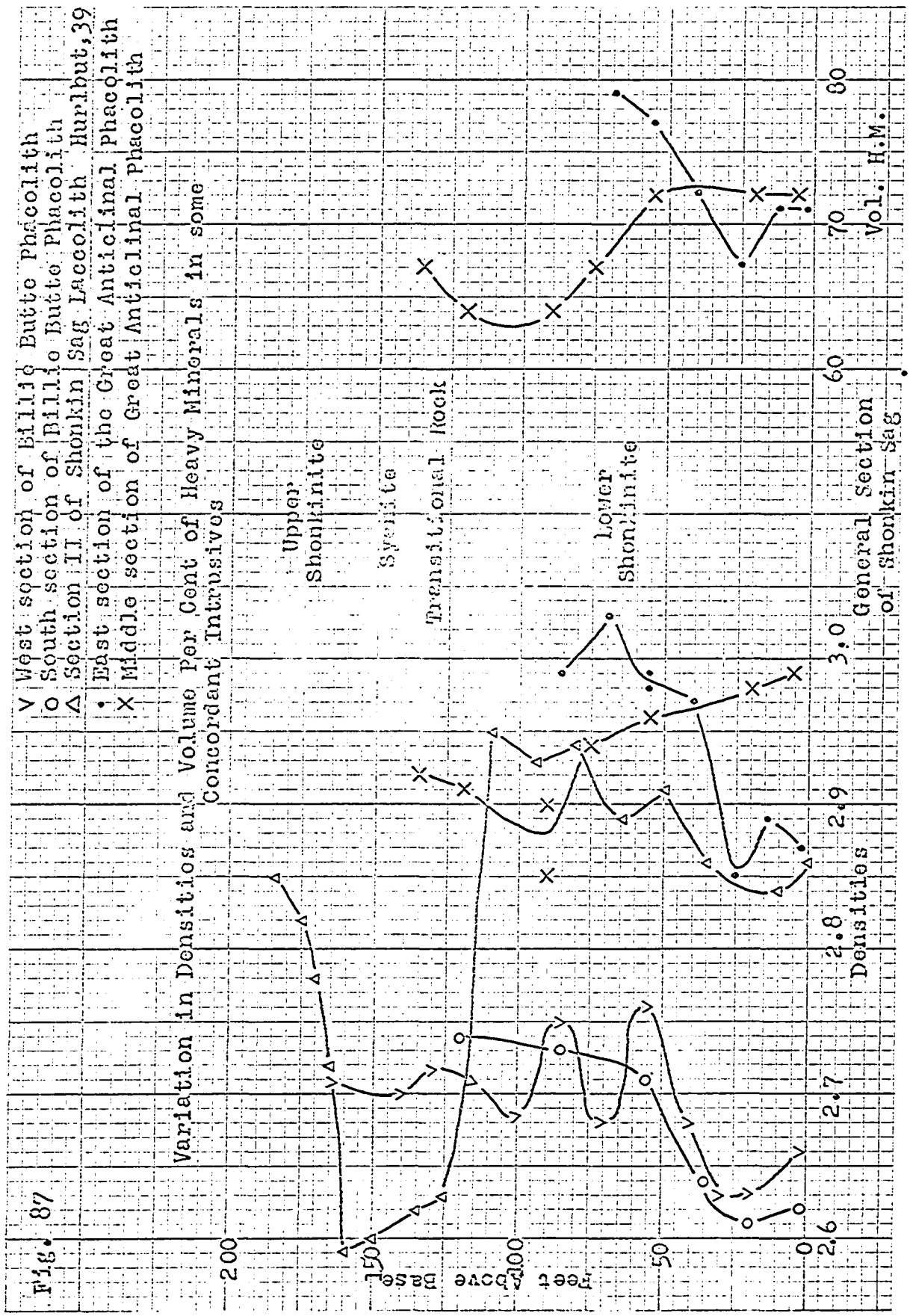

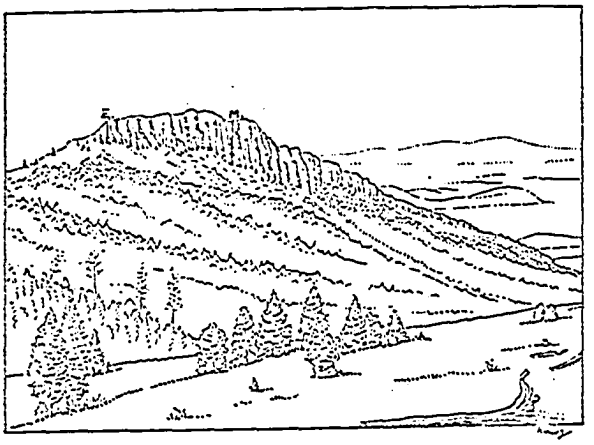

Fig. 88 Looking southwest at the Great Anticlinal Phacolith from the axis of the Robinson Anticline north and above the Shields River. Sketch by E. Raisz, from a photograph (Wolff, 1938). E. and M. respectively indicate the sections east and middle section shown on figure 87.

Irregular to geometrical shaped mineral segregations (pseudoleucite?)in fine-grained alkaline rocks

Associated with the malignites is a black mafic trachyte with abundant gray spots with irregular and geometric outlines (90,91); that occur in aggregates (Fig. 90,91,84). Also, more indistinctly spotted rocks occur in various places. Some of these structures may eventually prove to be pseudoleucite as is indicated by features described below. Elaboration here is worthwhile as pseudoleucite genesis has been described by many workers as important in the origin of feldspathoidal igneous rocks.

This occurrence is involved mainly with three samples of intermediate porphyries from a vertical, southward-terminated dike located along the axis of the Robinson Anticline (Plate 1, N.W. $\frac{1}{4}$, Sec. 22 T. 5 N., R. 10 E). Hornblende latite 626 is coarser grained than 625 (mafic phonolite?) and comes from the thicker part of the dike. Sample 625 is somewhat different mineralogically and chemically from 626. Sample 625 contains spotted structures and occurs near the terminus of the dike. Sample 624 also occurs near the terminus of the dike, is petrologically similar to 626, but contains white spots that are vague and more irregular but similar to those of 625. Associated with 625 is a gray porphyry (625c) that is megascopically similar to sill 636-635, which also has vague round to elongate pink patches (Fig. 89). The latter patches are made very distinct in hand by HF etching and staining with methyl blue and malachite green. In this case the spots take the methyl blue stain (the groundmass takes the stain in 625).

Because of the fine grain size, detailed work on these structures was not attempted. Tentative mineralogical and modal analysis of 625 and 626 follow separately in the appendix and Plate 2.

Several brief but definite statements can be made here: The chemical composition and overall mineralogy of 625 and 626 is similar to other pseudoleucite bearing rocks. (2) The white spots have a number of mineralogical similarities with pseudoleucites but are definitely different in certain respects (compare tentative descriptions of 625, 626 in appendix with other described occurrences). (3) The feeder dike 626 contains the next to highest potassium content of all the Crazy Mountains samples and should be the most favorable rock of pseudomorphs after leucite. But it is the slightly finer grained terminus of the dike (625) which contains the structures. This latter sample contains moderately high sodium content and less potassium. (4) The gray spots in 625 and 624 occur at the terminus of the dike where it is interbedded with a dipping sill. The capping malignite sill may have acted as a trap for upward accumulating leucites or analcites. The field situation is somewhat similar to the fergusite headed dike described by Buie (1941) in the Highwood Mountains.

Further, Fudali (1964, p. 1120-21) predicted that the most likely place for pseudoleucite to occur is in alkaline rocks with the following characteristics: (1) phonolitic with high sodium, (2) a. low to moderate vapor pressure if formed from sodium leucite or b. higher vapor pressure (4000 bars and up) and even higher sodium

content if formed from potash-rich analcite solid solutions, (3) lower temperature than extrusion temperature of some rocks (stabilizing the high sodium of the leucite). As the Crazy Mountains alkaline rocks are sodic hypabyssal intrusives, requirements 1, 2a and 3 met.

There is a good possibility that these structures are pseudoleucites, but it is by no means proven conclusively. Further study is necessary.

Fig. 89 Hand specimen 1 and thin section 2 are spotted mafic trachyte 625 (same as Fig. 90, 91). The matrix of the thin section is stained for methyl blue and some euhedral outlines are distinct. Slab 3 and 4 are spotted trachyte 635. Slab 3 has been etched with HCl which makes the spots more distinct on a cut. Slab 4 has been stained for methyl blue affording an indistinct wormy appearance though some definite spots are stained. These spots of 635 are very distinct on a weathered surface but vague in thin section.

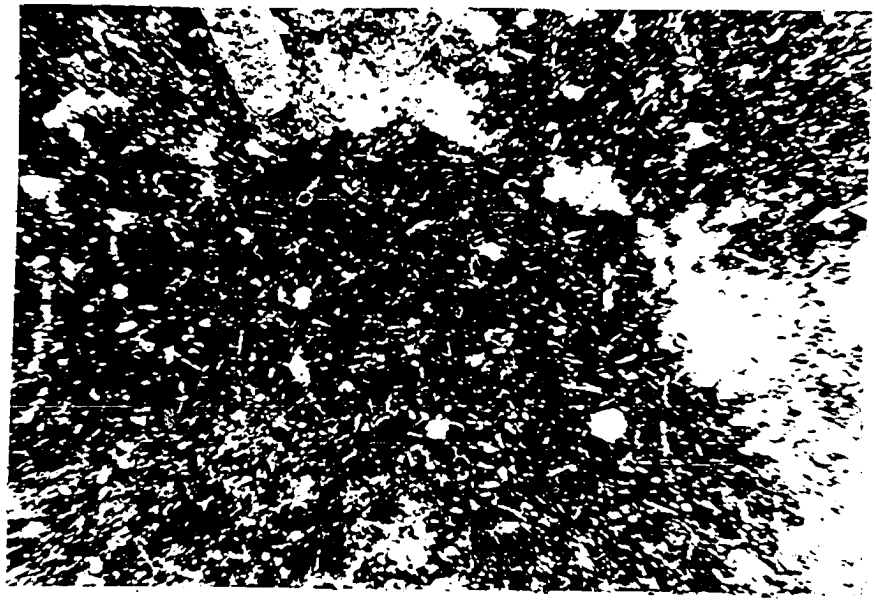

Fig. 90 Part of geometrical shaped mineral segregation (?) (dark euhedral part, lower 2/3 of photo) in mafic trachyte (625); X-nicols, 22X.

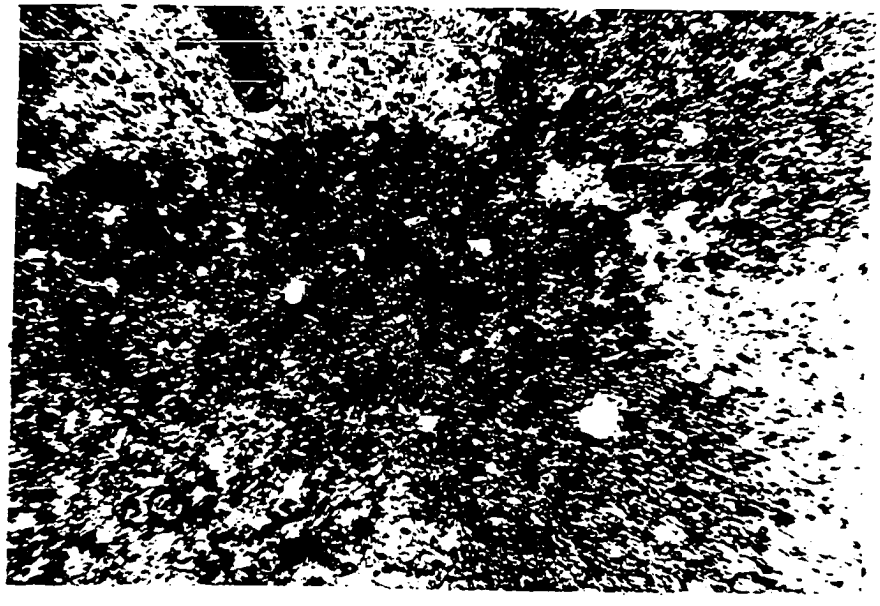

Fig. 91 Same as above; plane light, 22X.

Intrusive sequence

Wolff concluded (1938, p. 1590), on the basis of one small transecting dike (exposure 16, p. 147) that the alkalic series was younger in the Crazy Mountains than the more calcic series. Likewise Larsen, (1940, p. 891) observed: "Where the age relations of the different subprovinces have been determined the older rocks are commonly nearer the lime-alkali types".

Described on the succeeding pages are a number of exposures (mainly in the present map area) where relations should help establish an intrusive sequence. The pattern indicated by these exposures shows no overall sequence of intrusion of the various rock types. Yet it is possible to conclude there was an overlapping line of intrusion of diverse types. The latites and mafic trachytes were intruded early as well as late in the intrusive period.

Also the writer considers that Wolff's statement that the alkali series is younger than the other series has not been substantiated. In fact, if the interpretations of the time relationship indicated by Exposure 8 and, say, Exposure 7 is true than the alkali series overlapped in time of intrusion with the so-called calcic series. (It will be shown in the geochemistry sections that feldspathoid syenites are of the alkali series, while the quartz latites, andesites and basalts are of the

alkali-calcic series. This is a necessary statement in order to make the above conclusion).

Exposure descriptions that indicate a sequence of intrusion

Exposure 1: At 340, just north of the Shields River, a latite dike transects a thin basalt-diorite sill (339). The contact is not exposed between the two bodies but a transection can be inferred since the joints in the sill which parallel the dike increase in concentration toward the mutual contact (maximum concentration where joints are 2" to 3" apart).

Exposure 2: One hundred feet east of 253b in Lodgepole Creek, a latite dike has a fine-grained contact with two andesitic (?) basalt phases of the radiating dike system.

Exposure 3: At the head of the Upper Shields River, a diorite porphyry dike (652) transects a quartz latite dike (449). Both of these dikes are of the radiating dike system. 449 varies considerably in thickness in a vertical direction.

Exposure 4: Along the Upper Shields River, a diorite porphyry (260B) has a fine-grained contact with an altered basaltic phase (a complex dike of the radial system).

Exposure 5: Along the Upper Shields River, a hornblende latite dike (445C) has a fine-grained contact with a basaltic dike (445B) (a complex dike of the radial system).

Exposure 6: On Dugout Creek, a latite sill (443) appears to transect a biotite lamprophyre dike (442). The exposure is poor.

Exposure 7: East of Beverley Peak, a north trending basaltic dike (408) and a composite basaltic-diorite porphyry dike transect a quartz latite sill (401).

Exposure 8: A quartz latite sill (126) was probably intruded contemporaneously with or later than the aegerine syenite (116) of Target Peak Laccolith. These two possibilities are considered to be most likely because the sill abruptly terminates below and just to the west of Target Peak Laccolith and a downfold occurs beneath the laccolith. This relation indicates that the laccolith restricted the intrusion of the sill beneath.

Exposure 9: On the Robinson Anticline at X-143, a thin biotite lamprophyre sill terminates as a thin, short dike 10 feet to the east of a hornblende akerite dike (625, 634, 626). The earlier akerite dike apparently impeded intrusion of the malignite sill. This exposure also indicates that the sill was not intruded from the west up the dip, but from the east toward the anticlinal axis.

Exposure 10: On the Robinson Anticline an akerite dike (625, 624, 626) transects a malignite phacolith (627, 704) and a malignite sill (623). The malignite sill at exposure 9 is stratigraphically lower than the malignites at exposure 10, although it was intruded later. This indicates that a superimposed succession of sills does not always occur.

Exposure 11: On the Upper Shields River, an inclined biotite lamprophyre dike (574) transects an upper leuco-malignite sill (217).

Exposure 12: North trending dikes of blue felsite (610a), altered malignite (?) (609), malignite (707) and calcite-bearing

yellow felsite (613) transect sills of altered hornblende latite (612, 610b) in the north side of the Great Cliffs.

Exposure 13: Thin hornblende latite (597) which is similar to 112 trends north, transecting the lowest leuco-malignite laccolith (598 et al) in the south side of the Great Cliffs.

Exposure 14: A north-west trending hornblende latite dike (600) transects the lowest-leucomalignite laccolith (598).

Exposure 15: Biotite lamprophyre (?) dike (607) has a fine-grained contact with the base of the lowest leuco-malignite sill (598) in the north side of the Great Cliffs.

The following exposures are indicated by Wolff:

Exposure 16: A gray porphyry dike which is described by Wolff (1938, p. 1590)--"Specimen 170 07' is from an outcrop at the eastern diorite contact in Sweet Grass Canyon, which forms narrow irregular bands cutting an older gray porphyry sill. The norm is shonkinose and is the only rock found in place, cutting the diorite series, which belongs with northern alkaline series". It contains hornblende and no nepheline.

Exposure 17: The Comb Creek syenite sheet transects a sill of theralite (p. 1611).

Exposure 18: The Cottonwood Creek akeritic necks contain no inclusions of malignites which surround the neck, though the necks do contain inclusions of the other kinds of rock. Wolff, (p. 1616) reaches two alternative conclusions: (1) Any malignite fragments were implaced at higher levels or (2) The akeritic necks formed previous to the malignite.

Exposure 19: The Three Peaks neck is composed of a malignite matrix and contains granite and alkali syenite similar to the laurvikite stock and similar rocks in the Comb Creek area to the north of the map area (p. 1617).

Exposure 20: On the north side of the Great Cliffs is a limited exposure of coarse nepheline syenite grading into malignite (p. 1599) indicating contemporousness. This exposure was not observed by the writer.

Several other exposures have been seen by the writer more recently:

Exposure 21: A mafic trachyte sill 530 (like 515) has a chilled contact with a malignite dike north of Forest Lake.

Exposure 22: A malignite porphyry dike (29) transects an akerite sill (28) near the south end of Forest Lake.

Petrographic summary and discussion

In this section the mineralogical characteristics of the main rock types are summarized in the text and in diagrams (Figs. 93, 92). When evident, the order of magmatic crystallization is given. Contrasting post-magmatic mineralization is also briefed.

The main igneous rocks of the map area consist of nearly equal amounts of trachyte-feldspathoid syenite, intermediate rocks and quartz latite-rhyolite. Lesser amounts of basalt and andesite porphyry and rare biotite lamprophyres occur.

Malignite and trachyte - feldspathoid syenite

The malignites consist mainly of aegerine-augite, olivine, biotite, sanidine and/or orthoclase, nepheline, natrolite and other zeolites, opaques and magnesio-katopherite (the latter mineral occurs only in the two thickest intrusives). The central stratigraphic malignite sills are the most mafic. The variations within the thickest bodies are about the same as those which occur within the shonkinite layer of Shonkin Sag. Some of the malignites are as leucocratic as the syenites but distinct from them since the related syenites contain mainly aegerine-augite, aegerine, microperthite, albite, zeolite and minor amounts of nepheline and analcite.

The sequence of crystallization in these two groups is as follows: The magnesian olivine reacted with magma to form magnesian biotite at about the stage that aegerine-augite initiated crystallization on augite. Some of the magnetite may have been formed in the olivine-biotite reaction. Nepheline initiated crystallization before

biotite. Nepheline is succeeded by orthoclase (orthoclase-low albite series) and/or sanidine. Aegerine and biotite crystallized simultaneously. In the two thickest concordant bodies magnesio-katophorite crystallized with the above minerals. Apparently these bodies cooled more slowly with the drop in pressure and the liquid left the biotite stability field enabling the formation of magnesio-katophorite. The formation of the magnesio-katophorite is not particularly dependent on MgO content as the thin feeder dike 645 has high MgO and no katophorite while the lowest phacolith which contains katophorite is a leucocratic malignite.

Syenite was intruded after the intrusion of the malignite (some at least was intruded later, according to the cross-cutting intrusive relationships). These syenites crystallized aegerine-augite and aegerine with a feldspar of the orthoclase - low albite series and minor nepheline and analcite. Occasional olivine with a biotite rim occurs and indicates that this syenitic liquid could have been derived from a malignite magma by imperfect segregation. The irregular leucocratic segregations in the malignite may be due to imperfect segregation of the leucocratic fraction. In any case the differentiation of the syenite from the malignite was probably pre-intrusion (p. 134). At this point we might make a comparison: "The mafic-poor nepheline syenites of the Highwood Mountains have essentially the same minerals as the mafic-rich shonkinites except that they have no olivine, little pyroxene, and considerable biotite. Rarely nepheline syenites contain hornblende", (Larsen, 1940, p. 928).

Latites and mafic trachytes

The intermediate rocks include latites and mafic trachytes (Fig. 92). The mafic minerals in these are augite, hornblende, biotite and opaques. Pyroxene predominates among the mafic trachytes while hornblende is the most common mafic mineral among the latites. The mafic trachytes contain albite-oligoclase and microperthite or anorthoclase phenocrysts in a matrix of alkali-feldspar and sometimes quartz. The latites contain oligoclase-andesine phenocrysts in an andesine to alkaline feldspar and sometimes quartz matrix. These two groups are gradational. A few of the pyroxene rich types grade along strike into hornblende rich types.

Yet the hornblende latites predominate as dikes and sills in association with the eastern basalt-andesite porphyry and quartz latite-rhyolite porphyries. In fact, the latites fit as an intermediate group between the diorite porphyries and the quartz latites and rhyolite porphyries (Fig. 93). The latites seem to contain more dioritic and other inclusions than the trachytes. This has not been proven quantitatively. Augite and hornblende in these rocks appear to have reacted to form biotite, magnetite, sphene and apatite. Similar reactions are evident in the inclusions. No doubt partial assimilation by these inclusions plays an important role in the overall chemistry of these rocks and the quartz latite. The extent of contamination will not be evaluated here.

The mafic trachytes occur most often on the Robinson Anticline in association with other alkaline rocks. But many of their mineralogical and geochemical characters are not intermediate to the malignites and the trachytes-feldspathoid syenites. (This position appears to be played by some of the leucomalignites).

Diorite porphyries and basalts

The diorite porphyries are mineralogically intermediate to and transitional with the hornblende latites and the basalts. The diorites consist mainly of oligoclase-andesine, hornblende, augite, chlorite and opaques, while the basalts consist of andesine-labrodorite, augite, biotite, chlorite and opaques. The Barth value of 122 for the basalt indicates augite and plagioclase initiated crystallization simultaneously. The texture does not negate this possibility.

Quartz latite-rhyolite porphyries

The quartz latites are composed of phenocrysts of albite-oligoclase and perthite, and alkali feldspar-quartz matrix, plus biotite, hornblende and chlorite as matrix and phenocrysts. Potash feldspar is often rimmed by albite-oligoclase. These rocks also contain numerous xenoliths as do the latites. The rounded quartz grains are probably xenocrysts. A mineralogical and chemical break (Pg. 82) occurs between the latites and quartz latites though one intrusive may contain both types. The sequence basalt - andesite porphyry - hornblende latite - quartz latite, rhyolite

porphyry forms a continuous mineralogical series. An overlapping sequence of intrusion of the felsic and mafic types occurred within this series and this series overlapped in intrusion time with the feldspathoidal series.

Post magmatic history

Zeolitization

In the alkaline rocks, post magmatic minerals are zeolites, sodalite, sericite, aegerine, apatite, calcite, serpentine and rare chlorite. The feldspathoids, especially nepheline, are often pseudomorphed by natrolite and other zeolites. The feldspar is often fresh beside the completely replaced nepheline, though it may contain thin zeolite veins. In some of these zeolitized rocks, the feldspar is weathered out in relief. In leucocratic members, clear nepheline is sometimes replaced along rims and cleavage by sodalite, while nearby feldspars are zeolitized. Turbid brown feldspar is commonly associated with clear, secondary analcite. The analcite is often replaced by other zeolites. Sub-microscopic, turbid, brown alteration products conform to zones and various phases of perthite. Similar feldspar alteration is reported in other alkaline rock privinces. The feldspar and analcite are often replaced by aegerine microlites, apatite and a fine red biotite (?). Occasionally sericite is common. Calcite is especially striking where it replaces euhedral analcite (?). Chlorite is rare and has been observed as a replacement of augite near one basal contact. Yet chlorite is supposed to a common alteration product of aegerine. Cancrinite is rarely developed, if at all.

Serpentine rims the olivine.

In a seven-year-old, 30 foot-deep road cut, the zeolitization appears to be as common as in other long exposed outcrops indicating the pervasiveness of the alteration or rapid weathering. The coarser malignites display less zeolitization than the finer examples possibly reflecting the influence of enclosing strata and their contact solutions. Zeolite and calcite veins parallel and transect these alkaline rocks. Intense zeolitization has been described for the alkaline rocks of most of the central Montana sub-provinces.

Propylitization

The post magmatic mineralization of the latites, quartz latites, diorite porphyries, basalts and lamprophyres differs considerably from the alkalic rocks. It consists predominantly of chloritization of biotite, hornblende and augite. Chlorite and calcite replace these minerals. Some chlorite succeeds the calcite. In amygdules, less common zeolite and quartz may have preceded the formation of some of the calcite. This intense propylitization is most common in the radial dike set and some composite sills (especially near contacts). The feldspar phenocrysts and matrix are invariably turbid from sericite and other submicroscopic alteration products. Evidently dikes control post magmatic solutions. Later intimate intrusives may have affected the post magmatic reactions of earlier intrusives.

Minerals and Paragenesis of the Malignites, Feldspathoid Syenites -Trachytes-Variants and the Latites-Mafic Trachytes

Magmatic — Post-magmatic

Malignite

Opaques max. 3%
Mg. Kataphorite 0-9%
Olivine (Fa. 10) 0-20% — Serpentine occ.
Mg. Biotite 4-21% — Apatite
Augite → Aegerine-augite → Aegerine 14-60% — Calcite
Nepheline max. 15% — Natrolite max. 56%
Orthoclase
Sanidine max. 20% — Sodalite
Perthite — Other Zeolites
Analcite
Sphene — Cancrinite ?

Feldspathoid Syenites, Syenites and Variants

Olivine surrounded by Mg. Biotite rare — Chlorite minor
Aegerine-augite → Aegerine 6-17% — Apatite
Analcite max. 6% — Sericite
Nepheline max. 4% — Sodalite
Microperthite, Albite, Anorthoclase ? } 53-94% — Zeolitic Feld. max. 20%
Sphene, Opaques — Calcite
Cancrinite

Rhomb Porphyries consist of alkali feldspar, plagioclase, augite, biotite, chlorite and opaques.

Latite Porphyries to Mafic Trachyte Porphyries*

Augite → Aegerine-augite 0-8%, 8-16%* — Chlorite
Hornblende 8-18%, 0-3%* — Calcite
Biotite 0-8%
Andesine → Oligoclase 0-25% — Sericite
Oligoclase → Albite, Microperthite, Anorthoclase } 25%* — Epidote
Matrix of Andesine to Alkali Feldspar, Quartz } 52-75% — Zeolite
Analcite max. 5%
Opaques 1-8% — Apatite

Fig. 92

Minerals and Paragenesis of the Basalt-Andesite-Latite-Quartz Latite, Rhyolite Series

Magmatic	Post-magmatic
Basalt	
Opaques 2-6%	
Augite 19-22%	
Biotite 10-15%	Chlorite 7-30%
Labradorite → Andesine 25-40%	Calcite
Quartz	Zeolite
Other Accessories	
Andesite Porphyry	
Opaques 0-3%	
Augite approx. 5%	
Hornblende 10-20%	Chlorite 15%
Andesine → Oligoclase 50-60%	Sericite
Quartz	Calcite
Other Accessories	Zeolite
Latite Porphyries	
Opaques 1-8%	Chlorite 0-17%
Augite — Aegerine-augite* 0-8%	
Hornblende 8-18%	
Biotite 0-8%	
Phenocrysts of Andesine → Oligoclase 0-25%	Calcite
Matrix of Andesine, Alkali Feldspar, Quartz } 52-73%	Sericite, Epidote, Zeolite
	Apatite
*Aegerine-augite rims occasionally	
Rhyolites and Quartz Latite Porphyries	
Augite (rare)	Chlorite 0-5%
Hornblende 0-7%	Calcite
Biotite 0-9%	Sericite
Phenocrysts of Andesine → Albite 20-39%	Epidote
Perthite 0-11%	
Quartz in ameboid and string shapes max. 5%	
Matrix of Alkali Feldspar, Quartz } 41-71%	
Magnetite, Zircon, Sphene, Apatite	

The Lamprophyres contain augite, biotite, alkali feldspar, magnetite, chlorite, calcite and zeolite.

Fig. 93

GEOCHEMISTRY OF IGNEOUS ROCKS OF THE NORTHERN CRAZY MOUNTAINS

Previous work on the geochemistry and petrogenesis of the Central Montana Petrographic Province and Crazy Mountains

Iddings (1892), (p. 31) first noted the alkali rich igneous rocks in various mountain ranges along and to the east of the northern Rocky Mountain front. Pirsson (1905 b) discussed the regional characters of these igneous rocks and defined the Central Montana petrographic province.

At this time, Wolff had made only a few brief reports on the Crazy Mountains (1885, 1890, 1893, 1898). On the basis of this information and his own experience, Pirsson did not include the Crazy Mountains in the petrographic province because of certain different characters such as high sodium content and red-brown color of the biotite in the Crazy Mountain igneous rocks. Pirsson also discussed a chemical zoning and "regional progression of types" within the province. He meant by this latter term that a gradual geographic overlap of rock types occurs between the various mountain ranges.

Daly (p. 514, 1933) made short work of the genesis of the alkaline rocks of the Crazy Mountains by noting that the theralites (malignites) are underlain by limestones while the sub-alkaline rocks are not. Wolff (1938) wrote that the Crazy Mountains igneous rocks are especially characterized by high contents of sodium, barium, and strontium. Esper Larsen (1940) made a comprehensive study of the central Montana petrographic province by comparing the chemistry of the sub-provinces on various binary and ternary diagrams. He also included the Crazy Mountains and volcanic areas as far south as

Yellowstone Park in his discussion. He noted that high contents of barium and stontium characterized all of the province, not only the Crazy Mountains. Further, he concluded (p. 946) that the magma for the various sub-provinces differentiated from a basaltic magma by crystal settling of calcic plagioclase and hypersthene with some olivine at depth. He suggests that the alkaline rocks are derived from the basaltic types in that there are gradational types between the gabbros and shonkinites (basic alkaline rocks) in some provinces. He further suggested that a long period of quiet differentiation at depth would be required to form the alkaline rocks. The relatively flat-lying Cretaceous-Tertiary sediments of the plains area indicate a long period without much deformation and this would favor slow differentiation. This would also be substantiated by Larsen's observation that the younger rocks are commonly nearer the alkali types. The variation of the rocks in each sub-province, according to Larsen, is due to crystal settling combined with assimilation of siliceous material. The amount of assimilated material in the Crazy Mountains and Little Belt sub-provinces was large, according to Larsen. He also indicates that limestone assimilation may not have been important in the formation of the alkaline rocks as "there is no reason why this area would be more susceptible for limestone assimilation than any surrounding area with sub-alkaline rocks".

One anomoly in Larsen's scheme according to himself and Turner and Verhoogen (1960) is that it does not explain the consistent high BaO and SrO contents.

As far as the Crazy Mountains are concerned, Wolff and Larsen described two igneous series, an alkaline series in the northern Mountains and lime-alkalic series in the southern Mountains. It is this latter feature which has received primary attention in the present study.

The present geochemical study

The following geochemical considerations characterize the igneous rocks of the northern Crazy Mountains. Various geochemical diagrams have been used to compare the features. Some of the various petrogenetic hypotheses that have been put forth previously have been tested. Part of the task has been to define and describe the various possible rock series and determine genetic relations between them.

For this study chemical analyses of the writer (18 samples) and Wolff (20 samples) from the northern Crazy Mountains were used. Also chemical analyses of John Tappe (5 samples) and a varying number of Wolff from the southern Crazy Mountains were used in certain considerations. Chemical analyses, norms, geochemical parameters and modes of these samples are listed on Plate 2, including those analyses from the northern mountains and Tappe's five samples from the southern mountains. Other geochemical data not used in this study can be found in the appendix. The various geochemical parameters used are explained in following geochemical sections. In addition they are briefly described in the appendix.

Conclusions are given on pp. 213-219.

Alkali-lime index

A widely used geochemical index of a igneous complex is the alkali-lime index, (Peacock, 1931). The index is computed from a variation diagram of SiO2 versus K2O plus Na2O and CaO and equals the per cent SiO2 corresponding to K2O plus Na2O equal to CaO on the variation curve. Peacock arbitrarily distinguished four chemical classes of igneous rocks on the basis of this index: alkalic (less than 51), alkalic-calcic (51-56), calc-alkalic (56-61) and calcic (greater than 61).

From the writer's and Wolff's data, Fig. 94 was prepared. Two series are shown. Indicated Peacock indices are 47 with a range of 44 to 48 (alkali) and 55 with a range of 53 to 56 (alkali-calcic). The width of the trends on Fig. 94 is distorted because the SiO2 co-ordinate is compressed by one-half for convenience. Barth (1951-1959) computed a single index of 51.5 (alkalic-calcic) from Wolff's (1938) data, which is intermediate with respect to the above values. Larsen (1940) had termed the Southern Crazy Mountains series as "lime-alkalic", being as calcic as the Yellowstone subprovince (calc-alkaline according to Barth, 1951).

The rocks on the variation curves for the alkali index are those from the northern Crazy Mountains and one shonkinitic rock, 170 07' from the southern Crazy Mountains. The SiO2 content of the shonkinite is in the SiO2 range of 47.7 to 52.5 of the curve in which are no other examples for the alkali series.

The curves indicating the alkalic-calcic index represent rocks

from the southern stock, including surrounding dikes, a few akerites in the intermediate SiO2 range and quartz latites from the northern area. Similar to the alkalic curve, the alkali-calcic curves have no values in a range of SiO2= 58.3 - 64.4 except for akerite 282 from the northern area.

The blank range in the two sets of curves may indicate that continuous variation does not occur with respect to these geochemical parameters thus indicating more than two series. The fact that a few samples from different areas occur within these ranges for each set of curves may indicate the deficiencies are due to incomplete sampling. Rocks with these SiO2 contents may be located in areas such as the northern stock which have not been sampled or are not exposed. Another alternative is that the data represents only one series of rocks through which simple curves cannot be fit with any degree of closeness. This last alternative is not in accordance with the Larsen variation diagram (Fig. 104, 105) for instance which indicates two different series of chemical variations within the Crazy Mountains.

The alkalic index of 47 is lower than that of the Highwood Mountains (50, less alkaline?) and is about equal to that of the Tahitian province (Williams, 1932) and the Ponape Islands (Yagi, 1960). The crossing of the two curves of this alkaline set is vague because of erratic chemical variations which are in part probably due to alteration. The alkali-lime index of 55 is equivalent to that determined by Barth (1952, 1959) for the Little Belt Mountains. The

olivine-basalt trachyte phonolite sequence of E. Otago, New Zealand has a similar set of alkali-lime indices which are variously estimated at 50.1 (for the whole series which is near to Barth's value for all of the Crazy Mountain rocks), 46.5 (for rocks with feldspathoids), and 52.5 (for non-feldspathoidal rocks) according to Benson, (1941). The basic rocks of the feldspathoidal sequence of the East Otago sequence (basalts) are not like the malignites of the Crazy Mountains. This indicates that the alkali-lime index should not be cited alone. The per cent K_2O+Na_2O (=CaO) should also be given when the curves are not shown in order to give a better picture of the chemical variations; not just the SiO_2 value alone. For example, feldspathoidal series of East Otago has an alkali-lime index of 46.5 (SiO_2) - 7.8 (alkali-lime), as the alkaline series of the Crazy Mountains has alkali-lime index of 47.0 - 9.+ which brings out the differences between the two provinces. The Japanese geologists have been following this procedure (for instance, Sugimura, 1960).

The geographic overlap of the rock series as is indicated by the alkali-lime curves and other curves bears out Pirsson's idea of "regional progression of types" (1950b, p. 48). This idea was not emphasized by Larsen (1940).

Tappe's sample 38, that with the least amount of SiO_2, can be placed with both series of curves at their mafic ends. This indicates that rocks intermediate to basaltic types and mafic

Fig. 94

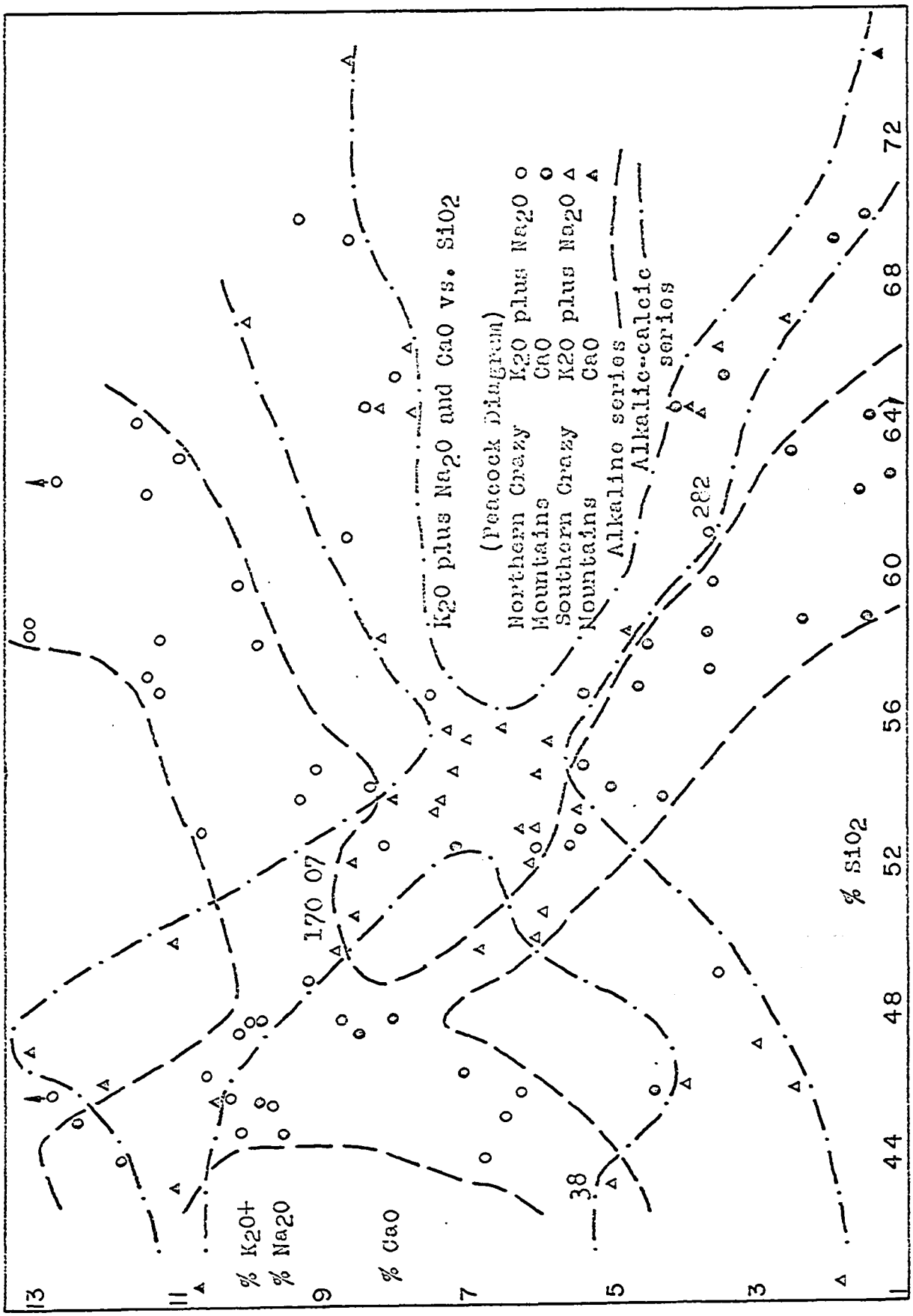

alkaline rocks do occur. Larsen (1940) observed this throughout the central Montana petrographic province and used it as evidence that the alkaline rocks were derived from the basalts. This sample has not been studied in detail and is tentatively called a hornblende diorite.

Potassium-Rubidium ratios

At an early stage of the research (1963), Peter Lessing of Syracuse University kindly determined potassium-rubidium ratios of five samples from the northern Crazy Mountains (Table 2, Fig. 95). Samples studied are malignite, hornblende latite, aegerine syenite from the map area, diorite and biotite diorite (?) from the northern stock. These samples represent major rock variants of this northern area, but quartz latite and basaltic types are not represented.

The values as determined by Lessing are as follows:

Table 2

Sample No.	Rock Type	Per cent K	Rb. ppm	K/Rb.
S-91	Hornblende latite	3.80±2.8%	117±13	324
S-140	Aegerine Syenite	4.06±2.8%	122±13	333
S-217	Malignite	2.40±2.8%	87± 9	276
S-217	Malignite	2.40*		
S-241	Diorite	2.08±2.8%	65± 7	320
S-242	Biotite Diorite	2.00±2.8%	64± 7	312

Accuracy of Analytical method is described by Reynolds (1963)
* Analysis by the Japan Analytical Chemistry Research Institute of the potassium content.

As a comparison, in the Lovozero alkaline massif, Kola Penninsula, the K/Rb. ratios range from 280 to 170 (Volkov and Savinova, 1959). Other igneous provinces have even greater ranges (Taubeneck, 1965).

Therefore the range of 276-333 is narrow and indicates that K/Rb is relatively constant in Crazy Mountain samples. The ratios are near the K/Rb ratio of 230±50 that occurs in many magmatic crystal rocks (Heir, 1965) though he reports miaskitic nepheline syenites with K/Rb ratios well over 500.

Ahrens et al (1952) and other workers had considered that the K/Rb ratio of igneous rocks is nearly constant during the major phases of differentiation. Yet Taubeneck (1965) has shown strong evidence that the ratio decreases with differentiation in some igneous rock series as is indicated by the decrease in the ratio with increase in potassium in the rocks (Fig. 95) or succeeding intrusions. There is no evidence from the present data to indicate a decrease in the ratios with respect to K content in the Crazy Mountain analyzed types.

At least the close similarity between the K/Rb ratios for the alkaline rocks and the dioritic rocks of the northern stock suggests that the types represented are co-magmatic (personal communication, Lessing, 1963). Further, the northern stock may be alkali-calcic as is indicated by known rock types, and the abundance of quartz latite (alkali-calcic) sills and dikes which trend into the main body. This alkali-calcic nature cannot be fully ascertained until this northern stock is studied. With this in mind, the constant K/Rb ratios suggest that the two possible series (alkali, alkali-calcic) in the Crazy Mountains are related. Concerning the K/Rb ratios, Butler et al (p. 93, 1962) have found a different situation in the Nigerian Younger Granites. "Rocks intruded at a later stage tend to have lower K/Rb ratios but they do not necessarily have lower K/Rb ratios than those emplaced earlier. The range in the K/Rb ratios varies from

complex to complex; this is to be expected if the rocks were derived from relatively isolated magma or fluid chambers existing under the site of the complexes". This observation tends to point to a close relationship for the Crazy Mountains two possible series.

Taubeneck (1965) suggests K/Rb ratios may be used to characterize rock series. This writer thinks that the central Montana petrographic province may be a good area in which to test this possibility as a number of apparent series occur which in part overlap geographically.

A specific recommendation is that K/Rb ratios be obtained from a quartz latite and basalt from the map area as well as dioritic samples from the southern stock and the Castle Mountains. These few additional analyses should provide enough information to ascertain the feasibility of such a project.

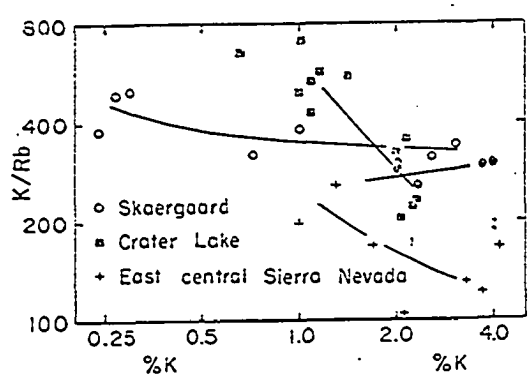

K/Rb ratios versus percentage of K for three rock suites.

Fig. 95 K/Rb ratios versus percentage of K for four igneous complexes; Skaergaard (circles), Crater Lake, Calif. (solid squares), East Central Sierra Nevada (crosses) and the Crazy Mountains (dots). Diagram modified from Taubeneck, 1965.

Niggli K-values

Moore, (1962) determined the Niggli K-value (molecular proportion of K20/K20+Na20) for 150 Cenozoic (some may be late Cretaceous) volcanic areas of the western United States including the Crazy Mountains (using Wolff's data). He plotted these values against the weight per cent of SiO2 and fitted curves from which he selected K-values for 50 and 60 per cent SiO2. These were plotted on a map of the western U.S. and contoured. The "selected" K-values range from .03 to at least .83.

The Crazy Mountains selected K-values for 50 and 60 per cent SiO2 are thus .33 and .32. The writer recalculated these values using Wolff's and the writer's new data. The values thus obtained are about .29 and .32 respectively indicating a slight positive slope to the curve (Fig. 96). (Moore had computed 14 geographic areas with horizontal trends including the Crazy Mountains). Although the writer's values are slightly different than those of Moore they do not alter his map contours. No different trends were ascertained for the two main rock series of the Crazy Mountains on the plot on Niggli K-value vs. SiO2 (Fig. 96), although the alkali (containing low SiO2) samples generally had a higher Niggli index than the alkali-calcic (containing low SiO2) samples.

Moore's contours indicate that a general increase in the K-value occurs from the West Coast eastward to the Colorado Plateau and in the middle and northern Rocky Mountains. Further east the values decrease, but the data are widely separated. He also indicates there is a strong correlation between the contours of the Bouguer anomaly map (Lyons, 1950) and his K-value maps (the correlation coefficient indicates that a probability of less than 1 in 1000 exists that such a correlation is due to chance). Where the K-value is high the Bouguer gravity is low and vice-versa (a large negative Bouguer anomaly indicates the crust is thick or especially light, possibly silicic). In addition, the quartz diorite line of the western United States (Moore, 1959) is an indication of the increase of potassium relative to sodium toward the east. To the west of this line the Mezozoic and Cenozoic batholithic rocks are dominantly quartz diorite while to the east they are dominantly granodiorite and quartz monzonite. Moore (1962, pp. 10-11) concludes:

> "The fact that the Cenozoic igneous rocks and the older granitic rocks show similar trends and that these trends parallel the continental margins as well as the regional Bouguer gravity pattern, suggest that the chemical differences from place to place are controlled chiefly by broad changes in the make-up of the earth's crust. The regional variation in K-value of the Cenozoic rocks could not likely have resulted from the differentiation of a single magma series inasmuch as the rocks of the Pacific Coast region are characterized by low K-value through their entire range, and those of the continental interior are characterized by high K-value through their ranges. The K-value appears to be related more to the geographic position of the magma chamber than to its age or the processes which took place in it....The alkali ratio of the Cenozoic igneous rocks apparently reflects a quasi-equilibrium with pre-existing rocks in their local environment even though

> locally magmatic differentiation may greatly alter the bulk composition of the specific igneous suites."

Gilluly (1965), (p. 28) in general agrees with Moore's views though he specifically criticizes the supposed relationship between the K-value and the gravity anomalies on the basis of more recent geophysical data. The present writer would also like to point out that it can be shown on Moore's maps that his generalities concerning the supposed relationship between the K-value and the gravity map does not hold in the south-central Montana area. This local discordance does not necessarily negate Moore's ideas as he was concerned mainly with regional trends.

In conclusion, Moore's method of drawing the best fit curve by eye appears to be valid since insignificantly different values were obtained by the writer even with more data. Moreover, Moore's major conclusions are validated.

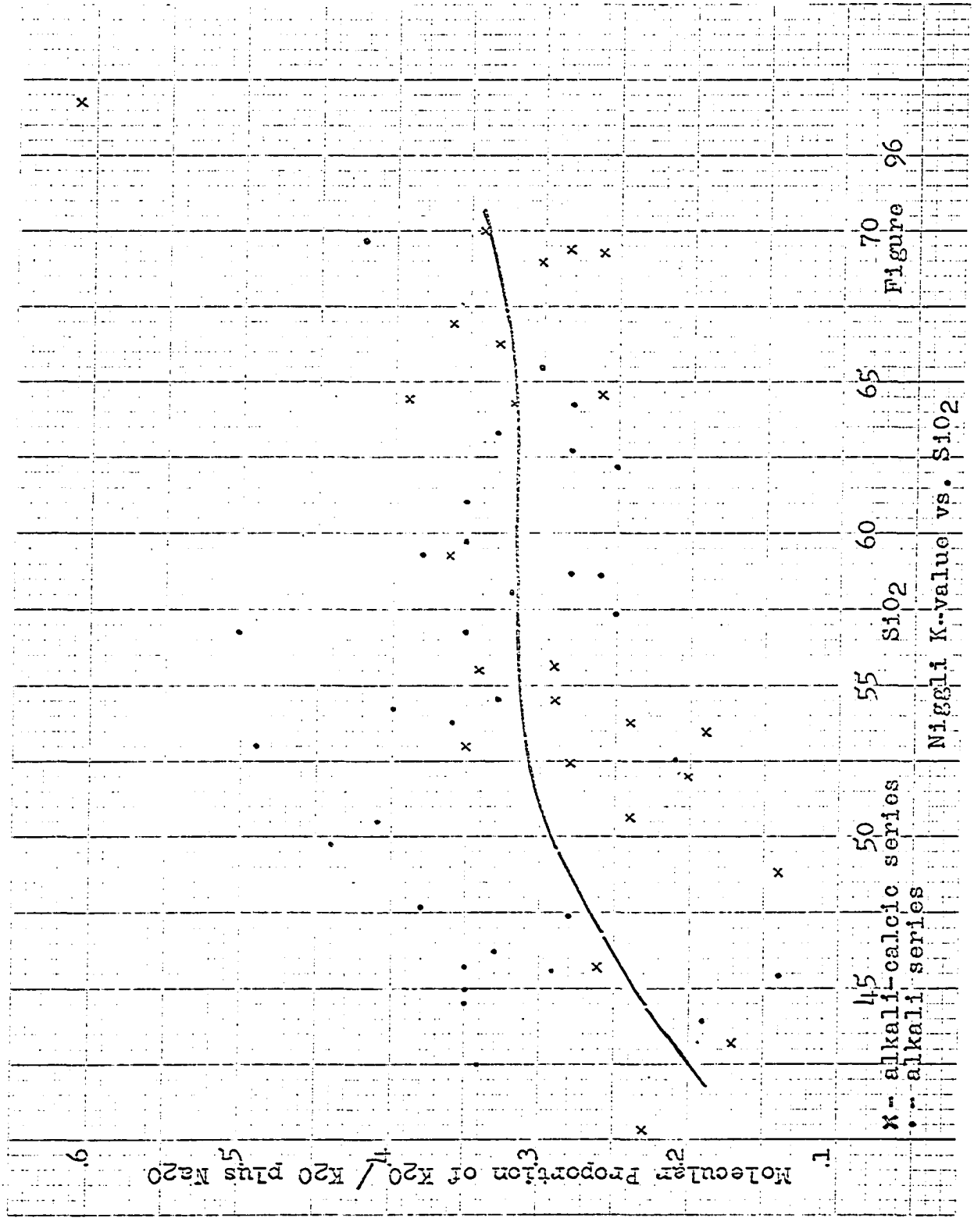

Differentiation and Crystallization indices

Because of recent interest and controversy concerning the differentiation index (Tuttle and Thornton, 1960, 1965) and the crystallization index (Poldervaart and Parker, 1964, 1965) as parameters of igneous differentiation, the writer has considered in detail various aspects of these indices.

The differentiation index is based on Bowen's concept of Petrogeny's Residua System. Bowen (1937) showed from six petrographically important, experimentally determined chemical systems that the residual liquids formed by fractional crystallization are enriched in alkali-alumina silicates. He considered that all magmatic liquids moved toward the system SiO_2—$NaAlSiO_4$—$KalSiO_4$, Petrogeny's Residual System. Thornton and Tuttle (1960) have reviewed and strengthened this concept in the light of more recent experimental data. They have attempted to make quantitative petrologic use of this concept by defining a measure of "basicity", the differentiation index. The differentiation index, D.I., is the relative amount of salic normative constituents of Petrogeny's Residua System in a magmatic rock. More exactly the D.I. is the sum of the weight percentages of normative quartz plus orthoclase plus albite plus nepheline, plus leucite plus kalsilite, and there are no more than three of these constituents in any norm. These are the salic constituents of the CIPW norm exclusive of anorthite and several other minor exceptions, zircon, corundum, halite, thenardite, sodium carbonate and others.

Figures 97-101 are those of Thornton and Tuttle (1960) in which D.I. is plotted against the major oxides for Washington's (1917) 5000 superior analyses of igneous rock. These data are indicated by contours. Also superimposed are curves for the Katmai, Alaska "average" igneous province and the Highwood Mountains alkaline sub-province. The dots represent all available chemical data for the Northern Crazy Mountains. (See explanation on p. 176.) The following discussion indicates the main geochemical relationships that can be ascertained from these figures.

SiO2 On the diagram of SiO2 versus D.I. (Fig. 97) the various rock groups are outlined and labeled. Some of these outlined groups are isolated while others are in juxtaposition. The malignite group has a definite trend toward ultra-alkaline rocks and is more undersaturated with respect to silica than the mafic part of the Highwoods Mountains trend. This characteristic is also possibly expressed by the smaller alkali lime index for the Crazy Mountains than for the Highwoods Mountains (p. 161). Distinctly separated from the malignites are the akerites and feldspathoid syenites and related rocks. The quartz latites are also isolated from the other groups. The single basalt, diorite, and quartz syenite (HA) and quartz latites are all representatives of the alkali-calcic trend according to the Larsen and Peacock diagram. These latter points fall nearly in a straight line which is lower in SiO2 but parallel to the main contoured trend, possibly being an expression of its alkali-calcic nature. In a sense,

this diagram is misleading in that the akeritic (AT, HL) rocks are shown intermediate in the sequence with respect to the malignite group and related feldspathoid syenites which is not in accord with the mineralogy and some other geochemical characters. (See petrography section and p. 187).

Al2O3 Aluminum Oxide variation (Fig. 98) is similar to the Highwoods in that the trend crosses the main contoured trend at about a D.I. of 60 with the mafic rocks being low in alumina. The scatter at high D.I. is due in large part to the presence of alkali-calcic rocks.

Fe2O3 Ferric iron (Fig. 100) is higher but parallel with the main contoured trends and slightly higher than the trend of the Highwoods province which is not shown. (Highwoods curves were not drawn by Thornton and Tuttle though points were plotted).

FeO Ferrous iron (Fig. 101) is lower than the main contoured maximum and the Highwoods trend at the felsic end. (FeO is so erratic for the Highwoods Mountains province that no curve was drawn by Thornton and Tuttle).

MgO Magnesium (Fig. 101) is higher than the contoured maxima and similar to the Highwoods curve though slightly lower. The scatter at the mafic end is due in part to the superposition of the two main series.

CaO The trend of calcium oxide (Fig. 102) is in general higher than the main maxima and the Highwood trend. The few examples at the mafic end which are slightly lower than the Katmai trend (andesite porphyry 652, basalt, 445B) are alkali-calcic according to other

diagrams. These are on line with a few akerites which are off the main trend (just below the crossing of the H and K lines). One akerite (35) ~~which~~ is alkali-calcic according to the Peacock index. Even though these rocks are mostly alkalic, this diagram shows them to be more CaO rich than a so-called calcic series such as the Katmai province.

Na2O Sodium oxide (Fig. 99) coincides with the maximum at the mafic end and rises at a greater rate than the maximum toward the felsic end. The trend is nearly parallel with that of the Highwoods trend, but is one to two per cent higher throughout.

K2O Potassium oxide (Fig. 99) is slightly higher than the main maximum at the mafic end and apparently slightly lower at the felsic end with a slight downward concavity at a D.I. between 70 and 80. The Highwoods curve is two to four per cent higher and nearly parallel to this trend.

Although only samples from the northern Crazy Mountains are plotted on these diagrams, there is evidence though vague for the two proposed main trends. There is also evidence of discontinuous chemical variation in the main alkali series as is indicated by the SiO2 vs. D.I. diagram.

Explanation of Differentiation index diagrams

The diagrams on the five following pages are contoured oxide vs. differentiation index diagrams. The contours are based on 5000 rock analyses from Washington's 1917 tables. Contour increments represent, from the outermost contour, 1-25, 26-50, 51-75, etc. points in a 0.16 per cent area. The silica diagram has two extra contours such that the increments represented are 1-12, 12-25, 26-38, 39-50, 51-75, 76-100 etc. points. Crosses represent average extrusive igneous rocks (Nockolds, 1954) and are as follows: (1) alkali trachyte, (2) phonolite, (3) calc-alkali trachyte, (4) latite, (5) rhyodacite, (6) andesite, (7) alkali basalt, (8) tholeitic basalt, (9) dellenite. Dots represent chemical analyses of northern Crazy Mountains igneous rocks.

Symbols representing names of Crazy Mountain Types according to the author and Wolff, 1938, are as follows: QL - quartz latite, and related types, As - aegerine syenite, NS - nepheline syenite, BO - Bostonite, SO - Soelvesbergite, AT - augite trachyte, HL - hornblende latite, LM - leucomalignite, M - Malignite, MM - Magnesian malignite, LA - Laurvikite, B - basalt, A - andesite porphyry, MP - mafic phonolite.

Lines drawn from the silica content of orthoclase and albite to anorthite largely separate silica-oversaturated, saturated and undersaturated types.

The variation curves for alkaline Highwood Mountains Montana

subprovince (Hurlbut, 1939; Larsen, 1941; Buie, 1941; and Burgess, 1941) and the "average" Katami, Alaska petrographic province (Fenner, 1926) are illustrated respectively with short dashes with an "H" and long dashes with a "K".

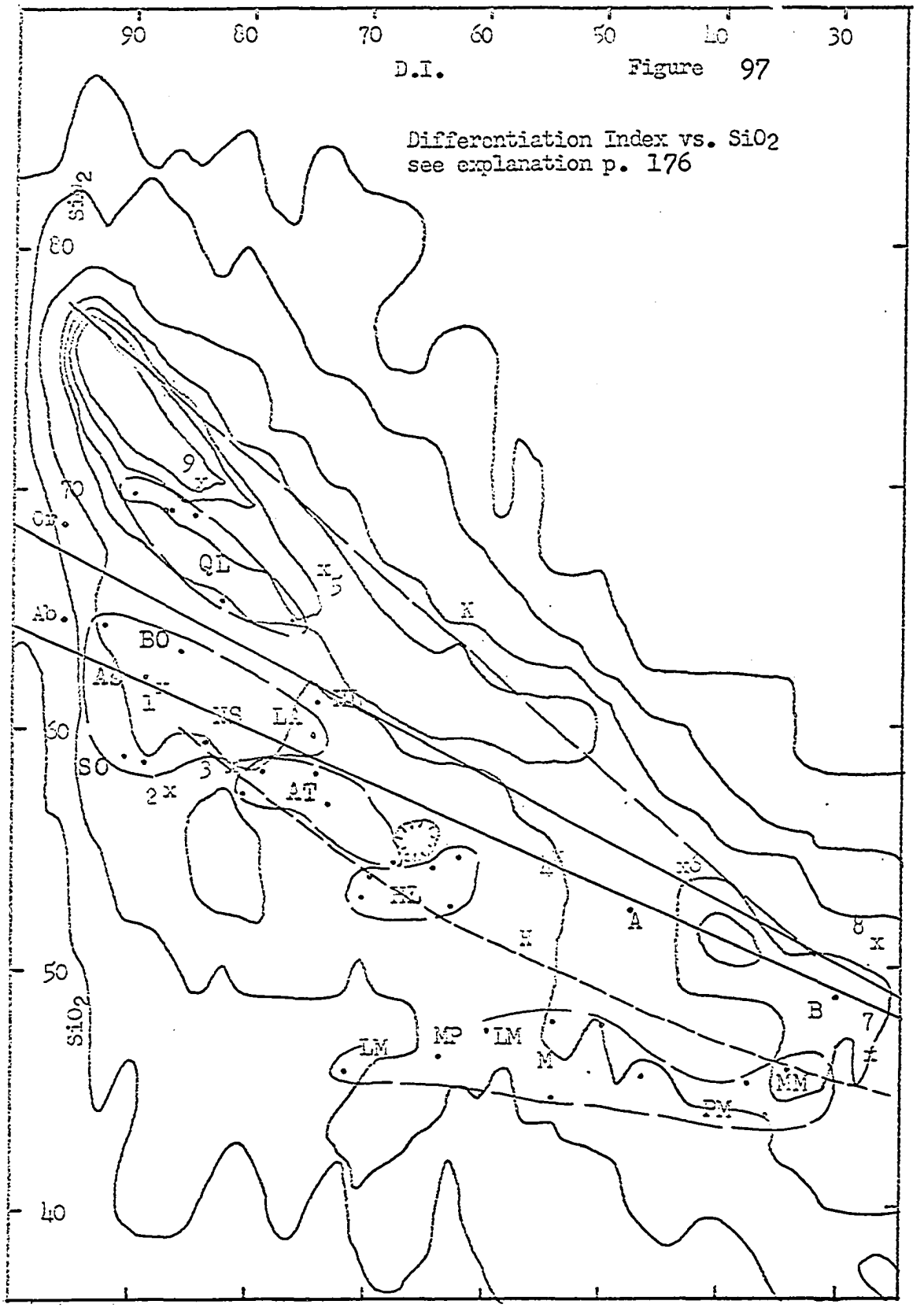

Figure 97

Differentiation Index vs. SiO_2
see explanation p. 176

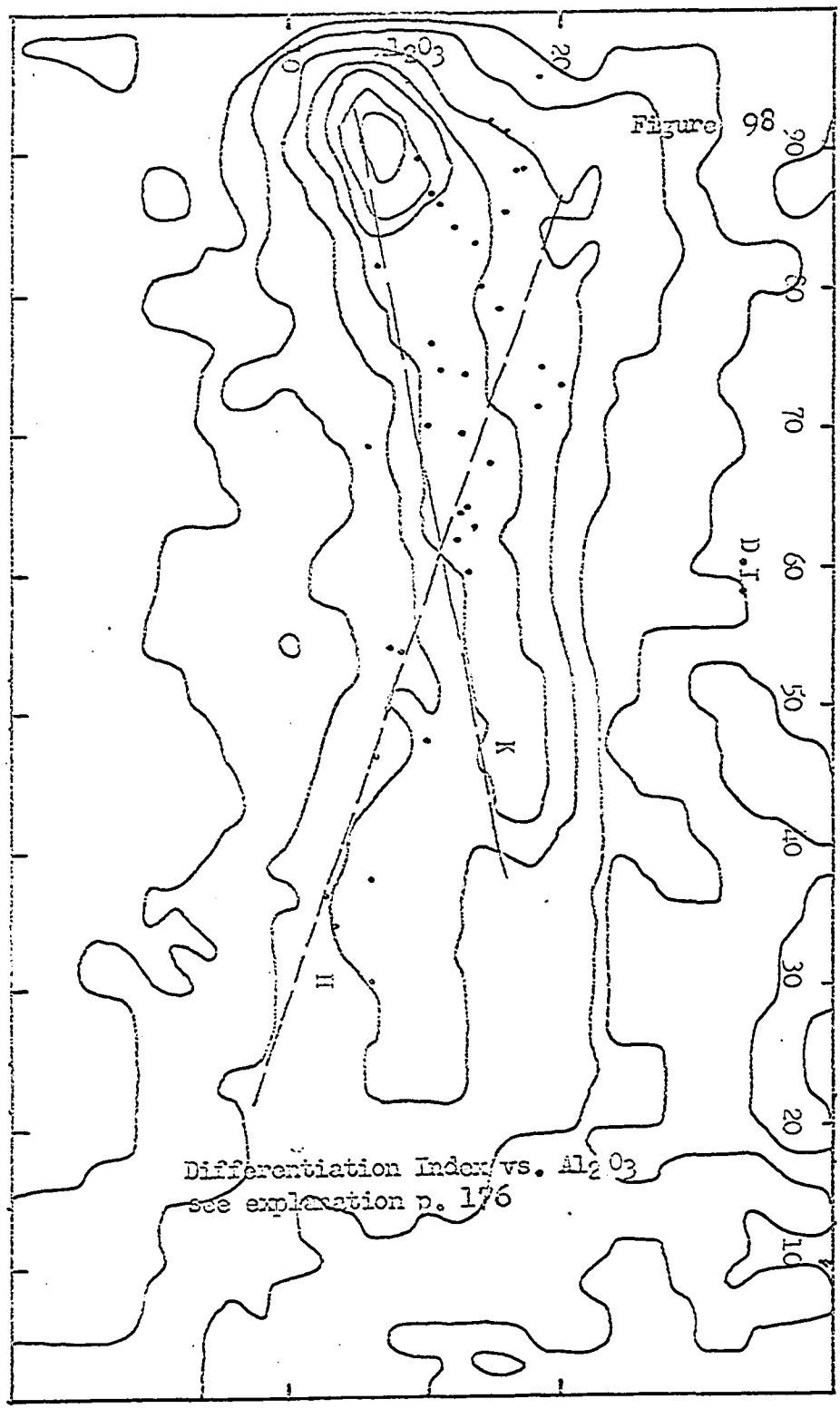

Figure 98

Differentiation Index vs. Al_2O_3

see explanation p. 176

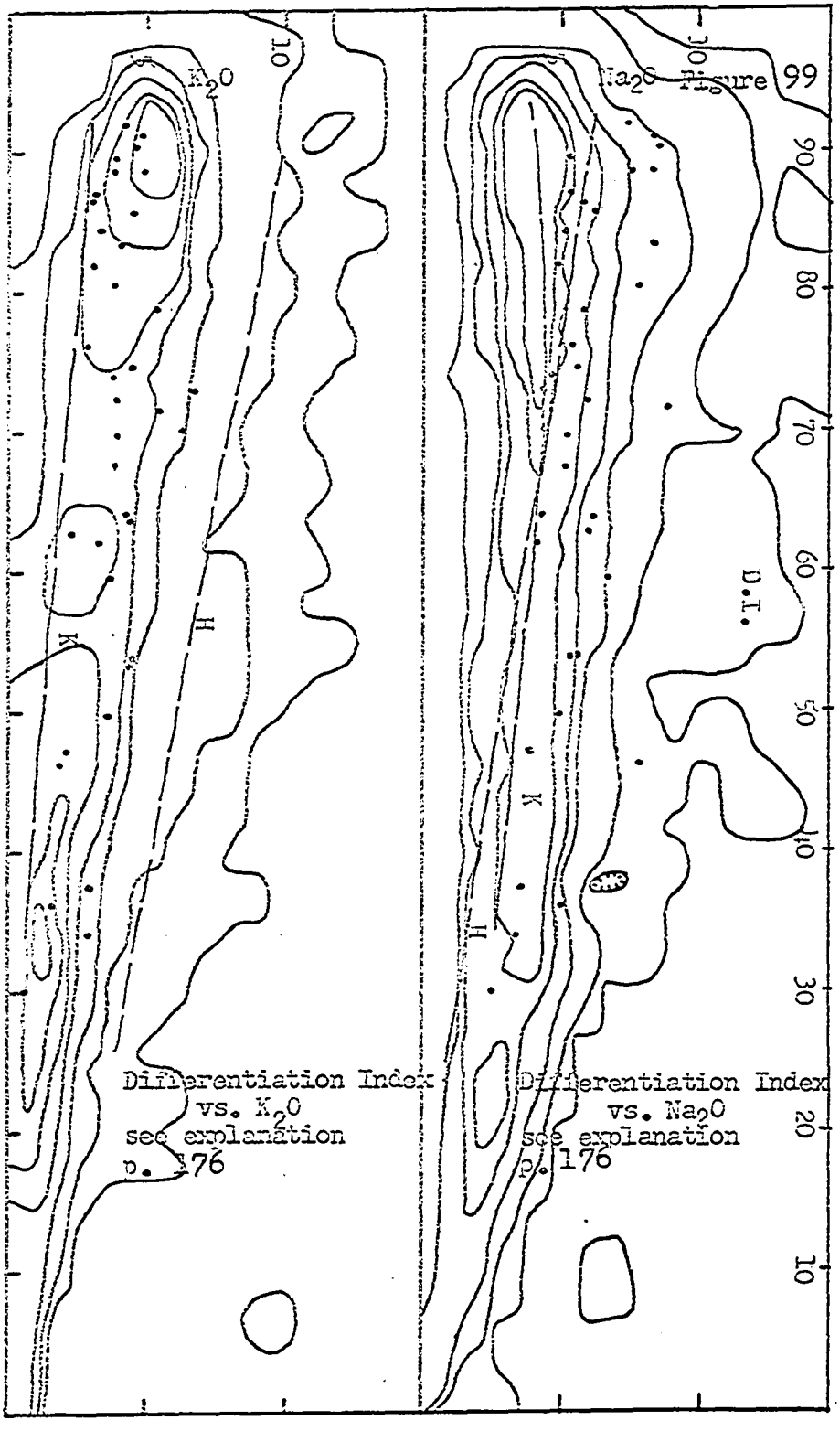

Figure

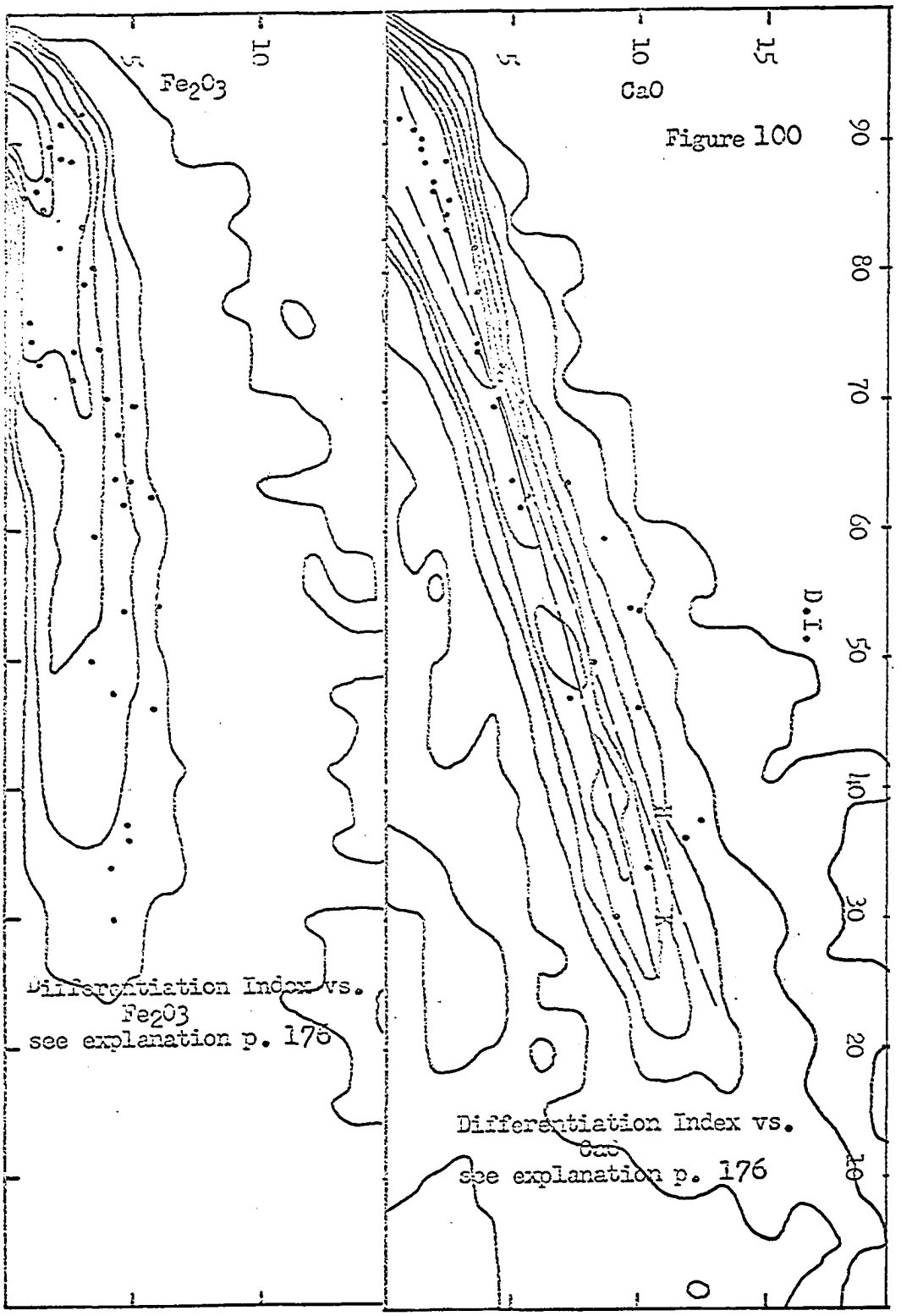

Figure 100

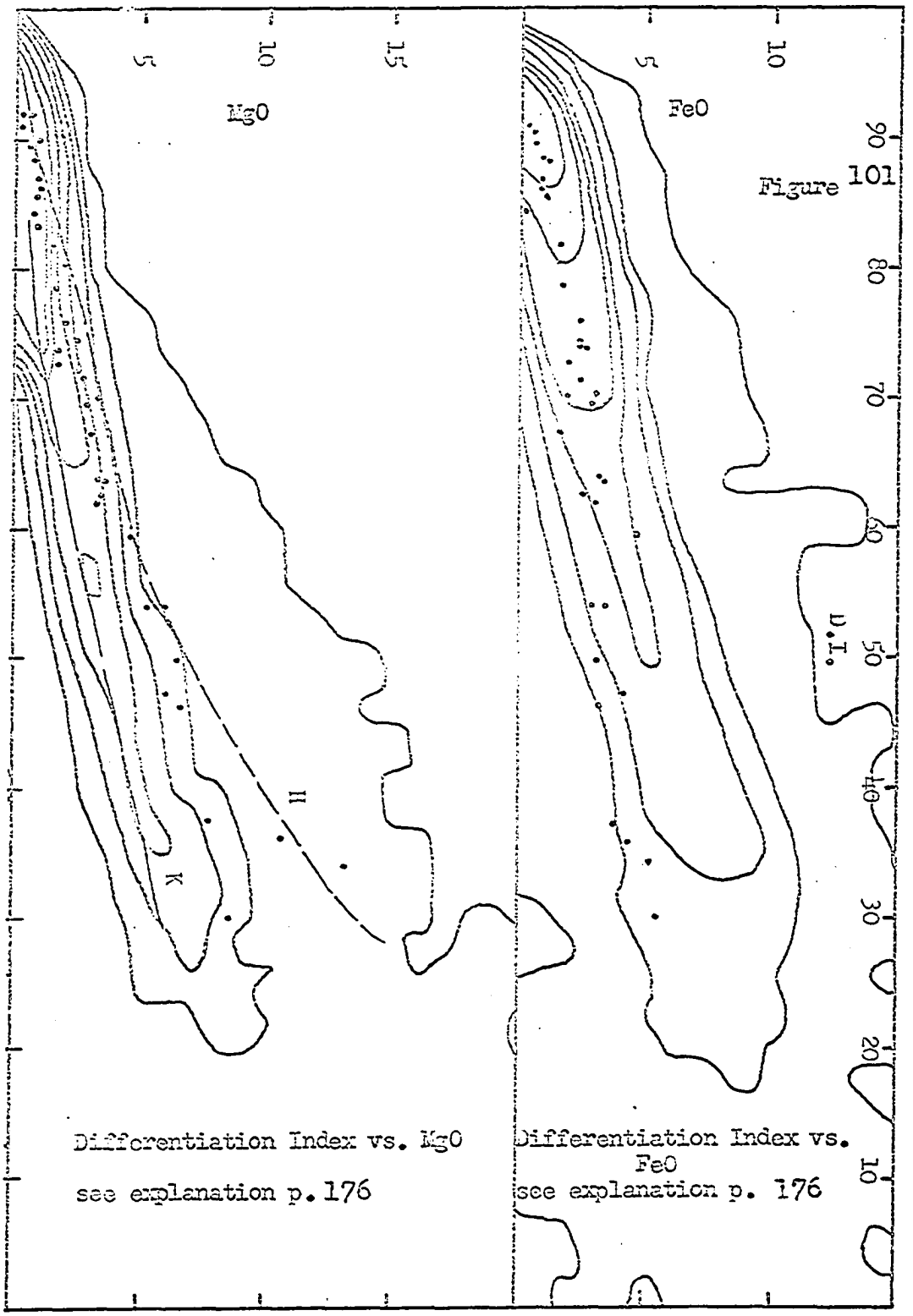

Figure 101

Differentiation Index vs. MgO

see explanation p. 176

Differentiation Index vs. FeO

see explanation p. 176

According to Poldervaart and Parker, (1964):

> "...Petrogeny's residua system SiO_2—$NaAlSiO_4$—$KAlSiO_4$ (Bowen, 1937, p. 11), contains different terminal points for oversaturated, saturated and undersaturated melts demonstrating that magmas differentiate toward more than one residium. Moreover, sodic melts that contain appreciable amounts of Fe_2O_3 probably crystallize considerably below the minimum temperature of the system SiO_2—$NaAlSiO_4$—$KAlSiO_4$ and many ultra-alkaline rocks are characterized by noteworthy amounts of Fe_2O_3 (see Nockolds, 1954, p. 1028-1029, Table 12). The system SiO_2—$NaAlSiO_4$—$KAlSiO_4$ is therefore not entirely representative of the residua of magmas, mainly because it lacks iron."

According to these workers a generally applicable parameter of igneous differentiation should be aimed at the "Onset" of crystallization and not the residua of magmas. The system anorthite—diopside—forsterite contains all the earliest phases of magmatic crystallization; it represents Petrogeny's primitive system. The system is expressed by the Crystallization Index which is defined as the sum of normative anorthite, normative magnesium diopside, normative forsterite, plus normative enstatite converted to forsterite, and magnesium spinel calculated from normative corundum in ultra-basic rocks.

Yet Thornton and Tuttle (1965) state that the sum of the salic constituents minus anorthite (D.I.) of a rock equals 100 minus mafic constituents and there is a simple linear relationship between CI and DI when there is no iron enrichment such as in the Skaegaard intrusion. But Poldervaart and Parker think that "iron enrichment is an important normal trend in differentiation of basaltic magmas"

(1965, p. 279) and differentiation can be best described by the C.I. As these workers show (Fig. 102) there are a number of igneous series in which there is not a simple linear relationship between C.I. and D.I. The northern (and five southern) Crazy Mountain samples follow a curved trend on C.I. vs. D.I. which is similar to those curves of the other series but much subdued.

These latter workers have plotted C.I. against excess or deficient normative quartz and have outlined four differentiation trends (Fig. 103). These trends are the normal ones for oversaturated, saturated, and undersaturated rocks and a rare ultra-alkaline series. Thornton and Tuttle (1965) have explained these four apparent trends on the basis of averaging (Poldervaart and Parker had used Nockold's average igneous types in the determination of trends). Superimposed on Figure 103 are the northern Crazy Mountains' samples plus five dike rocks from the southern Crazy Mountains. The diagram indicates the great diversity of igneous rocks that occur in the fifty-five square mile map area and nearby as examples occur along the major trends as well as intermediate areas.

Superimposed on the diagram are five per cent contours for the per cent of K20 plus Na20 minus CaO. The zero contour along which K20 plus Na20 equals CaO indicates a Peacock "index" with respect to C.I. of about 33 for all samples including the five dike rocks of the southern Crazy Mountains implying a Peacock "index" with respect to C.I. that would be equivalent for both main series of rocks. This

should be verified by plotting the other available analyses from the southern area on this diagram.

In one respect this diagram (Fig. 103) might be more enlightening than the SiO2 versus D.I. diagram (Fig. 97). On the Qu vs. C.I. Diagram, the akerites occur both saturated and slightly undersaturated with respect to SiO2 while on the D.I. versus SiO2 diagram they all appear undersaturated. Mineralogically, the first case is true. In addition, the akerites (latites - mafic trachytes) do not appear in an intermediate position with respect to the malignites and related feldspathoid syenites - trachytes as they do on the SiO2 vs. D.I. diagram. The malignite trend leads gradually to the position of the undersaturated syenitic rocks in the C.I. diagram which may be more expressive of the evolution of the series. Also, the ultra alkaline trend indicated by Poldervaart and Parker may be the subdued ridge which is indicated by contours on Thornton and Tuttle's C.I. vs. SiO2 diagram. Yet, the contour method may give a better visual representation as one does not have to know Nockold's method of determining the average igneous rock types to interpret the diagram as is necessary in the Poldervaart and Parker diagram.

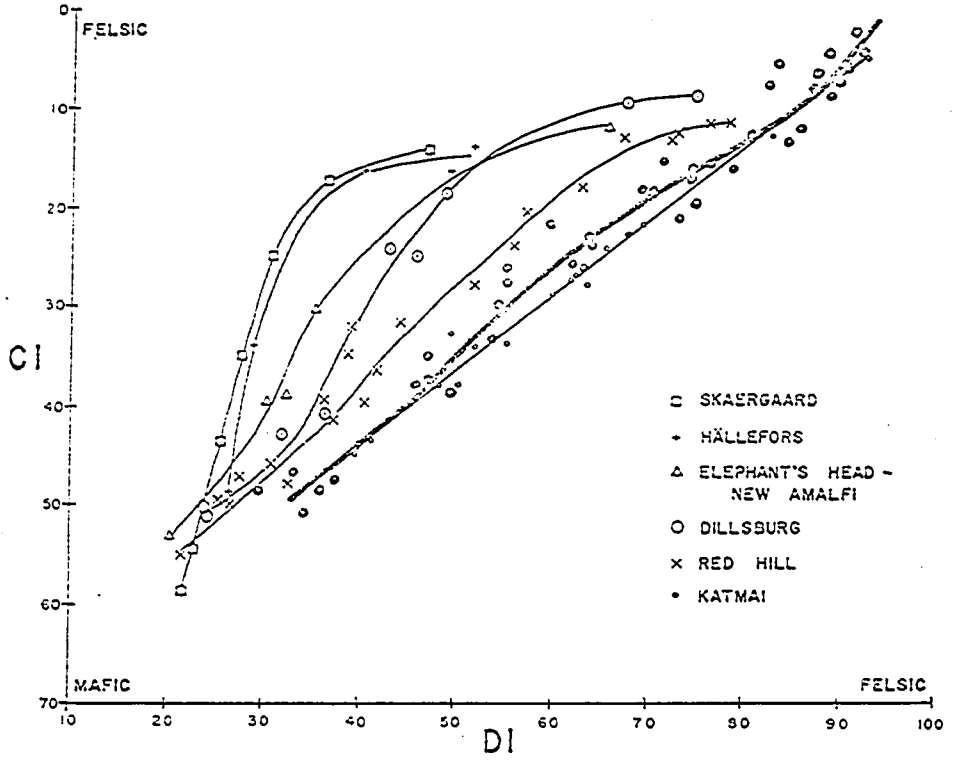

Fig. 102 Diagram of Crystallization Index (CI) vs Differentiation Index (DI) from Poldervarrt and Parker, 1965. Data for northern Crazy Mountains have been added (solid dots) for comparison.

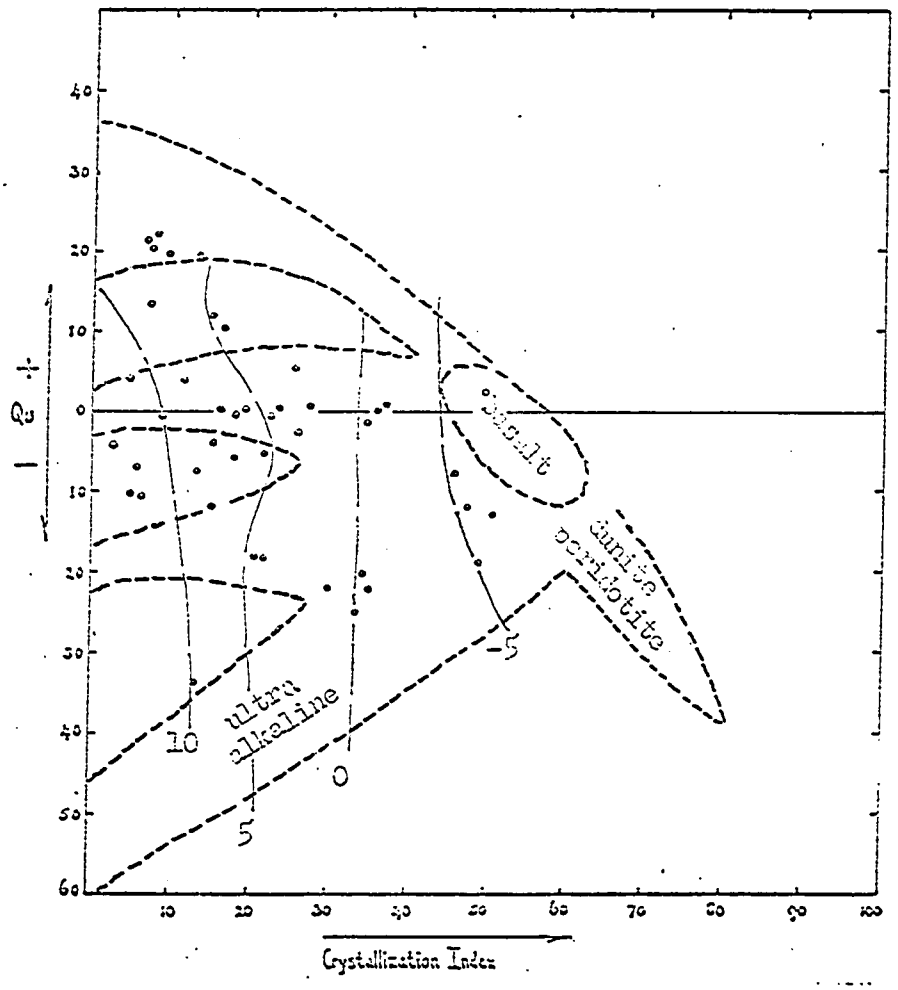

Fig. 103 Diagram of CI Against Qu. +Qu is normative Quartz, -Qu the weight per cent SiO_2 required to saturate the silica-deficient normative minerals. The various dashed trends as described in the text were ascertained by plotting Nolkolds' (1954) average igneous rocks. (They are not shown here). Dots represent the northern Crazy Mountains samples plus 5 samples from the southern Crazy Mountains. Contours represent the weight per cent of K_2O+Na_2O-CaO for Crazy Mountain rocks (see text).

Larsen binary variation diagrams

A binary variation diagram was used by Larsen, (1940) to describe and relate the chemistry of the various subprovinces of the Central Montana Petrographic Province, The parameters of this diagram are weight per cent of oxides taken separately versus an index considered to represent the degree of differentiation in a magma series. The Larsen index equals 1/3 SiO2 plus K2O-MgO- (CaO plus BaO plus SrO) - (FeO plus 0.9 Fe2O3 plus MnO). This index is calculated after SiO2, Al2O3, FeO plus 0.9 Fe2O3 plus MnO, MgO, CaO plus BaO plus SrO, K2O and Na2O are adjusted so that their sum is one hundred per cent. Because of the weight that was placed on the above diagram by Larsen in his petrogenetic considerations, the writer has reconsidered the diagram in light of recent chemical analyses and other geologic information. Larsen plotted the analyses of the Crazy Mountains on two sets of variation curves. Strongest weight was placed by him on geographic location in the determination of the set of curves which a particular analysis belonged to (Fig. 105, 106). The writer has reconsidered these curves with respect to other types of variation diagrams, mineralogy and other geologic aspects. It became evident to the writer that less complicated curves than Larsen's could be derived, assuming that two major overlapping series occur as indicated by the Peacock diagram. The following discussion presents methods and results.

Many of the present writer's chemical data are plotted with

Larsen's data for the northern Crazy Mountains (1940, Fig. 9, p. 904) and are shown here as Figure 104. Some of the writer's and Wolff's data lies closer to the curves of Larsen's variation diagrams for the southern Crazy Mountains (dotted samples on Fig. 105). These samples are 479A, 394, 578 which are not plotted on Fig. 104, and 445B, 652A, 282, 145 and 45 89' which are plotted on Fig. 104 to show how poorly they fit on this diagram. These particular samples are the very ones of the northern area which are closer to the Peacock curves (alkali-calcic) more typical for the southern area (Fig. 94). Also Shonkinose (?) dike 170 07 of the southern area plots on the northern variation curve as might be expected from the Peacock diagram. Akerite 45 89 is the only exception to the above statements in that it occurs on the southern Peacock curves but northern Larsen curves. As with the Peacock diagrams, those northern samples which fall closer to the southern (alkali-calcic) curve and visa versa are in the range of those curves where there is an absence of examples on Larsen's diagrams.

For the Larsen diagram of the northern area (Fig. 104), not considering samples transferred to the other diagram (Fig. 105) as indicated above, a simple curve has been constructed by sight and represents the general overall trend of the data. These curves are similar to those ascertained by Larsen. The sodium curve is higher but parallel to Larsen's curve. Otherwise the curves differ mainly at the basic and felsic ends. Complexities in Larsen's curves at the felsic end have been eliminated and better approximation of the trends

at the basic end have been made possible. These latter data are especially important as Larsen (1940) in his consideration of the primary magmas of the subprovince proposed compositions of the various subprovince primary magmas from basic ends of variation curves, i.e. the most basic rock types. It is evident from the new curves that the composition of the primary magma of the Crazy Mountains would be somewhat different than that of Larsen (1940, p. 922). Thus some of his conclusions need to be reconsidered (p. 192).

It is also evident that Larsen's southern curves will be changed in certain parts by the additional data from the northern area. Without constructing new curves for the southern area the main differences between the two sets of variation curves can be stated: (1) The alkalic (northern) curves have higher Na2O and (F2O +0.9 Fe2O3) in the intermediate and felsic parts and higher CaO at the basic end than the alkali-calcic curves. (2) the alkali-calcic curves have higher SiO2 throughout and higher CaO for the intermediate and felsic types than the alkalic curves (reflecting the alkali-calcic nature). The two sets of curves are similar in the intermediate values which may have genetic implications.

The variation of Al2O3 is very erratic on both of these sets of curves. This scatter is common in igneous rock series as was noted by Larsen (1938). It was due to this scatter that he did not account for Al2O3 in his index. Also Na2O and K2O are very erratic in the alkalic curves. Part of the spread of the data and complexi-

ties of the curves is due to the fact that each of the two series is made up of groups of related rocks some of which may be subseries. For instance, the hump in the left part of the Na2O curve of the alkalic series is due to the highly sodic basic malignites in conjunction with the intermediate akerites. Another reason for scatter is the significant deuteric alteration in these rocks.

A further indication of the geographic overlap of these rock series is indicated by the following considerations: Larsen (1940, p. 902) noted that the diorite stocks of the Castle Mountains do not lie on the variation curves of the Little Belt - Castle Mountains subprovince and must belong to another series. The two samples accord with both of the Crazy Mountain variation diagrams, but best with the alkalic curves. Tanner (1948) attempted to compare these samples with the Crazy Mountain curves but apparently did not realize that the Highwood and Crazy Mountain alkalic subprovince diagrams are reversed by printer's error in Larsen's (1940) paper.

In summary, the considerations above indicate that a wide overlapping of rock series of several subprovinces occurs. Also, the two main series are similar in the intermediate ranges. In fact some of the intermediate akerites could almost as well be placed on the alkali-calcic curves providing examples in range devoid of samples. The Peacock Diagram concurs with the present arrangement except 45 89' (which is one of the above mentioned akerites). Part of the reason that the above show the two trends as being similar in the intermediate range is due to the non-consideration of alumina in the indices.

The table below lists various estimated compositions of the original magma of the alkali series of the northern Crazy Mountains. The estimate in column 1 was ascertained by Larsen (1940, P. 921) from the "...variation diagrams taking into account the position near the mafic ends beyond which the rocks do not fit a regular variation curve." Methods of other estimates are not given by him. Column 2 is an estimate made by the writer using the newly ascertained curves. The estimates were made at a Larsen index position of minus 16. Column 3 is Wolff's (1938, p. 1606) estimate for the parent magma of the alkali series which is the average of 97 07, the laurvikite stock at the head of Comb Creek and the mean of four theralites (malignites).

Table 3

	(1)	(2)	(3)
SiO2	48.8	46.5	53.71
Al2O3	15.0	14.7	16.58
Fe2O3			2.90
FeO	9.1	9.7	3.26
MgO	5.2	11.5	4.81
CaO	11.1	12.7	6.62
Na2O	5.9	2.5	5.49
K2O	4.8	2.0	4.24
BaO	0.4	?	0.52
SrO	0.1	?	
MnO	0.1	?	
TiO2	0.9	?	0.75
P2O5	0.9	?	0.91
H2O+	0.9		0.90

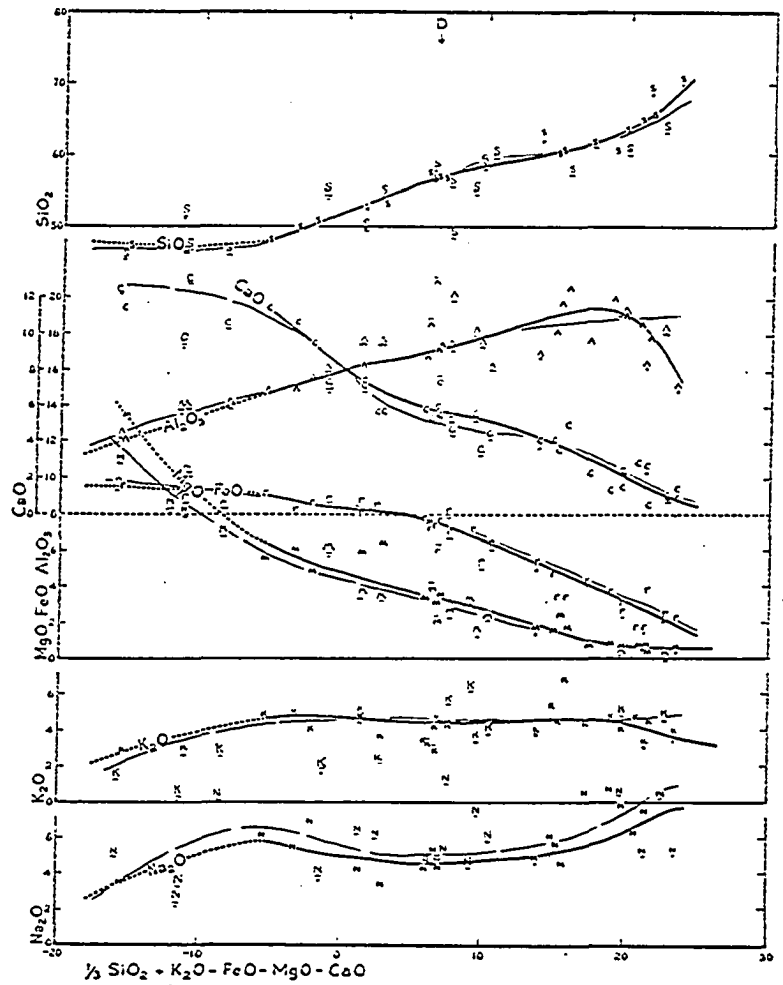

Fig. 104 Variation diagram of rocks of the northern Crazy Mountains (Larsen, 1940, p. 904). Underlined letters indicate the writer's data which have been added. Revised curves have been ascertained from all these data except that with the dots below. New curves are indicated by the narrow long dash lines. The dotted analyses are closer to the curves of the southern Crazy Mountains as is indicated by the following figure. Also superimposed are analyses of the two diorite stocks of the Castle Mountains, Montana. These are indicated by the "D" and the dashes above the letters. Considering the undotted analyses, the left hand side of curves represent malignites. From an index of about 0 to over 10 the analyses are the latito-mafic trachyte group and the higher indices are nepheline syenites, syenites and related types. The dotted mafic samples are basalt and diorite and felsic dotted samples are quartz latites and related types.

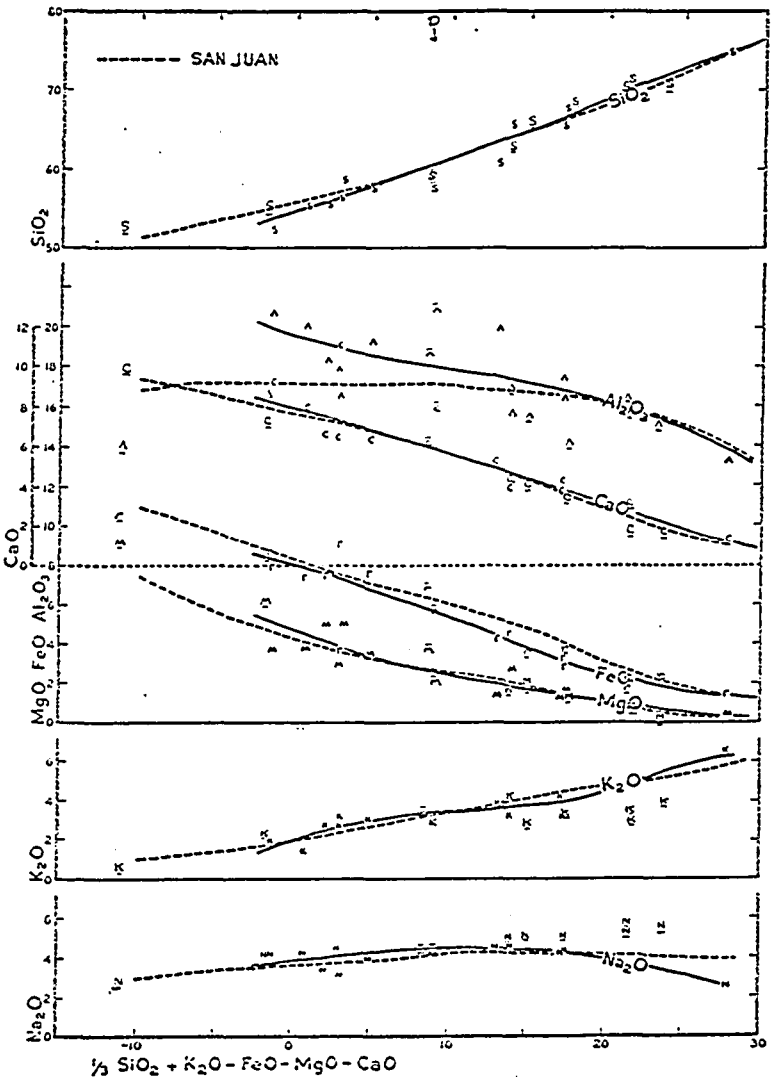

Fig. 105 Variation diagram of rocks of the southern Crazy Mountains compared to the San Juan, Colorado province (Larsen, 1940, p. 900). Superimposed underlined letters are samples from the northern Crazy Mountains which overall are closer to these curves than the curves of the northern area. Letters with lines above indicate the two diorite stocks of the Castle Mountains.

Larsen tertiary variation diagrams

Larsen (1938, p. 517) introduced two superimposed triangular chemical variation diagrams based on modifications of rock norms. One plot represents per cent Or, An, and Ab of the total normative feldspar after calculation of nepheline and leucite to feldspar. The second plot is of relative amounts of normative feldspar, femic minerals and quartz or deficient SiO_2 computed from the formation of feldspar from nepheline and leucite, as well as the formation of pyroxene from olivine. On the diagram these plots are connected by a line.

On these diagrams Larsen compiled the chemical data of each subprovince of the central Montana petrographic province, including the two Crazy Mountain subprovinces. It is obvious from his diagram that many of the quartz-bearing rocks on the diagram for the alkalic subprovince of the Crazy Mountains fit better on the diagram for the alkalic-calcic subprovince (Larsen's lime-alkalic subprovince). They would plot in the part of the diagram where there is an absence of data.

Because of this discrepancy, the writer has replotted Wolff's data as well as the more recent analyses on this type of variation diagram, taking into account geographic overlapping of the two series. The same samples of the northern area, which fit best on the Peacock and Larsen binary variation diagrams (p. 188) of the alkalic-calcic series also fit best on the Larsen terniary diagram for the same series (Fig. 106, 107). These two diagrams display the

continuous variation of the two main series, with the (latite-mafic trachyte) group intermediate to the feldspar end of both of the main series. This relation is also indicated by the C.I. vs. quartz plus or minus diagram (Fig. 103) and the D.I. vs. SiO2 diagram (Fig. 97). The Larsen ternary diagrams also indicates that some of the latites-mafic trachytes are near the alkalic-calcic trend while others are near the alkali trend. This spread is also indicated by the akerite (latite-mafic trachytes) mineralogical variations and other chemical variation diagrams. The rapid change in the amount of femics at the introduction of normative quartz into the alkalic-calcic trend (Fig. 107) may be due to omission of representative samples. Some of the intermediate group might fall in this gap.

Of all the subprovinces treated by Larsen (1938-1940), on this type of ternary diagram the alkalic-calcic subprovince of the Crazy Mountains is most similar to the Yellowstone and Crandall subprovinces, and is somewhat like the Little Belt subprovince.

On the alkali series diagram, the malignite series, represented by the longest lines to the most silica-deficient points, with decreasing mafics lead to the feldspathoid syenites and trachytes. A number of these have converging lines indicating a similar normative An, Ab, Or ratio. The ratio (not recalculating Ne, plus Lc to feldspar) for these samples (with the least An content; generally less than one per cent) is about Or 34-35, Ab 66-64.

These diagrams indicate two continually varying series, though the variation displayed for the normative feldspar of the

malignites is erratic which is also characteristic for other alkaline subprovinces such as the Highwoods Mountains. This character may give some indication as to the nature of the genetic process. On the other hand, the discussed diagram may not be particularly suitable for showing continual variations in highly alkaline series because of the nature of the calculations. Also indicated by the diagram is a group of rocks intermediate to these widely varying series which may be partly related to both (akerites).

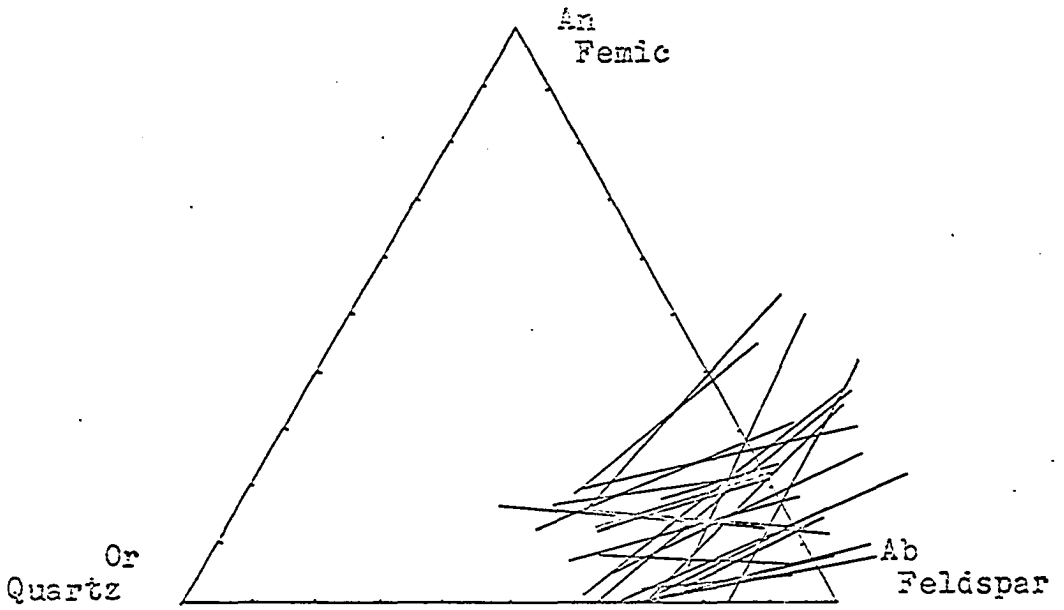

Fig.106 Same as Larsen's (1940) diagram below but including the writer's chemical data and excluding the more quartz-rich samples which fit better on alkali-calcic diagram. Left hand end of each line represents the composition of the normative feldspar.

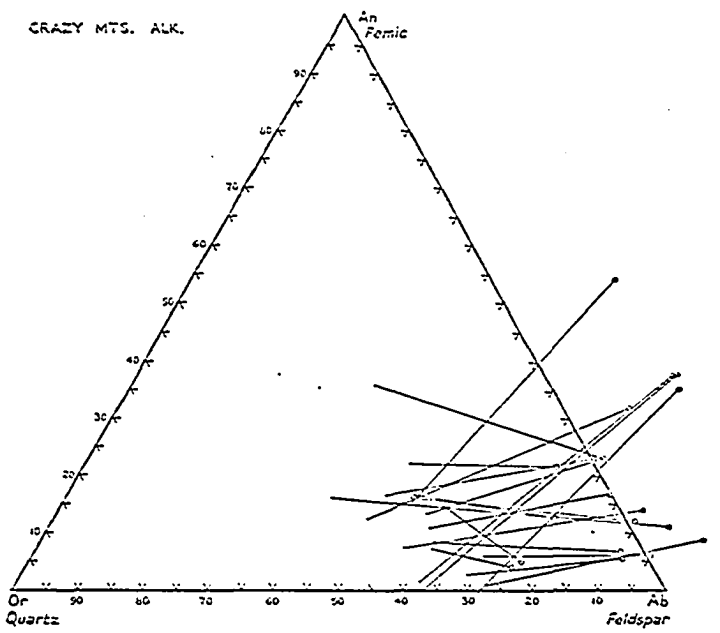

—*Triangular diagram of the norms for the northern (alkalic) subprovince of the Crazy Mountains*

Dots = Composition of normative feldspar.
Circles = Feldspar-femic-quartz or deficiency in SiO_2.

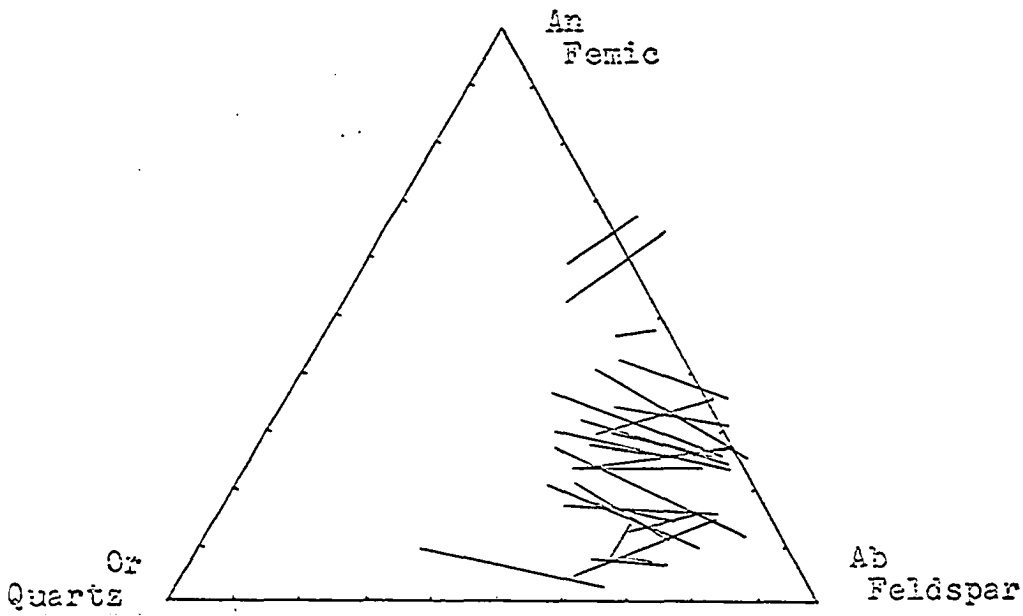

Fig. 107 Same as Larsen's (1940) diagram below, but replotted with some samples from the northern Crazy Mountains and some of the writer's chemical data. Left hand end of each line represents the composition of the normative feldspar.

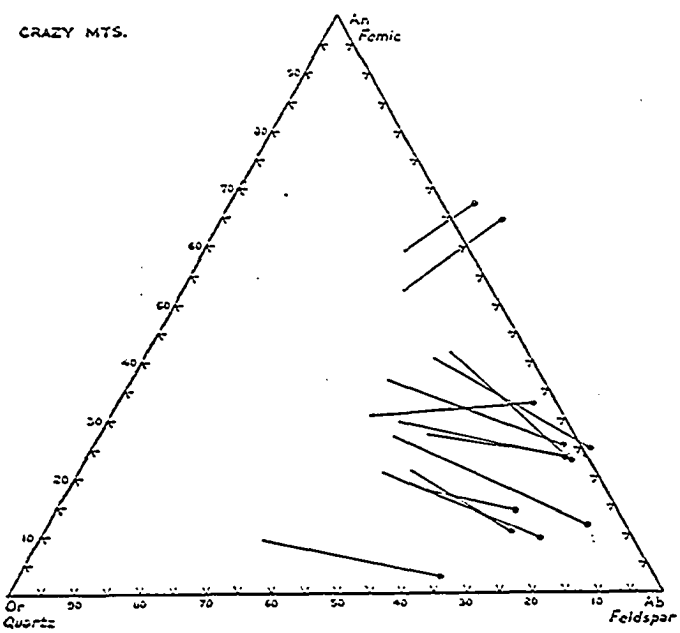

FIGURE 10.—*Triangular diagram of the norms for the southern (lime-alkalic) subprovince of the Crazy Mountains*

Dots = Composition of normative feldspar.
Circles = Feldspar-femic-quartz or deficiency in SiO_2.

Na2O- K2O-CaO and Alkali - FeO-MgO ternary variation diagrams

Plotted on these two ternary diagrams are the relative weight per cent of Na2O-K2O-CaO and Alkali (Na2O plus K2O)-FeO (FeO plus Fe2O3) -MgO (Fig. 108). Although these diagrams are easy to compute they have not been popular possibly because of considerations mentioned below.

Poldervaart (1950) used these diagrams to show basaltic trends. LeMaitre (1962) considered a slight variation of this diagram (total iron is computed as FeO). He used these diagrams to show that the igneous trend of Gough Island is chemically very similar to five other islands of the mid-Atlantic Ridge. Using these variation diagrams igneous trends of the northern Crazy Mountains are similar to those of the Oceanic islands mentioned above, especially the Tristan De Cuhna (Fig. 108). Broader trends are indicated for the Crazy Mountains than those of the Oceanic islands. This may be due in part to the more numerous samples and overlapping of series in the Crazy Mountains. These Oceanic islands consist mainly of basalt and less amounts of trachyandesite, trachyte, phonolite and rhyolite. The northern Crazy Mountains contain equivalents but little basaltic material is represented.

Insight into the usefulness of these diagrams is expressed by the statement of LeMaitre (p. 1336, 1962): "Although these types of diagrams may be useful in distinguishing major differences between rock series, e.g. alkali or tholeiitic, they can be very deceptive in the detailed comparison of similar provinces."

More subtle differences and similarities might be brought out by superimposing the two diagrams and drawing the lines between equivalent points similar to the Larsen triangular diagrams (Fig. 107, 108). This proved somewhat unsuccessful for the northern Crazy Mountains because of overlapping abundant data.

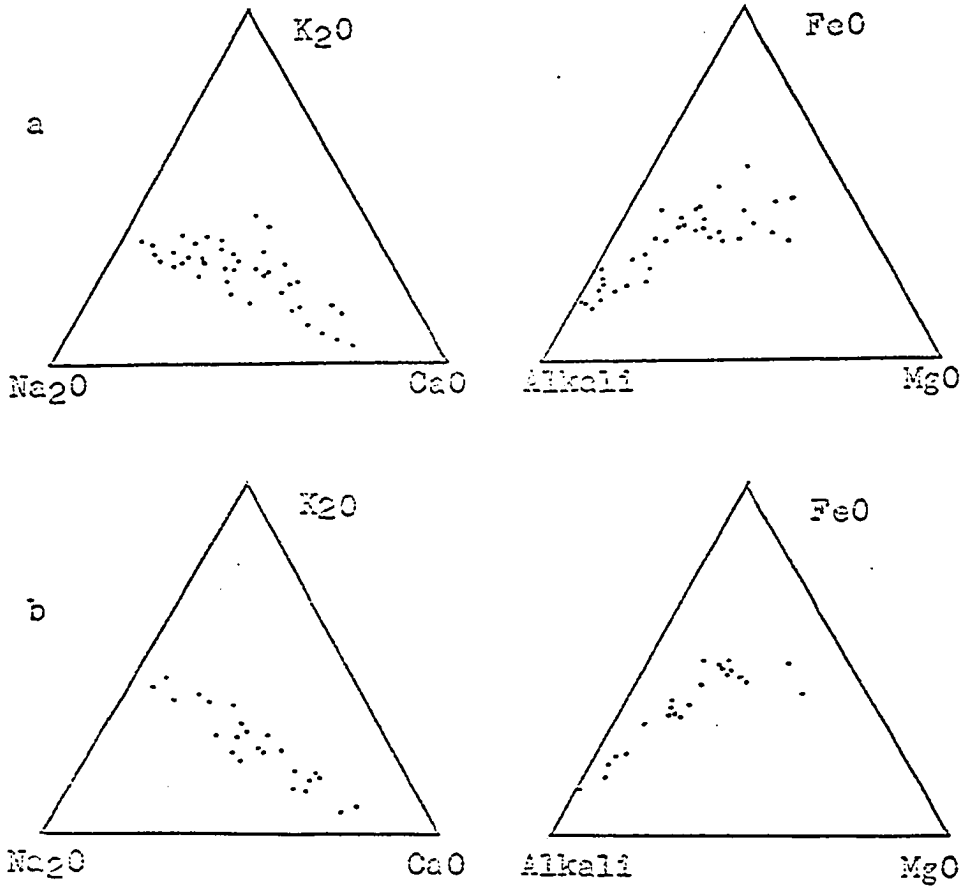

Fig. 108 Ternary diagrams of Na_2O-K_2O-CaO and Alkali-FeO-MgO for (a) the northern Crazy Mountains and (b) the Oceanic Island of Tristan De Cunha; see explanation p. 200

The leucocratic rock types with respect to the system NaAlSiO4-KalSiO4-SiO2 and related systems

Of the 43 chemically analyzed rocks that have been studied, 14 consisted of at least 80 per cent normative salic constituents (Plate 2) and 3 more have at least 76 per cent salic constituents. Therefore, these rocks lie approximately in the system NaAlSiO4-KAlSiO4-SiO2 (Fig. 109) where they occur as two rather distinct groups: (1) the quartz latites and rhyolite porphyries (2) the feldspathoidal syenites, trachytes and variants (bostonites, soelvsbergites, laurvikites,) and one mafic trachyte. All of these samples fall in the low temperature trough of this system indicating that the IMMEDIATE cause of their various types could be fractional crystallization of a magma by separation of alkalic feldspars. Partial melting must be eliminated because it would take unusual rocks to form nepheline syenite by this method. Further, the two distinct groups appear to be leucocratic members of two gradually varying series according to other chemical diagrams and petrography.

This might be compared with the Cenozoic petrographic provinces of New Zealand studied by Benson (1941). Intermediate types occur between two main groups found there. (Only the trachytes and phonolite field are shown on diagram 109a).

The feldspathoid syenites, trachytes and variants lie across the silica saturation line in character with their names.

The quartz latites and rhyolite porphyries lie near the ternary minimum in the system Or-Ab-Qu, from above 10,000 to 5,000 p H20 (Fig. 109, 110, Samples 173 and 205 from the southern stock are also plotted on this diagram). The calculated matrix of 479A plots near the "Average Granite" to the right of the low temperature trough as does aplite 205.

Kleeman (1965) emphasized the nonsuperposition of the "Average Granites" on the low temperature trough and showed that "Average Granite" coincides better with the low temperature trough in the system Or-Ab-An. He thereby concludes that the diagram Or-An-Ab may be more useful in ascertaining the evolution of granitic magmas.

It is interesting that the northern Crazy Mountains acid rocks plot in the converse relation to which Kleeman shows: while they occur along the ternary minimum in the system Ab-Or-Si02 they are in the plagioclase field in the diagram Ab-An-Or.

The calculated composition of the matrix of 479A is on the projection of the curves drawn through 479A total composition. It occurs near the "Average Granite" in both systems and therefore the thermal trough of the diagram Ab-An-Or. This indicates that by separation of the feldspar phenocrysts one could derive a magma composition such as aplite 205 which occurs as dikes in the southern stock (though it does not explain aplite 22).

It should be noted that the data fall fairly close to a sharply bending curve on the An-Or-Ab plot while some of the data

are not near the main curve for the Qu-Ab-Or diagram. If one eliminates Wolff's analyses and especially analyses outside the map area a very smooth curve is obtained leading to the matrix of 479A for this latter diagram. In this smooth curve representing the writer's analyses (394, S-70, 479A, 578) a systematic decrease in the amount of plagioclase phenocrysts occurs in the direction of the granitic end which concurs with the possibility indicated in the last paragraph. Detailed study on the feldspars, particularly the interesting small 2V potash feldspar is necessary before definite conclusions can be made.

In conclusion, two fairly well separated groups of rocks fall in the low temperature trough of Petrogeny's residua system indicating that fractional crystallization could have been important in deriving these residual rocks (at least the feldspathoid syenites and syenites). The separateness of the two groups coupled with the other geochemical considerations indicates these are likely residual fractions of two magmatic series.

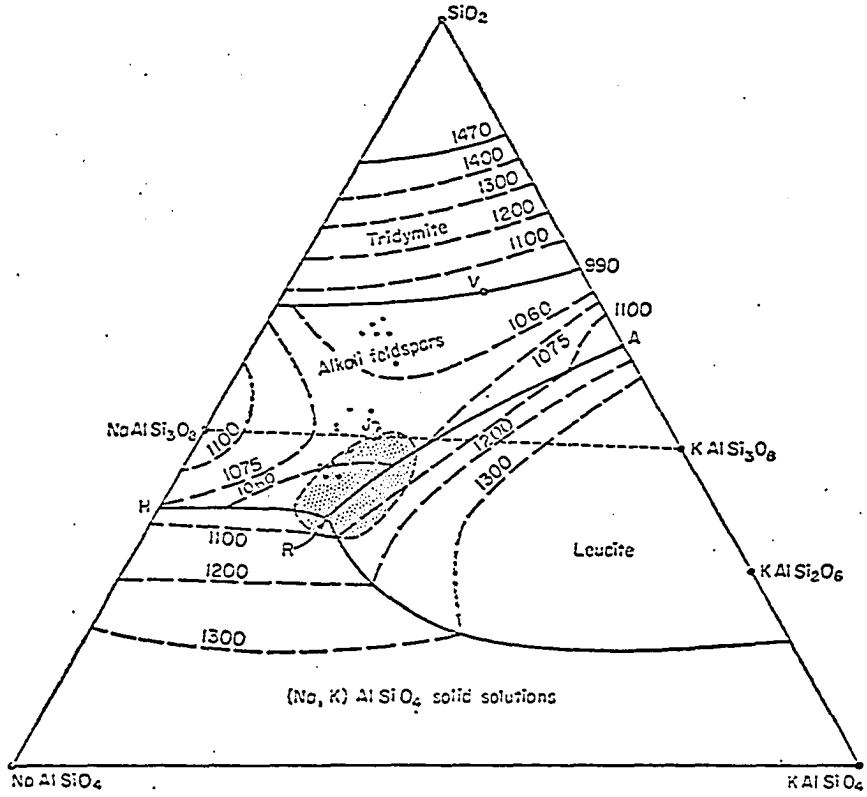

Fig. 109A

Temperatures of crystallization in the anhydrous system $NaAlSiO_4$-$KAlSiO_4$-SiO_2 at atmospheric pressure. (*After J. F. Schairer.*) Minimal temperatures, marking the axis of a low-temperature trough are at *R* (1020°C.), *J* (1063°C.), and near *V* (less than 990°C.). Stippled area marks the range of composition of salic portions (less anorthite) of trachytes and phonolites of eastern Otago volcanic province, New Zealand. (*After W. N. Benson.*) From Turner and Verhoogen, 1960

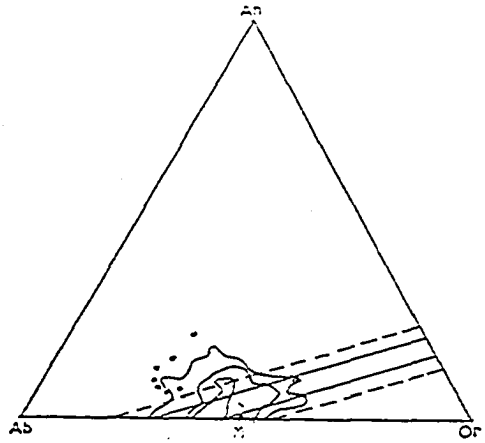

The relation of the "Average Granite" to the low-temperature trough of the Or-Ab-An-SiO_2 system. Dashed lines show the uncertainty due to possibility of analytical error. The contours (after Tuttle & Bowen, 1958, Fig. 67) represent the normative Or:Ab:An ratio in 1,269 rocks that carry more than 80% normative Ab+Or+Q.

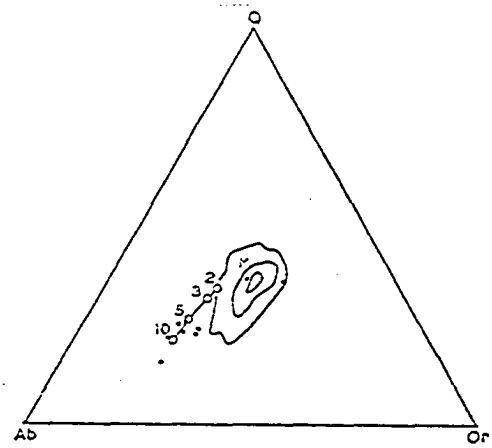

The relation of "Average Granite" to the Or-Ab-SiO_2 minima at 2,000; 3,000; 5,000; and 10,000 bars P_{H_2O} in the system Or-Ab-SiO_2 (after Luth, Jahns & Tuttle, 1964).

These diagrams from Kleeman, 1965

Fig. 109 On the diagrams above are plotted rocks with over 76 per cent normative salic constituents from the northern Crazy Mountains plus two samples from the southern Crazy Mountains. M represents the matrix of 479A. The same data are not plotted on all of the diagrams. See next diagram.

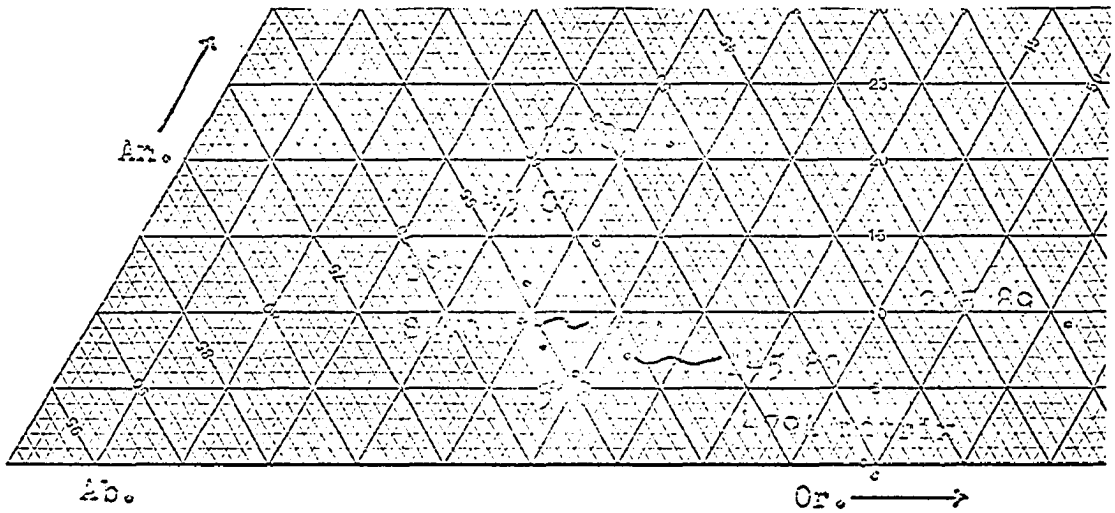

Enlargement of An-Ab-Or diagram of previous page.

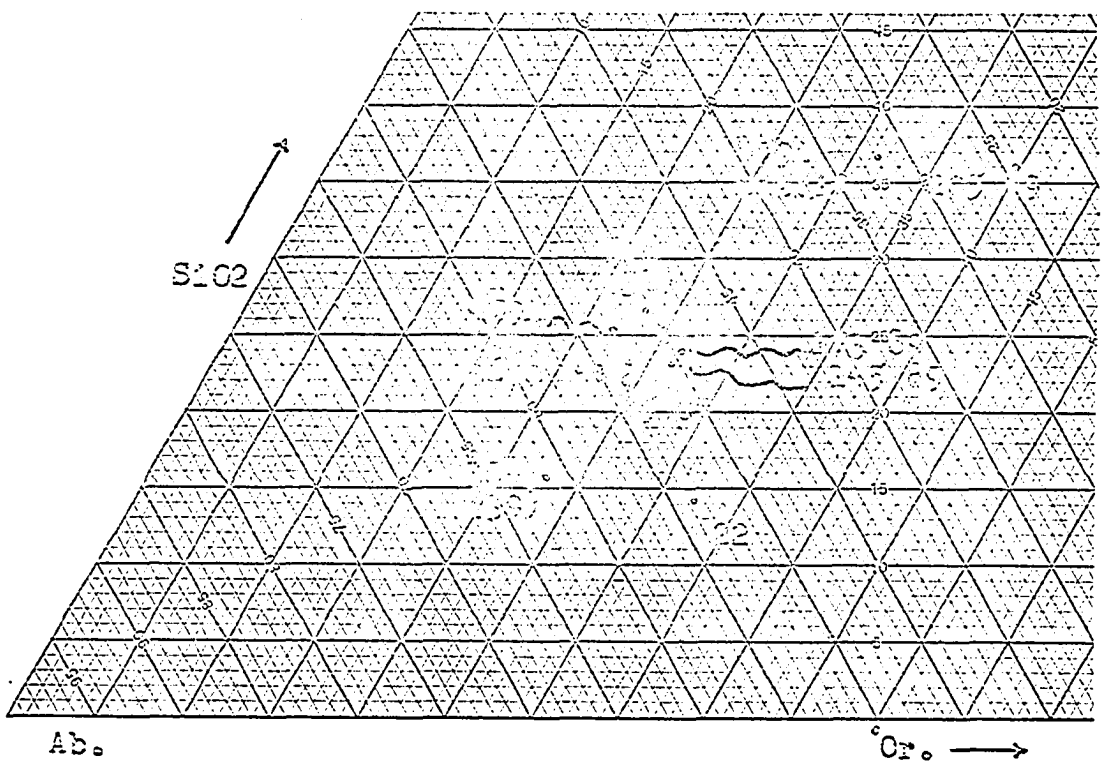

Enlargement of Or-Ab-SiO_2 diagram of previous page. Numbers in parenthesis are the amounts of plagioclase phenocrysts.

Fig. 110

MgO vs. Al203/Si02 variation diagram

Murata (1960) introduced a chemical variation diagram for basaltic and other rocks in which MgO is plotted with respect to Al203/Si02 (Fig. 111). He explains the basis of the diagram as follows:

> "A single fundamental tholeiitic magma (A) is believed to produce all members of the tholeiitic and alkalic series through fractional crystallization. As has been noted by previous investigations, the composition of such a fundamental magma corresponds essentially to a mixture of clinopyroxene and plagioclase feldspar (An~60)...
> The parallelism in composition between the tholeiitic basalt series (EaABCD) and the alkalic basalt series (J'-J-G-H-I) is well shown in figure (111). Both series have olivine-rich members (E-a-A and J'J) and a group of closely related differentiates with progressively increasing content of silica (B-C-D and G-H-I). In the tholeiitic series, this group includes rocks such as granophyre (D) that are rich in quartz whereas in the alkalic series even the most siliceous members (I, 62 per cent Si02) are free of quartz or have only minor amounts of it.
> Line E-a-A-B clearly shows the effect of early fractional crystallization of olivine and thus corresponds to Powers' olivine-control line (1955). Compositions resulting from the removal of olivine from the fundamental magma lie along A to B, while those due to the addition of olivine to the subjacent magma lie along A-a-E.
> The parallel trend (B-C-D and G-H-I in the two series is mainly the result of fractional syncrystallization of clinopyroxene and plagioclase feldspar. The progressive change in the composition of the plagioclase toward albite along this path of differentiation is nicely shown...
> The alignment of points in Figure 11[1] strongly suggests that fractional crystallization of clinopyroxine is the general mechanism for converting tholeiitic magmas into alkalic magmas.

> In figure (111b) the paths of such a differentiation involving fractional crystallization of clinopyroxene are indicated starting from four illustrative points (a, A, B and C) in the tholeiitic series...
> If settling of clinopyroxene is the key process in converting magmas of the tholeiitic series into those of the alkalic series, a question immediately arises as to the possible existence of series intermediate between these two. In figure (111b) for example, fractional crystallization of clinopyroxene along B-G may conceivably be interrupted at any point on the line and be succeeded by fractional syncrystallization of clinopyroxene and plagioclase feldspar. Such a course of differentiation might be along B-g-i in figure 2B (fig. 111b). Many of the basaltic lavas from Easter Island (Bandy 1937) and members of tonalite-quartz monzonite series of Ardamurchan (Richey and others, 1930) do plot along g-i and thereby support the idea that intermediate series are possible. The nomenclature of such series intermediate between the tholeiitic and the alkalic presents new problems."

The analyses for the northern Crazy Mountains sample plus five dike rocks for the southern Crazy Mountains are plotted on the last diagram (fig. 111b), and indicate that the chemical analyses occur astride the two trends shown by Murata. Two malignites plot near a-A (645 near A has considerable olivine and near F is 183 07' which has considerable olivine and magnesian hastingsite); near B is the basalt 445B and a malignite; from B to g are several malignites and an andesite porphyry, from J to G are two malignites and a basic dike rock from the southern stock; along g-i, the hornblende latites, quartz latites and rhyolite porphyries occur; along G-H-I are the fafic trachytes, laurvikite, feldspathoid syenite and trachyte (mafic trachyte 545A is an exception; it lies on g-i).

The two trends indicated by g-i and G-I respectively represent the alkali and alkali-calcic trends indicated by other variation diagrams, though there are complicating factors involved. The two trends are connected in the region C-H which is also indicated by the other diagrams. In fact some of the alkali? hornblende latites (945, 282, 70, 445c and 112) which occur along the g-i trend may occur on alkali-calcic trends on, say, the Peacock diagram. Other exceptions are 24, 35 and 38 which have been placed on the alkali-calcic trend on the other diagrams have appeared with the alkali trends (38 could just as easily lie on the alkali trend, for instance, for Peacock curve).

The position of the g-i trend which is intermediate to the tholeiitic and alkali basalt trends may be in accordance with the alkali-lime designation which has been given to the Crazy Mountains samples, which lie on this trend. This might be one acceptable answer to Murata's question as regards the designation of this series.

For the malignites the distance away from the pyroxene pole is approximately inversly proportional (except for 101 07) to the amount of clinopyroxene and magnesium biotite. But most of the malignites are lined up parallel to the olivine fractionation direction (except 390A, 577) and are alkalic near the pyroxene pole before "pyroxene fractionation". The fact that samples along the g-i trend contain more hornblende and less pyroxene (about equal amounts of pyrobole) than those samples along the G-H-I trend

suggests that other factors are involved besides simple clinopyroxene fractional crystallization in the development of these two trends.

Murata also plotted Al_2O_3/SiO_2 vs CaO and Na_2O plus K_2O for the same basaltic rocks as discussed above. These diagrams also indicated two different trends for the basaltic series. Although he considered these diagrams not quite as instructive it might be worth while to plot the Crazy Mountains samples on these diagrams to see if the hornblende latites occur on the intermediate (alkali-calcic) trend.

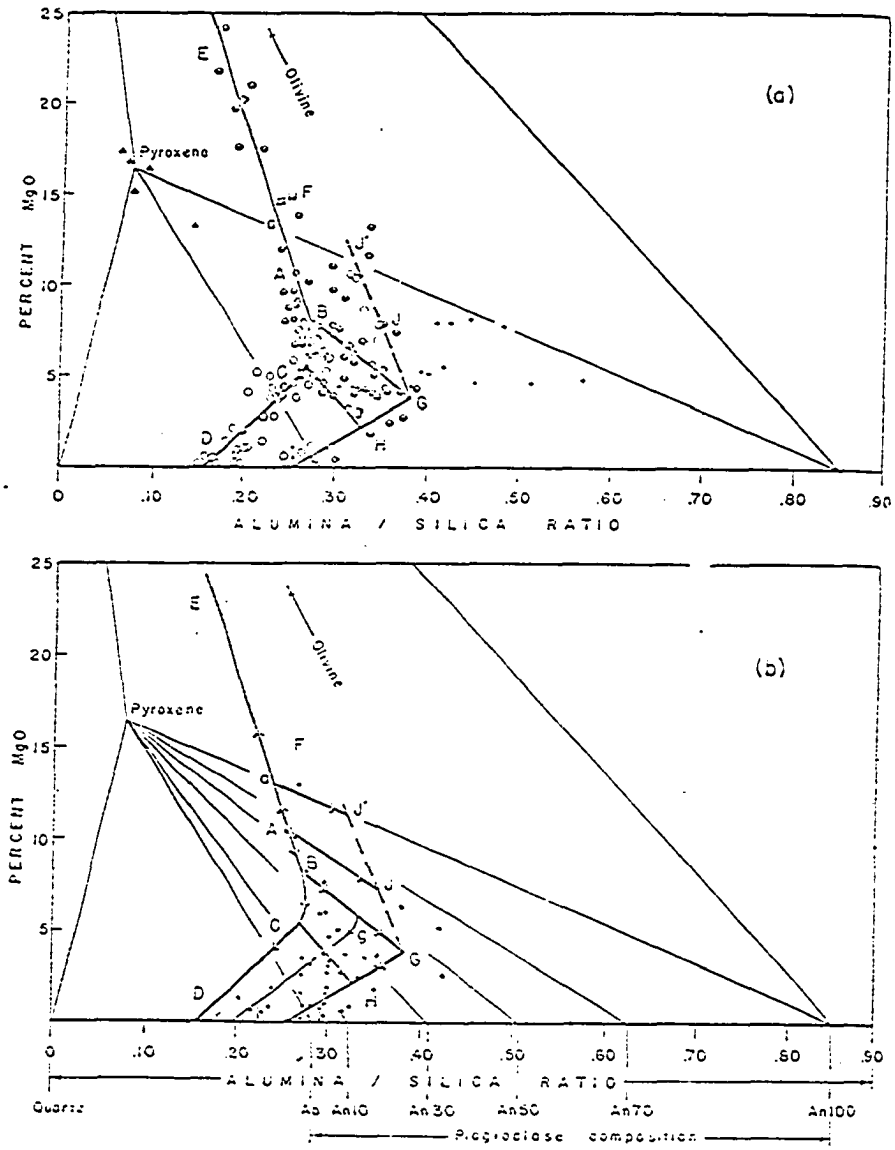

Trends in bulk composition of Hawaiian and British Hebridean rocks as indicated by a plot of MgO against the Al_2O_3/SiO_2 weight ratio (diagram a). The symbols are the same as in fig. 1. Average Hawaiian olivine, which plots off the diagrams, has the following composition: MgO, 47.2%; CaO, 0.25%; Al_2O_3/SiO_2, 0.009. Diagram (b) is a skeletonized version of diagram (a), and shows changes in composition arising from fractional crystallization of one or more minerals. The tholeiitic series of basalts lie along E-a-A-B-C-D, and the alkalic series, along J'-J-G-H-I. Rocks representing trends intermediate between these two major series lie along g-i.

Note the absence of Hebridean rocks with composition along E-a-A—B, and the absence of Hawaiian rocks corresponding to the plagioclase-rich rocks of the Hebrides. Hawaiian rocks with compositions along C-D are scarce.

Fig.111 The dots on the lower diagram represent Crazy Mountains samples. See text. Murata, 1960

Conclusions of the geochemical study

CaO, Na2O + K2O vs. SiO2 (alkali-lime index)

The Peacock diagram indicates the probability of two main continually varying igneous series (alkali, alkali-calcic) which overlap geographically. Gaps in curves of these series could be due to sampling and/or discontinuous chemical variations of CaO, and K2O + Na2O thus defining subseries. The curves are close together at intermediate values of SiO2. One sample which appears intermediate to the two series at the mafic end concurs with Larsen's (1940) observation that transitional types occur between the basalts and mafic alkaline types and suggests that mafic alkaline rocks could be derived from the basalt clan.

K/Rb.

The K/Rb ratios for some of the main rock types from the northern Crazy Mountains are relatively constant and are similar to other magmatic rocks. The close similarity of the ratios from the two main series indicates that they may be related in some way. More determinations are necessary.

K/K + Na) vs. SiO2 (Niggli K-values)

The Niggli-K values at 50 and 60 per cent SiO2 are not significantly different from those values obtained by Moore (1962) who concluded that the alkali ratio of the western United States Cenozoic igneous rocks. "...apparently reflects a quasi-equilibrium with

with pre-existing rocks in their local environment even though locally magmatic differentiation may greatly alter the bulk composition of the specific igneous suites" (Moore, 1962, pp. 10, 11).

Differentiation index and Crystallization index

These diagrams indicate a strong diversity of igneous rocks in the Crazy Mountains. The variations of C.I. and D.I. with SiO_2 or $Qu^{\pm}$ are not the same as far as the Crazy Mountains igneous rocks are concerned. The C.I. vs $Qu^{\pm}$ appears to jibe better with the mineralogy than D.I. vs SiO_2 for relationships of malignites and feldspathoidal syenites and akerites. Also the mineralogy of akerites is better expressed by C.I. vs $Qu^{\pm}$ than the D.I. vs SiO_2. Although only a few rocks are plotted from the southern Crazy Mountains there are enough data to suggest two series. Also akerites appear to link the two chemical series near the intermediate C.I. and D.I. values.

Larsen index vs the various main oxides

These Larsen diagrams indicate the possibility of two main series that are similar chemically in their intermediate ranges. Again, there are deficient areas along each curve representative of certain areas which are in part filled in with data from other areas. The Castle Mountain diorite stock fits well with the alkali series but not far from the alkali-calcic series. In addition the redetermined primary magma of the northern Crazy Mountains is somewhat different than that as determined by Larsen (using his method) thereby negating his discussion to a large extent.

Or: An: Ab, and Feldspar: Femics: $Qu^{\pm}$

These Larsen Ternary diagrams indicate two continually varying series with the quartz rich rocks of the northern Crazy Mountains

fitting well with the alkali-calcic curves (typical of the southern area). As is indicated by other curves some of the akerites are possibly positioned intermediate to the two series.

Na2O: K2O: CaO and alkali: FeO: MgO

This diagram indicates that the chemical variations of the northern Crazy Mountains igneous rocks are broadly similar to some of the oceanic islands that have been plotted in a similar manner. As has been previously suggested this diagram may not have the capacity to show detailed characteristics of an igneous series. On this diagram FeO and Fe_2O_3 are lumped and therefore do not take into account the fact that the rocks of the northern Crazy Mountains have a higher Fe_2O_3 to FeO ratio (expressing the aegerine and aegerine-augite) than the rocks of the southern Crazy Mountains (Wolff, 1938, p. 1624).

The systems SiO_2-$NaAlSiO_4$-$KalSiO_2$; Or-Ab-An

The concordance of the feldspathoid syenites - trachytes and the rhyolites-quartz latites along the thermal trough in these systems (except for the Or - Ab - An diagram) suggests that variability among these rocks (especially the nepheline syenites) is due to fractional crystallization of feldspars from melts in this system. The sodic quartz latites and rhyolite porphyries trend toward an "Average Granite". By separation of the plagioclase phenocrysts, aplites such as those that transect the stocks could be formed.

MgO vs Al_2O_3 / SiO_2

The data from the Crazy Mountains plots moderately well along two trends that were defined by Murata for the alkali series and a series intermediate to it and the tholeiitic series. Its intermediate nature would also be expressed by its alkali-calcic designation. But the mineralogy of these particular rocks is not in accordance with Murata's conclusion that clinopyroxene removal is important in the generation of the alkaline series from a tholeiitic series (at least on the basis of this diagram).

The major underlying causes for magmatic variations

Many of the previously discussed diagrams have similar curving patterns which are expressive of the main underlying causes for geochemical variations in the Crazy Mountain igneous rocks, as well as other igneous series.

The bend of the MgO vs Al2O3/SiO2 trends is equivalent to: (1) the bends in Qu± vs. C.I. trends (p. 187), (2) the bends in the SiO2 vs. D. I. trends (connecting each of the alkaline groups: malignite-mafic trachyte-feldspathoid syenite-trachyte, (except the mafic trachyte) and each of the alkali-calcic groups: basalt-andesite-latite-quartz latite-rhyolite (p. 178), (3) the bend in the FeO-MgO-Alkali trend (p. 202), the curve is broad because the two series have not been differentiated here), (4) the bends in Or-An-Ab and Femic-Feldspar-Quartz trends (p. 198, 199). These trends also are expressed in the other variation diagrams in more subtle ways which will be described as causation is developed.

Tuttle and Thorton (1960, 1965) indicate that fractional crystallization differentiation in the system SiO2-NaAlSiO4-KaISiO4 is most important and more expressive of most rock series, while Poldervaart and Parker (1964, 1965) place the most weight on fractional crystallization differentiation in the system Forsterite-Diopside-Anorthite. The two limbs of the above mentioned curves probably are a reflection of these two processes, with the mafic system being most important in the early, evolutionary stages and the leucocratic system being most important in the later stages. This is again probably expressed

slightly in the Crazy Mountain series in the C.I. vs. D.I. diagram. This diagram shows how the C.I. index is more important in the early phases of evolution and D.I. in the later phases of many provinces. The rather gentle curve for the Crazy Mountain trend expresses slight increase in the Fe in the residual melt, with evolution of the series (p. 181, 182), not extreme Fe fractionalism as in the Skærgaard intrusion.

The following discussion presents the two Crazy Mountain series in the light of the above mentioned two systems. In the basic (petrogeny's primitive) system, (representing the early limb of the trends) if the primary magma is MgO rich, as in the alkaline series (p. 182, p. 193 compared to 194), the pair olivine-diopside will crystallize first while the calc-alkaline series containing less MgO might crystallize diopside-plagioclase first (Turner and Verhoogen, 1960, p. 130). This is the case as is indicated by the mineralogy of the malignites compared to the basalt-andesites. Yet more CaO was withdrawn from the magma in the so-called alkaline series over a longer part of the evolutionary sequence (vaguely indicated by p. 181 because no data from the southern Crazy Mountains is plotted, but fairly well indicated by p. 193 vs. 194, not by p. 164). The terms alkalic and alkalic-calcic can be misleading for these series during this stage.

The high MgO content of the alkaline series is reduced to that of the calc-alkaline series by strong fractional crystallization

of olivine and pyroxene (p. 194, 193, 182). During this limb of the trends, SiO2 has not been fractionated to any great degree in the alkalic series (p. 178, 193), explaining the reason that p. 164 does not show long early withdrawel of CaO. Also Al2O3 has been strongly fractionated by the end of the mafic stage (p. 179, 193). More Al2O3 was used at an early part of this stage in the alkali-calcic series in the form of calcium plagioclase and diopside (p. 194, 198, 199).

At the bend, petrogeny's residua system became predominant. This is well expressed by the K2O plus Na2O - CaO zero contour which crosses both trends at their bends (p. 187). In the alkaline series, the high alumina, Na2O, etc. placed the magma in the system where nepheline began to use the high alumina to silica ratio and the residual magma moved in the direction of less Qu -. Similarly at the bend in the alkali-calcic series, feldspar-quartz became important as a comparison partly because the Al2O3/SiO2 ratio was lower than the alkaline series.

The primary cause of the variations in these two magmatic series is probably the composition of their primary magmas and fractional crystallization differentiation in petrogeny's primitive system gradually succeeded by petrogeny's residua system. The origin of the primary magmas and more subtle variations like the relationship of the latites-mafic trachytes to the two series are subjects of further work.

SUMMARY

Major conclusions, comparisons, speculations

This discussion combines the major conclusions, comparisons and speculations of petrography and geochemistry with structural aspects.

1) The Crazy Mountains (and the map area as a representative part of the entire mountains) contain a diverse range of igneous rocks (mainly Eocene Age). The map area does not contain the silicic aplites and the most mafic subalkaline types of the southern stock.

2) The petrography and many of the geochemical variation diagrams indicate two main series occur which overlap geographically. There are some gaps in the trends. Some evidence indicates that these are in part due to sampling. Further study may indicate that they may define subseries. For instance, the quartz latite-rhyolite porphyry group is distinctly chemically separate from the other groups. The latites - mafic trachytes appear to bridge the gap between the middles of the two series.

3) Simple and complex hypabyssal intrusives are intimately placed around two main stocks. Within the map area, complex dikes show strong petrographic variations due mainly to multiple intrusion. Variation within the concordant intrusives is not as dramatic, but many are due to multiple intrusion also. In situ differentiation is not an impossible process in some of the mafic alkaline bodies (similar to that conceived by Hurlbut, 1939 for Shonkin Sag). If differentiation in place has occurred, it was much less pronounced than in the Highwood Mountains, for instance. The

degree and type of simultaneous tectonism may not have allowed quiet in situ differentiation, or caused differentiates to be implaced separately. The intrusives of the Crazy Mountains are associated with folded and faulted strata while the differentiated bodies of the Highwoods and Bearpaw Mountains occur in rather undisturbed flat lying strata.

A similar situation occurs in the East Otago, New Zealand Province where well-known bodies occur differentiated in situ in the moderately deformed subprovince while in the strongly deformed subprovince not strongly differentiated bodies are reported (Benson, 1941).

There are other similarities between the Crazy Mountains and the East Otago province (1) The rock types are not dissimilar (2) A nepheline syenite intrusion occurs along the main anticline of each region (the main anticline is definitely faulted in the strongly deformed subprovince of East Otago),

4) The arrangement of the concordant intrusives is symmetrical. At the lower stratigraphic interval on the Robinson anticline, the most basic malignite sills are the stratigraphic middle intrusives as on the monocline the most felsic sills are the middle quartz latite - rhyolite porphyry group. These concordant bodies predominate in areas of high dip as dikes predominate in areas of low dip. Probably much intrusion occurred in the later

phases of folding (in the map area at least).

5) An apparent overlapping of time of intrusion of the many rock types occurs yet complex intrusions of the same composition have chilled border phases indicating pauses between intrusions. The akerites, consisting of mafic trachytes to latites, appear to have been early to late intrusives. These rocks have wide distribution in the Crazy Mountains. Similar felsic rocks in the Bearpaw Mountains have a wide age range. Larsen had previously reported that later intrusives of the province are usually alkalic (longer differentiation allowed).

6) Many authors have emphasized the stable or simple tensional tectonic environment of alkaline rocks. Yet a number of areas of alkaline rocks are associated with moderately folded (many superficially) and faulted strata (Bearpaw Mountains, East Otago, Terlingua - Solitario, Crazy Mountains). These and some others are associated with doming, block tectonics and monoclines; (Devils Tower, Leucite Hills).

7) The close geographic association of granitic rocks and nepheline syenites is not unusual (p. 394, Turner and Verhoogan 1960). This association does not necessarily indicate that they are immediately related. They both seem to represent two distinct groups of residual differentiates from two different series. The fact that they fall along the low temperature trough in Petrogeny's

residua system and other chemical variation diagrams indicate that the variance among them could be due to fractional crystallization of feldspars. Some syenites (soelvesbergites, implying aegerine) contain normative quartz indicating an unstable assemblage which might mean immediate contamination or low Al_2O_3. Also the acid rocks contain abundant xenoliths. Therefore contamination might have an important role as Larsen (1940) suggests. Similar felsic rocks in the Bearpaw Mountains also contain noticeable basement inclusions.

8) In regard to what has been said above, most of the variation diagrams show that many of the latites-mafic trachytes are intermediate to the malignites and the feldspathoidal syenite clan. In more detail, the D.I. vs SiO_2 diagram could be interpreted to mean that the feldspathoidal syenites, quartz syenites, quartz latites and rhyolite porphyries are immediately related to the akerites (mafic trachytes and latites). This is the relationship that Barth (1945) pictures for the Oslo, Norway Petrographic province where mafic types are minor. It is only the C.I. vs Qu± diagram that shows a separate distinct transition from the malignites to the feldspathoidal syenites, in accordance with what is indicated by the mineralogy. It is probable that some of the syenites and quartz syenites could be immediately derived from the akeritic magma. A break occurs between the malignites and

akerites on some of the diagrams which could be in part explained by sampling. (Those diagrams in which the break occurs do not have samples from the southern Crazy Mountains).

9) Fudali (1964) would predict the Crazy Mountains alkaline rocks might present the proper conditions in which to find vague geometric structures that would have a bearing on the pseudoleucite problem. Such structures of varying degrees of distinctness do occur in the alkaline rocks occasionally.

10) The pegmatites of the nepheline syenites are similar to the pegmatites in similar rocks of the Bearpaw Mountains but do not have any major concentration of rare minerals (see Gerasimovskii, 1956).

11) The irregular leucocratic segregations in the malignites probably indicate that they were able to generate a feldspathoidal syenite magma or at least were associated with one at some stage.

12) The apparent differences in post-magmatic alteration of the two main series indicates that the alteration is in part related to the waning stages of magmatic activity. Later intrusives may have affected alteration of earlier intrusives. This needs to be verified.

13) The primary cause of the variations in these two magmatic series is the composition of their primary magmas and fractional crystallization differentiation in petrogeny's primitive system gradually succeeded by petrogeny's residua system.

Problems for further study

1. The degree of contamination should be evaluated by a study of xenocrysts and xenoliths. It is interesting that alkaline(?) breccia pipes which were studied in some detail by Wolff contain no limestone xenoliths, but numerous xenoliths of gneiss, red quartzite, granite and hornfels. Yet a quartz latite sill contains a large xenolith of Paleozoic algal limestone.

2. More study on the complex dikes should be possible especially around the southern stock.

3. A study of the northern stock should complete the structural picture and afford a better understanding of the relation of the monoclinal sills and the stock.

4. A few more K/Rb ratios of some of the main rock types should give a better picture of the usefulness of this characteristic in determining the degree of relatedness between the two possible series.

5. As Larsen (1940), and Turner and Verhoogen (1960) have written, the high contents of Ba and Sr in the Central Montana Petrographic Province igneous rocks are difficult to explain. More Ba and Sr determinations are necessary before an evaluation can be made.

6. As new chemical analyses and modern geochemical concepts are available, a restudy of the geochemistry of the Central Montana Petrographic Province is in order.

7. A more detailed mineralogical study should add valuable information in understanding the genesis of these rocks. Zeolites are an important phase of all the subprovinces but have been ignored. A study of the olivines of all the subprovinces would focus on the beginning of crystallization and should afford information about primary magmas.

8. Wones and Eugster (1965, p. 1229) indicates that: "The biotite assemblages will provide, if properly studied, definite limits on the possible temperatures and fugacity of components such as H_2O, O_2 and H_2 in geologic processes. This especially is possible when the critical assemblage biotite - sanidine - magnetite is present as in the Crazy Mountain rocks.

9. Some of the rocks (especially mafic) of the alkali-calcic series contain more TiO_2 than those of the alkali series. Can one discriminate between the two or more series as Chayes (1965) has done?

10. A more detailed consideration of the lamprophyres is in order.

APPENDIX

Explanation of the computor output for the geochemical study

This section explains the computor output which is presented on the following pages

Each sample is designated on each row of the output data by the first six letters or numbers on the left end of the row. The first one or two symbols on the left of these six are: (A) indicating Wolff's samples; (AT) indicating John Tappe's samples; (B) indicating the writer's samples. The next two or three numbers or a letter to the right are the sample numbers. In many cases these numbers are not the full sample numbers. Wolff lists the year as the next designating symbols. The ambiguous designated samples are as follows: 45=45 07'; 945 = 45 89'. Wolff lists nepheline syenite 149 89 as 145 89' at the top of the column in his list of analyses. It has been corrected here. In addition, 445B contains 2.57 normative quartz as 445C contains no quartz which distinguishes these two samples.

The letter in the fifth column from the left indicates the row of the sample data. The (A) or (Z) of the sixth column from the left indicate respectively that total normative mineral weight per cent was not or was recalculated to 100 per cent anhydrous.

From the chemical analyses listed (Plate 2) the following geochemical parameters have been computed by the normative analyses program.

1) Weight per cent of normative minerals using 1964 atomic weights.
2) RMGFE equals 100 x the molecular ratio of MgO to MgO plus FeO for

the formation of normative olivine and pyroxene.

3) ANABW equals 100 x the weight per cent ratio of An to An plus Ab.

4) CI is the crystallization index which equals An plus magnesium Di plus Fe plus En converted to Fe plus magnesium spinel calculated from corundum in ultra basic rocks.

5) FeO/Fe203 equals the ratio the weight per cent of FeO to Fe203.

6) TFE equals total FeO plus Fe203 as weight per cent Fe.

7) MUR equals the Murata index which is the ratio of weight per cent of Al203 to Si02.

8) DIT equals the differentiation index which is Qu plus Or plus Ab plus Ne plus Lc plus Kp.

9) PEQ equals .53 x Ne minus .47 Qu. For basaltic rocks, if this value is negative the rock is an olivine tholeiite, if positive an alkali basalt (Poldervarrt, 1964).

10) PQU equals with a plus sign the amount of Qu; with a minus sign indicates the amount of Si02 necessary to saturate the silica defficient minerals.

11) NE KP QU represents the relative proportions of Nepheline, Kaliophilite, and Quartz for plotting Petrogeny's Residua system.

12) MIL which is the modified Larsen Index equals(Si3) plus K plus Ca plus Mg.

13) BHY equals the Barth value which is Ab plus 2.0 Di plus 2.3 Hy. For basaltic rocks if this number is greater than 123 pyroxene initiated crystallization before plagioclase; if less than 123, plagioclase initiated crystallization before pyroxene; if approximately equal to 123 than pyroxene and feldspar initiated crystallization

simultaneously (Barth, 1962, p. 115, 116).

14) BHYOL equals the Barth value (olivine included) which is Ab plus 2.0 plus Di plus 2.3 Hy plus Ol. converted to pyroxene.

	Q	OR	AB	AN	NE	LC	KP	AC	NS	KS	C
AT16AA	.61	16.72	37.65	16.61	0.00	0.00	0.00	0.00	0.00	0.00	0.00
	WO	DW	DE	DF	EN	OF	FO	FA	CS	MT	HM
AT16BA	0.00	5.08	2.78	2.12	6.26	4.77	0.00	0.00	0.00	2.09	0.00
	IL	TN	PF	RU	AP						
AT16CA	2.81	0.00	0.00	0.00	1.40				H2O	1.76	T 98.90
AT16DA	DI 9.98	HY	11.03	OL	0.00	RMGFE	63.293	ANABW	30.61	CI	27.29
AT16EA	FEO/FE2O3	3.92	TFE	5.39	MUR	.296	DIT	55.59	PEQ	1.72	PQU .61
AT16ZA	NE 37.10	KP	17.28	QU	45.62	MLI	4.28	BHY	110.25	BHYOL	110.25

	Q	OR	AB	AN	NE	LC	KP	AC	NS	KS	C
AT16AZ	.62	16.91	38.07	16.79	0.00	0.00	0.00	0.00	0.00	0.00	0.00
	WO	DW	DE	DF	EN	OF	FO	FA	CS	MT	HM
AT16BZ	0.00	5.14	2.81	2.14	6.33	4.82	0.00	0.00	0.00	2.11	0.00
	IL	TN	PF	RU	AP						
AT16CZ	2.84	0.00	0.00	0.00	1.41				H2O	1.76	T 100.00
AT16DZ	DI 10.09	HY	11.15	OL	0.00	RMGFE	63.293	ANABW	30.61	CI	27.29
AT16EZ	FEO/FE2O3	3.92	TFE	5.39	MUR	.296	DIT	55.59	PEQ	1.72	PQU .61
AT16ZZ	NE 37.10	KP	17.28	QU	45.62	MLI	4.28	BHY	110.25	BHYOL	110.25

	Q	OR	AB	AN	NE	LC	KP	AC	NS	KS	C
AT22AA	13.49	27.48	45.86	3.25	0.00	0.00	0.00	0.00	0.00	0.00	0.00
	WO	DW	DE	DF	EN	OF	FO	FA	CS	MT	HM
AT22BA	1.22	2.10	1.22	.78	0.00	0.00	0.00	0.00	0.00	1.94	0.00
	IL	TN	PF	RU	AP						
AT22CA	1.27	0.00	0.00	0.00	.61				H2O	1.11	T 99.22
AT22DA	DI 4.10	HY	0.00	OL	0.00	RMGFE	67.268	ANABW	6.62	CI	5.93
AT22EA	FEO/FE2O3	1.19	TFE	2.18	MUR	.226	DIT	87.50	PEQ	-4.80	PQU 13.59
AT22ZA	NE 28.61	KP	17.98	QU	53.40	MLI	12.38	BHY	101.60	BHYOL	101.60

	Q	OR	AB	AN	NE	LC	KP	AC	NS	KS	C
AT22AZ	13.59	27.69	46.22	3.27	0.00	0.00	0.00	0.00	0.00	0.00	0.00
	WO	DW	DE	DF	EN	OF	FO	FA	CS	MT	HM
AT22BZ	1.23	2.12	1.23	.79	0.00	0.00	0.00	0.00	0.00	1.96	0.00
	IL	TN	PF	RU	AP						
AT22CZ	1.28	0.00	0.00	0.00	.62				H2O	1.11	T 100.00
AT22DZ	DI 4.13	HY	0.00	OL	0.00	RMGFE	67.268	ANABW	6.62	CI	5.93
AT22EZ	FEO/FE2O3	1.19	TFE	2.18	MUR	.226	DIT	87.50	PEQ	-4.80	PQU 13.59
AT22ZZ	NE 28.61	KP	17.98	QU	53.40	MLI	12.38	BHY	101.60	BHYOL	101.60

	Q	OR	AB	AN	NE	LC	KP	AC	NS	KS	C
AT24AA	0.00	13.77	39.55	23.02	1.54	0.00	0.00	0.00	0.00	0.00	0.00
	WO	DW	DE	DF	EN	OF	FO	FA	CS	MT	HM
AT24BA	0.00	5.58	3.94	1.16	0.00	0.00	2.53	.82	0.00	3.54	0.00
	IL	TN	PF	RU	AP						
AT24CA	2.96	0.00	0.00	0.00	1.25				H2O	1.11 T	99.65
AT24DA	DI 10.68	HY	0.00	OL	3.35	RMGFE	81.689	ANABW	36.79	CI	34.16
AT24EA	FEO/FE2O3	1.48	TFE	4.51	MUR	.357	DIT	55.05	PEQ	6.62	PQU -2.63
AT24ZA	NE 41.86	KP	14.26	QU	43.88	MLI	2.83	BHY	83.16	BHYOL	91.95

	Q	OR	AB	AN	NE	LC	KP	AC	NS	KS	C
AT24AZ	0.00	13.82	39.69	23.10	1.54	0.00	0.00	0.00	0.00	0.00	0.00
	WO	DW	DE	DF	EN	OF	FO	FA	CS	MT	HM
AT24BZ	0.00	5.60	3.95	1.16	0.00	0.00	2.54	.82	0.00	3.55	0.00
	IL	TN	PF	RU	AP						
AT24CZ	2.97	0.00	0.00	0.00	1.25				H2O	1.11 T	100.00
AT24DZ	DI 10.72	HY	0.00	OL	3.36	RMGFE	81.689	ANABW	36.79	CI	34.16
AT24EZ	FEO/FE2O3	1.48	TFE	4.51	MUR	.357	DIT	55.05	PEQ	6.62	PQU -2.63
AT24ZZ	NE 41.86	KP	14.26	QU	43.88	MLI	2.83	BHY	83.16	BHYOL	91.95

	Q	OR	AB	AN	NE	LC	KP	AC	NS	KS	C
AT35AA	0.00	10.05	36.81	23.42	0.00	0.00	0.00	0.00	0.00	0.00	0.00
	WO	DW	DE	DF	EN	OF	FO	FA	CS	MT	HM
AT35BA	0.00	6.42	3.87	2.20	3.03	1.72	1.47	.92	0.00	5.34	0.00
	IL	TN	PF	RU	AP						
AT35CA	2.72	0.00	0.00	0.00	1.42				H2O	1.39 T	99.36
AT35DA	DI 12.49	HY	4.75	OL	2.38	RMGFE	69.830	ANABW	38.89	CI	35.59
AT35EA	FEO/FE2O3	1.52	TFE	6.91	MUR	.338	DIT	47.15	PEQ	3.59	PQU -.90
AT35ZA	NE 42.56	KP	12.18	QU	45.26	MLI	1.24	BHY	93.85	BHYOL	99.38

	Q	OR	AB	AN	NE	LC	KP	AC	NS	KS	C
AT35AZ	0.00	10.11	37.04	23.57	0.00	0.00	0.00	0.00	0.00	0.00	0.00
	WO	DW	DE	DF	EN	OF	FO	FA	CS	MT	HM
AT35BZ	0.00	6.46	3.90	2.21	3.05	1.73	1.47	.92	0.00	5.37	0.00
	IL	TN	PF	RU	AP						
AT35CZ	2.73	0.00	0.00	0.00	1.43				H2O	1.39 T	100.00
AT35DZ	DI 12.57	HY	4.78	OL	2.40	RMGFE	69.830	ANABW	38.89	CI	35.59
AT35EZ	FEO/FE2O3	1.52	TFE	6.91	MUR	.338	DIT	47.15	PEQ	3.59	PQU -.90
AT35ZZ	NE 42.56	KP	12.18	QU	45.26	MLI	1.24	BHY	93.85	BHYOL	99.38

	Q	OR	AB	AN	NE	LC	KP	AC	NS	KS	C
AT38AA	0.00	6.97	15.62	28.84	9.32	0.00	0.00	0.00	0.00	0.00	0.00
	WO	DW	DE	DF	EN	OF	FO	FA	CS	MT	HM
AT38BA	0.00	8.05	5.05	2.50	0.00	0.00	5.50	3.00	0.00	7.15	0.00
	IL	TN	PF	RU	AP						
AT38CA	4.35	0.00	0.00	0.00	2.49				H2O	1.55	T 98.84
AT38DA	DI 15.60	HY	0.00	OL	8.50	RMGFE	72.657	ANABW	64.86	CI	45.77
AT38EA	FEO/FE2O3	1.54	TFE	9.34	MUR	.422	DIT	32.29	PEQ	12.35	PQU-11.24
AT38ZA	NE 55.72	KP	12.41	QU	31.86	MLI	-3.48	BHY	77.95	BHYOL	102.79

	Q	OR	AB	AN	NE	LC	KP	AC	NS	KS	C
AT38AZ	0.00	7.05	15.81	29.18	9.43	0.00	0.00	0.00	0.00	0.00	0.00
	WO	DW	DE	DF	EN	OF	FO	FA	CS	MT	HM
AT38BZ	0.00	8.14	5.11	2.53	0.00	0.00	5.56	3.03	0.00	7.23	0.00
	IL	TN	PF	RU	AP						
AT38CZ	4.40	0.00	0.00	0.00	2.52				H2O	1.55	T 100.00
AT38DZ	DI 15.78	HY	0.00	OL	8.60	RMGFE	72.657	ANABW	64.86	CI	45.77
AT38EZ	FEO/FE2O3	1.54	TFE	9.34	MUR	.422	DIT	32.29	PEQ	12.35	PQU-11.24
AT38ZZ	NE 55.72	KP	12.41	QU	31.86	MLI	-3.48	BHY	77.95	BHYOL	102.79

	Q	OR	AB	AN	NE	LC	KP	AC	NS	KS	C
B390AA	0.00	11.29	4.39	0.00	29.17	0.00	0.00	7.06	0.00	0.00	0.00
	WO	DW	DE	DF	EN	OF	FO	FA	CS	MT	HM
B390BA	0.00	17.71	13.89	1.85	0.00	0.00	1.82	.27	0.00	5.13	0.00
	IL	TN	PF	RU	AP						
B390CA	1.31	0.00	0.00	0.00	2.38				H2O	3.78	T 96.27
B390DA	DI 33.45	HY	0.00	OL	2.09	RMGFE	90.776	ANABW	0.00	CI	33.01
B390EA	FEO/FE2O3	.54	TFE	6.70	MUR	.294	DIT	46.59	PEQ	22.82	PQU-26.51
B390ZA	NE 70.35	KP	14.30	QU	15.35	MLI	-2.50	BHY	188.39	BHYOL	191.39

	Q	OR	AB	AN	NE	LC	KP	AC	NS	KS	C
B390AZ	0.00	11.72	4.56	0.00	30.30	0.00	0.00	7.33	0.00	0.00	0.00
	WO	DW	DE	DF	EN	OF	FO	FA	CS	MT	HM
B390BZ	0.00	18.39	14.43	1.93	0.00	0.00	1.89	.28	0.00	5.33	0.00
	IL	TN	PF	RU	AP						
B390CZ	1.36	0.00	0.00	0.00	2.47				H2O	3.78	T 100.00
B390DZ	DI 34.75	HY	0.00	OL	2.17	RMGFE	90.776	ANABW	0.00	CI	33.01
B390EZ	FEO/FE2O3	.54	TFE	6.70	MUR	.294	DIT	46.59	PEQ	22.82	PQU-26.51
B390ZZ	NE 70.35	KP	14.30	QU	15.35	MLI	-2.50	BHY	188.39	BHYOL	191.39

	Q	OR	AB	AN	NE	LC	KP	AC	NS	KS	C	
B394AA	11.87	17.20	46.54	8.68	0.00	0.00	0.00	0.00	0.00	0.00	0.00	
	WO	DW	DE	DF	EN	OF	FO	FA	CS	MT	HM	
B394BA	0.00	3.13	1.84	1.14	2.94	1.81	0.00	0.00	0.00	1.59	0.00	
	IL	TN	PF	RU	AP							
B394CA	.80	0.00	0.00	0.00	1.38					H2O 1.70 T		98.92
B394DA	DI	6.11	HY	4.75	OL	0.00	RMGFE	68.035	ANABW	15.73	CI	14.88
B394EA	FEO/FE2O3	2.22	TFE	2.67	MUR	.238	DIT	76.42	PEQ	-4.11	PQU	11.99
B394ZA	NE	33.35	KP	12.93	QU	53.73	MLI	8.64	BHY	105.46	BHYOL	105.46

	Q	OR	AB	AN	NE	LC	KP	AC	NS	KS	C	
B394AZ	12.00	17.38	47.04	8.78	0.00	0.00	0.00	0.00	0.00	0.00	0.00	
	WO	DW	DE	DF	EN	OF	FO	FA	CS	MT	HM	
B394BZ	0.00	3.17	1.86	1.15	2.97	1.83	0.00	0.00	0.00	1.61	0.00	
	IL	TN	PF	RU	AP							
B394CZ	.81	0.00	0.00	0.00	1.39					H2O 1.70 T		100.00
B394DZ	DI	6.18	HY	4.81	OL	0.00	RMGFE	68.035	ANABW	15.73	CI	14.88
B394EZ	FEO/FE2O3	2.22	TFE	2.67	MUR	.238	DIT	76.42	PEQ	-4.11	PQU	11.99
B394ZZ	NE	33.35	KP	12.93	QU	53.73	MLI	8.64	BHY	105.46	BHYOL	105.46

	Q	OR	AB	AN	NE	LC	KP	AC	NS	KS	C	
B445AA	2.44	4.02	22.00	22.09	0.00	0.00	0.00	0.00	0.00	0.00	0.00	
	WO	DW	DE	DF	EN	OF	FO	FA	CS	MT	HM	
B445BA	0.00	8.43	6.27	1.33	15.04	3.18	0.00	0.00	0.00	6.45	0.00	
	IL	TN	PF	RU	AP							
B445CA	2.60	0.00	0.00	0.00	1.27					H2O 5.38 T		95.13
B445DA	DI	16.03	HY	18.23	OL	0.00	RMGFE	86.128	ANABW	50.11	CI	48.53
B445EA	FEO/FE2O3	1.25	TFE	7.44	MUR	.268	DIT	29.91	PEQ	-3.45	PQU	2.56
B445ZA	NE	41.88	KP	8.02	QU	50.10	MLI	-3.84	BHY	122.51	BHYOL	122.51

	Q	OR	AB	AN	NE	LC	KP	AC	NS	KS	C	
B445AZ	2.57	4.22	23.12	23.22	0.00	0.00	0.00	0.00	0.00	0.00	0.00	
	WO	DW	DE	DF	EN	OF	FO	FA	CS	MT	HM	
B445BZ	0.00	8.86	6.59	1.40	15.81	3.35	0.00	0.00	0.00	6.78	0.00	
	IL	TN	PF	RU	AP							
B445CZ	2.74	0.00	0.00	0.00	1.33					H2O 5.38 T		100.00
B445DZ	DI	16.85	HY	19.16	OL	0.00	RMGFE	86.128	ANABW	50.11	CI	48.53
B445EZ	FEO/FE2O3	1.25	TFE	7.44	MUR	.268	DIT	29.91	PEQ	-3.45	PQU	2.56
B445ZZ	NE	41.88	KP	8.02	QU	50.10	MLI	-3.84	BHY	122.51	BHYOL	122.51

	Q	OR	AB	AN	NE	LC	KP	AC	NS	KS	C
B445AA	0.00	23.70	44.44	9.65	.18	0.00	0.00	0.00	0.00	0.00	0.00
	WO	DW	DE	DF	EN	OF	FO	FA	CS	MT	HM
B445BA	0.00	2.06	1.78	0.00	0.00	0.00	3.75	0.00	0.00	5.25	1.61
	IL	TN	PF	RU	AP						
B445CA	3.00	0.00	0.00	0.00	2.49				H2O	2.68	T 97.89
B445DA	DI 3.83	HY 0.00	OL 3.75	RMGFE 100.000				ANABW 17.84		CI	17.60
B445EA	FEO/FE2O3 .56	TFE 5.95	MUR .308	DIT 69.78				PEQ 6.28		PQU	-1.78
B445ZA	NE 35.50	KP 19.71	QU 44.79	MLI 7.32				BHY 89.96		BHYOL	101.79

	Q	OR	AB	AN	NE	LC	KP	AC	NS	KS	C
B445AZ	0.00	24.21	45.39	9.86	.18	0.00	0.00	0.00	0.00	0.00	0.00
	WO	DW	DE	DF	EN	OF	FO	FA	CS	MT	HM
B445BZ	0.00	2.10	1.82	0.00	0.00	0.00	3.83	0.00	0.00	5.37	1.64
	IL	TN	PF	RU	AP						
B445CZ	3.07	0.00	0.00	0.00	2.54				H2O	2.68	T 100.00
B445DZ	DI 3.92	HY 0.00	OL 3.83	RMGFE 100.000				ANABW 17.84		CI	17.60
B445EZ	FEO/FE2O3 .56	TFE 5.95	MUR .308	DIT 69.78				PEQ 6.28		PQU	-1.78
B445ZZ	NE 35.50	KP 19.71	QU 44.79	MLI 7.32				BHY 89.96		BHYOL	101.79

	Q	OR	AB	AN	NE	LC	KP	AC	NS	KS	C
B459AA	0.00	29.01	55.80	0.00	5.73	0.00	0.00	4.36	0.00	0.00	0.00
	WO	DW	DE	DF	EN	OF	FO	FA	CS	MT	HM
B459BA	.60	.61	.52	0.00	0.00	0.00	0.00	0.00	0.00	.53	.38
	IL	TN	PF	RU	AP						
B459CA	.46	0.00	0.00	0.00	.94				H2O	1.39	T 98.93
B459DA	DI 1.13	HY 0.00	OL 0.00	RMGFE 100.000				ANABW 0.00		CI	1.14
B459EA	FEO/FE2O3 .16	TFE 1.85	MUR .290	DIT 91.52				PEQ 11.23		PQU	-4.90
B459ZA	NE 39.72	KP 18.21	QU 42.07	MLI 13.20				BHY 101.98		BHYOL	101.98

	Q	OR	AB	AN	NE	LC	KP	AC	NS	KS	C
B459AZ	0.00	29.33	56.40	0.00	5.79	0.00	0.00	4.41	0.00	0.00	0.00
	WO	DW	DE	DF	EN	OF	FO	FA	CS	MT	HM
B459BZ	.60	.61	.53	0.00	0.00	0.00	0.00	0.00	0.00	.54	.38
	IL	TN	PF	RU	AP						
B459CZ	.46	0.00	0.00	0.00	.95				H2O	1.39	T 100.00
B459DZ	DI 1.14	HY 0.00	OL 0.00	RMGFE 100.000				ANABW 0.00		CI	1.14
B459EZ	FEO/FE2O3 .16	TFE 1.85	MUR .290	DIT 91.52				PEQ 11.23		PQU	-4.90
B459ZZ	NE 39.72	KP 18.21	QU 42.07	MLI 13.20				BHY 101.98		BHYOL	101.98

```
          Q       OR      AB      AN      NE      LC      KP      AC      NS      KS       C
B479AA  21.95  18.91  45.86   5.28   0.00   0.00   0.00   0.00   0.00   0.00    .93
          WO      DW      DE      DF      EN      OF      FO      FA      CS      MT      HM
B479BA   0.00    0.00    0.00    0.00    2.19    0.00    0.00    0.00    0.00    1.76    .27
          IL      TN      PF      RU      AP
B479CA    .66    0.00    0.00    0.00    1.60                                H2O 1.13 T   99.41
B479DA DI   0.00 HY   2.19 OL   0.00  RMGFE 100.000  ANABW  10.33  CI   6.86
B479EA FEO/FE2O3    .57 TFE   1.70 MUR   .220 DIT 87.23 PEQ-10.47 PQU 22.07
B479ZA NE 28.65  KP 12.39  QU 58.96  MLI 11.75  BHY  95.44  BHYOL  95.44

          Q       OR      AB      AN      NE      LC      KP      AC      NS      KS       C
B479AZ  22.08  19.02  46.13   5.31   0.00   0.00   0.00   0.00   0.00   0.00    .94
          WO      DW      DE      DF      EN      OF      FO      FA      CS      MT      HM
B479BZ   0.00    0.00    0.00    0.00    2.20    0.00    0.00    0.00    0.00    1.77    .27
          IL      TN      PF      RU      AP
B479CZ    .67    0.00    0.00    0.00    1.60                                H2O 1.13 T  100.00
B479DZ DI   0.00 HY   2.20 OL   0.00  RMGFE 100.000  ANABW  10.33  CI   6.86
B479EZ FEO/FE2O3    .57 TFE   1.70 MUR   .220 DIT 87.23 PEQ-10.47 PQU 22.07
B479ZZ NE 28.65  KP 12.39  QU 58.96  MLI 11.75  BHY  95.44  BHYOL  95.44

          Q       OR      AB      AN      NE      LC      KP      AC      NS      KS       C
B545AA    .07  23.22  50.26   4.71   0.00   0.00   0.00   0.00   0.00   0.00   0.00
          WO      DW      DE      DF      EN      OF      FO      FA      CS      MT      HM
B545BA   0.00    5.21    4.36    .19    1.74    .08    0.00    0.00    0.00    5.60    0.00
          IL      TN      PF      RU      AP
B545CA   1.50    0.00    0.00    0.00    1.97                                H2O 1.05 T   98.90
B545DA DI   9.76 HY   1.82 OL   0.00  RMGFE  96.802  ANABW   8.56  CI  15.50
B545EA FEO/FE2O3    .64 TFE   4.63 MUR   .271 DIT 74.37 PEQ   5.35 PQU    .07
B545ZA NE 37.02  KP 17.94  QU 45.04  MLI  7.85  BHY 111.14  BHYOL 111.14

          Q       OR      AB      AN      NE      LC      KP      AC      NS      KS       C
B545AZ    .08  23.48  50.82   4.76   0.00   0.00   0.00   0.00   0.00   0.00   0.00
          WO      DW      DE      DF      EN      OF      FO      FA      CS      MT      HM
B545BZ   0.00    5.27    4.41    .19    1.76    .08    0.00    0.00    0.00    5.66    0.00
          IL      TN      PF      RU      AP
B545CZ   1.52    0.00    0.00    0.00    1.99                                H2O 1.05 T  100.00
B545DZ DI   9.86 HY   1.84 OL   0.00  RMGFE  96.802  ANABW   8.56  CI  15.50
B545EZ FEO/FE2O3    .64 TFE   4.63 MUR   .271 DIT 74.37 PEQ   5.35 PQU    .07
B545ZZ NE 37.02  KP 17.94  QU 45.04  MLI  7.85  BHY 111.14  BHYOL 111.14
```

	Q	OR	AB	AN	NE	LC	KP	AC	NS	KS	C
B577AA	0.00	26.85	0.00	0.00	37.20	4.20	0.00	5.25	0.00	0.00	0.00
	WO	DW	DE	DF	EN	OF	FO	FA	CS	MT	HM
B577BA	0.00	6.90	5.14	1.08	0.00	0.00	.85	.20	0.00	4.00	0.00
	IL	TN	PF	RU	AP						
B577CA	1.37	0.00	0.00	0.00	1.99				H2O 4.58 T		95.01
B577DA	DI 13.12	HY	0.00	OL	1.04	RMGFE	86.258	ANABW		CI	12.57
B577EA	FEO/FE2O3	.54	TFE	5.13	MUR	.421	DIT 71.83	PEQ 38.38	PQU-34.77		
B577ZA	NE 54.51	KP 26.81	QU 18.68	MLI 7.48	BHY 200.00	BHYOL 203.00					

	Q	OR	AB	AN	NE	LC	KP	AC	NS	KS	C
B577AZ	0.00	28.26	0.00	0.00	39.15	4.42	0.00	5.52	0.00	0.00	0.00
	WO	DW	DE	DF	EN	OF	FO	FA	CS	MT	HM
B577BZ	0.00	7.26	5.41	1.13	0.00	0.00	.89	.21	0.00	4.21	0.00
	IL	TN	PF	RU	AP						
B577CZ	1.44	0.00	0.00	0.00	2.09				H2O 4.58 T		100.00
B577DZ	DI 13.81	HY	0.00	OL	1.10	RMGFE	86.258	ANABW		CI	12.57
B577EZ	FEO/FE2O3	.54	TFE	5.13	MUR	.421	DIT 71.83	PEQ 38.38	PQU-34.77		
B577ZZ	NE 54.51	KP 26.81	QU 18.68	MLI 7.48	BHY 200.00	BHYOL 203.00					

	Q	OR	AB	AN	NE	LC	KP	AC	NS	KS	C
B578AA	21.38	18.79	40.78	3.69	0.00	0.00	0.00	0.00	0.00	0.00	.70
	WO	DW	DE	DF	EN	OF	FO	FA	CS	MT	HM
B578BA	0.00	0.00	0.00	0.00	3.46	.50	0.00	0.00	0.00	3.23	0.00
	IL	TN	PF	RU	AP						
B578CA	.84	0.00	0.00	0.00	4.92				H2O 1.76 T		98.28
B578DA	DI 0.00	HY	3.96	OL	0.00	RMGFE	90.116	ANABW	8.29	CI	6.22
B578EA	FEO/FE2O3	.72	TFE	2.81	MUR	.205	DIT 82.37	PEQ-11.58	PQU 21.75		
B578ZA	NE 27.29	KP 13.19	QU 59.52	MLI 10.02	BHY 103.02	BHYOL 103.02					

	Q	OR	AB	AN	NE	LC	KP	AC	NS	KS	C
B578AZ	21.75	19.12	41.50	3.75	0.00	0.00	0.00	0.00	0.00	0.00	.71
	WO	DW	DE	DF	EN	OF	FO	FA	CS	MT	HM
B578BZ	0.00	0.00	0.00	0.00	3.52	.51	0.00	0.00	0.00	3.29	0.00
	IL	TN	PF	RU	AP						
B578CZ	.85	0.00	0.00	0.00	5.00				H2O 1.76 T		100.00
B578DZ	DI 0.00	HY	4.03	OL	0.00	RMGFE	90.116	ANABW	8.29	CI	6.22
B578EZ	FEO/FE2O3	.72	TFE	2.81	MUR	.205	DIT 82.37	PEQ-11.58	PQU 21.75		
B578ZZ	NE 27.29	KP 13.19	QU 59.52	MLI 10.02	BHY 103.02	BHYOL 103.02					

	Q	OR	AB	AN	NE	LC	KP	AC	NS	KS	C
B625AA	0.00	26.59	13.53	4.11	20.77	0.00	0.00	0.00	0.00	0.00	0.00
	WO	DW	DE	DF	EN	OF	FO	FA	CS	MT	HM
B625BA	0.00	8.48	6.98	.47	0.00	0.00	1.06	.08	0.00	7.29	0.00
	IL	TN	PF	RU	AP						
B625CA	1.88	0.00	0.00	0.00	3.87				H2O	4.28 T	95.10
B625DA	DI	15.92	HY	0.00	OL	1.14	RMGFE	95.172	ANABW	23.28	CI 21.26
B625EA	FEO/FE2O3		.66	TFE	6.10	MUR	.355	DIT	64.03	PEQ	23.31 PQU -18.97
B625ZA	NE	46.14	KP	24.82	QU	29.04	MLI	4.22	BHY	135.20	BHYOL 139.56

	Q	OR	AB	AN	NE	LC	KP	AC	NS	KS	C
B625AZ	0.00	27.96	14.23	4.32	21.84	0.00	0.00	0.00	0.00	0.00	0.00
	WO	DW	DE	DF	EN	OF	FO	FA	CS	MT	HM
B625BZ	0.00	8.92	7.33	.49	0.00	0.00	1.12	.08	0.00	7.67	0.00
	IL	TN	PF	RU	AP						
B625CZ	1.98	0.00	0.00	0.00	4.07				H2O	4.28 T	100.00
B625DZ	DI	16.74	HY	0.00	OL	1.20	RMGFE	95.172	ANABW	23.28	CI 21.26
B625EZ	FEO/FE2O3		.66	TFE	6.10	MUR	.355	DIT	64.03	PEQ	23.31 PQU -18.97
B625ZZ	NE	46.14	KP	24.82	QU	29.04	MLI	4.22	BHY	135.20	BHYOL 139.56

	Q	OR	AB	AN	NE	LC	KP	AC	NS	KS	C
B626AA	0.00	37.40	23.91	3.38	6.94	0.00	0.00	0.00	0.00	0.00	0.00
	WO	DW	DE	DF	EN	OF	FO	FA	CS	MT	HM
B626BA	0.00	6.86	5.42	.68	0.00	0.00	1.81	.25	0.00	5.93	0.00
	IL	TN	PF	RU	AP						
B626CA	1.60	0.00	0.00	0.00	2.64				H2O	2.79 T	96.82
B626DA	DI	12.96	HY	0.00	OL	2.06	RMGFE	91.289	ANABW	12.39	CI 17.42
B626EA	FEO/FE2O3		.74	TFE	5.21	MUR	.287	DIT	70.49	PEQ	11.76 PQU -6.93
B626ZA	NE	29.15	KP	31.14	QU	39.71	MLI	8.15	BHY	123.80	BHYOL 130.94

	Q	OR	AB	AN	NE	LC	KP	AC	NS	KS	C
B626AZ	0.00	38.63	24.69	3.49	7.17	0.00	0.00	0.00	0.00	0.00	0.00
	WO	DW	DE	DF	EN	OF	FO	FA	CS	MT	HM
B626BZ	0.00	7.09	5.59	.70	0.00	0.00	1.87	.26	0.00	6.12	0.00
	IL	TN	PF	RU	AP						
B626CZ	1.65	0.00	0.00	0.00	2.73				H2O	2.79 T	100.00
B626DZ	DI	13.39	HY	0.00	OL	2.12	RMGFE	91.289	ANABW	12.39	CI 17.42
B626EZ	FEO/FE2O3		.74	TFE	5.21	MUR	.287	DIT	70.49	PEQ	11.76 PQU -6.93
B626ZZ	NE	29.15	KP	31.14	QU	39.71	MLI	8.15	BHY	123.80	BHYOL 130.94

	Q	OR	AB	AN	NE	LC	KP	AC	NS	KS	C
B634AA	0.00	22.45	47.25	1.40	9.24	0.00	0.00	0.00	0.00	0.00	0.00
	WO	DW	DE	DF	EN	OF	FO	FA	CS	MT	HM
B634BA	.23	5.50	4.76	0.00	0.00	0.00	0.00	0.00	0.00	4.89	.29
	IL	TN	PF	RU	AP						
B634CA	.87	0.00	0.00	0.00	1.03				H2O	2.73 T	97.92
B634DA	DI 10.26	HY	0.00	OL	0.00	RMGFE	100.000	ANABW	2.89	CI	11.91
B634EA	FEO/FE2O3	.50	TFE	3.99	MUR	.299	DIT	80.62	PEQ	12.41	PQU -7.98
B634ZA	NE 44.13	KP	16.16	QU	39.71	MLI	8.64	BHY	115.03	BHYOL	115.03

	Q	OR	AB	AN	NE	LC	KP	AC	NS	KS	C
B634AZ	0.00	22.93	48.26	1.43	9.43	0.00	0.00	0.00	0.00	0.00	0.00
	WO	DW	DE	DF	EN	OF	FO	FA	CS	MT	HM
B634BZ	.24	5.62	4.86	0.00	0.00	0.00	0.00	0.00	0.00	4.99	.29
	IL	TN	PF	RU	AP						
B634CZ	.89	0.00	0.00	0.00	1.05				H2O	2.73 T	100.00
B634DZ	DI 10.48	HY	0.00	OL	0.00	RMGFE	100.000	ANABW	2.89	CI	11.91
B634EZ	FEO/FE2O3	.50	TFE	3.99	MUR	.299	DIT	80.62	PEQ	12.41	PQU -7.98
B634ZZ	NE 44.13	KP	16.16	QU	39.71	MLI	8.64	BHY	115.03	BHYOL	115.03

	Q	OR	AB	AN	NE	LC	KP	AC	NS	KS	C
B645AA	0.00	10.28	2.59	4.08	21.70	0.00	0.00	0.00	0.00	0.00	0.00
	WO	DW	DE	DF	EN	OF	FO	FA	CS	MT	HM
B645BA	0.00	20.80	16.62	1.79	0.00	0.00	6.61	.78	0.00	7.32	0.00
	IL	TN	PF	RU	AP						
B645CA	1.61	0.00	0.00	0.00	1.70				H2O	4.00 T	95.89
B645DA	DI 39.21	HY	0.00	OL	7.39	RMGFE	92.437	ANABW	61.19	CI	48.53
B645EA	FEO/FE2O3	.87	TFE	6.95	MUR	.266	DIT	36.05	PEQ	16.48	PQU-22.32
B645ZA	NE 66.83	KP	16.90	QU	16.27	MLI	-6.87	BHY	176.57	BHYOL	186.48

	Q	OR	AB	AN	NE	LC	KP	AC	NS	KS	C
B645AZ	0.00	10.72	2.70	4.26	22.63	0.00	0.00	0.00	0.00	0.00	0.00
	WO	DW	DE	DF	EN	OF	FO	FA	CS	MT	HM
B645BZ	0.00	21.69	17.33	1.86	0.00	0.00	6.89	.82	0.00	7.64	0.00
	IL	TN	PF	RU	AP						
B645CZ	1.68	0.00	0.00	0.00	1.78				H2O	4.00 T	100.00
B645DZ	DI 40.89	HY	0.00	OL	7.71	RMGFE	92.437	ANABW	61.19	CI	48.53
B645EZ	FEO/FE2O3	.87	TFE	6.95	MUR	.266	DIT	36.05	PEQ	16.48	PQU-22.32
B645ZZ	NE 66.83	KP	16.90	QU	16.27	MLI	-6.87	BHY	176.57	BHYOL	186.48

```
          Q       OR      AB      AN      NE      LC      KP      AC      NS      KS      C
B652AA    .54   12.70   32.83   17.98    0.00    0.00    0.00    0.00    0.00    0.00   0.00
          WO      DW      DE      DF      EN      OF      FO      FA      CS      MT     HM
B652BA  0.00    6.70    5.16     .83    9.63    1.54    0.00    0.00    0.00    6.48   0.00
          IL      TN      PF      RU      AP
B652CA   2.26    0.00    0.00    0.00     .48                                H2O 3.58 T  97.14
B652DA DI 12.69 HY 11.17 OL   0.00  RMGFE  89.137  ANABW  35.39  CI 36.92
B652EA FEO/FE2O3    .95 TFE   6.42 MUR   .291 DIT 47.43 PEQ  1.01 PQU   .55
B652ZA NE 38.60  KP 15.67  QU 45.73  MLI  1.35  BHY 112.37  BHYOL 112.37
```

```
          Q       OR      AB      AN      NE      LC      KP      AC      NS      KS      C
B652AZ    .56   13.08   33.80   18.51    0.00    0.00    0.00    0.00    0.00    0.00   0.00
          WO      DW      DE      DF      EN      OF      FO      FA      CS      MT     HM
B652BZ  0.00    6.90    5.31     .85    9.92    1.59    0.00    0.00    0.00    6.67   0.00
          IL      TN      PF      RU      AP
B652CZ   2.33    0.00    0.00    0.00     .49                                H2O 3.58 T 100.00
B652DZ DI 13.06 HY 11.50 OL   0.00  RMGFE  89.137  ANABW  35.39  CI 36.92
B652EZ FEO/FE2O3    .95 TFE   6.42 MUR   .291 DIT 47.43 PEQ  1.01 PQU   .55
B652ZZ NE 38.60  KP 15.67  QU 45.73  MLI  1.35  BHY 112.37  BHYOL 112.37
```

```
          Q       OR      AB      AN      NE      LC      KP      AC      NS      KS      C
BS70AA  19.61   18.20   48.48    6.87    0.00    0.00    0.00    0.00    0.00    0.00    .42
          WO      DW      DE      DF      EN      OF      FO      FA      CS      MT     HM
BS70BA  0.00    0.00    0.00    0.00    2.47     .13    0.00    0.00    0.00    1.94   0.00
          IL      TN      PF      RU      AP
BS70CA    .65    0.00    0.00    0.00     .90                                H2O  .82 T  99.66
BS70DA DI   0.00 HY   2.60 OL   0.00  RMGFE  96.107  ANABW  12.40  CI  8.62
BS70EA FEO/FE2O3    .72 TFE   1.69 MUR   .227 DIT 86.58 PEQ -8.62 PQU 19.67
BS70ZA NE 30.44  KP 11.99  QU 57.58  MLI 11.54  BHY  93.98  BHYOL  93.98
```

```
          Q       OR      AB      AN      NE      LC      KP      AC      NS      KS      C
BS70AZ  19.67   18.26   48.65    6.89    0.00    0.00    0.00    0.00    0.00    0.00    .43
          WO      DW      DE      DF      EN      OF      FO      FA      CS      MT     HM
BS70BZ  0.00    0.00    0.00    0.00    2.47     .13    0.00    0.00    0.00    1.95   0.00
          IL      TN      PF      RU      AP
BS70CZ    .65    0.00    0.00    0.00     .90                                H2O  .82 T 100.00
BS70DZ DI   0.00 HY   2.61 OL   0.00  RMGFE  96.107  ANABW  12.40  CI  8.62
BS70EZ FEO/FE2O3    .72 TFE   1.69 MUR   .227 DIT 86.58 PEQ -8.62 PQU 19.67
BS70ZZ NE 30.44  KP 11.99  QU 57.58  MLI 11.54  BHY  93.98  BHYOL  93.98
```

	Q	OR	AB	AN	NE	LC	KP	AC	NS	KS	C
B112AA	0.00	13.95	44.93	13.49	2.11	0.00	0.00	0.00	0.00	0.00	0.00
	WO	DW	DE	DF	EN	OF	FO	FA	CS	MT	HM
B112BA	0.00	4.33	3.74	0.00	0.00	0.00	3.43	0.00	0.00	6.05	1.79
	IL	TN	PF	RU	AP						
B112CA	1.82	0.00	0.00	0.00	1.42				H2O	2.16	T 97.07
B112DA	DI 8.07	HY	0.00	OL	3.43	RMGFE	100.000		ANABW	23.09	CI 25.75
B112EA	FEO/FE2O3	.43	TFE	6.19	MUR	.323	DIT	62.82	PEQ	7.41	PQU -3.34
B112ZA	NE 43.37	KP	12.99	QU	43.64	MLI	4.29	BHY	91.85	BHYOL	101.33

	Q	OR	AB	AN	NE	LC	KP	AC	NS	KS	C
B112AZ	0.00	14.37	46.29	13.90	2.17	0.00	0.00	0.00	0.00	0.00	0.00
	WO	DW	DE	DF	EN	OF	FO	FA	CS	MT	HM
B112BZ	0.00	4.46	3.86	0.00	0.00	0.00	3.54	0.00	0.00	6.24	1.85
	IL	TN	PF	RU	AP						
B112CZ	1.88	0.00	0.00	0.00	1.46				H2O	2.16	T 100.00
B112DZ	DI 8.32	HY	0.00	OL	3.54	RMGFE	100.000		ANABW	23.09	CI 25.75
B112EZ	FEO/FE2O3	.43	TFE	6.19	MUR	.323	DIT	62.82	PEQ	7.41	PQU -3.34
B112ZZ	NE 43.37	KP	12.99	QU	43.64	MLI	4.29	BHY	91.85	BHYOL	101.33

	Q	OR	AB	AN	NE	LC	KP	AC	NS	KS	C
B116AA	0.00	28.72	44.80	0.00	13.07	0.00	0.00	1.15	0.00	0.00	0.00
	WO	DW	DE	DF	EN	OF	FO	FA	CS	MT	HM
B116BA	2.40	1.82	1.57	0.00	0.00	0.00	0.00	0.00	0.00	1.41	1.34
	IL	TN	PF	RU	AP						
B116CA	.70	0.00	0.00	0.00	.50				H2O	3.41	T 97.48
B116DA	DI 3.38	HY	0.00	OL	0.00	RMGFE	100.000		ANABW	0.00	CI 3.47
B116EA	FEO/FE2O3	.26	TFE	2.45	MUR	.318	DIT	88.82	PEQ	16.55	PQU-11.33
B116ZA	NE 43.12	KP	18.85	QU	38.03	MLI	11.53	BHY	107.02	BHYOL	107.02

	Q	OR	AB	AN	NE	LC	KP	AC	NS	KS	C
B116AZ	0.00	29.46	45.96	0.00	13.40	0.00	0.00	1.18	0.00	0.00	0.00
	WO	DW	DE	DF	EN	OF	FO	FA	CS	MT	HM
B116BZ	2.47	1.86	1.61	0.00	0.00	0.00	0.00	0.00	0.00	1.45	1.37
	IL	TN	PF	RU	AP						
B116CZ	.72	0.00	0.00	0.00	.52				H2O	3.41	T 100.00
B116DZ	DI 3.47	HY	0.00	OL	0.00	RMGFE	100.000		ANABW	0.00	CI 3.47
B116EZ	FEO/FE2O3	.26	TFE	2.45	MUR	.318	DIT	88.82	PEQ	16.55	PQU-11.33
B116ZZ	NE 43.12	KP	18.85	QU	38.03	MLI	11.53	BHY	107.02	BHYOL	107.02

	Q	OR	AB	AN	NE	LC	KP	AC	NS	KS	C
B217AA	0.00	17.08	5.45	11.31	13.60	0.00	0.00	0.00	0.00	0.00	0.00
	WO	DW	DE	DF	EN	OF	FO	FA	CS	MT	HM
B217BA	0.00	17.58	14.36	1.09	0.00	0.00	3.39	.28	0.00	7.09	0.00
	IL	TN	PF	RU	AP						
B217CA	2.24	0.00	0.00	0.00	3.02				H2O	4.30	T 96.47
B217DA	DI 33.03	HY	0.00	OL	3.67	RMGFE	94.560		ANABW	67.48	CI 47.35
B217EA	FEO/FE2O3		.80	TFE	6.45	MUR	.293	DIT	37.44	PEQ	13.62 PQU -13.50
B217ZA	NE 45.81	KP	26.87	QU	27.32	MLI	-4.36	BHY	143.63	BHYOL	151.81

	Q	OR	AB	AN	NE	LC	KP	AC	NS	KS	C
B217AZ	0.00	17.70	5.65	11.72	14.09	0.00	0.00	0.00	0.00	0.00	0.00
	WO	DW	DE	DF	EN	OF	FO	FA	CS	MT	HM
B217BZ	0.00	18.22	14.89	1.13	0.00	0.00	3.51	.29	0.00	7.35	0.00
	IL	TN	PF	RU	AP						
B217CZ	2.32	0.00	0.00	0.00	3.13				H2O	4.30	T 100.00
B217DZ	DI 34.23	HY	0.00	OL	3.81	RMGFE	94.560		ANABW	67.48	CI 47.35
B217EZ	FEO/FE2O3		.80	TFE	6.45	MUR	.293	DIT	37.44	PEQ	13.62 PQU -13.50
B217ZZ	NE 45.81	KP	26.87	QU	27.32	MLI	-4.36	BHY	143.63	BHYOL	151.81

	Q	OR	AB	AN	NE	LC	KP	AC	NS	KS	C
A145AA	20.67	23.58	44.84	5.22	0.00	0.00	0.00	0.00	0.00	0.00	0.00
	WO	DW	DE	DF	EN	OF	FO	FA	CS	MT	HM
A145BA	0.00	.04	.03	0.00	1.46	0.00	0.00	0.00	0.00	.82	1.22
	IL	TN	PF	RU	AP						
A145CA	.63	0.00	0.00	0.00	.72				H2O	.44	T 99.21
A145DA	DI .07	HY	1.46	OL	0.00	RMGFE	100.000		ANABW	10.42	CI 6.36
A145EA	FEO/FE2O3		.31	TFE	1.67	MUR	.214	DIT	89.79	PEQ	-9.99 PQU 20.83
A145ZA	NE 27.27	KP	15.04	QU	57.69	MLI	13.01	BHY	93.70	BHYOL	93.70

	Q	OR	AB	AN	NE	LC	KP	AC	NS	KS	C
A145AZ	20.83	23.76	45.20	5.26	0.00	0.00	0.00	0.00	0.00	0.00	0.00
	WO	DW	DE	DF	EN	OF	FO	FA	CS	MT	HM
A145BZ	0.00	.04	.03	0.00	1.48	0.00	0.00	0.00	0.00	.82	1.23
	IL	TN	PF	RU	AP						
A145CZ	.63	0.00	0.00	0.00	.73				H2O	.44	T 100.00
A145DZ	DI .07	HY	1.48	OL	0.00	RMGFE	100.000		ANABW	10.42	CI 6.36
A145EZ	FEO/FE2O3		.31	TFE	1.67	MUR	.214	DIT	89.79	PEQ	-9.99 PQU 20.83
A145ZZ	NE 27.27	KP	15.04	QU	57.69	MLI	13.01	BHY	93.70	BHYOL	93.70

```
          Q      OR     AB     AN     NE     LC     KP     AC     NS     KS     C
A045AA 19.57 20.03 44.17 10.92  0.00  0.00  0.00  0.00  0.00  0.00  0.00
          WO     DW     DE     DF     EN     OF     FO     FA     CS     MT     HM
A045BA  0.00    .36    .31   0.00   1.43   0.00   0.00   0.00   0.00   0.00   1.59
          IL     TN     PF     RU     AP
A045CA    .46    .18   0.00   0.00   0.00                                H2O   .47 T  99.04
A045DA DI    .68 HY   1.43 OL   0.00  RMGFE 100.000  ANABW  19.83  CI 12.72
A045EA FEO/FE2O3    .14 TFE   1.28 MUR   .236 DIT 84.58 PEQ -9.46 PQU 19.76
A045ZA NE 28.56  KP 13.59  QU 57.85  MLI 11.55  BHY  85.33  BHYOL  85.33

          Q      OR     AB     AN     NE     LC     KP     AC     NS     KS     C
A045AZ 19.76 20.23 44.60 11.03  0.00  0.00  0.00  0.00  0.00  0.00  0.00
          WO     DW     DE     DF     EN     OF     FO     FA     CS     MT     HM
A045BZ  0.00    .37    .32   0.00   1.44   0.00   0.00   0.00   0.00   0.00   1.61
          IL     TN     PF     RU     AP
A045CZ    .47    .19   0.00   0.00   0.00                                H2O   .47 T 100.00
A045DZ DI    .68 HY   1.44 OL   0.00  RMGFE 100.000  ANABW  19.83  CI 12.72
A045EZ FEO/FE2O3    .14 TFE   1.28 MUR   .236 DIT 84.58 PEQ -9.46 PQU 19.76
A045ZZ NE 28.56  KP 13.59  QU 57.85  MLI 11.55  BHY  85.33  BHYOL  85.33

          Q      OR     AB     AN     NE     LC     KP     AC     NS     KS     C
A297AA  3.87 25.29 61.77  2.40  0.00  0.00  0.00  0.00  0.00  0.00  0.00
          WO     DW     DE     DF     EN     OF     FO     FA     CS     MT     HM
A297BA  0.00    .16    .14   0.00    .71   0.00   0.00   0.00   0.00   4.17    .18
          IL     TN     PF     RU     AP
A297CA  0.00   0.00   0.00   0.00   0.00                                H2O   .99 T  98.68
A297DA DI    .30 HY    .71 OL   0.00  RMGFE 100.000  ANABW   3.74  CI  3.23
A297EA FEO/FE2O3    .31 TFE   2.87 MUR   .272 DIT 92.14 PEQ  3.77 PQU  3.92
A297ZA NE 36.80  KP 15.81  QU 47.39  MLI 13.18  BHY  98.19  BHYOL  98.19

          Q      OR     AB     AN     NE     LC     KP     AC     NS     KS     C
A297AZ  3.92 25.63 62.59  2.43  0.00  0.00  0.00  0.00  0.00  0.00  0.00
          WO     DW     DE     DF     EN     OF     FO     FA     CS     MT     HM
A297BZ  0.00    .16    .14   0.00    .72   0.00   0.00   0.00   0.00   4.23    .19
          IL     TN     PF     RU     AP
A297CZ  0.00   0.00   0.00   0.00   0.00                                H2O   .99 T 100.00
A297DZ DI    .30 HY    .72 OL   0.00  RMGFE 100.000  ANABW   3.74  CI  3.23
A297EZ FEO/FE2O3    .31 TFE   2.87 MUR   .272 DIT 92.14 PEQ  3.77 PQU  3.92
A297ZZ NE 36.80  KP 15.81  QU 47.39  MLI 13.18  BHY  98.19  BHYOL  98.19
```

	Q	OR	AB	AN	NE	LC	KP	AC	NS	KS	C
A105AA	3.48	27.48	53.05	7.62	0.00	0.00	0.00	0.00	0.00	0.00	0.00
	WO	DW	DE	DF	EN	OF	FO	FA	CS	MT	HM
A105BA	0.00	1.85	1.33	.35	.43	.11	0.00	0.00	0.00	1.29	0.00
	IL	TN	PF	RU	AP						
A105CA	.78	0.00	0.00	0.00	.13				H2O	.66 T	97.91
A105DA	DI 3.53	HY .55	OL 0.00	RMGFE 83.449				ANABW 12.56		CI	11.03
A105EA	FEO/FE2O3 1.13	TFE 1.41	MUR .287	DIT 85.81				PEQ 3.45		PQU	3.55
A105ZA	NE 34.21	KP 18.59	QU 47.20	MLI 11.81				BHY 94.79		BHYOL	94.79

	Q	OR	AB	AN	NE	LC	KP	AC	NS	KS	C
A105AZ	3.56	28.06	54.18	7.78	0.00	0.00	0.00	0.00	0.00	0.00	0.00
	WO	DW	DE	DF	EN	OF	FO	FA	CS	MT	HM
A105BZ	0.00	1.89	1.36	.36	.44	.12	0.00	0.00	0.00	1.32	0.00
	IL	TN	PF	RU	AP						
A105CZ	.80	0.00	0.00	0.00	.13				H2O	.66 T	100.00
A105DZ	DI 3.61	HY .56	OL 0.00	RMGFE 83.449				ANABW 12.56		CI	11.03
A105EZ	FEO/FE2O3 1.13	TFE 1.41	MUR .287	DIT 85.81				PEQ 3.45		PQU	3.55
A105ZZ	NE 34.21	KP 18.59	QU 47.20	MLI 11.81				BHY 94.79		BHYOL	94.79

	Q	OR	AB	AN	NE	LC	KP	AC	NS	KS	C
A131AA	0.00	22.93	63.72	5.30	.13	0.00	0.00	0.00	0.00	0.00	0.00
	WO	DW	DE	DF	EN	OF	FO	FA	CS	MT	HM
A131BA	0.00	.77	.62	.05	0.00	0.00	.84	.08	0.00	3.12	0.00
	IL	TN	PF	RU	AP						
A131CA	0.00	0.00	0.00	0.00	.24				H2O	1.80 T	97.80
A131DA	DI 1.44	HY 0.00	OL .91	RMGFE 94.028				ANABW 7.68		CI	7.65
A131EA	FEO/FE2O3 .49	TFE 2.32	MUR .299	DIT 88.73				PEQ 7.01		PQU	-.50
A131ZA	NE 39.93	KP 15.01	QU 45.06	MLI 11.63				BHY 94.52		BHYOL	96.96

	Q	OR	AB	AN	NE	LC	KP	AC	NS	KS	C
A131AZ	0.00	23.44	65.16	5.42	.14	0.00	0.00	0.00	0.00	0.00	0.00
	WO	DW	DE	DF	EN	OF	FO	FA	CS	MT	HM
A131BZ	0.00	.78	.64	.05	0.00	0.00	.86	.08	0.00	3.19	0.00
	IL	TN	PF	RU	AP						
A131CZ	0.00	0.00	0.00	0.00	.25				H2O	1.80 T	100.00
A131DZ	DI 1.48	HY 0.00	OL .93	RMGFE 94.028				ANABW 7.68		CI	7.65
A131EZ	FEO/FE2O3 .49	TFE 2.32	MUR .299	DIT 88.73				PEQ 7.01		PQU	-.50
A131ZZ	NE 39.93	KP 15.01	QU 45.06	MLI 11.63				BHY 94.52		BHYOL	96.96

	Q	OR	AB	AN	NE	LC	KP	AC	NS	KS	C
A097AA	0.00	26.65	47.89	14.18	0.00	0.00	0.00	0.00	0.00	0.00	0.00
	WO	DW	DE	DF	EN	OF	FO	FA	CS	MT	HM
A097BA	0.00	.26	.17	.08	1.88	.88	2.77	1.44	0.00	1.52	0.00
	IL	TN	PF	RU	AP						
A097CA	1.01	0.00	0.00	0.00	1.11				H2O	.37 T	99.85
A097DA	DI	.51	HY	2.76	OL	4.22	RMGFE	73.584	ANABW	22.85	CI 18.66
A097EA	FEO/FE2O3	2.29	TFE	2.60	MUR	.325	DIT	74.65	PEQ	5.55	PQU -1.61
A097ZA	NE	34.81	KP	20.32	QU	44.88	MLI	9.14	BHY	84.57	BHYOL 96.47

	Q	OR	AB	AN	NE	LC	KP	AC	NS	KS	C
A097AZ	0.00	26.69	47.96	14.20	0.00	0.00	0.00	0.00	0.00	0.00	0.00
	WO	DW	DE	DF	EN	OF	FO	FA	CS	MT	HM
A097BZ	0.00	.26	.17	.08	1.88	.89	2.78	1.44	0.00	1.52	0.00
	IL	TN	PF	RU	AP						
A097CZ	1.01	0.00	0.00	0.00	1.12				H2O	.37 T	100.00
A097DZ	DI	.51	HY	2.76	OL	4.22	RMGFE	73.584	ANABW	22.85	CI 18.66
A097EZ	FEO/FE2O3	2.29	TFE	2.60	MUR	.325	DIT	74.65	PEQ	5.55	PQU -1.61
A097ZZ	NE	34.81	KP	20.32	QU	44.88	MLI	9.14	BHY	84.57	BHYOL 96.47

	Q	OR	AB	AN	NE	LC	KP	AC	NS	KS	C
A282AA	9.75	23.05	40.19	12.51	0.00	0.00	0.00	0.00	0.00	0.00	0.00
	WO	DW	DE	DF	EN	OF	FO	FA	CS	MT	HM
A282BA	0.00	.81	.58	.16	3.53	.97	0.00	0.00	0.00	4.16	0.00
	IL	TN	PF	RU	AP						
A282CA	1.39	0.00	0.00	0.00	1.38				H2O	1.41 T	98.46
A282DA	DI	1.55	HY	4.49	OL	0.00	RMGFE	82.770	ANABW	23.74	CI 16.49
A282EA	FEO/FE2O3	.89	TFE	4.00	MUR	.272	DIT	74.12	PEQ	-4.10	PQU 9.89
A282ZA	NE	29.83	KP	17.94	QU	52.22	MLI	9.44	BHY	91.29	BHYOL 91.29

	Q	OR	AB	AN	NE	LC	KP	AC	NS	KS	C
A282AZ	9.90	23.41	40.82	12.71	0.00	0.00	0.00	0.00	0.00	0.00	0.00
	WO	DW	DE	DF	EN	OF	FO	FA	CS	MT	HM
A282BZ	0.00	.82	.59	.16	3.58	.98	0.00	0.00	0.00	4.23	0.00
	IL	TN	PF	RU	AP						
A282CZ	1.41	0.00	0.00	0.00	1.40				H2O	1.41 T	100.00
A282DZ	DI	1.57	HY	4.56	OL	0.00	RMGFE	82.770	ANABW	23.74	CI 16.49
A282EZ	FEO/FE2O3	.89	TFE	4.00	MUR	.272	DIT	74.12	PEQ	-4.10	PQU 9.89
A282ZZ	NE	29.83	KP	17.94	QU	52.22	MLI	9.44	BHY	91.29	BHYOL 91.29

	Q	OR	AB	AN	NE	LC	KP	AC	NS	KS	C
A149AA	0.00	24.64	47.31	0.00	9.08	0.00	0.00	6.02	0.00	0.00	0.00
	WO	DW	DE	DF	EN	OF	FO	FA	CS	MT	HM
A149BA	.79	3.68	1.99	1.56	0.00	0.00	0.00	0.00	0.00	1.59	0.00
	IL	TN	PF	RU	AP						
A149CA	0.00	0.00	0.00	0.00	.31				H2O	2.60	T 96.96
A149DA	DI 7.23	HY	0.00	OL	0.00	RMGFE	62.703	ANABW	0.00	CI	4.43
A149EA	FEO/FE2O3	.36	TFE	3.12	MUR	.284	DIT	83.57	PEQ	12.89	PQU -7.91
A149ZA	NE 42.83	KP	17.28	QU	39.89	MLI	11.00	BHY	113.25	BHYOL	113.25

	Q	OR	AB	AN	NE	LC	KP	AC	NS	KS	C
A149AZ	0.00	25.41	48.79	0.00	9.36	0.00	0.00	6.21	0.00	0.00	0.00
	WO	DW	DE	DF	EN	OF	FO	FA	CS	MT	HM
A149BZ	.81	3.79	2.05	1.61	0.00	0.00	0.00	0.00	0.00	1.64	0.00
	IL	TN	PF	RU	AP						
A149CZ	0.00	0.00	0.00	0.00	.32				H2O	2.60	T 100.00
A149DZ	DI 7.45	HY	0.00	OL	0.00	RMGFE	62.703	ANABW	0.00	CI	4.43
A149EZ	FEO/FE2O3	.36	TFE	3.12	MUR	.284	DIT	83.57	PEQ	12.89	PQU -7.91
A149ZZ	NE 42.83	KP	17.28	QU	39.89	MLI	11.00	BHY	113.25	BHYOL	113.25

	Q	OR	AB	AN	NE	LC	KP	AC	NS	KS	C
	WO	DW	DE	DF	EN	OF	FO	FA	CS	MT	HM
A065AA	0.00	26.77	48.23	.80	13.06	0.00	0.00	0.00	0.00	0.00	0.00
A065BA	.15	2.19	1.89	0.00	0.00	0.00	0.00	0.00	0.00	1.87	2.08
	IL	TN	PF	RU	AP						
A065CA	0.00	0.00	0.00	0.00	.22				H2O	2.64	T 97.25
A065DA	DI 4.08	HY	0.00	OL	0.00	RMGFE	100.000	ANABW	1.62	CI	5.02
A065EA	FEO/FE2O3	.17	TFE	2.81	MUR	.328	DIT	90.54	PEQ	15.88	PQU-11.36
A065ZA	NE 44.50	KP	17.27	QU	38.22	MLI	11.81	BHY	106.19	BHYOL	106.19

	Q	OR	AB	AN	NE	LC	KP	AC	NS	KS	C
A065AZ	0.00	27.52	49.59	.82	13.43	0.00	0.00	0.00	0.00	0.00	0.00
	WO	DW	DE	DF	EN	OF	FO	FA	CS	MT	HM
A065BZ	.16	2.25	1.95	0.00	0.00	0.00	0.00	0.00	0.00	1.92	2.14
	IL	TN	PF	RU	AP						
A065CZ	0.00	0.00	0.00	0.00	.22				H2O	2.64	T 100.00
A065DZ	DI 4.20	HY	0.00	OL	0.00	RMGFE	100.000	ANABW	1.62	CI	5.02
A065EZ	FEO/FE2O3	.17	TFE	2.81	MUR	.328	DIT	90.54	PEQ	15.88	PQU-11.36
A065ZZ	NE 44.50	KP	17.27	QU	38.22	MLI	11.81	BHY	106.19	BHYOL	106.19

	Q	OR	AB	AN	NE	LC	KP	AC	NS	KS	C
A059AA	0.00	31.55	41.80	6.61	4.36	0.00	0.00	0.00	0.00	0.00	0.00
	WO	DW	DE	DF	EN	OF	FO	FA	CS	MT	HM
A059BA	0.00	4.25	3.67	0.00	0.00	0.00	.06	0.00	0.00	3.92	.50
	IL	TN	PF	RU	AP						
A059CA	1.22	0.00	0.00	0.00	.57				H2O	1.15	T 98.49
A059DA	DI 7.92	HY	0.00	OL	.06	RMGFE	100.000		ANABW	13.65	CI 14.81
A059EA	FEO/FE2O3	.54	TFE	3.58	MUR	.307	DIT	78.90	PEQ	9.80	PQU -3.76
A059ZA	NE 34.74	KP	23.08	QU	42.18	MLI	10.24	BHY	102.33	BHYOL	102.53

	Q	OR	AB	AN	NE	LC	KP	AC	NS	KS	C
A059AZ	0.00	32.04	42.44	6.71	4.42	0.00	0.00	0.00	0.00	0.00	0.00
	WO	DW	DE	DF	EN	OF	FO	FA	CS	MT	HM
A059BZ	0.00	4.31	3.73	0.00	0.00	0.00	.06	0.00	0.00	3.98	.51
	IL	TN	PF	RU	AP						
A059CZ	1.23	0.00	0.00	0.00	.58				H2O	1.15	T 100.00
A059DZ	DI 8.04	HY	0.00	OL	.06	RMGFE	100.000		ANABW	13.65	CI 14.81
A059EZ	FEO/FE2O3	.54	TFE	3.58	MUR	.307	DIT	78.90	PEQ	9.80	PQU -3.76
A059ZZ	NE 34.74	KP	23.08	QU	42.18	MLI	10.24	BHY	102.33	BHYOL	102.53

	Q	OR	AB	AN	NE	LC	KP	AC	NS	KS	C
A182AA	0.00	39.41	26.79	15.28	5.88	0.00	0.00	0.00	0.00	0.00	0.00
	WO	DW	DE	DF	EN	OF	FO	FA	CS	MT	HM
A182BA	0.00	2.76	1.84	.73	0.00	0.00	1.71	.75	0.00	2.04	0.00
	IL	TN	PF	RU	AP						
A182CA	1.04	0.00	0.00	0.00	.42				H2O	1.25	T 98.66
A182DA	DI 5.33	HY	0.00	OL	2.46	RMGFE	76.879		ANABW	36.32	CI 21.24
A182EA	FEO/FE2O3	1.40	TFE	2.52	MUR	.354	DIT	73.07	PEQ	12.45	PQU -6.01
A182ZA	NE 28.30	KP	31.07	QU	40.63	MLI	10.26	BHY	79.00	BHYOL	89.15

	Q	OR	AB	AN	NE	LC	KP	AC	NS	KS	C
A182AZ	0.00	39.95	27.15	15.49	5.96	0.00	0.00	0.00	0.00	0.00	0.00
	WO	DW	DE	DF	EN	OF	FO	FA	CS	MT	HM
A182BZ	0.00	2.80	1.86	.74	0.00	0.00	1.74	.76	0.00	2.07	0.00
	IL	TN	PF	RU	AP						
A182CZ	1.06	0.00	0.00	0.00	.42				H2O	1.25	T 100.00
A182DZ	DI 5.40	HY	0.00	OL	2.49	RMGFE	76.879		ANABW	36.32	CI 21.24
A182EZ	FEO/FE2O3	1.40	TFE	2.52	MUR	.354	DIT	73.07	PEQ	12.45	PQU -6.01
A182ZZ	NE 28.30	KP	31.07	QU	40.63	MLI	10.26	BHY	79.00	BHYOL	89.15

	Q	OR	AB	AN	NE	LC	KP	AC	NS	KS	C	
A945AA	5.91	19.85	35.45	16.02	0.00	0.00	0.00	0.00	0.00	0.00	0.00	
	WO	DW	DE	DF	EN	OF	FO	FA	CS	MT	HM	
A945BA	0.00	3.10	2.52	.20	5.50	.44	0.00	0.00	0.00	6.93	0.00	
	IL	TN	PF	RU	AP							
A945CA	1.63	0.00	0.00	0.00	1.14					H2O 1.22 T		98.69
A945DA	DI 5.82	HY 5.93	OL 0.00	RMGFE	94.281	ANABW	31.12	CI	25.65			
A945EA	FEO/FE2O3	.65	TFE 5.75	MUR	.289	DIT	62.03	PEQ	-1.98	PQU	5.99	
A945ZA	NE 31.37	KP 18.43	QU 50.20	MLI	6.06	BHY	96.07	BHYOL	96.07			

	Q	OR	AB	AN	NE	LC	KP	AC	NS	KS	C	
A945AZ	5.99	20.12	35.92	16.23	0.00	0.00	0.00	0.00	0.00	0.00	0.00	
	WO	DW	DE	DF	EN	OF	FO	FA	CS	MT	HM	
A945BZ	0.00	3.14	2.56	.20	5.57	.44	0.00	0.00	0.00	7.02	0.00	
	IL	TN	PF	RU	AP							
A945CZ	1.65	0.00	0.00	0.00	1.15					H2O 1.22 T		100.00
A945DZ	DI 5.90	HY 6.01	OL 0.00	RMGFE	94.281	ANABW	31.12	CI	25.65			
A945EZ	FEO/FE2O3	.65	TFE 5.75	MUR	.289	DIT	62.03	PEQ	-1.98	PQU	5.99	
A945ZZ	NE 31.37	KP 18.43	QU 50.20	MLI	6.06	BHY	96.07	BHYOL	96.07			

	Q	OR	AB	AN	NE	LC	KP	AC	NS	KS	C	
A070AA	0.00	23.22	41.57	10.20	1.27	0.00	0.00	0.00	0.00	0.00	0.00	
	WO	DW	DE	DF	EN	OF	FO	FA	CS	MT	HM	
A070BA	0.00	5.01	4.30	.04	0.00	0.00	2.21	.02	0.00	6.58	0.00	
	IL	TN	PF	RU	AP							
A070CA	1.73	0.00	0.00	0.00	1.60					H2O 1.37 T		97.75
A070DA	DI 9.35	HY 0.00	OL 2.23	RMGFE	99.257	ANABW	19.70	CI	22.18			
A070EA	FEO/FE2O3	.62	TFE 5.38	MUR	.302	DIT	67.58	PEQ	6.71	PQU	-2.06	
A070ZA	NE 36.01	KP 19.98	QU 44.01	MLI	6.44	BHY	98.61	BHYOL	105.11			

	Q	OR	AB	AN	NE	LC	KP	AC	NS	KS	C	
A070AZ	0.00	23.76	42.53	10.44	1.30	0.00	0.00	0.00	0.00	0.00	0.00	
	WO	DW	DE	DF	EN	OF	FO	FA	CS	MT	HM	
A070BZ	0.00	5.12	4.40	.04	0.00	0.00	2.26	.02	0.00	6.73	0.00	
	IL	TN	PF	RU	AP							
A070CZ	1.77	0.00	0.00	0.00	1.63					H2O 1.37 T		100.00
A070DZ	DI 9.56	HY 0.00	OL 2.28	RMGFE	99.257	ANABW	19.70	CI	22.18			
A070EZ	FEO/FE2O3	.62	TFE 5.38	MUR	.302	DIT	67.58	PEQ	6.71	PQU	-2.06	
A070ZZ	NE 36.01	KP 19.98	QU 44.01	MLI	6.44	BHY	98.61	BHYOL	105.11			

	Q	OR	AB	AN	NE	LC	KP	AC	NS	KS	C
A035AA	0.00	25.82	36.55	13.22	0.00	0.00	0.00	0.00	0.00	0.00	0.00
	WO	DW	DE	DF	EN	OF	FO	FA	CS	MT	HM
A035BA	0.00	3.27	2.57	.33	4.41	.57	.82	.12	0.00	6.37	0.00
	IL	TN	PF	RU	AP						
A035CA	1.71	0.00	0.00	0.00	1.40				H2O	1.54 T	97.15
A035DA	DI	6.17	HY	4.99	OL	.93	RMGFE	90.992	ANABW	26.55 CI	23.33
A035EA	FEO/FE2O3		.74	TFE	5.59	MUR	.308	DIT	64.20	PEQ 3.98	PQU -.39
A035ZA	NE	31.75	KP	23.53	QU	44.73	MLI	6.86	BHY	99.07	BHYOL 101.84

	Q	OR	AB	AN	NE	LC	KP	AC	NS	KS	C
A035AZ	0.00	26.58	37.62	13.60	0.00	0.00	0.00	0.00	0.00	0.00	0.00
	WO	DW	DE	DF	EN	OF	FO	FA	CS	MT	HM
A035BZ	0.00	3.36	2.64	.34	4.54	.59	.84	.12	0.00	6.55	0.00
	IL	TN	PF	RU	AP						
A035CZ	1.76	0.00	0.00	0.00	1.44				H2O	1.54 T	100.00
A035DZ	DI	6.35	HY	5.13	OL	.96	RMGFE	90.992	ANABW	26.55 CI	23.33
A035EZ	FEO/FE2O3		.74	TFE	5.59	MUR	.308	DIT	64.20	PEQ 3.98	PQU -.39
A035ZZ	NE	31.75	KP	23.53	QU	44.73	MLI	6.86	BHY	99.07	BHYOL 101.84

	Q	OR	AB	AN	NE	LC	KP	AC	NS	KS	C
A095AA	0.00	27.60	1.38	1.08	23.68	0.00	0.00	0.00	0.00	0.00	0.00
	WO	DW	DE	DF	EN	OF	FO	FA	CS	MT	HM
A095BA	0.00	17.86	14.49	1.23	0.00	0.00	0.00	0.00	0.00	6.93	0.00
	IL	TN	PF	RU	AP						
A095CA	1.35	0.00	0.00	0.00	1.88				H2O	1.39 T	97.49
A095DA	DI	33.59	HY	0.00	OL	0.00	RMGFE	93.917	ANABW	43.91 CI	33.18
A095EA	FEO/FE2O3		.71	TFE	5.97	MUR	.298	DIT	54.02	PEQ 21.56	PQU-20.54
A095ZA	NE	46.39	KP	29.78	QU	23.83	MLI	.80	BHY	190.15	BHYOL 190.15

	Q	OR	AB	AN	NE	LC	KP	AC	NS	KS	C
A095AZ	0.00	28.31	1.42	1.11	24.29	0.00	0.00	0.00	0.00	0.00	0.00
	WO	DW	DE	DF	EN	OF	FO	FA	CS	MT	HM
A095BZ	0.00	18.32	14.87	1.27	0.00	0.00	0.00	0.00	0.00	7.11	0.00
	IL	TN	PF	RU	AP						
A095CZ	1.38	0.00	0.00	0.00	1.93				H2O	1.39 T	100.00
A095DZ	DI	34.45	HY	0.00	OL	0.00	RMGFE	93.917	ANABW	43.91 CI	33.18
A095EZ	FEO/FE2O3		.71	TFE	5.97	MUR	.298	DIT	54.02	PEQ 21.56	PQU-20.54
A095ZZ	NE	46.39	KP	29.78	QU	23.83	MLI	.80	BHY	190.15	BHYOL 190.15

		Q	OR	AB	AN	NE	LC	KP	AC	NS	KS	C
A110AA	0.00	26.53	.17	0.00	25.01	0.00	0.00	1.44	0.00	0.00	0.00	
		WO	DW	DE	DF	EN	OF	FO	FA	CS	MT	HM
A110BA	1.30	14.84	12.83	0.00	0.00	0.00	0.00	0.00	0.00	7.28	.54	
		IL	TN	PF	RU	AP						
A110CA	1.80	0.00	0.00	0.00	3.28					H2O 3.05 T	95.02	
A110DA	DI 27.67 HY		0.00 OL	0.00	RMGFE 100.000				ANABW	0.00	CI 29.12	
A110EA	FEO/FE2O3		.49 TFE	6.52 MUR	.311 DIT 54.42 PEQ 25.10 PQU-22.26							
A110ZA	NE 48.55	KP 29.15	QU 22.30	MLI	.80	BHY 199.39	BHYOL 199.39					

		Q	OR	AB	AN	NE	LC	KP	AC	NS	KS	C
A110AZ	0.00	27.92	.18	0.00	26.32	0.00	0.00	1.51	0.00	0.00	0.00	
		WO	DW	DE	DF	EN	OF	FO	FA	CS	MT	HM
A110BZ	1.37	15.62	13.50	0.00	0.00	0.00	0.00	0.00	0.00	7.66	.57	
		IL	TN	PF	RU	AP						
A110CZ	1.90	0.00	0.00	0.00	3.45					H2O 3.05 T	100.00	
A110DZ	DI 29.12 HY		0.00 OL	0.00	RMGFE 100.000				ANABW	0.00	CI 29.12	
A110EZ	FEO/FE2O3		.49 TFE	6.52 MUR	.311 DIT 54.42 PEQ 25.10 PQU-22.26							
A110ZZ	NE 48.55	KP 29.15	QU 22.30	MLI	.80	BHY 199.39	BHYOL 199.39					

		Q	OR	AB	AN	NE	LC	KP	AC	NS	KS	C
A	UAA	0.00	22.57	6.67	16.30	18.99	0.00	0.00	0.00	0.00	0.00	0.00
		WO	DW	DE	DF	EN	OF	FO	FA	CS	MT	HM
A	UBA	0.00	9.83	6.96	2.01	0.00	0.00	6.21	1.98	0.00	5.29	0.00
		IL	TN	PF	RU	AP						
A	UCA	0.00	0.00	0.00	0.00	0.00					H2O 3.35 T	96.80
A	UDA	DI 18.80 HY		0.00 OL	8.18	RMGFE 81.960				ANABW	70.97	CI 38.76
A	UEA	FEO/FE2O3		1.05 TFE	5.55 MUR	.382 DIT 49.82 PEQ 20.02 PQU-19.92						
A	UZA	NE 46.86	KP 26.60	QU 26.54	MLI	1.06	BHY 105.97	BHYOL 132.59				

		Q	OR	AB	AN	NE	LC	KP	AC	NS	KS	C
A	UAZ	0.00	23.32	6.89	16.84	19.61	0.00	0.00	0.00	0.00	0.00	0.00
		WO	DW	DE	DF	EN	OF	FO	FA	CS	MT	HM
A	UBZ	0.00	10.15	7.19	2.08	0.00	0.00	6.41	2.04	0.00	5.47	0.00
		IL	TN	PF	RU	AP						
A	UCZ	0.00	0.00	0.00	0.00	0.00					H2O 3.35 T	100.00
A	UDZ	DI 19.42 HY		0.00 OL	8.45	RMGFE 81.960				ANABW	70.97	CI 38.76
A	UEZ	FEO/FE2O3		1.05 TFE	5.55 MUR	.382 DIT 49.82 PEQ 20.02 PQU-19.92						
A	UZZ	NE 46.86	KP 26.60	QU 26.54	MLI	1.06	BHY 105.97	BHYOL 132.59				

	Q	OR	AB	AN	NE	LC	KP	AC	NS	KS	C
A101AA	0.00	22.04	15.12	0.00	21.10	0.00	0.00	.29	0.00	0.00	0.00
	WO	DW	DE	DF	EN	OF	FO	FA	CS	MT	HM
A101BA	0.00	12.21	8.48	2.71	0.00	0.00	1.94	.69	0.00	5.16	0.00
	IL	TN	PF	RU	AP						
A101CA	2.66	0.00	0.00	0.00	4.81				H2O	1.33 T	97.21
A101DA	DI 23.40	HY	0.00	OL	2.63	RMGFE	80.423	ANABW	0.00	CI	20.82
A101EA	FEO/FE2O3	1.29	TFE	6.24	MUR	.307	DIT	59.93	PEQ	19.71	PQU-19.42
A101ZA	NE 50.28	KP	21.50	QU	28.22	MLI	1.80	BHY	160.76	BHYOL	166.77

	Q	OR	AB	AN	NE	LC	KP	AC	NS	KS	C
A101AZ	0.00	22.67	15.55	0.00	21.71	0.00	0.00	.30	0.00	0.00	0.00
	WO	DW	DE	DF	EN	OF	FO	FA	CS	MT	HM
A101BZ	0.00	12.56	8.73	2.79	0.00	0.00	2.00	.70	0.00	5.31	0.00
	IL	TN	PF	RU	AP						
A101CZ	2.74	0.00	0.00	0.00	4.95				H2O	1.33 T	100.00
A101DZ	DI 24.07	HY	0.00	OL	2.70	RMGFE	80.423	ANABW	0.00	CI	20.82
A101EZ	FEO/FE2O3	1.29	TFE	6.24	MUR	.307	DIT	59.93	PEQ	19.71	PQU-19.42
A101ZZ	NE 50.28	KP	21.50	QU	28.22	MLI	1.80	BHY	160.76	BHYOL	166.77

	Q	OR	AB	AN	NE	LC	KP	AC	NS	KS	C
A183AA	0.00	16.78	2.03	8.42	14.67	0.00	0.00	0.00	0.00	0.00	0.00
	WO	DW	DE	DF	EN	OF	FO	FA	CS	MT	HM
A183BA	0.00	16.51	12.80	1.93	0.00	0.00	13.73	2.28	0.00	6.25	0.00
	IL	TN	PF	RU	AP						
A183CA	1.44	0.00	0.00	0.00	1.31				H2O	1.35 T	98.15
A183DA	DI 31.24	HY	0.00	OL	16.01	RMGFE	89.719	ANABW	80.60	CI	50.71
A183EA	FEO/FE2O3	1.23	TFE	7.12	MUR	.259	DIT	34.11	PEQ	12.38	PQU-19.30
A183ZA	NE 47.10	KP	28.49	QU	24.42	MLI	-6.00	BHY	154.73	BHYOL	181.15

	Q	OR	AB	AN	NE	LC	KP	AC	NS	KS	C
A183AZ	0.00	17.10	2.07	8.58	14.94	0.00	0.00	0.00	0.00	0.00	0.00
	WO	DW	DE	DF	EN	OF	FO	FA	CS	MT	HM
A183BZ	0.00	16.82	13.04	1.96	0.00	0.00	13.99	2.32	0.00	6.37	0.00
	IL	TN	PF	RU	AP						
A183CZ	1.47	0.00	0.00	0.00	1.34				H2O	1.35 T	100.00
A183DZ	DI 31.83	HY	0.00	OL	16.31	RMGFE	89.719	ANABW	80.60	CI	50.71
A183EZ	FEO/FE2O3	1.23	TFE	7.12	MUR	.259	DIT	34.11	PEQ	12.38	PQU-19.30
A183ZZ	NE 47.10	KP	28.49	QU	24.42	MLI	-6.00	BHY	154.73	BHYOL	181.15

	Q	OR	AB	AN	NE	LC	KP	AC	NS	KS	C
A945AA	5.91	19.85	35.45	16.02	0.00	0.00	0.00	0.00	0.00	0.00	0.00
	WO	DW	DE	DF	EN	OF	FO	FA	CS	MT	HM
A945BA	0.00	3.10	2.52	.20	5.50	.44	0.00	0.00	0.00	6.93	0.00
	IL	TN	PF	RU	AP						
A945CA	1.63	0.00	0.00	0.00	1.14				H2O	1.22 T	98.69
A945DA	DI 5.82	HY	5.93	OL	0.00	RMGFE	94.281	ANABW	31.12	CI	25.65
A945EA	FEO/FE203	.65	TFE	5.75	MUR	.289	DIT	62.03	PEQ	-1.98	PQU 5.99
A945ZA	NE 31.37	KP	18.43	QU	50.20	MLI	6.06	BHY	96.07	BHYOL	96.07

	Q	OR	AB	AN	NE	LC	KP	AC	NS	KS	C
A945AZ	5.99	20.12	35.92	16.23	0.00	0.00	0.00	0.00	0.00	0.00	0.00
	WO	DW	DE	DF	EN	OF	FO	FA	CS	MT	HM
A945BZ	0.00	3.14	2.56	.20	5.57	.44	0.00	0.00	0.00	7.02	0.00
	IL	TN	PF	RU	AP						
A945CZ	1.65	0.00	0.00	0.00	1.15				H2O	1.22 T	100.00
A945DZ	DI 5.90	HY	6.01	OL	0.00	RMGFE	94.281	ANABW	31.12	CI	25.65
A945EZ	FEO/FE203	.65	TFE	5.75	MUR	.289	DIT	62.03	PEQ	-1.98	PQU 5.99
A945ZZ	NE 31.37	KP	18.43	QU	50.20	MLI	6.06	BHY	96.07	BHYOL	96.07

	Q	OR	AB	AN	NE	LC	KP	AC	NS	KS	C
A070AA	0.00	23.22	41.57	10.20	1.27	0.00	0.00	0.00	0.00	0.00	0.00
	WO	DW	DE	DF	EN	OF	FO	FA	CS	MT	HM
A070BA	0.00	5.01	4.30	.04	0.00	0.00	2.21	.02	0.00	6.58	0.00
	IL	TN	PF	RU	AP						
A070CA	1.73	0.00	0.00	0.00	1.60				H2O	1.37 T	97.75
A070DA	DI 9.35	HY	0.00	OL	2.23	RMGFE	99.257	ANABW	19.70	CI	22.18
A070EA	FEO/FE203	.62	TFE	5.38	MUR	.302	DIT	67.58	PEQ	6.71	PQU -2.06
A070ZA	NE 36.01	KP	19.98	QU	44.01	MLI	6.44	BHY	98.61	BHYOL	105.11

	Q	OR	AB	AN	NE	LC	KP	AC	NS	KS	C
A070AZ	0.00	23.76	42.53	10.44	1.30	0.00	0.00	0.00	0.00	0.00	0.00
	WO	DW	DE	DF	EN	OF	FO	FA	CS	MT	HM
A070BZ	0.00	5.12	4.40	.04	0.00	0.00	2.26	.02	0.00	6.73	0.00
	IL	TN	PF	RU	AP						
A070CZ	1.77	0.00	0.00	0.00	1.63				H2O	1.37 T	100.00
A070DZ	DI 9.56	HY	0.00	OL	2.28	RMGFE	99.257	ANABW	19.70	CI	22.18
A070EZ	FEO/FE203	.62	TFE	5.38	MUR	.302	DIT	67.58	PEQ	6.71	PQU -2.06
A070ZZ	NE 36.01	KP	19.98	QU	44.01	MLI	6.44	BHY	98.61	BHYOL	105.11

Thin section descriptions

The thin section descriptions are listed numerically by group in the following order: feldspathoid syenite and trachytes, quartz latites and rhyolites, mafic trachytes and latites, lamprophyres, andesites and basalts, followed by malignites.

Sample S-61

Location: basal contact of Target Peak aegerine syenite laccolith, southern cliff.

Megascopic: light-green, fine-grained slightly porphyritic.

Texture: trachytic.

Aegerine-augite:

Magnetite: minor subophitic texture with feldspar.

Feldspar: laths replaced by calcite, zeolite.

Analcite: phenocrysts abundant, some partly altered to polycrystalline zeolite, pseudomorphed by calcite and minor chlorite for at least up to 2 cm. from the contact.

Apatite:

Contact is sharp, some 1-2 mm. feldspar laths at contact, abundant calcite for 1 mm. distance from contact, some calcite veining in country rock sericite.

See S-62, S-63 has some calcite and primary (?) analcite (5 Ft. from the contact).

Sample S-62

Location: 2' above the base of the southern cliff of Target Peak aegerine syenite laccolith.

Aegerine-augite: chloritized in centers.

Feldspar phenocrysts, 2V is less than 60 degrees in the center of crystal, elsewhere is perthitic.

Analcite:

Calcite:

Apatite:

Zeolite:

Counts	Aegerine-augite	Feldspar Phenocrysts	Feldspar Matrix
200	13.5	9.0	43.5

Analcite	Zeolite	Calcite
6.0	19.5	2.5

Sample S-116

Location: 65 ft. above the base of lower cliff at the southern end of Target Peak laccolith.

Megascopic: medium-grained, gray to green with deep-red irregular spots (sodalite).

Specific Gravity: 2.54.

Texture: medium-grained, trachytic.

Aegerine, Aegerine-augite: zoned, contains glass and other minute inclusions, one colorless center has complicated extinction, associated with high birefringence, high relief mineral (?), euhedral, with 2 directions of cleavage, diopsidic augite(?).

Opaques: magnetite, anhedral.

Feldspars: laths, polysynthetic twinning, twin boundaries sharp to vague, straight to irregular, straight twin planes do not extend the length of lath always, turbid, laths penetrate each other, but a later albite boundry may follow the outline of the penetrated lath, similar to that on page 502 of the (Retiev, 1964), extinction angles for the smaller well twinned laths are 10, 19.5, 15.5, 6, on stained slide 0, 0 degrees, some of the laths have very patchy to wormy perthites similar to that reported by Retiev, in that case it represents intersection of the solvus with unmixing as well as direct precipitation of sodium feldspar (?), in second stained slide (slide 3) moderate calcium stain, outline not stained indicating less than 3 per cent An. molecule in rims, irregular light staining for potassium occurred, yet in another part of slide the feldspar did not take the stain while analcite did take the calcium stain, index of refraction less than 1.54 mainly an antiperthite on basis of chemical analysis and phenocryst 2 mm. by 5 mm. and albite; various parts of feldspar laths take potassium stain well usually rim does not stain, microperthite.

Nepheline: clear anhedral, with inclusions as surrounding feldspars, took stain for calcium lightly, which does not necessarily indicate calcium, altered to light yellow and pink-red sodalite on rims.

Analcite: colorless, clear, not turbid, poor cubic cleavage, interstitial, etched slide displays cubic cleavage, may be late analcite, six sided in nepheline, birefringent, speckled with alteration products, zeolitized, pyroxene (?) microlites are abundant, also turbid hexagonal isotropic areas elsewhere primary(?).

Sodalite: yellow and dusty pink, isotropic, possibly 2 minerals, as alteration product of nepheline.

Sample S-116 (continued)

Zeolite: often associated with isotropic areas or holes in slides radial aggregates of laths, subhedral to anhedral, some six-sided pseudomorphs with radial zeolites, associated brown opaque alteration.

Sericite(?): replacing analcite, some have a light tinge of yellow radiating needles, could be a zeolite, moderate birefringence.

Apatite: up to 1.5 mm. long.

Sphene(?):

Calcite: anhedral.

			Primary(?) Analcite			Interstitial
	Aegerine					
Counts	Augite	Feldspar	Isotropic	Nepheline	Sodalite	Analcite
500	8.4	71.6	6.8	1.2	1.4	3.6

Zeolite, Sericite and Unidentified Alteration Products	Calcite	Apatite
6.6	.4	.2

Sample 135

Location: 15 ft. above the curving base of the southwest side of Target Peak aegerine syenite laccolith.

Megascopic: gray, fine-grained porphytic.

Texture: trachytic.

Aegerine-augite: in aggregates, as matrix and phenocrysts.

Olivine: trace, in 3-4 mm. aggregate, colorless, surrounded by serpentine succeeded by biotite followed by aegerine augite, fine-grained magnetite rims olivine, apatite associated, indicates relation between the malignites and aegerine syenites.

Biotite: trace besides that which surrounds the olivine, surrounded by pyroxene, sphene (?) inclusion, indicates that dependence of biotite on olivine.

Feldspar phenocrysts: prominent Carlsbad twinning, clear and turbid, turbid brown alteration product isotropic, hexagonal and square isotropic, some light blue sodalitic inclusions, minor gird twinning developed in part of phenocrysts, some appear microperthitic.

Feldspar matrix: microperthitic and albite, turbid and zeolitized.

Analcite: clear triangular secondary, minor, some polycrystalline pseudomorphs after analcite (?).

Nepheline: turbid, minor, altered.

Sodalite (?): light blue isotropic to slightly birefringent, six-sided outline, turbid.

Apatite: minor.

Counts	Aegerine-Augite	Feldspar Matrix	Feldspar Phenocrysts	Isotropics plus nep. alteration products
200	17.5	70.5	6.0	6.0

Sample S-142

Location: 20' from the top of Target Peak laccolith associated with pegmatite pods.

Megascopic: light gray with pink spots of sodalite alteration, fine-grained, slightly porphyritic.

Texture: see above.

Aegerine-augite: zoned light-green to medium-green, pleochroic medium-brown to light-brown, aegerine needles are absent.

Opaques: as alteration product.

Feldspar: turbid as compared to the analcite, as laths, multiple twinning, perthitic, parallel extinction in untwinned parts, rims often clear while centers are turbid, alteration conforms to parts of twins suggesting compositional differences, index of refraction less than 1.54, one small lath had extinction angle of 12.5 degrees, centers contain numerous inclusions, laths stain for potassium, rims often do not stain for potassium suggesting albite, staining is often irregular, grid twinning not evident, all the above indicates microperthite with albite rims, 2V may be moderate in size (microperthite is less than 100 u or one-tenth mm. in size according to Tuttle's classification).

Nepheline: clear, anhedral, partly replaced by light-yellow isotropic sodalite (?), also rimmed by pink turbid isotropic sodalite, cleaved, often associated with white eyes described below, in one case nepheline has one square edge and contains a hexagonal white eye, with turbid brown border but fairly sharp, also another curving boundary.

White eyes: six-sided, square, anhedral areas of polycrystalline material, in contact with augite and partly surrounded by aegerine indicating that the mineral was formed at least before the aegerine, usually surrounded by nepheline which is altered to pink and yellow sodalite, sometimes there is a narrow turbid zone between nepheline and white eyes, euhedral against feldspar, with 400X magnification, the contact is wavy and sometimes sharp, one example appears to be partly zeolitized isotropic mineral which is rimmed by pink nepheline alterations, finer polycrystalline material is less than .01 mm. in size while the coarser material is .1 mm. to .01 mm. in size, these polycrystalline areas did not take the potassium stain.

Analcite: triangular areas between feldspar laths, typical cleavage.

Calcite:

Apatite: euhedral, tabular.

Sericite: alteration, in plucked areas, moderate birefringence.

Sample S-142 (continued)

Unidentified mineral: extremely high relief, high birefringence, uniaxial, euhedral feldspar laths extend into it, also replacing feldspars, good cleavage.

Sodalite: light-yellow and pink turbid replacing nepheline, isotropic, complex extinction in pegmatite.

Counts	Aegerine-augite	Feldspar	Analcite	Nepheline Sodalite	White Eyes	Sericitic Alteration
200	11.0	70.5	6.0	4.0	2.5	3.0

Unidentified
1.5

Note: S-108 also has the zeolitized six-sided shaped mineral but with not as good an intergrowth as this slide, in many slides the intergrowth has yellow birefringence.

Sample 705

Location: dike on axis of Robinson Anticline, on creek north of Meadow Creek, same as 680.

Megascopic: light green, fine-grained.

Texture: trachytic.

Aegerine: needles, minor aegerine augite phenocrysts, maximum 2 mm. long.

Feldspar phenocryst: trace, Carlsbad twinning, rim altered to light green isotropic noselite.

Matrix feldspar: microperthite and albite, turbid.

Analcite (?): altered, hexagonal and square, aegerine inclusions along cleavage, some are light yellow and dusty-purple indicating sodalization, also zeolitization, do not stain for potassium, also clear anhedral with complex twinning occasionally, turbid feldspars stick into clear analcite.

Zeolite:

Unidentified: blue birefringent, colorless, prismatic.

Aegerine trachyte.

Sample S-498

Location: east contact of the north end of Virginia Peak laccolith.

Megascopic: medium-green with pink feldspar phenocrysts.

Texture: fine-grained porphyritic, trachytic.

Aegerine: as minute needles in groundmass, minor phenocrysts.

Feldspar: phenocrysts, Carlsbad twinning prominent, euhedral, estimated 2V is 60-70 degrees, turbid, optic axis is perpendicular to Carlsbad twin plane, slight stain for K, turbid parts of phenocrysts stained, etched for 20 sec. and one min., a few entire matrix feldspar stained where turbid, vague polysynthetic twinning, 1 cm. phenocrysts, few took staining moderately, matrix feldspar had alternating laths stained for potassium, and is a microperthite, the phenocrysts stained irregularly, and could be an untwinned anorthoclase (X-ray perthite?) which might be expected at the contact of a hypabyssal intrusion, a vague multiple twinning is developed occasionally.

Analcite: minor phenocrysts, anhedral.

Sample 499 (459)

Location: Virginia Peak laccolith, at north end, near the west contact.

Megascopic: gray, fine-grained, porphyritic, several slides.

Specific Gravity: 2.58.

Microscopic:

Texture: fine-grained, porphyritic, trachytic, feldspar phenocrysts 1-4 cm. in length.

Aegerine: little or no zoning, pleochroic green, usually maximum 2 cm. in length and 1 cm. in width, part of matrix, parallel extinction, minor aegerine augite cores, centers sometimes deep blue, as inclusions in feldspar, associated once with fibrous, radiating mineral with high relief and high birefringence, (colorless aegerine).

Opaques: anhedral magnetite-limonite(?) intergrowth, alteration.

Microperthite: phenocrysts more turbid than the groundmass, most stain for potassium lightly, phenocrysts display polysynthetic twinning throughout or in part, perthitic, twinned feldspars in untwinned feldspars ~~in untwinned feldspars~~ which are diagonal to the long direction of the untwinned feldspar, multiple twinned feldspar has higher index of refraction than untwinned feldspar, also some antiperthite development, turbid areas are usually near edges of phenocrysts, percline twinning and vague grid twinning developed, polysynthetic parts of phenocrysts, are unstained for potassium, while the rest of the feldspar is, also these latter parts are not as turbid, these characters indicate the perthitic character, turbidities similar to that of the Pilansburg complex, see slides in the University of Cincinnati collection, reference in the Transactions of the Geological Society of South Africa, vol. 31, 1938, Wolff states that the phenocrysts are anorthoclase, using his analysis of anorthoclase in computation of the chemical analysis from the mode indicates that the feldspar of this rock sample has an average composition of his anorthoclase, large 2V, "Sodium rich sanidine and anorthoclase breaks down into albite, microcline", extinction angle 12.5 degrees.

Zeolite: minor, some with moderate birefringence, irregular extinction.

Analcite(?): isotopic, clear, some cleavage.

Unidentified Mineral: colorless, yellow, birefringent, parallel extinction, moderate relief, prismatic, trace.

Sample 499 (continued)

Sericite: trace, cryptocrystalline, light brown.

S-15 is a little coarser grained, but mainly fine-grained, less brown alteration.

S-17 has much less alteration as 478.

S-17 contains isotropic irregular areas in phenocrysts which are turbid purple-blue (sodialite?), also contains light brown biolite or amphibole with parallel extinction, also more analcite than 499, interstitial. Calcium stain test positive for most feldspars.

Counts	Aegerine	Feldspar Phenocrysts	Feldspar Matrix	Zeolite	Analcite	Sericite
400	9.8	38.5	49.2	0.75	1.0	0.75

Sample 678

Location: poorly exposed concordant body in center of Robinson Anticline, 5' thick.

Megascopic: pink, fine-grained with feldspar phenocrysts 3 cm. long, pyrobole 5 mm. long (?).

Texture: fine-grained, porphyritic, with trachytic groundmass.

Pyroxene: zoned light to medium-green, subhedral to euhedral, associated with biotite, magnetite, hornblende, biotite, magnetite pyroxene surrounded by chlorite.

Magnetite: with limonitic alteration, anhedral.

Biotite: pleochroic light brown to red-brown.

Amphibole: pleochroic light to green-brown, c:Z' is 20 degrees which indicates common hornblende.

Alkali Feldspar Matrix: turbid brown, trachytic laths with parallel extinction, cryptocrystalline aegerines or augites, biotites and opaques in the matrix.

Feldspar phenocrysts: euhedral, penetration twins, surrounded by narrow margin of chlorite, irregular multiple twinning, alternating twins are turbid, very altered, take potassium stain, at least the larger phenocrysts, anorthoclase (?), plagioclase, S-26 is very similar.

Apatite: subhedral, maximum one mm. long.

Calcite: anhedral, minor.

Counts	Augite	Magnetite	Biotite	Hornblende	Feldspar Phenocrysts
200	6.5	1.5	t	3.0	21.0

Matrix Feldspar	Chlorite	Calcite
67.0	1.0	1.0

Pegamite Pods of Target Peak Feldspathoid Syenite Laccolith

Location: from near the top of both benches of Target Peak, S-118 from the lower bench and (T) of 142A is taken from the base of Target Cliff, the pods occur 20' from the top.

Megascopic: elongate pods, maximum dimensions are 1' by 3', feldspars and aegerines extend at right angles to the border.

Texture: coarse-grained hypautomorphic.

Aegerine: brown-green to green only slightly zoned in 142A, in 118 light green aegerine-augite occurs, much has parallel extinction, sprays of aegerine needles often grow into analcite, prismatic.

Feldspar: alkali, altered to a perthitic intergrowth of zeolite, alternating irregular laminae take the potassium stain well, often very turbid, laths are 1 cm. in length, numerous light green to colorless pyroxene and apatite inclusions in altered materials, a very low 2V was obtained in the center of the lath which was perthitic elsewhere, the low 2V material looked almost uniaxial and was turbid, predominate mineral.

Nepheline: rims altered to light brown sodalite and other alteration products which may be pyroxene microlites and red-brown translucent biotite (?) as well as zeolite, sodalization (?) occurs in irregular waves, nepheline is hexagonal and rectangular and subhedral, two directions of good cleavage.

Sodalite (?): has complicated extinction in places, light yellow to orange, zoned, pink megascopically, uniaxial positive sign was obtained once, also some purple dusty isotropic alteration of nepheline, the light brown material is isotropic and will be gradational to abrupt in contact with the light orange birefringent material, slab treated with 70% HNO_3 until dry causing the formation of the NaCl cubes, irregularly distributed across the crystal, minor prismatic $CaSO_4 H_2O$ (?) crystals formed in veinlike areas on alteration product and surrounds the red edge of the alteration product in radiating groups of fibers, the red coloration appears to have diffused to the edge of the crystal in the process of salt formation, also contains aegerine-augite microlites, did not fluoresce with long or short wave ultraviolet light, did not stain with methyl blue.

Analcite: triangular areas between feldspar laths, clear, often complex extinction, poor cubic cleavage, zeolitized in which case includes microlites of aegerine often giving these interstitial areas a megascopic green cast.

Sericite (?): very fine crystalline replacement of six-sided mineral.

Calcite:

Target Peak Pegmatite Pods (continued)

Unidentified: brown birefringent alteration product near edges of six-sided shaped outline, minor, radial aggregates minor.

Opaques: magnetite with oxidized stain.

Unidentified: high relief, good cleavage, high birefringent material.

Sample S-31

Location: near top of 40' sill overlooking Forest Lake from the East.

See description of S-32.

Chlorite: with numerous sphene inclusions parallel the cleavage, these are subhedral, chlorite, calcite, apatite and sphene are pseudomorphing hornblende, biotite(?).

Biotite: brown and green chlorite is interbedded.

Plagioclase: zones with quartz between zones, as phenocrysts, extinction angles are 3.5 degrees, higher index of refraction than 1.54.

Kspar: minor as phenocrysts, some patch perthite(?).

Matrix: cryptocrystalline, stained for potassium, contains a significant amount of quartz.

Quartz: in matrix, in elongated attached groups.

Sphene:

Calcite: rimmed with quartz, also contains green chlorite.

Magnetite: is associated with the chlorite pseudomorphs.

Sample 32

Location: about 10' above base of 40' sill, S-3 from the top, overlooks Forest Lake from the east.

Megascopic: fine-grained, porphyritic, light brown groundmass and white feldspar laths.

Texture: felsic matrix, laths up to 4 mm. long.

Biotite: red-brown to light brown, shredded, associated with chlorite, high relief inclusions parallel the cleavage, interbedded green and brown zones.

Chlorite: light green to light brown pleochroic.

Opaques: black in reflected light, anhedral.

Plagioclase: laths 4.5, 0, are only observed extinction angles, clear, estimated 2V 75-85 degrees, index of refraction higher than balsam, calcium oligoclase.

Kspar: euhedral, center phenocrysts of one group of phenocrysts stained for K.

Matrix: .1 - .01 mm., felsic, quartz and alkali feldspar which stains for potassium.

Apatite: euhedral.

Counts	Biotite	Chlorite	Plagioclase Phenocrysts	Kspar Phenocrysts	Matrix	Magnetite
200	2.0	3.0	26.0	0.5	68.0	0.5

Color Index: 5.5, very similar to S-70, 479a.

Sample S-70

Location: same body as 479A and 45 07', approximately 500 feet north of Cottonwood Creek, on ridge near south end of the body.

Megascopic: white to gray with limonitic stain.

Texture: fine-grained porphyry, plagioclase laths up to 3 cm. in length, subparallel orientation of plagioclase and biotite.

Hornblende: light to medium-green, simple twinning, trace.

Biotite: pleochroic, black to dark brown to light yellow, euhedral to anhedral.

Magnetite: anhedral to euhedral, trace.

Plagioclase: as laths, some zoning, one extension angle equals 4.2, other laths have 0-degree extinction angle, index of refraction higher than balsam indicating approximate An 23 to 24, vein and patch extinction, some jagged outlines.

Perthite: rectangular with lath plagioclase inclusions that extend into matrix, .4 cm. across.

Quartz: round as polycrystalline aggregates, inclusions abundant but absent near quartz edges and cracks, some of the inclusions are pyroxene, one quartz grain contains a vein-like area of microcrystalline quartz (?).

Matrix: microcrystalline quartz and alkali feldspar, microgranitic texture .1 to .01 mm. in size.

Sphene: subhedral, trace.

Sample S-126

Location: sill maximum 40 ft. thickness, below, and to the west of Target Peak, terminating in irregular noses, inclusion of shale in the nose.

Megascopic: pink, with white feldspar phenocrysts, fine-grained porphyry with plagioclase black amphibole and biotite phenocrysts.

Texture: see above.

Hornblende: euhedral, light green-brown to green pleochroic, c:Z' are 15, 16, 20, 21 degrees.

Biotite: red-brown to light brown pleochroic.

Opaques: magnetite, anhedral.

Plagioclase: laths altered along cracks, zoning, albite and minor pericline, Carlsbad, narrow twinning. Narrow potassium stain on rims, minor antiperthitic (?) development, lower index of refraction than 1.54, extinction angles are 4.5, 16.5, 4.5, 6, 10.5 degrees, in perthite 11 degrees, (max. An is 5 per cent) .1 - .01 mm. size.

Perthite: rectangular with rectangular plagioclase inclusions that extend into matrix, rare rimming of orthoclase by plagioclase, stained.

Quartz: anhedral in matrix, in strings, rare association with biotite rare round phenocrysts.

Apatite: euhedral.

Counts	Hornblende	Biotite	Opaques	Matrix	Quartz	Plagioclase
300	2.0	2.7	1.0	71.3	2.1	20.3

Perthite
0.3

Matrix: small feldspar laths, turbid, stained for potassium, quartz.

Color index 5.7.

Sample 394

Location: sill at top of cirque just south of Lebo Peak.

Megascopic: gray with green mafics, fine-grained, porphyritic.

Specific Gravity: 2.68.

Texture: fine-grained porphyritic, parallel orientation of phenocrysts.

Pyroxene (?): anhedral, colorless, trace.

Hornblende: pleochroic medium to light brown, zoned with green rims, anhedral to euhedral, another more common hornblende is medium green to light green which is usually ragged in outline, with not very prominent cleavage, chloritized in part, c:Z' approximately 17 degrees second hornblende is probably first being chloritized.

Biotite: pleochroic deep red to blue-brown to light yellow, anhedral to subhedral, biotite in aggregates, interbedded layers of biotite and hornblende, similar to the Boulder Bathylith samples, replaced by quartz along layers, high relief inclusions associated, some bent crystals.

Chlorite: light green, slightly pleochroic, berlin blue interference colors, associated with hornblende, 3 mm. across chlorite mass, surrounded by biotite on one side, with some euhedral outlines.

Plagioclase: laths slightly turbid, altered in part to epidote (light green to yellow), calcite; rims often stained for potassium parallel extinction indicating An 20, only phenocrysts stained for Ca., Norm indicates total An content as An 16.

Quartz: anhedral, matrix and phenocrysts, in polycrystalline masses, replacing hornblende.

Matrix: 1 mm. to .02 mm. in size, quartz, alkali feldspar (stains for potassium), felsophyric, took Ca stain in places where no potassium stain, indicating plagioclase in groundmass.

Apatite: minor euhedral.

Counts	Hornblende Chlorite	Biotite	Plagioclase	Matrix	Quartz	Epidote
1000	5.2	4.5	38.8	46.1	4.9	0.4

Apatite
0.1

Norm indicates 12 per cent quartz.
Quartz micromonzonite.
Rhydacite (quartz latite) on basis of chemical analysis, type of plagioclase, hornblende.

Sample 425

Location: 35' sill north of Beverly Peak.

Megascopic: cream to pink with green mafics, fine-grained porphyry.

Texture: see above, felsic cryptocrystalline matrix.

Hornblende: green to light brown pleochroic, euhedral, altered to chlorite.

Chlorite: light green, numerous high relief inclusions parallel to the cleavage.

Magnetite: anhedral, in aggregates.

Plagioclase: euhedral to subhedral, laths, extinction angles are 10, 11, 12, 5, 0.6 degrees, index of refraction less than 1.54 indicating albite (An 10 per cent).

Matrix: turbid, stains for potassium, .1 - .01 mm. felsic, quartz and alkali feldspar.

Perthite: stained for Kspar, euhedral, with plagioclase inclusions some 2.5 mm. across, some occurances of Kspar surrounded by plagioclase, anhedral to euhedral, small 2V.

Biotite: black to red-brown, pleochroic, minor.

Calcite: anhedral in matrix.

Apatite: subhedral.

Quartz: anhedral in matrix.

High relief, high birefringent alteration product.

Counts	Hornblende	Opaques	Plagioclase	Kspar	Quartz	Matrix
400	4.5	1.2	35.2	8.0	1.2	51.5

Chlorite	Alteration product
0.2	0.5

Color index: 5.9

Sample 479A

Location: same as S-70, or Wolff's 45 '07, linear body 200 to 300 feet wide and 200 feet high at north end; this particular sample was collected from near center of the body, ridge north of Target Peak.

Specific Gravity: 2.63.

Megascopic: white to gray with limonitic stain.

Texture: fine-grained porphyry.

Biotite: dark-brown to light yellow pleochroic, subhedral to anhedral with apatite inclusions, magnetite with exsolved texture.

Opaques: anhedral magnetite.

Plagioclase: laths are euhedral to subhedral, zoned slightly polysynthetic twinning not abundant, most have parallel extension indicating An 20, vein-like extinction in one half of twin and not other, narrow border and irregular spots stained for potassium, patches and veins do not stain for potassium.

Quartz: as phenocrysts anhedral usually, also subhedral, several grains in contact, straight extinction, few inclusions, grains not fractured.

Matrix: according to staining about one half of the matrix is orthoclase and the rest is quartz and plagioclase.

Zircon:

Apatite: subhedral, prismatic.

Counts	Biotite	Altered Hornblende	Magnetite	Plagioclase	Quartz	Matrix
400	4.5	1.5	0.5	32	1.0	60.5

Color index
6.5

Sample 578

Location: sill on the west side of Beverly Cirque, 55' thick, sill 579 is in contact.

Megascopic: white, with green hornblende phenocrysts, many basic inclusions.

Specific gravity: 2.67.

Texture: fine-grained porphyritic, matrix is very fine-grained to cryptocrystalline, about one-half of the matrix stained irregularly for potassium.

Hornblende: light green to medium green to olive-green pleochroic, mainly euhedral, twins display different pleochroism due to orientation (?), extinction angles 20, 29, 20 degrees for c:Z', X' is yellow, Y is dark green; sphene inclusions.

Biotite: dark brown associated with hornblende, minor.

Chlorite: alteration product of hornblende, berlin blue interference color indicates penninite possibly.

Magnetite: subhedral, limonitic alteration.

Plagioclase: as phenocrysts; some of which are rimmed by brown, fine-grained material surrounded by albite, contains apatite inclusions; plagioclase sometimes rims the orthoclase, subhedral to euhedral; phenocrysts often turbid, zoned penetration twins, rare complex twin pattern, albite and peracline twinning, index refraction lower than balsam, extinction angles of 10, 1.5, 4.5, 5.5, 5.5 degrees indicating oligoclase (Ab 11), zoned, growth rims on plagioclase are idented.

Orthoclase and perthite: mainly euhedral, but also subhedral and anhedral, often contains plagioclase phenocrysts, simple twinning, zones of quartz near boundary, hornblende phenocryst inclusions; some of the plagioclase inclusions are in the same optical orientation, others are not, some plagioclase inclusions extend beyond the orthoclase border indicating it is not an exsolution perthite; one rare example contains plagioclase laths near the rim and is surrounded by a continuous rim of finely crystalline material that looks somewhat like the matrix, some may be quartz, the outer edge of this rim is gradational in places and sharp in others with the matrix; the rim did not stain for potassium while the matrix stained lightly; hornblende occurs in the outer mantle. The stain of the potassium feldspar appears to be related to optical orientation (?) as far as intensity is concerned, phenocrysts usually larger than plagioclase, extinction angles of plagioclase inclusions are 24.5, 13.0, 2.5, indicating andesine (An 45), one plagioclase inclusion was zoned equally toward potassium feldspar and matrix boundaries.

Sample 578 (continued)

Quartz: anhedral, near rims of potassium feldspar.

Matrix: .1 - .01 mm. in size, felsic texture, quartz and alkali feldspar.

Apatite: subhedral, to euhedral, prismatic, one grain is .5 mm. long.

Sphene:

Unidentified mineral: high relief, high birefringent, associated with chlorite.

Counts	Hornblende	Magnetite	Biotite	Plagioclase	Albite Rims
1000	7.5	1.8	.25	30.6	0.8

Potassium Feldspar	Matrix	Apatite	Sphene	Unidentified
7.5	51.2	0.2	.3	.1

Color Index
9.5

Two slides counted, the one with more intense has epoxy cement.

Sample 582

Location: sill 10' thick on the west side of Beverly Cirque.

Megascopic: cream fine-grained porphyry with pink feldspar phenocrysts, green mafics, two samples of the contact, one rippled, the other sheared.

Texture: fine-grained porphyry.

Chlorite: light green to light brown, up to 2 mm. masses, associated with calcite magnetite, limonite, apatite, perfectly pseudomorphic after hornblende (?).

Opaques: anhedral, black in reflected light, some limonite (?).

Plagioclase: as laths, one clear lath surrounded by larger lath which is sericitic clear lath is probably orthoclase, while other is plagioclase, 1-3 mm. long, much is turbid, zoned, euhedral, extinction angles are 5, 4.5, 10.5, 2.5, 8, 12.5, combined Carlsbad, albite 11.5 to 6. degrees, index of refraction more than 1.54 indicating low Ca. andesine, maximum 4 mm. long.

Matrix: turbid, stained for potassium, felsic texture, quartz, and alkali feldspar, 1-.01 mm.

Quartz: as phenocrysts and in groundmass, embayed, stained slides show circular zones around the quartz.

Perthite: patches displayed well by staining, plagioclase has good combined Carlsbad--albite twins, orthoclase rarely surrounded by plagioclase, 2V less than 60 degrees, plagioclase probably about An 20.

Calcite: mainly in matrix, surrounding the feldspar phenocrysts, but not replacing them, surrounded by chlorite in pseudomorphs after hornblende, rarely associated with quartz, but not replacing it.

Counts	Chlorite	Opaques	Plagioclase Phenocrysts	Plagioclase In Perthite	Kspar	Matrix
200	5.0m	0.5	27.5	2.5	11.0	46.0

Calcite	Quartz
3.0	3.0

Color Index: 5.5

On the basis of the Kspar plagioclase ratio of the phenocrysts, which actually places it on the border between dacite and rhyodacite, similar to 578, this rock is called a rhyodacite.

Sample S-14 equals 467

Location: dike exposed along road below Forest Lake, 25' exposure, hornblende and feldspars are lineated N.40W and horizontal, many inclusions of coarse basic altered material and felsic material, sample of the basic inclusion is also 467.

Megascopic: light brown groundmass, pink feldspar and black hornblendes, one inclusion 1 cm. by 2 cm. containing hornblende and medium grained pink felsic minerals.

Texture: fine-grained porphyritic, slightly cumulorporphyritic.

Augite: very light green to colorless, simple twins, positive sign estimated 2V is 60 to 70 degrees, euhedral, some prismatic (?) c:Z' is 27. 52. 58 degrees.

Hornblende: dark green to light brown pleochroic, euhedral mostly, mainly as phenocrysts, much simple twinning, zoned 3-4 mm. long as a maximum, associated with magnetite, seam twinning, in aggregates 2 mm. across with magnetite, c:Z' is 15, 15 to 11 degrees on the edge.

Biotite: brown, minor.

Chlorite: light green to colorless, berlin blue interference color, interbedded with biotite, associated with numerous high relief inclusions parallel the cleavage, chlorite is likely Penninite, sphene, radial extinction.

Opaques: euhedral to anhedral, some brassy black, magnetite associated with hornblende, bimodal size.

Quartz: anhedral to euhedral, higher index than the feldspar matrix.

Calcite: associated with quartz, cut by sericite vein (?) and associated with zeolite or feldspar, calcite euhedral with zeolite.

Feldspar: plagioclase phenocrysts, turbid, index of refraction less than 1.54, maximum length 3 mm. long, extinction angles are 9, 11.5, 13.5, 15, 15 degrees, matrix feldspars also lower index than 1.54, matrix stains for potassium, also contains minute augites, hornblende, magnetite, may be epoxy in which case feldspar equals An 33, trachytic feldspar matrix.

Apatite: subhedral.

Sphene: high relief, high birefringence, parting not parallel the crystal outline, associated with zeolite and quartz, euhedral, no complete extinction.

Counts	Augite	Hornblende Phenocrysts	Plagioclase Phenocrysts	Matrix Feldspar	Opaques	Chlorite
200	3.0	10.0	11.5	72.0	3.5	0.5

Color index: 17.0

Sample S-76A

Location: 2" above the base of the upper sill exposed along the road about a half-mile east of Bennett Cabin, sill is 15' thick, poor slide.

Megascopic: dark brown, very fine-grained matrix with white feldspar phenocrysts.

Texture: very fine-grained porphyritic.

Chlorite: light orange-brown, pseudomorphic after hornblende.

Magnetite: anhedral surrounded by limonite stain.

Plagioclase: as laths, did not stain for K, multiple twinning not common, extinction angles of 13, 15 degrees indicate andesine An 33 (?).

Matrix: stained evenly for K, turbid, microlitic feldspar, trachytic, less than 0.1 mm.

Zeolite: clear, anhedral, light yellow birefringence, did not take K stain, elongate.

Calcite: associated with chlorite in pseudomorphs of hornblende.

Counts	Chlorite	Magnetite	Plagioclase	Matrix	Zeolite	Calcite
200	7.5	3.5	15.5	68.0	3.5	2.0

Color Index: 11.0

Sample S-76B

Location: near middle of sill as described in S-76A.

Megascopic: altered, light brown matrix, plagioclase and hornblende phenocrysts, limonite stained, very similar to a few of Davis' dikes, poor thin section.

Texture: porphyritic.

Hornblende: light green to medium green pleochroic.

Magnetite: anhedral.

Biotite: orange-brown to brown pleochroic.

Plagioclase: phenocrysts are altered, zoned, limonite stained, most with parallel extinction, usually not as turbid as groundmass feldspars, other extinction angles are 6.5, 4.5, 11 degrees, higher index than 1.54 An 29 (?), zoned slightly.

Matrix: mainly feldspar, turbid, stained for K, less than 0.2 mm. in size.

Quartz: minor in matrix.

Apatite: minor.

Calcite: minor.

Counts	Hornblende	Biotite	Plagioclase Phenocrysts	Feldspar Matrix	Magnetite
200	12.5	3.0	20.0	61.0	3.5

Color Index: 20.0

Hornblende oligoclase latite.

Sample S-78

Location: along the Upper Shields River, one-half mile east of Bennett Cabin, same sill as S-76 A and B.

Megascopic: 12' to 15' thick, vesicules parallel the bedding, mostly in the upper 5', no obvious contact effects, chilled top and bottom, medium-brown with cream plagioclase laths and black hornblende.

Texture: trachytic.

Hornblende: olive-green to brown pleochroic, one c:Z' equals 15 degrees.

Biotite: brown to yellow-brown, associated with magnetite.

Magnetite: anhedral.

Chlorite: minor, associated with biotite.

Plagioclase: phenocryst laths, negative K stain, index of refraction higher than 1.54, euhedral, Carlsbad twins, multiple twins, some patchy extinction, sericitic alteration, extinction angles 11, 0, 0, 0, 0; An 29 (?).

Matrix: mostly feldspar which stains for K, turbid, less than 0.1 mm. in size.

Quartz: anhedral in matrix, minor.

Calcite: minor.

Counts	Hornblende	Magnetite	Biotite	Plagioclase Phenocrysts	Matrix
200	14.0	1.5	3.0	14.0	67.0

Color Index: 18.5

Sample S-112

Location: 5' sill or low angle dike 200 feet below the lower cliff of Target Peak analcite syenite.

Megascopic: light brown, fine-grained, oriented sample.

Texture: fine-grained glomerophyritic, this feature was noted for the akerites by Wolff (1939).

Pyroxene: colorless, subhedral, some wavy extinction, multiple and simple twinning, positive sign, estimated 2V is between 45 and 80 degrees, altering to biotite and magnetite, replaced initially along a network of fractures, pyroxene surrounded by biotite which is surrounded by hornblende with the pyroxene outline remaining inclusions of apatite, magnetite, and calcium stained anhedral feldspar, schiller structure, minor zoning, highest extinction angle of c:Z' is 49.5 degrees indicating augite, some centers may be diopsidic.

Amphibole: pleochroic greenish-brown to light brown, slight zoning with green or brown in the middle, usually less than 1 mm. in length some up to 2 mm., euhedral to subhedral, more inclusions near the centers (opaques) masses of radial biotite (?) may be a chlorite near centers, also inclusions of apatite and magnetite, maximum c:Z' 20 degrees indicating hornblende, twin seams and simple twins, magnetite inclusions in zones.

Biotite: pleochroic brown, to red-brown to yellow to light brown, as shreds associated with a green to reddish-brown chlorite (?) which also surrounds the altered pyroxene probably chlorite-anamolous interference colors, slightly pleochroic.

Magnetite: and other opaques, anhedral.

Feldspar: groundmass, tabular, turbid, largest grain almost 1 mm. in length, zoned simple, and multiple twins, twin boundaries usually not sharp, sections perpendicular to prism are not as turbid as laths, altering to radial zeolite natrolite (?) extinction angles range from 0 to 25 degrees for matrix feldspar, phenocrysts 15 degrees, most plagioclase has higher index than balsam indicating up to 46 per cent An, twinning has broken down across some crystals, clear rims and interstitial material, isotropic areas in the feldspars, sericite alteration rims of matrix feldspar stained unevenly for potassium. .6 mm. to less than .05 mm. is the size of groundmass.

Quartz(?): anhedral, fine-grained, but nepheline occurs in the norm.

Apatite: tabular, euhedral to subhedral, inclusions in hornblende, associated with magnetite.

Sample S-112 (continued)

Calcite: partly replacing feldspar, usually has sharp boundaries with it, associated with pyroxene breakdown.

Counts	Augite	Hornblende	Biotite	Opaques	Feldspar Phenocrysts	Feldspar Matrix
400	1.7	13.7	5.5	5.2	1.2	69.5

Apatite	Calcite	Limonite
0.2	2.0	0.2

Color Index: 26.3

Inclusion is 6 mm. across; composed of fine to medium-grained brown hornblende with apatites, fine to medium-grained augite, medium-grained altered feldspar which are plagioclase according to staining the feldspars are turbid and have complicated extinction in another inclusion pyroxene is probably converted to hornblende and biotite, also magnetite in these inclusions.

Sample 266

Location: dike of radiating set along the Upper Shield's River Valley.

Megascopic: light brown, fine-grained, zeolite amygdules, megascopically similar to 445C except coarser.

Texture: fine-grained.

Pyroxene: colorless, subhedral, associated with other mafics, as matrix.

Hornblende: light brown to brown pleochroic, euhedral phenocrysts minor.

Opaques: anhedral, associated with biotite, in aggregates.

Biotite: irregular shreds, light brown to medium brown, irregular extinction, minor.

Chlorite: irregular shreds associated with biotite, brown to light green zoned, pleochroism negligible, pennine (?); took potassium stain. Stilpnomelane (?) probably not, because anomalous interference colors.

Feldspar: many laths with polysynthetic twinning with parallel extinction, turbid, boarders of laths and between laths stained for potassium, difficult to distinguish from chlorite with the nicols not crossed, one half of slide stained, other extinction angles are 7, 15, 13, 12.5, 21.5, indicating oligoclase to andesine, some twins also stained, An 35.

Zeolite: clear, radial extinction, cleavage is radial.

Counts	Pyroxene	Hornblende	Opaques	Biotite	Chlorite	Feldspar Plagioclase
200	8.0	?	6.0	1.5	16.0	55.0

Zeolite	Kspar (?)
1.5	12.0

Color Index: 32.5

Sample 297

Location: dike along the Upper Shields River.

Megascopic: mainly fine-grained, rarely porphyritic, gray.

Texture: see above, hypidomorphic.

Augite: colorless to light green pleochroic, altered to hornblende and chlorite, euhedral to subhedral, indistinct extinction, zoned, multiple twins some 4 mm. across, rare hour-glass structure, c:Z' angles are 24, 39, 31, 28, 51 degrees.

Hornblende: medium to light brown, some light green terminations, c:Z' extinction angles are 12, 21, 19 degrees.

Chlorite: light brown-green to medium brown, anhedral, associated with hornblende, generally interstitial, also larger pools often with sharp straight-outlines with major minerals, some secondary, others look primary (?).

Magnetite and other Opaques: surrounded by thin rim of high birefringent high-relief mineral (sphene).

Feldspar: as laths, rims stain lightly for K, turbid, subophitic with hornblende and chlorite, various twins take K stain, rims often clear with turbid centers, index of refraction is lower than balsam, extinction angles are 12.5, 11.5, 10.5, 13.5 indicating a maximum of 8% An.

Zeolite: radial extinction, clear.

Apatite:

Counts	Augite	Hornblende	Chlorite	Magnetite	Feldspar	Zeolite
200	10.0	5.5	17.0	8.0	54.5	5.0

Color Index: 40.5

Sample 351

Location: 5' plus, sill on Dugout Creek.

Megascopic: fine-grained porphyry, gray, plagioclase and hornblende phenocrysts, subparallel orientation of phenocrysts, good stained section.

Texture: see above, trachytic, matrix.

Hornblende: light brown to green-brown pleochroic, euhedral phenocrysts mostly, plagioclase inclusions, seam twinning, simple twinning, c:Z' 15, 16, 15, 14, and 17 degrees, up to 2 mm. long, usually less than 1 mm., apatite inclusions, altered to brown chlorite (?), minor zoning.

Chlorite: green and light brown anhedral and pseudomorphic with high birefringence, high relief inclusions (?), associated with magnetite.

Opaques: some oxidized, as phenocrysts, in aggregates, associated with apatite in reflected light, black and steel gray in one phenocryst, magnetite.

Matrix: mostly trachytic feldspar which stains for potassium, also some minor anhedral quartz, turbid, lower index of refraction than 1.54, phenocrysts less than 2 mm. long.

Plagioclase: turbid, altered in evenly distributed patches to sericite and epidote, minor zoning, maximum 2 mm. long, extinction angles 25, 15, 6, 25, 24 degrees, albite twinning, An 46 Andesine.

Apatite:

Calcite: minor,

Unidentified mineral: high relief, high birefringence, turbid.

Counts	Hornblende	Chlorite	Plagioclase	Feldspar Matrix	Opaques	Quartz
500	16.2	2.8	24.8	50.0	5.8	.2

Unidentified
.2

Color Index: 24.8

Sample 445C

Location: later dike phase of the radiating dike set near the Upper Shield's River road.

Megascopic: fine-grained against the outer basalt phase, elongate round calcite amygdules parallel to contact and horizontal indicating horizontal or vertical last movement of magma, light brown.

Texture: fine-grained, trachytic, glomeroporphyritic.

Hornblende: light brown to medium brown pleochroic, simple twinning, bimodal sizes, extinction angles 14, 13, 16 degrees, phenocrysts in groups 2V 70-85 degrees.

Biotite: associated with chlorite.

Chlorite: anhedral brown to light yellow zoned, slightly pleochroic, anomolous extinction.

Opaques: anhedral to subhedral, very fine, some cubic, oxidized, magnetite, some black in reflected light with red rims.

Plagioclase: turbid, minor phenocrysts with extinction angles of 0, 0, 0, 15, 11.5, 5; matrix feldspar 0 extinction angle, potassium stain negative, calcium stain slight, oligoclase also indicated by norm.

Zeolite: as rounded amygdules, two directions of cleavage at right angles, undulatory and complicated extinction narrow isogyres, biaxial, second order blue indicating thomsonite, distinct negative relief with surrounding feldspar, perfect radial aggregate, parallel extinction zoned concentrically, impinging into a rounded calcite grain; another zeolite area has lower relief than cement, 2 right angle cleavages.

Calcite: rounded elongated phenocrysts, up to 2 mm. in length, preferred orientation, carbonate cleavage, stained slightly for calcium.

Apatite: prismatic, anhedral with parallel extinction.

Unidentified minerals: a trace of an irregular isotropic mineral which took the calcium stain.

Counts	Hornblende	Opaques	Biotite	Chlorite	Plagioclase Phenocrysts	Groundmass Phenocrysts
200	16.5	4.0	0.5	6.0	3.0	68.0

Zeolite	Calcite
t	2.6

Sample 445C (continued)

Norm compares favorably with 70'89 an akerite according to Wolff which is monzonese.

Color index: 27.0

Sample 482A

Location: upper reaches of Cottonwood Creek 0.5 mile south of the junction with Eagle Creek, rooftop intrusion.

Megascopic: medium-brown with black hornblende and pink plagioclase phenocrysts, fine grained porphyritic.

Texture: fine-grained porphyritic.

Augite: colorless, euhedral to subhedral, minor, estimated 2V 60-70 degrees, positive sign, good cleavage, one c:Z' is 46 degrees, surrounded by biotite, converted also to chlorite, high relief inclusions.

Hornblende: pleochroic medium green to light brown, zoned medium green to light brown-green on rims, as euhedral phenocrysts and prismatic groundmass, simple twins, magnetite inclusions abundant near one center, c:Z' 13, 25 degrees.

Opaques: anhedral, magnetite oxidized.

Biotite: red-brown to light yellow-brown pleochroic, associated with next mineral in radial aggragate.

Chlorite: green-brown (?) intermediate position biotite and hornblende or pyroxene.

Plagioclase: as phenocrysts, some turbid, others clear, do not stain for K, zoning minor, multiple twinning not abundant, index of refraction of some of phenocrysts and matrix is less than 1.54, altering to sericite, 0.5 mm., grain in inclusion replaced by calcite, rims of matrix feldspar stain unevenly for K (matrix size is 0.1 to 0.4 mm.) combined Carlsbad-albite twinning angle indicates An 35, less calcic plagioclase indicated by index of refraction, orthophyric texture.

Quartz: anhedral in groundmass, also surrounds feldspar in inclusions.

Calcite: 1 mm. anhedral grain in part surrounded by anhedral clear plagioclase plus quartz (?) in ameboid area 1 mm. by 2.5 mm. in size; all this is surrounded by a turbid brown zone which appears glassy in part as well as cryptocrystalline; elsewhere occurs an area of anhedral carbonate with a fibrous nature, also associated with quartz, biotite also surrounds exenocryst (?).

Sample 482A (continued)

Apatite: anhedral.

Sphene: subhedral associated with biotite.

Counts	Augite	Hornblende Phenocrysts	Hornblende Matrix	Plagioclase Phenocrysts	Feldspar Matrix
400	0.5	11.7	3.7	8.2	65.7

Chlorite	Biotite	Apatite	Calcite	Opaques
1.2	6.5	t	t	2.0

Sample 515

Location: 10' sill exposed in saddle between Target Peak and Goat Mountain near the Forest Lake Road.

Megascopic: pink, fine-grained with minor feldspar and light green augite phenocrysts, cumulophyric.

Augite: light green, zoning prominant under crossed nicols, replaced by calcite.

Amphibole: trace, green to light green, replaced by calcite.

Biotite: black to light brown pleochroic, with sphene parallel the cleavage often surrounded by chlorite which is greenish brown.

Magnetite: some phenocrysts, anhedral.

Feldspar: phenocrysts and groundmass are plagioclase, groundmass is turbid, stains for potassium, calcite alteration, matrix has lower index than balsam, twinning is not well developed, matrix size, 1 mm. albite-oligoclase.

Apatite: euhedral associated with calcite often.

Quartz: anhedral in matrix.

Calcite: some euhedral outlines, others look like replacement.

Counts	Augite	Biotite	Chlorite	Magnetite	Matrix Feldspar	Phenocryst Feldspar
200	9.5	8.0		6.0	72.5	2.0

Quartz	Apatite
2.0	0.5

Similar to 634E

Color index: 23.5

Sample 545A

Location: in middle of anticline south of Virginia Peak, along Crow Creek, 40' upper sill, not finer grained at lower contact with middle sill.

Megascopic: Pink with green mafic phenocrysts and white feldspar laths, fine-grained porphyry, pyroxene and plagioclase both up to 1.5 mm. across.

Texture: matrix is well crystallized laths of feldspar which are turbid.

Augite: colorless to light green to medium green zoned, mostly light green with slight zoning, multiple twinning, angle c:Z' is indicated by 46, 46, 39, 42, 39, 28, degrees, positive sign, some medium green with light green rims, inner colorless parts may be diopsidic, as aggregates, rarely associated with magnetite and biotite, sometimes darker green rim, altered to biotite.

Amphibole: green to light yellow pleochroic, rarely surrounding pyroxene, angle c:Z' is 18 degrees indicating hornblende.

Biotite: black to light-orange pleochroic, some euhedral, apatite inclusions.

Magnetite: anhedral to euhedral.

Feldspar: plagioclase phenocrysts zoned, parallel extinction in phenocrysts, even centers, Peracline and Albite twins, potassium stain on rims of phenocrysts and matrix feldspars, larger grains often as groups of intergrown phenocrysts minor clear albitic material, all feldspars have index of less than 1.56, matrix .5 - .1 mm., albite oligoclase.

Quartz: anhedral in matrix and phenocrysts.

Apatite: euhedral to anhedral, associated with magnetite.

Sphene: minor, anhedral, associated with magnetite.

Triangular shaped isotropic (?) mineral with cleavage, analcite.

Zeolite: anhedral, multiple twinning.

Counts	Augite	Amphibole	Biotite	Magnetite	Plagioclase Phenocrysts	Matrix Feldspar
400	14.0	1.0	6.5	2.5	14.5	61.0

Quartz	Apatite
2.7	0.2

Norm indicates 0.10 quartz, 23 per cent orthoclase and about 55 per cent albite.

Mafic trachytic.

Color Index: 23.0

Sample 587B

Location: 15' from contact of sill over 300' thick, b, c, d, e, are other types, which occur at various intervals throughout sill.

Megascopic: light green, fine-grained porphyritic, feldspar subhedral, and smaller than other porphyries, 2 mm. across, altered, black inclusion.

Pyroxene: light green, euhedral, positive sign, estimated 2V 60-70 degrees Z:c are 25, 37, 38, 34, 46 degrees, multiple twinning extinction angles 25, 45, 40 augite.

Magnetite: associated with pyroxene, anhedral.

Chlorite: light green to light brown pleochroic, often associated with calcite in pseudomorph, uniaxial.

Biotite: zoned brown to light green in centers.

Plagioclase: as phenocrysts, complicated twinning, sericitic zeolitized (?) stained for potassium along the borders, one large phenocryst had 30 degree extinction angle, smaller phenocrysts 4, 5, 0 degrees, matrix feldspars take especially potassium stain, all that stained for potassium counted as Kspar. Labradorite (?) phenocrysts, albite matrix. In second slide, altered plagioclase phenocrysts took potassium lightly, while rims went unstained, index of refraction less than lakeside, other extinction angle 0, 7, 0, 6.5, 12.5, An 9 (?).

Apatite:

Calcite:

Quartz: anhedral in matrix.

Unidentified mineral: very high birefringent mineral, high relief, associated with pseudomorphism, sphene.

Counts	Pyroxene	Chlorite	Magnetite	Plagioclase	Kspar	Quartz
200	8.5	9.0	2.5	37.5(?)	42.5(?)	0.5

Color Index: 19.1

Latite

Sample 625

Location: dike on plunging axis of the Robinson Anticline, exposure surrounded by malignite, but contact not exposed, related 624 to the west, indicates that the dike has intruded a malignite sill nearly parallel the contacts, 626 is the vertical feeder dike for these intrusives. 625A-C are other fine grain types found in rock pile.

Megascopic: black with gray pseudomorphs, groundmass and pseudomorphs are lighter near surface of samples, with zeolites especially near pseudomorph centers.

Texture: fine-grained cumlophyric.

Augite: in about the same concentration in white spots and matrix subhedral, often minute needles less thick than thin section, one larger grain in white spots has green zone apparently near middle, occur as groups of phenocrysts, associated with biotite, positive sign, 60 degrees estimated 2V, occur as radial bunches in white spots, simple and multiple twinning, groundmass augite contained calcite veinlets and irregular inclusions.

Biotite: yellow-brown to light brown pleochroic, often shredded, tends to be rounded.

Opaques: anhedral to square to triangular (in groundmass at least), more opaques near rims of white spots, with maximum light, high power they are opaque with very narrow brown translucent border and black in reflected light, indicating some may be ilmanite, Larsen observed that many appeared blue translucent, indicating sodalite but negative short and long wave flourescent light reaction and negative methyal blue stain, especially, negative diffraction data negates this possibility, minor iron oxide stain, opaques are extremely fine.

White Spots: euhedral to anhedral, equidimendional, some eight-sided, often in groups in contact, irregularly distributed, outlines are straight and sharp or irregular within one spot, some smaller irregular areas are gradational with matrix the definite white spots are 3 to 5 mm. across while the smaller irregular areas are about 1 mm. across, inclusions are magnetite, calcite, zeolites, augite, apatite and biotite. These are all common in pseudoleucite (Hatch, Wells, and Wells 1952 p. 97).

Nepheline (?) or Sodic zeolite is restricted to groundmass according to the methyl blue test (no nepheline, sodalite, or analcite in white spots), has radial extinction reminiscent of a zeolite, some parts of groundmass did not stain properly, fiberous to prismatic to anhedral, undulatory extinction, almost medium grained in places, fine-grained

Sample 625 (continued)

very low birefringence fibrous isotropic material associated, groundmass and white spots (?) stained for the Ca test.

Glass or leucite or analcite: only in white spots, isotropic under 25 power objective and condensor, light brown without condensor and lower power, stained poorly for potassium.

Zeolite: often in middle of white spot, biaxial figure.

Calcite: anhedral, often associated with zeolite in center of white spot, similar occurance described by Proskurho (1960), in matrix hexagonal carbonate and associated zeolite the latter is surrounded by biotite, some association of pyroxene.

Apatite: in groundmass and white spots, euhedral to subhedral.

Note: Composite diffractogram of white spots had a large isolated peak at 15,8 which could well indicate an analcite structure (see Fudali, 1964, p. 1104), but they stain for potassium and not for sodium. Seperation of various white spot phases is necessary before definite identification can be made.

Augite	in Pseudo-leucite 11.8	in matrix 12.2	Rock Total 24.0	Within Pseudoleucite 29.8	Within Matrix 20.2
lt. brown isotropic	12.4		12.4	31.3	
Magnetite	4.2	4.4	8.6	10.6	7.3
Nepheline?		34.4	34.4		56.9
Biotite	5.6	8.2	13.8	14.1	13.5
Calcite	1.6	0.6	2.2	4.0	1.0
Zeolite	4.0		4.0	10.1	
Isotropic	39.6	0.6 60.4	0.6 100.0	99.9	1.0 99.9

Sample 626

Location: vertical dike along the plunging axis of the Robinson Anticline, 625, 624, are samples at south terminus of dike.

Megascopic: light green, fine-grained, porphyry with biotite and other mafic phenocrysts.

Texture: trachytic, glomeroporphyritic, mafics, euhedral.

Augite with Aegerine Rims: light green, zoned maximum 3 mm. across, multiple twinning, bimodel sizes, hornblende inclusions, extinction angles are 23, 51, 46 degrees.

Biotite: brown, in matrix and in hornblende.

Hornblende: dark green to light green, some poly-zoned, multiple twinning, distinctly euhedral, 3 mm. long, magnetite, biotite inclusions, extinction angles are 14, 15, 24 degrees.

Magnetite: and some brassy opaques, one hexagonal grain indicating magnetite, bimodel sizes.

Feldspar phenocrysts: over 1 mm. in length, multiple twinning does not extend the length of crystals, replaced by calcite and analcite extinction angles 23, 27, 29 degrees indicating An. 49 (andesine).

Matrix Feldspar Laths: stain for potassium, turbid, less than 0.2 mm. in length.

Analcite: euhedral and interstitial, clear, lower relief than surrounding feldspars, cleavage not apparent.

Calcite: euhedral to anhedral, intergrown with and pseudomorphing feldspars, calcite, apatite intergrowths.

Apatite: subhedral, .1 to .3 mm. across, cumulate of apatites, associated with mafics.

Sphene: euhedral, associated with calcite.

Zeolite: radial laths, each with parallel extinction, associated with calcite.

Unidentified: hexagonal, 1 mm. long, with light brown innerpart surrounded by clear rim, has trachytic-like feldspar texture under X nicols, some has high birefringence, trace.

Color Index: 26.2

Sample 626 (continued)

Counts	Augite	Hornblende	Magnetite	Plagioclase Phenocrysts	Feldspar Matrix	Analcite
500	7.8	13.8	4.6	0.2	70.8	0.6

Calcite	Zeolite	Apatite
1.0	0.4	0.2

Note: 624 is very similar to 626 generally, it contains calcite mass 3.5 X 5.5 mm. elongated with numerous rounded inclusions of apatite, also sericite veining. It contains anhedral to hexagonal turbid glassy spots similar to those in 625 and especially those in 636.

Sample 634B

Location: 20' above base of the southern exposure of Billie Butte Laccolith.

Megascopic: fine-grained porphyry, pink, 1.2 cm. feldspar phenocrysts with preferred orientation, .6 cm. pyrobole phenocrysts.

Specific Gravity: 2.61.

Texture: fine-grained porphyritic, trachytic, groundmass, poor slide.

Augite to Aegerine Augite: euhedral, subhedral, mainly medium green, slightly pleochroic and zoned, simple twins, one grain with ragged ends surrounded by hornblende and contains apatite inclusions parallel the long direction, pyroxene is converting to hornblende and biotite, no aegerine.

Hornblende: pleochroic dark brown to dark green-brown to light green, multiple twinning zoned to darker edges, contain magnetite and apatite inclusions, zoned extinction, extinction angles c:Z' indicated by 28, 34, 17, 17, and 12 degrees.

Magnetite: subhedral, associated with pyroxene and hornblende.

Feldspars: one phenocryst has grid twinning in one Carlsbad twin and multiple twinning in the other, phenocrysts are zoned, outer edge take potassium stain irregular at times, microperthitic in part, grid twins are not spindle-shaped, one phenocryst took potassium stain except for inner twin, in feldspars, part of twins stained, larger matrix feldspars are irregularly stained. The feldspars are irregularly turbid which contrasts with the clear analcite secondary (?), the grid twinning occurs only on parts of feldspars vaguely, the turbid parts of the feldspars are the part that stain for potassium, parallel extinction probable, but multiple twinning not helpful, zoned plagioclase takes potassium along zones in minor cases, phenocrysts are replaced by analcite, estimated 2V about 70 - 80 degrees, negative sign.

Analcite: interstitial patches and anhedral to euhedral crystals with two equal cleavages at right angles, colorless in thin section and hand specimen, does not stain for potassium, radially arranged aegerines and feldspar laths, one phenocryst has clearer and higher relief center, contain low birefringent veins which are turbid, maximum 1.5 mm. across.

Calcite: minor, anhedral.

Apatite: euhedral, turbid brown in middle.

One irregular equant 1 mm. across area has center stained for potassium surrounded by an isotropic area with a network of low birefringent turbid material.

Sample 634B (continued)

Counts	Aegerine Augite	Hornblende	Biotite	Plagioclase	Kspar	Matrix Feldspar
400	12.0	3.0	2.2	11.8	7.7,	56.7

Analcite	Magnetite
4.5	2.0

Sample 634E

Location: 85' above the base of the southern exposure of Billie Butte Laccolith.

Megascopic: pink to green, fine-grained.

Specific Gravity: 2.73.

Texture: fine-grained glomoporphyritic.

Augite to Aegerine Augite: slightly pleochroic light green, moderate zoning which is well displayed under crossed nicols, zoning is asymetrical, being more abrupt on the rim side, no aegerine, some diopsodic cores. Some c:Z' extinction angles are a maximum of 45 degrees.

Hornblende: medium to light brown, associated with biotite, augite, magnetite, inclusions of biotite, and magnetite.

Biotite: dark red-brown to light brown.

Feldspars: laths with parallel extinction, sharp brown rims, laths up to 3.5 mm. long, simple twins, multiple twins not abundant, matrix and rims stain for potassium which are also the turbid parts, larger phenocrysts minutely altered to sericite, also a minor amount of clear albite (?) around feldspars. (An 20?) finer material, .3 - .5 mm., orthophyric, some could be potassium oligoclase.

Opaques: anhedral, magnetite.

Zeolite: clear interstitial, triangular areas which may be altered analcite.

Apatite: .5 mm. euhedral to anhedral.

Counts	Pyroxene	Hornblende	Biotite	Opaques	Plagioclase Phenocrysts	Matrix Feldspar
400	16.2	0.2	8.0	4.2	2.0	68.0

Apatite	Zeolite
0.5	0.7

Color Index: 28.6

Pyroxene trachyte.

Sample 442

Location: Northwest-trending dike, northwest of Target Peak, on monocline, cut by latite sill, offset along bedding (see picture).

Megascopic: gray-green, fine-grained, biotite books 1 cm. across, zeolite or calcite amygdules, hematitic stain.

Texture: trachytic with calcite segregations.

Chlorite: light green, some yellow, occurs especially as narrow borders on calcite grains, with minute opaque (magnetite) grains, surrounding ragged brown phenocrysts (altered biotite), chlorite has replaced biotite in part, also formed in the calcite replacement of mafics.

Biotite: dark green to light brown pleochroic, laths, interbedded with calcite layers (lens shaped), calcite has spread the biotite layers apart rather than replaced them.

Magnetite: euhedral to subhedral, mainly in matrix.

Feldspar: laths with parallel extinction, no twinning (?), mostly replaced by zeolite.

Zeolite: radial extinction, up to yellow birefringence.

Calcite: tabular and hexagonal phenocrysts, intergrown with zeolites in matrix, mafic replacement (?) surrounded by chlorite; chlorite, opaques along boundaries and parallel in the pseudomorphs.

Apatite: subhedral, in groups.

Some turbid spots.

Counts	Chlorite	Biotite	Magnetite	Zeolitic Feldspar	Zeolite	Calcite	Apatite
200	18.0	4.5	9.5	5.5	43.0	18.5	0.5

Color Index: 32.5

This rock has many properties of a lamprophyre, such as the replacement texture and two sizes of biotites; slightly less than one-third of the total rock is composed of mafic minerals; calcite has replaced some mafics.

Sample 574

Location: westward dipping dike which transects an upper malignite sill on the banks of the Upper Shields River in the southwest part of the map area.

Megascopic: dark green-gray, fine-grained with biotite plates and calcite segregations.

Texture: trachytic, glomeroporphyritic.

Augite: light-green to light brown pleochroic, minor zoning, polysynthetic twinning, replaced by calcite, maximum extinction angle is 55 degrees, one augite aggregate included calcite and magnetite with stained potassium feldspar along cracks, as phenocrysts and microlites, chloritized.

Amphibole(?): minor, in aggregate of biotite.

Biotite: dark to light brown pleochroic, zoned to dark brown rims, euhedral to anhedral, in intergrown masses associated with magnetite and apatite, large plates containing zeolite, calcite and augite inclusions, rare magnetite inclusions near edges of biotite, some biotite have euhedral outlines of pyroxene or amphibole, intergrown masses also include calcite and augite, biotite occurs as small grains and large plates, some darker centers in large plates.

Magnetite: anhedral to subhedral, replacing augite (?) in segregation, that are 1.5 mm. across, associated with biotite and other opaques, some opaques black in reflected light and anhedral, occur on edges of pyroxene aggregates which are partly converted to biotite.

Calcite: much is associated with feldspar, some anhedral, others euhedral, replacing feldspar in matrix, interstitial and 1 mm. grains.

Feldspar: laths, most stain lightly for potassium, zoned, clear, minor polysynthetic twinning, no phenocrysts.

Apatite: a tabular subhedral to euhedral, in aggragates, large and small crystals, larger crystals 1 mm. long.

Counts	Augite	Biotite	Opaques including Magnetite	Chlorite	Feldspar	Calcite	Apatite
300	7.3	18.0	6.7	0.7	51.3	14.0	2.0

Color Index: 32.7

The stained thin section has Lakeside cement for a cover glass. The above characters indicate a biotite lamprophyre, possibly a minette.

Sample 322

Location: 1' plus sill north of Dugout Creek.

Megascopic: dark gray-brown, fine-grained porphyry.

Texture: see above.

Chlorite: light green, associated with calcite, pseudomorphic after plagioclase and mafics (?).

Biotite: red-brown to light brown pleochroic.

Magnetite: abundant as phenocrysts and in matrix, anhedral, oxidized in part.

Plagioclase: laths partly and completely replaced by chlorite and calcite seperately or together, extinction angle is 26 degrees indicating andesine.

Matrix: brown, turbid, abundant magnetite, similar to 712B.

Calcite: in rounded amygdals surrounded by radial fibrous zeolites, yellow birefringence Thomsonite (?), also pseudomorphic.

Zeolite: see above, fibrous, intergrown with calcite.

Apatite: minor.

Probably equivalent to the andesite porphyry (652), general texture is similar.

Sample S-338A

Location: 4' dike associated with thicker basaltic dike along the Upper Shields River.

Megascopic: see sample 652A.

Texture: See 652A.

Augite: light green to colorless, magnetite inclusions and glassy inclusions, altering to chlorite and magnetite, zoned, 3 mm. across, c:Z' 54 to 59 degrees at rim.

Hornblende: light brown to medium-brown, euhedral to subhedral, simple twins, c:Z' angles are 15, 10, 13, 15 degrees.

Chlorite: light green, interstitial between matrix feldspars, pseudomorphic.

Magnetite: subhedral, oxidized, as larger grains.

Matrix: plagioclase laths with possible albite rims, turbid, plus chlorite and hornblende, matrix is similar to all of 266.

Plagioclase: phenocrysts altered to sericite, zeolite, as inclusions in augite, polysynthetic twinning, also Carlsbad twinning, one c:Z' is 17 degrees, Andesine (?).

Apatite:

Quartz: anhedral in matrix.

Counts	Augite	Hornblende	Plagioclase Phenocrysts	Matrix Plagioclase	Chlorite	Opaques
200	5.0	12.5	5.5	58.5	15.1	3.0

Sample 445B

Location: early phase of complex dike along the upper Shields River unpaved road on Schofield Creek.

Megascopic: black, fine-grained porphyry.

Specific Gravity: 2.82.

Texture: cumulophyric.

Augite: euhedral to anhedral, as phenocrysts and as groundmass, maximum length 7 mm., estimated 2V is 70 to 80 degrees, positive sign, usually as aggregates, zoning indicated by extinction and location of magnetite inclusions, colorless, inclusions of biotite magnetite, quartz, optic plane parallel to the best cleavage, multiple twins, twin plane parallels the (100), poorer extinction indicates augite because of the greater dispersion of augite than diopside, c:Z' are 25, 25, 29, 29, 40, 35, 45 degrees.

Chlorite: light green, fibrous radial, romb and six-sided pseudomorphs, interstitial material and alterations of matrix feldspar, some represents alteration of hornblende, some uniaxial (?).

Biotite: dark brown to light brown pleochroic.

Hornblende: light yellow to brown, subhedral, ragged.

Plagioclase: as phenocrysts and as matrix laths, zoned, altered to chlorite and sericite, phenocrysts extinction angles are 29 zoned to 22, 17.5, 26, 29, 30.5, 32.5, 35.5 indicating that the centers are as calcic as An 62, matrix extinction angles are 18, 27, 29, 27, 28, 30.5, 27, 18, 15, 30 zoned outward to 18 degrees indicating An 54 to 35 (matrix is Labradorite to andesine).

Quartz: in matrix, anhedral indicated by etching.

Calcite: anhedral, minor, replacing plagioclase, occurs around chloritic areas.

Magnetite: anhedral to subhedral, often in aggregates, wormy.

No potassium feldspar indicated by staining.

Counts	Augite	Chlorite	Biotite	Magnetite	Hornblende	Plagioclase
400	22.6	30.2	9.5	2.4	.7	31

Calcite	Apatite	Quartz
.2	.2	2.2

Color Index: 65.4

Sample 652A

Location: at head of the Upper Shield's River, 10 ft. northwest trending dike which dips to east from 80 to about 20 degrees, transects hornblende latite 449.

Megascopic: medium brown, fine-grained porphyry, with cream colored plagioclase phenocrysts and dark green pyroboles.

Specific Gravity: 2.78.

Texture: cumlophyric fine-grained porphyritic.

Augite: 2V estimated to be 60 to 90 degrees, positive sign, c:Z' equals 47 degrees, inclusions of brassy opaques, brown inclusions stained red, multiple twinning, colorless to light green.

Hornblende: medium brown to light brown pleochroic, euhedral to subhedral, c:Z' are 17, 17, 15, 14, 14, 13, 13, 15 degrees, some large laths in plagioclase phenocrysts, parallel the twinning directions of plagioclase.

Chlorite: yellow-green to light green to colorless, anhedral equidimensional aggregates, associated pyroxene, opaques, sphene and zeolite (?) in six-sided outline, pseudomorphic after pyroxene or olivene, 338A indicates pyroxene, also interstitial between matrix feldspar laths.

Magnetite: anhedral, distributed through groundmass, some of the opaques appear brassy in center and black edges some wormy exolved intergrowths along preferred optical directions in zeolitic pseudomorphs.

Plagioclase: polysynthetic twinning not abundant in matrix or phenocrysts, extinction angles are 0, 0, 6, 5, 16.5 degrees, the last two are from large phenocrysts indicating andesine, phenocrysts have twins in which every other twin has complete perfect extinction interbedded with twins with patchy extinction, a plagioclase aggregate contains anhedral pyroxene which has controlled the optical orientation of the domains, twins often terminate partway along the phenocrysts, many phenocrysts subdivided into domains with slightly different optical orientation, phenocryst twins often offset along straight lines which appear cleaved, interlarded twins also took staining for calcium to different degrees, also alternately turbid, albite rims indicated by staining on the matrix feldspar also around some hornblendes and plagioclase phenocrysts, interstitial albite, Negative potassium stain reactions, chloritized in isolated evenly distributed spots.

Sphene: (?)

Counts	Augite	Hornblende	Plagioclase Phenocrysts	Matrix Plagioclase	Albite	Chlorite
500	5.2	19. plus	10.4	41.6	2.8	15 plus

Sample 712A

Location: center of terminal dike on the south fork of Lodgepole Creek, 10' thick, see also 712B.

Megascopic: dark brown, fine-grained porphyry.

Texture: see above, intersertal.

Augite: colorless, multiple twinning, inclusions of biotite, phenocrysts 5 mm. across and as interstitial material, c:Z' up to 51 degrees.

Chlorite: light green, replacing feldspars.

Biotite: dark brown to light brown pleochroic, associated with interstitial material and as phenocrysts which pluck on grinding, calcite occurs in the middle of biotite phenocrysts.

Magnetite: inclusions in augite, also as subhedral to anhedral phenocrysts.

Plagioclase: distinct zones in phenocrysts with extinction angles c:Z' of 25, 9.5, 23.5 indicating an An content of at least 46, matrix feldspars extinction angles are 13, 14, 21, 18.5, 15, 15 degrees indicating an An content of at least 40 (andesine groundmass, phenocrysts at least andesine).

Apatite:

Calcite:

Counts	Augite	Chlorite	Biotite	Magnetite	Plagioclase Phenocrysts	Matrix Plagioclase
200	19.0	7.0	16.5	5.5	13.0	36.5

Color Index: 48.0

Sample 712B

Location: same as 712A but 1 ft. from the west contact.

Megascopic: light brown, fine-grained porphyry.

Texture: see above, finer groundmass than 712A.

Augite: colorless, biotite inclusions, multiple twinning, zoning not apparent, maximum c:Z' is 60 degrees.

Chlorite: yellow-green, pseudomorphic, associated with zeolite, calcite, also as matrix between feldspar laths, some uniaxial.

Biotite: associated with chlorite, brown.

Magnetite: anhedral, phenocrysts, matrix.

Plagioclase: distinct zoning, laths, rounded, zeolite and calcite alteration, 20, 33.5, 9, 32.5 to 18, 20, 24, 23 are extinction angles for the phenocrysts indicating An content of at least 58 and rimmed to An 36, matrix extinction angles are 17, 26 degrees, indicating an An content of at least 48 (Andesine) groundmass, Labradorite to andesine zoned phenocrysts.

Counts	Augite	Biotite & Chlorite	Pseudomorphic Chlorite	Plagioclase Phenocrysts	Plagioclase Matrix
200	12	55.5	2.5	11.5	14.0

Plagioclase Matrix	Zeolite	Magnetite
14.0	0.5	4.0

Sample 217

Location: from 20' sill overlooking the Upper Shields River, opposite lower bridge, 2' above contact with middle dike, dip of contact N. 7 E., 6 W., straight and sharp.

Megascopic: dark green, not fresh.

Specific Gravity:

Texture: hypidomorphic, medium-grained.

Augite with Aegerine-Augite to Aegerine Rims: augite has 2V of 40 to 60 degrees, optical plane is parallel the long direction and cleavage, under crossed nicols zoning is displayed in otherwise homogenous looking augite centers, green zoning is abrupt and gradational depending on the optical orientation for one thing, upon terminations the zoning is often sharp and the outline of the early formed augite is apparent, extinction angles on the green rims varies, but is usually near zero and increases continuously toward the centers indicating aegerine to aegerine-augite inward, abundant inclusions of apatite, biotite, magnetite and zeolite, green rims sometimes occur around the inclusions, one large zoned crystal biotite zone between the augite and aegerine-augite zone. Aegerine has slender minute prisms and fibrous aggregates, sometimes associated with fibrous aggregates, opaque to turbid aggregates of aegerine (?).

Olivine: clear, irregular fractures common and antigorite (?) contains numerous magnetite inclusions.

Magnetite and other Opaques: anhedral six-sided, as inclusions in augite, commonly surrounded by biotite.

Biotite: pleochroic light brown to medium brown, zoned to red-brown border, red-brown color sometimes extends irregularly into the centers of the biotites, euhedral apatite inclusions which themselves contain numerous subparallel green inclusions, rare biotite grain with central anhedral olivine which is replaced along edges and cracks by light green mineral antigorite (?), biotite rims olivine.

Sanidine: 2V approximately 10 degrees, clear, vein, stringlet, patch perthitic replacement by zeolite, prominant cleavage parallel and perpendicular the optic plane.

Nepheline: searched for but not positively identified.

Zeolite: complex extinction, turbid to light brown, associated with sericite or microlitic cancrinite, and isotropic and as inclusions in pyroxene, associate with pink dust (sodalite).

Sample 217 (continued)

Apatite: hexagonal to prismatic long opaque prismatic inclusions.

Calcite: minor, anhedral.

Counts	Aegerine-Augite	Aegerine	Olivine	Magnetite	Biotite
500	44.4	2.8	0.4	1.2	11.2

Orthoclase	Zeolite-Sericite	Apatite	Analcite (?)
8.6	31.2	0.2	

Sample 224

Location: from sill exposed along Upper Shield's River Road, in roadcut not over seven years old, in southwest corner of map area, also location of 223 and a number of other oriented samples.

Megascopic: gray-green with white zeolitic areas.

Texture: hypidomorphic fine-grained.

Aegerine-Augite: augite is light green, aegerine-augite is pleochroic green to light brown, some is brown opaque, aegerine as radiating fibrous aggregates which have grown into the orthoclase, the green-brown fibrous material may not be aegerine, it is silver in reflected light, often extends out into the natrolite, maximum 3 mm. long.

Magnetite (?): steel gray in reflected light, also dusty opaque material, inclusions in pyroxene.

Biotite: pleochroic light brown to yellow-brown to black, zoned to black to orange-brown rims, euhedral laths of zeolite in biotite indicating biotite succeeded nepheline, spikes of aegerine on outlines, apatite inclusions, interbedded with aegerine and brown aegerine (?), also occurs as red and brown microlites.

Orthoclase (?): subhedral to lath shaped, colorless to turbid brown, replaced along alternating layers by zeolite which contain numerous minute red-brown to light green inclusions, 2V less than 60 degrees.

Nepheline: hexagonal and lath shaped, partly replaced with zeolite, euhedral with biotite, aegerine-augite, orthoclase not aegerine.

Analcite: interstitial clear, triangular, prominant cleavage at right angles, associated with clear zeolite with undulatory extinction.

Sample 224 (continued)

Zeolite: that replacing nepheline as lower relief than nepheline, modes include partly zeolitized orthoclase and nepheline, two zeolites indicated, that replacing analcite has higher relief than that replacing nepheline and orthoclase, some natrolite.

Alteration Products of Nepheline and Orthoclase: include, high birefringent colorless parallel extinct, probably aegerine (?), biotite.

Unidentified Minerals: trace of orange to liver-brown mineral associated with pyroxene.

Unidentified Mineral: trace of high relief, dark brown to opaque mineral.

Unidentified Mineral: trace of light brown mineral with subhexagonal outline, red-brown in reflected light, limonitic stained (?).

Apatite inclusions in biotite.

Counts	Aegerine-Augite	Aegerine	Biotite	Orthoclase	Nepheline
	28.5	11.0	5.0	8.0	10.5

Zeolite	Natrolite	Brown Opaque Mineral	Orange Mineral
30.0	4.0	1.0	0.5

Sample 390A

Location: near base of 20' sill on southeast part of the anticlinal nose.

Megascopic: dark green, fine-grained with white zeolite veins.

Specific Gravity: 2.81.

Texture: fine-grained, porphyritic.

Augite to Aegerine: colorless to dark green to yellow, subhedral, zones in colorless augite appear under crossed nicols, aegerine as radiating fibers.

Olivine: colorless, parallel extinction.

Opaques: anhedral magnetite and some brassy pyrite.

Biotite: anhedral to subhedral, associated with olivines.

Iddingsite: red-brown to orange pleochroic, right angles cleavages, replacing olivine, masses of iddingsite surrounded by biotite with exsolved (?) magnetite at their junction, some masses are not equant.

Orthoclase: tabular, slightly turbid, low birefringence.

Nepheline:

Analcite (?): euhedral, six-sided, low birefringence, lower relief than surrounding zeolite, poor cleavage development isotropic.

Sodalite: light blue isotropic, partly zeolitized.

Zeolite: lightly turbid to clear, wavy irregular extinction, light orange cast, contains numerous aegerine and opaque inclusions, some coarse zeolites, some positive uniaxial or low 2V positive, could be Chabazite or Gmelinite, probably Gemelinite, has distinct prismatic cleavage and basal parting, zeolitic mass surrounded by mafics.

Apatite: rough surface minor.

Counts	Augite	Aegerine-Augite	Aegerine	Olivine	Opaques	Biotite
500	27.8	10.8	2.0	0.4	1.4	8.2

Zeolite	Apatite	Calcite	Iddingsite
48.6	0.2	0.4	0.2

Sample 577

Location: on north of the Upper Shields River, near axis of the Robinson Anticline, sill with contacts not exposed.

Specific Gravity: 2.65.

Texture: medium-grained, hypidomorphic.

Aegerine-Augite: zoned to light green to medium green rims pleochroic euhedral to subhedral, prismatic to radiating aggregates of translucent fibrous, larger crystals are sometimes opaque toward edge, converted to biotite.

Biotite: pleochroic brown to brown-orange to black, zoned to darker edge, interbedded with aegerine and replaces it, significant titanium content according to X-ray flourescence.

Magnetite: steel gray with black rims in reflected light, anhedral in zeolite.

Aegerine altered: radiating to triangular to equidimensional, subhedral, light green to brown to gray to translucent, white in reflected light, associated with aegerine-augite.

Unidentified Minerals: prismatic mineral associated with radiating minerals described above, high birefringence, high relief.

Sphene: anhedral associated with opaques.

Apatite: subhedral, euhedral, minor.

Calcite: anhedral in zeolite, parallel to cleavage.

Sanidine: clear, some euhedral, 2V approximately 10 degrees, good cleavage, simply twinned, did not stain for calcium, well for potassium, some methalyine blue stain along zeolitized cracks, some triclinic phase or zeolite contamination indicated by X-ray pattern.

Zeolite: mostly natrolite according to X-ray pattern, stained lightly for calcium and potassium, but may not be indicative, tests for zeolites, in laths and hexagonal outlines indicating the probable replacement of nepheline, in lath shaped intergrowth in rectangular sections and patchy inter-growth within hexagonal sections, also as thin veins and blebs in sanidine, cancrinitic or sericitic material associated.

Counts	Augite	Aegerine-Augite	Aegerine	Biotite	Sanidine	Zeolite
1000	0.2	14.1	2.7	6.1	10.8	56.2

Sphene	Apatite
0.2	0.1

Sample 598

Locations: spotted theralite from the top of the Great [redacted] Cliffs, second pointed overlook down southside from top, east of dike, maximum 150' sill.

Megascopic: on fresh cut green-black anhedral areas (orthoclase) surrounded by matrix of white zeolites and mafics, on weathered surface feldspars laths stand out in relief.

Specific Gravity: 2.75 (?).

Texture: hypidomorphic bimodal grain-size, leucocratics over 1 mm. while mafics are less 1/2 mm. in length, cumulate 3 mm. - 4 mm. across of pyroxenes.

Aegerine-Augite: subhedral, zoned colorless to medium green rims, intergrown with magnetite and hastingsite, small (?) aggregates of small crystals, two small crystals with green centers.

Magnetite: anhedral, associated with pyroxene.

Biotite: pleochroic, light yellow to orange-brown, associated with aegerine, some have three zones, apatite inclusions, one green serpentine center of biotite, opaque to red translucent material between.

Hastingsite: pleochroic light brown to liver-brown, lath shaped.

Perthite: anhedral, clear to turbid brown, acute bisectrix figure isogyres go to edge of field, indicating maximum 2V of 60 degrees, includes dusty purple anhedral to euhedral hauynite, slight grid twinning, perthite-like zeolitization of feldspar, small aegerines and hastingsite rim feldspar lath as if they were formed later, the latter will lie within analcite or altered nepheline, often clear centers with turbid borders which display distinct polysynthetic twinning, clear areas in turbid borders display the twinning, poikilitically including other minerals, augites have not aegerine rims in this latter case, but toward the border where it is more turbid more aegerine rims occur, often sharp boundary between turbid and clear feldspars, angle on one feldspar is 13 degrees, yellow high birefringent material replacement.

Nepheline: difficult to distinguish from orthoclase, some clear, minor, some altered nepheline or orthoclase with aegerine microlites parallel fractures, sericite and sodalite, alteration.

Analcite: isotropic, interstitial, clear, cubic cleavage, some isotropic material is replaced by yellow birefringent zeolite.

Hauynite: blue isotropic, some with perfect hexagonal outlines in orthoclase, some square and speckled blue, some light yellow high birefringent mineral intergrown with hauynite.

Sample 598 (continued)

Zeolite: turbid, includes some isotropic parts parallel the cleavage biaxial figure, most zeolite is slightly altered orthoclase in count, some clear, radiating fibrous, myrmekitic-like.

Sericite or Cancrinite: moderate birefringence, radial aggregates or microlites, Wolff called it cancrinite.

Deep red translucent mineral associated with hastingsite, pyroxene, anhedral miner.

Apatite: subhedral, laths, a few 0.5 mm. long.

Sodalite (?): pink rose, dusty, replacing feldspar, surrounds irregular areas of sericite (?).

Counts	Aegerine-Augite	Magnetite	Biotite	Hastingsite	Anorthoclase
300	30.7	1.3	5.7	1.0	13.3

Nepheline	Partly Zeolitized Orthoclase or Nepheline	Zeolitized Anorthoclase with Multiple Twinning	Hauynite	Apatite
0.4	33.7	6.3	0.3	0.3

Isotropic	Sericite or Cancrinite
3.3	3.0

Sample 627A

Location: from Great Anticlinal Phacolith, 5' from top of section as described at 627D.

Megascopic: dark green like 627G, darker than others from this section, greenigh-brown phenocrysts of olivine.

Specific Gravity: 2.92.

Microscopic:

Texture: hypidiomorphic fine-grained, finer grained than 627B.

Aegerine-Augite: subhedral to euhedral, zoned light green to medium green rims, some green zones along cracks, pleochroic inclusions, aegerine is associated pleochroic medium green to yellow-green, one 3 mm. mass of augite crystals with minor leucocratics, no biotite or green zones in the middle of these masses.

Olivine: colorless surrounded by biotite, fractured, elongated, 1 mm. long.

Magnetite: anhedral.

Biotite: pleochroic medium brown to light brown, zoned dark brown rims, some brown zones in middle occasionally, smaller aegerine-augite and hastingsite on biotite grains.

Hastingsite: Liver to green-brown pleochroic, intergrown with biotite around replaced olivine.

Orthoclase: good cleavage, 2 mm. across poikilitically containing other minerals, simply twinned, surrounded zeolite areas, hexagonal isotropic crystals, partly zeolitized, colorless with aegerine, microlites, simple twins, in orthoclase (altered nepheline?) oriented section indicates a two 2V of about 10 degrees, this crystal has rectangular outline with zeolite veining (sanidine), veined with zeolites, much called orthoclase, probably sanidine.

Nepheline: minor, anhedral, moderate cleavage.

Analcite: anhedral, cubic cleavage, clear.

Zeolite: lower index than 1.56, turbid in part, that with radial extinction is often clear, with minute opaque inclusions, some has low 2V, that with moderate 2V plus sign equals natrolite or thomsonite.

Counts	Aegerine-Augite	Olivine	Magnetite	Biotite	Hastingsite	Sanidine
300	43.7	1.7	0.3	15.7	2.7	0.3

Analcite (?)	Zeolite	Aegerine
1.0	19.7	2.0

Sample 627B

Location: from the Great Anticlinal phacolith, 22' from the top of section as described in 627D.

Megascopic: dark green, medium to fine-grained, white zeolitic masses to 0.6 cm. across, light brown biotite masses, more mafics apparent than in 627D.

Specific Gravity: 2.91.

Texture: hypidomorphic granular, medium to fine-grained, preferred orientation of pyroxenes.

Aegerine-Augite: zoned colorless to green rims, pleochroic light green usually less than 1 mm. in length, some up to 3 mm. aegerine rims indicated by parallel extinction, twin seams, biotite and magnetite inclusions, interbedded with hastingsite.

Olivine: colorless, usually anhedral, surrounded by narrow rims of brown poorly (?) crystalline material (iddingsite ?) which grades outward into biotite.

Opaques: anhedral, much associated with biotite, surrounding olivine.

Biotite: zoned brown to light brown, some light brown, usually darker on edge, rare brown zone in center, associated iddingsite is a brighter brown.

Hastingsite: pleochroic light brown to liver-brown to light green.

Orthoclase: anhedral contain zeolite veins, cleaved.

Nepheline: poikilitically contains pyroxenes, partly zeolitized, clear, anhedral to rectangular rarely.

Analcite: clear, prominant cleavage, also some anhedral, translucent isotropic material.

Zeolite: colorless to turbid, radial and undulatory extinction, some medium-grained, contains numerous inclusions, yellow birefringence, lower relief than nepheline, which is sometimes euhedral against it, good cleavage, some clear zeolite veins with index greater than 1.56.

Apatite: subhedral.

Red translucent alteration products.

Counts	Aegerine-Augite	Aegerine	Olivine	Opaque	Biotite	Hastingsite
300	39.0	4.0	1.0	2.0	15.3	3.0

Orthoclase	Nepheline	Analcite	Zeolite	Translucent	Apatite
0.6	1.0	0.7	36.6	0.3	0.7

Sample 627C

Location: from Great Anticlinal Laccolith, 50' from top of section as described in 627D.

Megascopic: green with white zeolite veins $\frac{1}{4}$ to $\frac{1}{2}$ inch across, brown biotite aggregates.

Specific Gravity: 2.85 to 2.89.

Microscopic:

Texture: fine-grained, hypidiomorphic, pyroxenes up to 2 mm. long, some preferred orientation.

Aegerine-Augite: colorless to green zoned, anhedral, to subhedral, simple twins, wormy intergrowth of magnetite, associated aegerine needles.

Olivine: surrounded successively by iddingsite, biotite and once by aegerine.

Opaques: associated with mica, anhedral.

Biotite: brown to yellow pleochroic, zoned darker on rims, greenish-yellow serpentine separates it from olivine.

Hastingsite: brown to purple-brown pleochroic, subhedral, rarely intergrown with biotite, also with augite.

Orthoclase: large 2V, zeolite-veined, poikilitically enclosing other phenocrysts, cleavage not always apparent, some euhedral against aegerine.

Nepheline: clear, partly zeolitized, anhedral, poikilitically enclosing augite.

Analcite: colorless, isotropic, cleaved.

Zeolite: as vein, contains biotite, magnetite and pyroxene, often turbid, some clear and completely twinned.

Counts	Aegerine-Augite	Aegerine	Olivine	Opaques	Biotite	Hastingsite
400	40.7	0.7	.7		16.7	4.5

Orthoclase	Analcite	Nepheline	Zeolite	Apatite
2.5	0.5	1.2	32.0	0.3

Sample 627D

Location: from Great Anticlinal Phacolith, 65' from top, this series collected along a vertical section in middle of cliff, see location map, along vertical crevasse, which appears on air photos.

Megascopic: dark green with brown biotite aggregates, medium to fine-grained.

Specific Gravity: 2.94.

Texture: hypidomorphic and granular, subparallel orientation of pyroxenes and biotites.

Aegerine-augite: zoned colorless to medium green, pleochroic green to light brown to gray, up to 3 mm. in length, generally less than 1 mm. euhedral, many subhedral, minor anhedral, rare green zone without parallel extinction in center of augite, zonation sharp and gradational, aegerine-augite may be euhedral within aegerine, twinned simply. Biotite included only in the green veins of augite, they also occur as inclusions in augite centers.

Magnetite: anhedral, some square outlines, distributed evenly, partly oxidized.

Olivine: colorless, fractured surrounded by biotite, subhedral, replaced along fractures by biotite.

Hastingsite: light green to liver-brown pleochroic, intergrown with biotite.

Orthoclase: minor.

Nepheline: opaque inclusion, subhedral, romb shaped.

Analcite (?): anhedral, spotted with zeolites.

Zeolite: clear to slightly turbid, prominant cleavage occasionally radial extinction, high 2V, up to 1 mm. across poikilitically enclos - ing other minerals.

Apatite: subhedral, tabular to hexagonal, index lower than zeolite.

Counts	Aegerine-Augite	Olivine	Magnetite	Biotite	Hastingsite
300	41.0	2.0	0.7	16.3	7.0

Orthoclase	Nepheline	Analcite	Zeolite	Apatite
0.3	0.3	0.3	31.0	T

Sample 627E

Location: from Great Anticlinal Phacolith, 85' from top, section location described in 627D.

Megascopic: dark green similar to 627D, biotite aggregates and olivines are larger than 627D.

Specific Gravity: 2.96.

Texture: fine-grained to medium-grained granular, subparallel orientation of phenocrysts.

Aegerine-Augite: zoned colorless to green, rims, minor green centers, subhedral to euhedral, biotite and magnetite, twinned simply, maximum 3 mm. in length.

Olivine: anhedral, prominant cleavage, replaced along cracks by biotite, surrounded by biotite, maximum 3 mm. in length.

Opaques: anhedral to subhedral.

Biotite: zoned light brown to dark brown rims, pleochroic light brown to medium brown, parts liver-brown with higher birefringence several brown zones rarely occur within a crystal, much magnetite inclusions, often surrounds olivine.

Hastingsite: pleochroic, liver-brown to green, some light blue anhedral, intergrown with and surrounding aegerine-augite.

Nepheline: anhedral, minor.

Zeolites: prominant cleavage in two directions, higher index than 1.56, poikilitically encloses smaller augites.

Isotropic: minor isotropic material.

Apatite: minor.

Counts	Aegerine-Augite	Aegerine	Olivine	Magnetite	Biotite
300	44.3	1.0	2.3	2.0	15.3

Hastingsite	Nepheline	Zeolites	Apatite
7.3	1.0	29.7	0.3

Sample 627F

Location: from the Great Anticlinal Phacolith, 120' from top, section location described at 627A.

Specific Gravity: 2.98.

Texture: hypidomorphic, fine-grained.

Aegerine-Augite: zoned colorless to medium green, rare green zones in middle, zones sharp to gradational, inclusions of glass, altered to biotite, numerous smaller crystals have multiple twinning, maximum 2 mm. in length, one grain 6 mm. in length.

Olivine: colorless, rimmed with biotite succeeded by hastingsite, replaced along narrow channels initially, smaller segments of olivine have been rotated, maximum 2 mm. in length.

Opaques: intergrowth of black and metallic minerals (reflected light), anhedral.

Biotite: pleochroic light-brown to medium brown, zoned light brown to dark brown rims.

Hastingsite: liver-brown to reddish-brown pleochroic, anhedral, intergrown with pyroxene, some hastingsite in channels in olivine.

Orthoclase: anhedral, poikilitically includes smaller augites and biotites.

Zeolites: turbid with inclusions to clear, prominant cleavage, complex twinning, undulatory extinction, numerous magnetite inclusions, index lower than 1.56, some masses 2-3 mm. across.

Apatite: subhedral to euhedral, minor isotropic material.

Counts	Aegerine-Augite	Olivine	Opaques	Biotite	Hastingsite
400	50.8	2.0	0.2	15.0	3.5

Orthoclase	Isotropics	Zeolite	Apatite
1.0	0.2	27.0	0.3

Sample 627G

Location: from Great Anticlinal Phacolith, 135' from top, 5' from base, section location described in 627A.

Megascopic: darker green than 627D and E.

Specific Gravity: 2.99.

Texture: hypidomorphic, fine-grained, some medium-grained, some biotite, olivine and pyroxene up to 2 mm. long.

Aegerine-Augite: zoned light green to medium green rims, polysynthetic twinning, radiating fibrous masses of aegerine, inclusions of glass (?) and biotite, rare 1.2 cm. subtriangular aggregate of augite crystals without aegerine rimms, aggregate augites are homogenous in size.

Olivine: colorless, subhedral to anhedral, elongate, with biotite rims.

Opaques: most magnetite, anhedral to euhedral, much associated with zeolites.

Biotite: zoned light brown to dark brown rims, interbedded zones of different color-twinning (?), replaced olivine and augites along cracks.

Hastingsite (?): light green to medium green rims, polysynthetic twinning, radiating fibrous (?) intergrown with biotite, associated with biotite.

Orthoclase: clear, anhedral, 3-4 mm. area which is optically continous which poikilitically encloses augites and subhedral to hexagonal to rectangular shaped complexly twinned zeolites.

Nepheline: anhedral, minor.

Zeolite: prominant cleavage, some polysynthetically twinned like sample 577 natrolite or thomsonite.

Apatite: minor.

Minor turbid isotropic material - analcites.

Red translucent alteration product.

Counts	Aegerine-Augite	Aegerine	Olivine	Opaque	Biotite	Hastingsite
500	53.0	0.2	3.4	0.8	11.6	2.8

Orthoclase	Nepheline	Zeolite	Apatite	Turbid	Isotropic Red Translucent
4.4	1.8	20.8	0.2	0.6	0.2

Sample 643

Location: sill poorly exposed on nose of Robinson Anticline.

Megascopic: fine-grained porphyritic, dark green (?).

Specific Gravity: 3.01 (?).

Texture: fine-grained porphyritic, subparallel orientation of phenocrysts, augite and olivine up to 3 mm. long.

Aegerine-Augite: euhedral augite phenocrysts, light green, with narrow rims, aegerine-augite needles as groundmass, these are zoned and twinned.

Olivine: colorless, euhedral, surrounded by thinner rims of biotite than usual, thin veins of biotite along cracks, where olivine and augite are in contact no biotite has formed on the olivine and no aegerine occurs on the augite, some magnetite inclusions, some squares of magnetite between olivines, in aggregates with pyroxene, biotite, augite, leucocratic inclusions, elongate; index of beta and diffraction pattern indicate Fa. content is 10 per cent, diffraction pattern indicates that the olivines are homogenous and constant in composition; the reason for all of the olivine is that there has been only slight replacement of the olivine by biotite (?).

Magnetite: subhedral to square, other opaques with red translucent borders.

Biotite: zoned with darker rims, subhedral, mainly in groundmass and as thin rims around olivine.

Orthoclase(?): anhedral, $\frac{1}{4}$ mm. across, possibly zeolite, high 2V, simple twins.

Zeolite (?): turbid groundmass, microlitic, undulatory and zoned extinction.

A Minor Mineral: clear, moderate birefringent, relief higher than the turbid zeolite.

Counts	Augite Phenocrysts	Aegerine-Augite Groundmass	Olivine	Biotite	Orthoclase	Zeolite
300	26.3	28.0	20.0	10.7	1.0	12.7

High Birefringent Mineral in Matrix	Red translucent Mineral
0.7	0.3

Sample 645

Location: 10' dike in middle of Robinson Anticline.

Megascopic: dark green to dark gray, fine-grained porphyritic.

Specific Gravity: 2.88.

Texture: fine-grained porphyritic.

Augite: with narrow rims of aegerine, aegerine also in groundmass polysynthetic twinning.

Olivine: anhedral to euhedral, colorless, two directions of cleavage indicate biotite, a few phenocrysts altered to biotite and magnetite, magnetite is exsolved (?).

Magnetite: anhedral.

Biotite: zoned, as laths in matrix, some very light brown.

Sanidine: clear, unzeolitized, cleavage which does not extinguish straight, low 2V, stained.

Nepheline (?): anhedral, partly zeolitized, poor cleavage, no positive identification, probably sanidine.

Zeolite: groundmass, radial extinctions, turbid.

Apatite: subhedral to euhedral in aegerine at least.

Calcite: minor, replacing nepheline and orthoclase.

Isotropic material in matrix.

Unstained section.

Serpentine (?): pseudomorphic after olivine, yellow-brown.

Counts	Aegerine-Augite	Olivine	Magnetite	Biotite	Sanidine
1000	60.1	5.5	0.6	7.8	1.7

Nepheline (?)	Zeolite	Calcite	Isotropic
1.4	20.0	1.7	1.2

Sample 665

Location: Olivine-malignite sill, 20' thick, with thin sedimentary septa separating upper sill, along Meadow Creek below 640?

Megascopic: abundant inclusions composed of zeolite, biotite, fibrous aegerine and sanidine, the elliptical inclusion in the thin section is .6 cm. across and probably 1.3 cm. long: the zeolite is pink, most of the inclusions have gone over to zeolite, coarse-grained.

Mineralogy of inclusions.

Aegerine: dark green.

Biotite: dark brown to light brown pleochroic.

Magnetite: anhedral.

Sanidine: euhedral, tabular, fractured, turbid-brown inclusions, inclined extinction.

Zeolite: in triangular areas between sanidine laths, colorless, moderate 2V, positive sign.

Cancrinite (?): as laths in zeolites and around borders of laths, parallel extinction, may be the best cancrinite in all these rocks.

Sample 666

Location: from 20 to 25' thick sill on southwest part of nose of Robinson Anticline, foliation N 68° E. 75° N.W.

Megascopic: fine-grained, dark green, with inclusions of biotite and zeolite, elongate and also triangular, maximum dimension 1.2 cm.

Specific Gravity: 2.91.

Texture: fine-grained hypidiomorphic.

Aegerine-Augite: zoned colorless, to yellow-brown to light green subhedral, some needles of aegerite, apatite magnetite inclusions, polysynthetic twinning, masses of very fine-grained augite crystals 1 mm. across, these include biotite also, augite are fractured and parts are slightly separated and by zeolites.

Olivine: surrounded by biotite, clear maximum 3 mm. across.

Magnetite: inclusions.

Biotite: fan-shaped zones of dark brown and light yellow, rims are darker than many samples, one broken biotite with augite growing through it.

Zeolite: some hexagonal shapes indicating nepheline(?), complex extinction numerous inclusions of dark red and opaque anhedral microlites.

Minor fibrous translucent material.

Inclusion is composed of zeolite and some radiating fibrous aegerite; complexly extinct zeolite is turbid (pink in hand lense) while colorless zeolite has undulatory extinction, and sharp straight twin boundary, also dark brown biotite, analcite indicating by isotropic character and prominant cubic cleavage, good figure, low 2V, two directions of cleavage, index of refraction less than 1.56, lower than twin on one side, about the same as surrounding zeolite, could be Chabazite or Gemelinite, has prismatic cleavage and basal parting.

Counts	Aegerine-Augite	Biotite	Magnetite	Olivine	Zeolite
200	52.5	4.0	0.5	3.5	39.5

Sample 704A

Location: from the Great Anticlinal Phacolith, 3' above base, vertical section located at eastern end of east-west exposure.

Megascopic: dark green, similar in grain size to 627G.

Specific Gravity: 2.87.

Texture: hypidomorphic fine-grained, subparallel orientation of phenocrysts.

Aegerine-Augite: zoned light to medium green, aegerine is pleochroic light green to yellow-green, sharp and gradational zones, rare central green zones, inclusions of magnetite, biotite and isotropic material.

Olivine: colorless, subhedral and anhedral, surrounded by greenish-brown serpentine succeeded by biotite.

Magnetite: some square crystals.

Biotite: zoned colorless to light brown to reddish-brown rims, pleochroic light brown to colorless, some perfect hexagonal plates intergrown with hastingsite, magnetic inclusions, some with two dark zones.

Hastingsite: dark liver to light brown pleochroic, anhedral.

Orthoclase: interstitial, clear.

Nepheline: minor.

Zeolite: turbid and clear areas, turbid has opaque inclusions which are often light red in reflected light, complicated extinction, iron oxide staining on zeolite abundant.

Counts	Aegerine-Augite	Olivine	Magnetite	Biotite	Hastingsite
300	50	2.7	1.3	13.0	4.3

Orthoclase	Nepheline	Zeolitized Orthoclase	Zeolite
1.7	0.3	0.7	26.0

Sample 704B

Location: from Great Anticlinal Phacolith, 13' above base, section at east end of east-west exposure.

Megascopic: dark green, similar to 704A and 727G.

Specific Gravity: 2.89.

Texture: hypidomorphic, fine-grained, subparallel orientation of pyroxenes, some biotite and pyroxene aggregates 3 mm. across.

Aegerine-Augite: zoned colorless to green rims, aegerine is pleochroic yellow-green to green, magnetite inclusions, multiple seam twinning, orthoclase or nepheline occurs along twin seams, maximum 1.5 mm. across.

Olivine: colorless, anhedral, surrounded by biotite.

Magnetite: squares.

Biotite: poly-zoned light brown to medium brown, maximum 1.5 mm. across.

Hastingsite: anhedral, liver-brown to light greenish-blue, intergrown with augite, radiating fibrous.

Orthoclase: lath shaped occasionally, partly replaced by zeolite in perthitic fashion, 3 mm. across poikilitically enclosing augite, etc.

Nepheline: trace.

Zeolite: in parallel laths, some possibility of incipiently zeolitized nepheline, also zeolitized isotropic areas (analcite ?), turbid often.

Cancrinite: replacing orthoclase almost submicroscopic along veins with zeolites.

Counts	Aegerine-Augite	Olivine	Magnetite	Biotite	Hastingsite
300	46.7	5.0	0.3	16.3	3.0

Orthoclase	Zeolitic Orthoclase	Nepheline	Zeolitic Isotropics	Zeolite
4.3	4.0	0.3	0.3	19.7

Sample 704C

Location: from Great Anticlinal Phacolith, 25' above base, at vertical section at east end of east-west exposure.

Megascopic: dark green.

Specific Gravity: 2.86.

Texture: hypidomorphic medium-grained.

Aegerine-Augite: zoned light yellow-green to medium green (?), seam twins, magnetite and biotite inclusions, aegerine as fibrous radiating aggregates.

Olivine: colorless, lath-shaped, subhedral, not diopside because of parallel extinction, surrounded by biotite, aegerine and magnetic inclusions.

Magnetite: subhedral to square.

Biotite: poly-zoned light brown to dark brown, pleochroic light brown to reddish-brown, numerous apatite inclusions,

Hastingsite:

Orthoclase: matrix, partly zeolitized.

Nepheline: matrix, subhedral, turbid in centers.

Zeolite: some clear, some turbid, undulatory extinction.

Analcite (?): minor isotropic material.

Apatite: subhedral.

Counts	Aegerine-Augite	Olivine	Magnetite	Biotite	Hastingsite
300	37.0	7.0	1.7	21.0	1.3

Orthoclase	Nepheline	Zeolitized Orthoclase or Nepheline	Zeolite	Analcite (?)	Apatite
1.7	1.0	1.0	27.3	0.7	0.3

Sample 704D

Location: from the Great Anticlinal Phacolith, 40' above the base, vertical section located at the east end of the east-west exposure.

Megascopic: gray-green with white zeolitized areas, brown biotite masses around olivines, coarse biotite plates.

Specific Gravity: 2.97.

Texture: hypidomorphic medium-grained.

Aegerine-Augite: zoned light green to medium green, pleochroism, very slight, check other slides, rarely poly-zoned, subhedral, magnetite and biotite inclusions, idomorphic with biotite, no aegerine around augite, if surrounded by biotite, aegerine on augite if surrounded by leucocratic material, seam twinning.

Olivine: elongate, colorless, anhedral magnetite inclusions, replaced along channels by magnetite and biotite, fractured.

Magnetite: anhedral, pyrite replaced by limonite.

Biotite: pleochroic light brown perpendicular to cleavage, orange-brown parallel the cleavage, zoned with darker borders, often enclosing olivine, anhedral to euhedral, ideomorphism indicates it was formed after augite and before aegerine, magnetite inclusions.

Hastingsite: pleochroic light green to brown-green, anhedral to subhedral, surrounding augite often associated with biotite, radial needles as inclusions, apatite (?) as inclusions.

Orthoclase: clear to irregularly turbid brown, augite is ideomorphic against orthoclase if no aegerine rims, some 3 mm. laths poikilitically enclosed augites, simple twins, one grain had 2V such that the isogyres do not leave the field of view 60 degrees or less, partly zeolitized forming a perthitic-like intergrowth, along preferred directions, enclosed zeolite has yellow birefringence, undulatory extinction.

Zeolite: rectangular areas representing feldspar and nepheline, containing numerous aegerine inclusions, euhedral hexagonal zeolitized areas representing nepheline (?) zeolitized areas are euhedral against aegerine terminations on aegerine-augite, poor example on edge of slide, submicroscopic, complicated extinction.

Apatite: subhedral.

Counts	Aegerine-Augite	Olivine	Magnetite	Biotite	Hastingsite
300	41.3	9.0	1.3	11.3	9.3

Orthoclase	Zeolitized Orthoclase	Zeolite
8.0	6.7	13.0

Sample 704E

Location: from the Great Anticlinal Phacolith, 55' above base, vertical section located at east end of east-west exposure.

Megascopic: dark green more biotite masses than F and about the same as D, same amount of white zeolite blebs as D.

Specific Gravity: 2.98 - 2.99.

Texture: medium-grained, hypidomorphic, subparallelism of pyroxenes, some pyroxenes and especially biotite plates 3 mm. across.

Aegerine-Augite: zoned light green to green rims, seam twinning, biotite, magnetite and glass (?) inclusions.

Magnetite: anhedral associated with biotite, along cracks in olivine.

Olivine: colorless, anhedral, biotite along cracks and peripheral, twin planes are irregular.

Biotite: pleochroic orange-red to light brown, zoned to darker-brown rims, surrounding olivine.

Hastingsite: pleochroic liver-brown to light green-brown, numerous parallel needle inclusions which are colorless and in that part of the hastingsite next to augite, often surrounds the augite.

Orthoclase: clear, some brown turbid which could be iron because when zeolitized aegerine microlites occur, poikilitically enclosing augites etc., large 2V.

Nepheline: clear to turbid-like orthoclase, many opaque inclusions poikilitically enclosing augites, etc.

Zeolite: clear to turbid, often numerous aegerite (?) inclusions with parallel extinction, inclusions are often near borders, some have numerous inclusions, others without, undulatory complex twinning, often blade shaped replacement of orthoclase, different blades have parallel extinction, in one zeolitized orthoclase lath replacement has higher birefringence lower relief, symmetrical extinction while another example has inclined extinction, orthoclase replacement is much less regular (patchy), this stained blue by the methyl blue test, two euhedral laths (against orthoclase), anhedral augite has lath-like extinction parallel the cleavage, also an hexagonal--shaped zeolitized crystal, not usual in these slides, similar occurance in 577.

Counts	Aegerine-Augite	Olivine	Magnetite	Biotite	Hastingsite
300	48.7	8.7	1.0	14.7	4.0

Orthoclase	Nepheline	Zeolitized Orthoclase or Nepheline	Zeolite
5.0	1.7	1.3	15.0

Sample 704F

Location: from the Great Anticlinal phacolith, 70' above base, vertical section located at the east end of the east-west exposure.

Megascopic: gray-green, similar to 704D, white zeolite blebs, less biotite masses surrounding olivine.

Specific Gravity: 3.03.

Texture: hypidomorphic, medium-grained, subparallel orientation of pyroxenes, biotites and pyroxenes maximum 4 mm. across.

Aegerine-Augite: pleochroic, zoned colorless to green to deep green, usually light brown in basal sections, euhedral to subhedral, seam twinning, many large grains not surrounded by aegerine, biotite and rounded or euhedral magnetite inclusions, in aggregates.

Olivine: colorless, anhedral, surrounded by biotite, both contain magnetite inclusions, one twinned plane is curved, minor rimming by pyroxene.

Magnetite: larger grains than usual .3 mm., subhedral, in pyroxene.

Biotite: pleochroic light orange-brown to orange-brown, not zoned as usual, poikilitically enclosing augites.

Hastingsite: pleochroic liver-brown to light green, euhedral to subhedral, associated with biotite and pyroxene, some euhedral zeolites in hastingsite, euhedral with.

Orthoclase: medium-grained poikilitically enclosing augites, zeolitized along preferred directions parallel the cleavage (?), several stages of zeolitization.

Zeolite: undulatory extinction, yellow-birefringence due to thickness of slide often enclose microlite needles of aegerine which sometimes occur in radial aggregates, subhedral masses enclosed in pyroxene and opaques, equant clear zeolite masses adjacent to turbid areas, partly zeolitized areas with aegerine parallel the cleavages of the orthoclase, one area is euhedral against euhedral hastingsite, the clear areas represent natrolized analcite (?) while other areas represent feldspars and nepheline (?), initial zeolitization indicated by colorless rods, these rods have lower relief than orthoclase lower birefringence indicated, rarely they have the appearance of lath inclusions with slight twinning (?), higher relief parallel the extinction, Chabazite (?) clear zeolite with undulatory extinction has small 2V.

Sample 704F (continued)

Unidentified mineral: trace, pleochroic, dark-blue parallel the cleavage to blue-green perpendicular to the cleavage, intergrown with hastingsite, with apatite inclusions, appears to be isotropic and have anomolous pleocroism.

Apatite: subhedral, trace.

Counts	Aegerine-Augite	Olivine	Magnatite	Biotite	Hastingsite
300	59.3	2.3	0.7	0.7	6.0

Orthoclase	Zeolitic Orthoclase or Nepheline	Isotropic	Zeolite
6.3	7.7	0.3	8.0

Sample 707

Location: dike in the Great Theralite Cliffs, which transects sills, trends north 20° west.

Megascopic: contains inclusions composed of feldspar, biotite and zeolite, inclusion of baked sandstone and light porphyritic malignite, larger irregular inclusions are 3 cm. across, smaller elliptical and rounded inclusions are generally less than 1.2 cm. across, inclusions have subparallel orientation.

Mineralogy of inclusions.

Aegerine: occurs as microlites in analcite.

Biotite: black to red-brown zoned, pleochroic in inclusions, in the groundmass it is light yellow to brown centers, rims are black to red-brown.

Magnetite:

Sanidine: euhedral, well-cleaved, altered to zeolite, anhedral outside inclusion.

Zeolite: with curving fracture, with radial extinction, natrolite (?).

Analcite: six-sided shapes.

Calcite:

BIBLIOGRAPHY

Ahrens, L.H., Pinson, W.H., Kearns, M.M., 1952, Association of Rubidium and Potassium and their Abundance in Common Igneous Rocks and Meteorites: Geochem. et Cosmochem. Acta, V. 2, pp. 229-242.

Alden, William C., 1932, Physiography and Glacial Geology of Eastern Montana and Adjacent Area: U.S.G.S., Prof. Paper, 174.

Anderson, E.M., 1951, The Dynamics of Faulting and Dyke Formation with Application to Britain: Oliver and Boyd, Edinburgh, pp. 206.

Aoki, Ken-Ichiro, 1964, Clinopyroxenes from Alkaline Rocks of Japan: Amer. Min., V. 49, No. 9, 10, pp. 1199-1223.

Bailey, E.H., Stevens, R.E., 1960, Selective Staining of K-Feldspar and Plagioclase on Rock Slabs and Thin Sections: Amer. Min., V. 45, pp. 1020-1025.

Barksdale, J.D., 1951, The Shonkin Sag Laccolith Revisited: Abs., Amer. Min., V. 36, p. 310.

Barth, T.F., 1952, 1962, Theoretical Petrology: John Wiley and Sons, New York.

Benson, W.N., 1941, Cainozoic Petrographic Provinces in New Zealand and their Residual Magmas: Amer. Journal Sci., V. 239, pp. 537-552.

----------, 1941, The Basic Igneous Rocks of Eastern Otago and their Tectonic Environment: Royal Soc. New Zealand Transactions, V. 71, pt. 3, pp. 208-222.

Berg, R.R., 1961, Laramide Tectonics of the Wind River Mountains in Symposium on Lake Cretaceous Rocks, Wyoming and Adjacent Areas: Wyoming Geol. Association, 16th Annual Field Conference, 1961: Casper, Wyoming, Petroleum Information.

Bevan, A., 1925, Rocky Mountain Peneplains Northeast of Yellowstone Park: Journal of Geology, V. 33, pp. 563-587.

Bhattachargi, Somdev, Smith, C.H., 1964, Flowage Differentiation: Science, V. 145, pp. 150-153.

Bowen, C.F., 1918, Anticlines in a Part of the Musselshell Valley, Musselshell, Meagher and Sweetgrass Counties, Montana: U.S.G.S. Bul. 691, pp. 185-209.

Bowen, N.L., 1924, Fin Area in Telmark, Norway: Amer. Journal Sci., 5th series, V. 208.

----------, 1928, The Evolution of Igneous Rocks: Princeton University Press, Princeton, N.J., pp. 234-236, 240-257.

Brogger, W.G., 1943-1962, Studies on the Igneous Rock Complex of the Ohio Region: Skrift. Norske. Vidersk.-Akad. Oslo I. Mat. Nat. Klasse.

Buie, B.F., 1941, Igneous Rocks of the Highwood Mountains, Pt. III, Dikes and Related Intrusives: G.S.A. Bul., V. 52, pp. 1753-1808.

Butler, J.R., Bowden, P., Smith, A. Z., 1962, K/Rb. Ratios in the Evolution of the Younger Granites of Northern Nigeria: Geochem. et Cosmochem. Acta, V. 26, pp. 89-100.

Chayes, F., 1952, Notes on the Staining of Potash Feldspar with Sodium Cobaltinitrite in Thin Section: Geophysical Laboratory Paper No. 1160.

Czamanske, G.K., 1964, Petrologic Aspects of the Finnmark Igneous Complex, Oslo Area, Norway: Journal of Geo., V. 73, pp. 293-322.

Daly, R.A., 1910, Origin of Alkaline Rocks: G.S.A. Bul., V. 21, p. 92.

----------, 1933, Igneous Rocks and the Depth of the Earth: McGraw-Hills Co., N.Y., pp. 483-544.

Dana, E.S., Grinnell, G.B., 1876, Geological Report in Report of Reconnaissance into the Yellowstone National Park by William Ludlow, Washington, D.C., pp. 89-126.

Deer, W.A., 1935, The Cairnsmore of Carsphairn Igneous Complex: Quart. Jour. Geol. Soc., V. 91, p. 47.

----------, 1937, The Composition and Paragenesis of the Biotites of the Carsphairn Igneous Complex: Min. Mag., V. 24, p. 495.

De Sitter, L.U., 1956, Structural Geology: McGraw-Hill Book Co., N.Y., pp. 552.

Eardley, A.J., 1962, Structural Geology of North America: Harper and Row, N.Y., p. 358.

Edgar, A.D., 1965, The Mineralogical Composition of Some Nepheline Alteration Products: The American Mineralogist, V. 50, pp. 978-989.

Fenner, C.N., 1926, The Katmai Magmatic Province: Jour. Geol., V. 34, pp. 673-772.

Fenneman, N.M., 1931, Physiography of the United States: McGraw-Hill Book Co., p. 534.

Fudali, R.L., 1964, Experimental Studies Bearing on the Origin of Pseudoleucite and Associated Problems of Alkalic Rock Systems G.S.A. Bul., V. 74, pp. 1101-1126.

Gast, P.W., 1956, Terrestrial Ratio of Potassium to Rubidum and the Composition of the Earth's Mantle: Science, V. 47, pp. 858-860.

Gerasimovskii, V.I., 1956, Mineralogy of Nepheline Syenite Intrusives: Geochemistry, No. 5, pp. 495-510.

Gilluly, J., 1965, Volcanism, Tectonism and Plutonism in the Western United States, G.S.A. Special Paper No. 80, p. 69.

Graves, R.W., 1957, Billings Geological Society, 8th Annual Field Conference Guide Book.

Griggs, D.J., 1939, Structure and Mechanism of Intrusion, in Hurlbut, C.S., Jr., Igneous Rocks of the Highwood Mountains, Pt. 1; The Laccoliths: Geological Science of America Bul., V. 50, No. 7, pp. 1043-1112.

Gwinn, B.E., 1964, Thin-Skinned Tectonics in the Plateau and Northwestern Valley and Ridge Provinces of the Central Appalachians, G.S.A. Bul., V. 75, pp. 863-900.

Harris, S.A., 1957, The Tectonics of Montana as Related to the Belt Series: Billings Geological Society Guide Book, 8th Annual Field Conference Guidebook, pp. 22-23.

Hatch, F.H., Wells, A.K., Wells, M.K., 1952, The Petrology of the Igneous Rocks: Thomas Murby and Co., p. 469.

Hayden, F.V., 1961, Sketch of the Geology of the Country about the Headwaters of the Missouri and Yellowstone Rivers: Amer. Jour. of Sci., 2nd series, V. 31, p. 233.

Heir, K.S., Taylor, S.R., 1964, A Note in the Geochemistry of Alkaline Rocks: Norsk Geologisk, Tidskrift, Bind. 44 Hefte 2, pp. 197-203.

----------, 1965, A Geochemical Companion of the Blue Mountain (Ontario, Canada) and Stjernoey (Finnmark, North Norway) Nepheline Syenites: Norsk Geologisk, Tidskrift, Bind. 45, Hefte 1, pp. 41-51.

Hoskins, D.M., 1965, Relationship of Thrust Faults to Plunging Anticlines in South Central Pennsylvania (Abs.), G.S.A. Meetings Abstracts, p. 30.

Hunt, C.B., 1953, Geology and Geography of the Henery Mountains Region, Utah: U.S.G.S. Professional Paper 453.

Hurlbut, C.S., and Griggs, D., 1939, Igneous Rocks of the Highwood Mountains, Montana: Pt. 1, The Laccoliths, G.S.A. Bul., V. 50, pp. 1043-1112.

Iddings, J.P., 1892, Origin of Igneous Rocks: Bul. Phil. Soc., Washington, V. 12, p. 31.

----------, Weed, W.H., 1894, Description of the Livingston Montana Quadrangle, U.S.G.S., Geol. Atlas, Folio 1.

Johannsen, A., 1931, 32, 37, Petrography of the Igneous Rocks, University of Chicago Press, Chicago.

Keith, M.L., 1939, Selective Staining to Facilitate Rosiwal Analysis: Amer. Min., V. 24, pp. 561-565.

Kleeman, A.W., 1965, The Origin of Granitic Magmas: Journal of the Geol. Soc. of Australia, V. 12, Pt. 1, pp. 35-52.

Knopf, A., 1936, Igneous Geology of the Spanish Peak Region, Colorado: G.S.A. Bul., V. 47, No. 11, pp. 1727-1784.

---------, 1964, Time Required to Emplace the Boulder Bathylith, Montana: A First Approximation, Amer. Journal of Sci., V. 262, pp. 1207-1216.

Koizumi, M., 1953, The Differential Thermal Analysis Curves and Dehydration Curves of Zeolites: Mineralogical Journal (Japan), V. 1, p. 36.

Kureping, V.A., 1965, Pseudoleucite Rocks of Mt. Sukai in Gorniya Shorya: Akad Nauk. SSSR Doklady, Earth Science Sec., V. 150. No. 1-6, pp. 143-144.

Kushiro, Ikuo, 1960, Si-Al Relation in Clinopyroxenes from Igneous Rocks: Amer. Journal of Sci., V. 258, pp. 548-554.

Larsen, E.S., 1938, Variation Diagrams for Groups of Igneous Rocks: Journal of Geology, V. 46, pp. 506-570.

----------, Hurlbut, C.S., Griggs, D., Buie, B.F., Burgess, D.H., 1939, Igneous Rocks of the Highwood Mountains, Montana: G.S.A. Bul., V. 50, pp. 1733-1868.

----------, 1940, Petrographic Provinces of Central Montana: G.S.A. Bul., V. 51, No. 6, pp. 887-948.

Lehmann, E., 1965, Non Metosomatic Chlorite in Igneous Rocks: Geological Magazine, V. 102, No. 1, pp. 36-45.

Le Maitre, R.W., 1962, Petrology of Volcanic Rocks, Gough Island, South Atlantic: G.S.A. Bul., V. 73, pp. 1309-1340.

Lessing, P., Decker, R.W., Reynolds, R.C., 1963, Potassium and Rubidium Distribution in Hawaiian Lavas: Journal of Geophysical Research, V. 68, No. 20, pp. 5851-5855.

Lindgren, W., 1913, The Igneous Geology of the Cordillera and Its Problems: Problems of Amer. Geology, Yale University Press, New Haven, Conn., pp. 234-286.

Lyons, J.B., 1944, Igneous Rocks of the Northern Big Belt Range, Montana: G.S.A. Bul., V. 55, pp. 422-445.

Mansfield, G.R., 1909, Glaciation in the Crazy Mountains of Montana: G.S.A. Bul., V. 19, pp. 558-567.

McMannis, W.J., 1955, Geology of the Bridger Range, Montana: G.S.A. Bul., V. 66, pp. 1407-1413.

----------, 1965, Rocky Mountain Sedimentary Basins: Western Montana, Bul. of A.A.P.G., pp. 1801-1823.

Miyashiro, A., 1957, The Chemistry, Optics and Genesis of the Alkali-Amphiboles: Journal Fac. Sci. Univ. Tokyo, Sec. 2, V. 11, p. 57.

Moore, J.G., 1959, The Quartz Diorite Boundary Line in the U.S.: Journal of Geology, V. 67, pp. 198-210.

----------, 1962, K/Na Ratio of Cenozoic Igneous Rocks of the Western U.S.: Geochem. et Cosmochem. Acta, V. 26, pp. 101-130.

Murata, K.J., 1960, A New Method of Plotting Chemical Analyses of Basaltic Rocks: Amer. Journal Sci., V. 258A, pp. 247-252.

Nockolds, S.R., 1934, The Production of Normal Rock Types and their Bearing on Petrogenesis: Geol. Mag., V. 71, p. 31.

Ode, H., 1957, Mechanical Analysis of the Dike Pattern of the Spanish Peaks Area, Colorado: G.S.A. Bul., V. 38, pp. 567-576.

Oftedahl, C., 1946, Igneous Rock Complexes of the Oslo Region, VI, on Akerites and Romb-Porphyries: Skrift. Det. Norske Vidensk Akad. Oslo, No. 1.

----------, 1948, Igneous Rock Complexes of the Oslo Region, VI, The Feldspars: Skrift. Det. Norske Vidensk Akad., Oslo.

Peacock, M.A., 1931, Classification of Igneous Rocks: Journal of Geology, V. 39, pp. 54-67.

Pecora, W.T., 1942, Nepheline Syenite Pegmatites, Rocky Boy Stock, Bearpaw Mountains, Montana: Amer. Mineralogist, V. 27, pp. 397-424.

----------, et al, 1957, Preliminary Map of the Warrwick Quadrangle, Bearpaw Mountains, Montana, Miscellaneous Investigations Map I-237.

Perry, E.S., 1950, The Belt Series of Montana: Billings Geological Society, 1st Annual Guidebook, pp. 40-43.

Peterson, D.W., 1961, Descriptive Modal Classification of Igneous Rocks, A.G.I. Data Sheet, No. 23: Geotimes, V. 5, No. 6, pp. 31-36.

Phillips, W.R., 1963, A Differential Thermal Study of the Chlorites: Mineralogical Mag., V. 33, pp. 404-414.

Pirsson, L.V., 1905, The Petrographic Province of Central Montana: Amer. Jour. Sci., 3rd series, V. 20, pp. 35-49.

Poldervaart, A., 1949, Three Methods of Graphic Representation of Chemical Analyses of Igneous Rocks: Transactions of the Royal Society of South Africa, V. XXXII, Pt. II, pp. 177-188.

----------, 1964, Chemical Definition of Alkali Basalts and Theoleiites: G.S.A. Bul., V. 75, pp. 229-232.

----------, Parker, A.B., 1964, The Crystallization Index as a Parameter of Igneous Differentiation in Binary Variation Diagrams: Amer. Jour. Sci., V. 262, No. 2, pp. 281-289.

----------, ----------, 1965, Reply to Discussion by Dr. Thornton and Dr. Tuttle: Amer. Jour. of Sci., V. 263, No. 3, pp. 279-283.

Ransome, R.L., 1913, The Tertiary Orogeny of the North American Cordillera and Its Problems: Problems of Amer. Geology, Yale University Press, pp. 287-376.

Reeves, F., 1927, Geology of the Cat Creek and Devil's Basins Oil Field and Adjacent Areas in Montana: U.S.G.S. Bul., No. 786-B, pp. 54-55.

----------, 1929, Thrust Faulting and Oil Possibilities in the Plains Adjacent to the Highwoods, Montana: U.S.G.S. Bul., No. 806, pp. 155-195.

Retref, E.A., 1962, Preliminary Observations of the Feldspars from the Pilanesberg Alkaline Complex, Transvaal, South Africa: Norsk Geologisk Tidskrift, Bind. 42, Feldspar V., Halvbind, pp. 493-513.

Reynolds, R.C., 1963, Potassium-Rubidium Ratios and Polymorphism in Illites and Microclines from the Clay-Size Fraction of Proteozoic Carbonate Rocks: Geochem. et and Cosmochem. Acta, V. 27, No. 11, pp. 1097-1111.

Richards, P.W., 1957, Geology of the Area East and Southeast of Livingston, Park Co., Montana: U.S.G.S. Bul. 1021L.

Roberts, A.E., 1964, Geologic Map of the Bozman Pass Quadrangle, Montana: U.S.G.S. Map I-399.

Rosenbush, H., 1887, Mikroscopeshe Physiographie: pp. 248, 251.

----------, 1907, Elemente der Gesteinslehre, 3rd edition.

----------. Osann, A., 1922. Elemente der Gesteinslehre, 4th edition.

Rouse, J.T., et al., 1937, Petrology, Structure and Relations to Tectonics of Porphyry Intrusives in the Beartooth Mountains, Montana: Jour. Geol., V. 45, pp. 717-740.

Saether, E., 1948, On the Genesis of Paralkaline Rock Provinces: Rep. 18th Session International Geological Congress, London, V. 2, pp. 123-130.

Saha, P., 1958, Geochemical and X-ray Investigation of Natural and Synthetic Analcites: Amer. Min., V. 44, Nos. 3,4, pp. 300-314.

Seki, Y., Kennedy, G.C., 1964, An Experimental Study on the Leucite-Pseudoleucite Problem: Amer. Min., V. 49, No. 9, pp. 1267-1280.

Shand, J.S., 1943, Eruptive Rocks: Woodbridge Press, Guilford, pp. 332-436.

----------, 1945, The Present State of Daly's Hypothesis of the Alkaline Rocks: Amer. Jour. Sci., V. 243A, pp. 495-507.

Simpson, C.G., 1937, The Fort Union of the Crazy Mountain Field, Montana, and Its Mammalian Fauna: U.S. Nat. Museum Bul. 169.

Sims, J.D., 1964, A Sedimentary Petrographic Study of the Upper Fort Union Group, Northern Crazy Mountains, Montana: Unpublished M.S. thesis, University of Cincinnati.

Smith, J.V., Sahama, T.G., 1953-1955, May, Determination of the Composition of Natural Nephelines by an X-ray Method: Mineral. Mag., V. 30, pp. 439-449.

Smith, J.G., 1965, Fundamental Transcurrent Faulting in the Northern Rocky Mountains: A.A.P.G. Bul., V. 49, pp. 1398-1409.

Sorensen, H., 1960, On the Agpaitic Rocks, 21st Internat. Geol. Cong. Pt. 8, pp. 319-327.

Spencer, E.W., 1959, Structural Trends in the Beartooth Mountains, Montana and Wyoming: Billings Geol. Soc., 9th Annual Field Conference, pp. 16-23.

Steinhart, J.S., Meyer, R.P., 1961, Explosion Studies of Continental Structure: Carnegie Institution of Washington, Publication 622, Washington, D.C.

Stone, R.W., Calvert, W.R., 1910, Stratagraphic Relations of the Livingston Formation of Montana: Econ. Geol., V. 5, pp. 552-669, 741-764.

Sugimura, A., 1960, Zonal Arrangement of Some Geophysical and Petrological Features in Japan and Its Environs, Jour. Fac. Sci., Univ. Tokyo, Sect. 2, 12, pp. 133-153.

Tanner, J.T., 1949, Geology of the Castle Mountain Area, Montana, Unpublished Ph. D. dissertation, Princeton University.

Taubeneck, W.H., 1965, An Appraisal of Some Potassium-Rubidium Ratios in Igneous Rocks: Jour. of Geophysical Research, V. 70, No. 2, pp. 475-478.

Thom, W.T., Jr., 1923, The Relation of Deep Seated Faults to Structural Features of Central Montana: Amer. Assn. Petroleum Geologists, Bul., V. 7, No. 1, pp. 1-23.

----------, 1955, Wedge Uplifts and their Tectonic Significance in Crust of the Earth: G.S.A. Special Paper 62, pp. 369-376.

----------, 1957, Tectonic Relationships, Evolutionary History and Mechanics of Origin of the Crazy Mountain Basin: 8th Annual Field Conference Guidebook, Billings Geol. Soc., edited by R.W. Graves, pp. 9-21.

Thornton, C.P., Tuttle, O.F., 1960, Chemistry of Igneous Rocks, Pt. 1, Differentiation Index: Amer. Jour. Sci., V. 258, pp. 664-684.

----------, ----------, 1965, The Crystallization Index as a Parameter of Igneous Differentiation in Binary Variation Diagrams: A Discussion: Amer. Jour. Sci., V. 263, pp. 277-279.

Tilley, C.E., 1958, Problems of Alkali Rock Genesis: Quart. Jour. Geol. Soc. London, V. 113, pp. 323-360.

Turner, F.J., Verhoogen, J., 1960, Igneous and Metamorphic Petrol., McGraw-Hill Book Co., N.Y.

Tuttle, O.F., 1952a, Origin of Contrasting Mineralogy of Extrusive and Plutonic Salic Rocks: Jour. of Geol., V. 60, p. 107.

----------, 1952b, Optical Studies of Alkali Feldspars: Amer. Jour. Sci., Bowen V., p. 553.

Tyrrell, G.W., 1965, Distribution of Igneous Rocks in Space and Time: G.S.A. Bul., V. 66, pp. 405-426.

Volkov, V.P., Savinova, E.N., 1959, Distribution of Rubidium and K/Rb Ratio in the Rocks of the Lovezero Alkali Massif: Geochem., No. 6, pp. 635-642.

Vororbieva, O.A., Alkali Rocks of the U.S.S.R., 21st Inter. Geol. Cong., Pt. 13, pp. 7-18.

Washington, H.S., 1900, Igneous Complex of Magnet Cove: G.S.A. Bul. V. 11, pp. 389-400.

----------, 1917, Chemical Analysis of Igneous Rocks, pub. from 1884 to 1913: U.S.G.S. Prof. Paper 99.

Watkinson, D.H., Wyllie, P.J., 1964, The Limestone Assimilation Hypothesis: Nature, V. 204, No. 4963, pp. 1053-54.

Weed, W.H., 1899, Description of the Little Belt Mountains Quadrangle: U.S. Geol. Survey, Geol. Atlas, Folio 56.

Wilkinson, J.F.G., 1963, Some Natural Analcite Solid Solutions: Min. Mag., V. 33, pp. 498-505.

Williams, H., 1933, Geology of Tahiti, Moorea and Maiso: B.P. Bishop Mus., Bul. 105.

Witkind, I.J., Geology of the Abajo Mountain Area San Juan County, Utah: (1964) Geological Survey, Prof. Paper No. 453.

Wolf, P.E., 1964, Late Cenozoic Uplift and Exhumed Rocky Mountains of Central Western Montana: G.S.A. Bul., V. 75, pp. 493-502.

Wolff, J.E., 1885, Notes of the Petrography of the Crazy Mountains and Other Localities in Montana Territory: Northern Transcontinental Survey, pp. 8-13.

----------, 1890, Notes on the Petrography of the Crazy Mountains: Neues Jarib. Min. etc., p. 1192.

----------, 1892, The Geology of the Crazy Mountains, Montana, G.S.A. Bul., V. 3, pp. 445-452.

----------, 1893, On the Occurrence of Theralite in Costa Rica, Central America: Amer. Jour. of Sci., pp. 271-72.

----------, Tarr, ----, 1893, Acmite-Trachyte from the Crazy Mountains, Harv. Mus. Comp. Zool. Bul., V. 16, No. 12, pp. 227-28.

----------, 1898, Theralite in J.S. Diller, The Educational Series of Rock Specimens: U.S.G.S. Bul. 150. pp. 197-201.

----------, 1938, Igneous Rocks of the Crazy Mountains, Montana: G.S.A. Bul., V. 49, pp. 1569-1628.

Wones, D.R. Eugster, H.P., 1965, Stability of Biotite, Experiment Theory and Application: Amer. Min., V. 50, pp. 1228-72.

Yagi, K., 1959, Petrochemistry of the Cenozoic Alkalic Rocks of Japan and Surrounding Areas (JwE): Bul. V Soc. Japan, Ser. 2,3, pp. 63-75.

--------, 1960, Petrochemistry of the Alkalic Rocks of the Ponape Island, Western Pacific Ocean: Rept. 21st, Inter. Geol. Cong., Copenhagen, Pt. 13, pp. 108-122.

Zies, E.G., Chaynes, F., 1960, Pseudoleucite in a Tinguaite from the Bearpaw Mountains, Montana: Jour. of Petrology, V. 1, Pt. 1, pp. 86-98.

Zlobin, B.I., 1959, Paragenesis of Dark-Colored Minerals of the Alkaline Rocks in Connection with the New Term for the Agpaitic Coefficient: Geochemica (English summary), pp. 507-19.

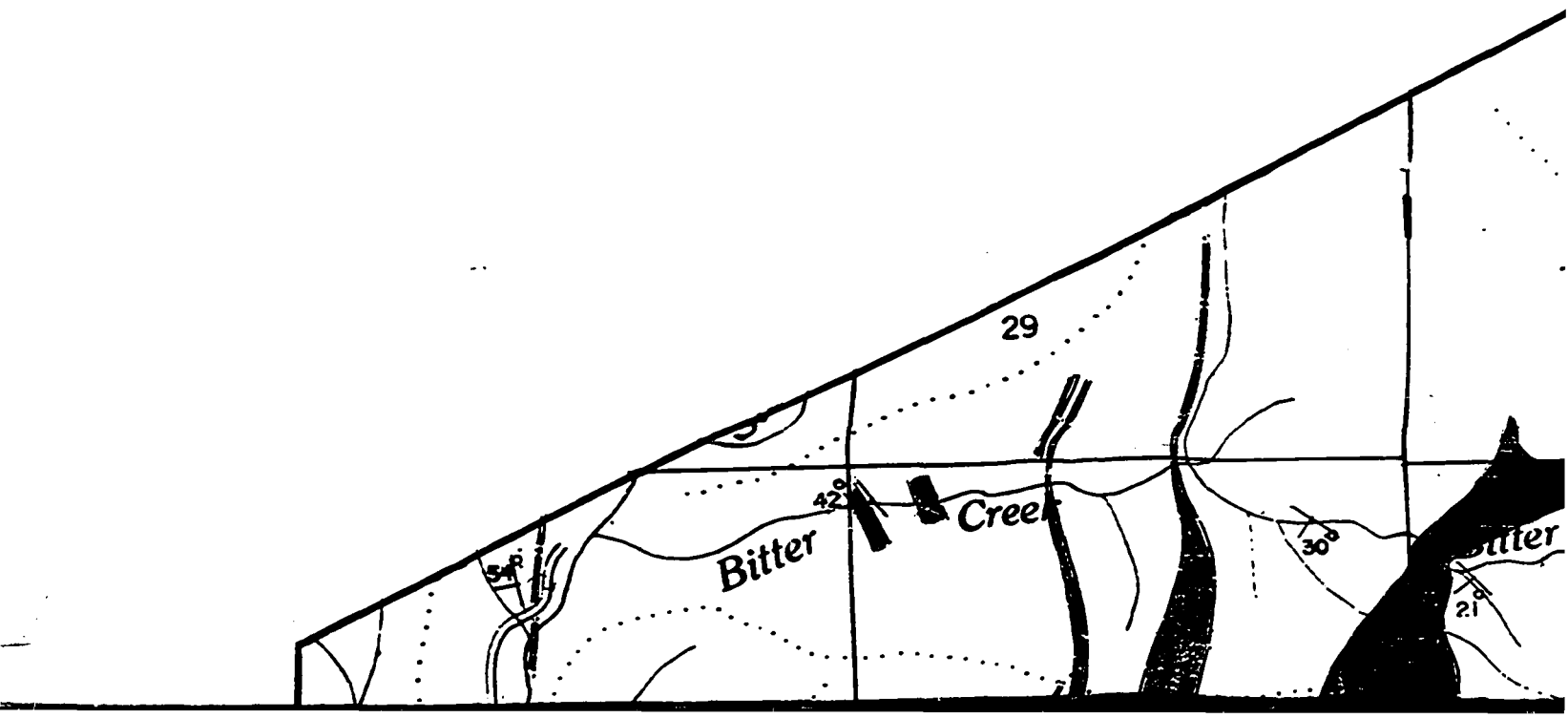

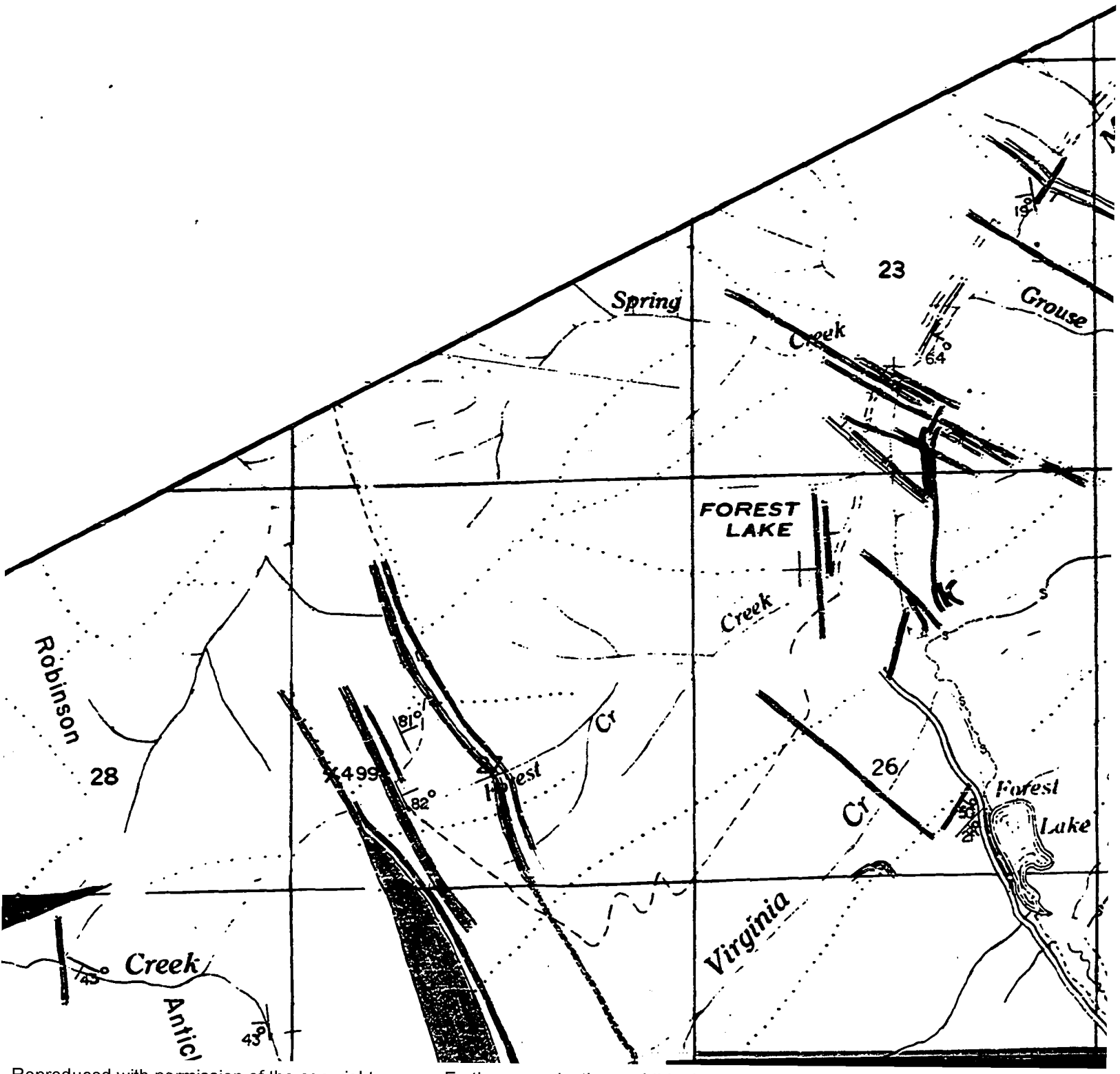

GEOLOGY OF PART

by F.E. Simms, assisted

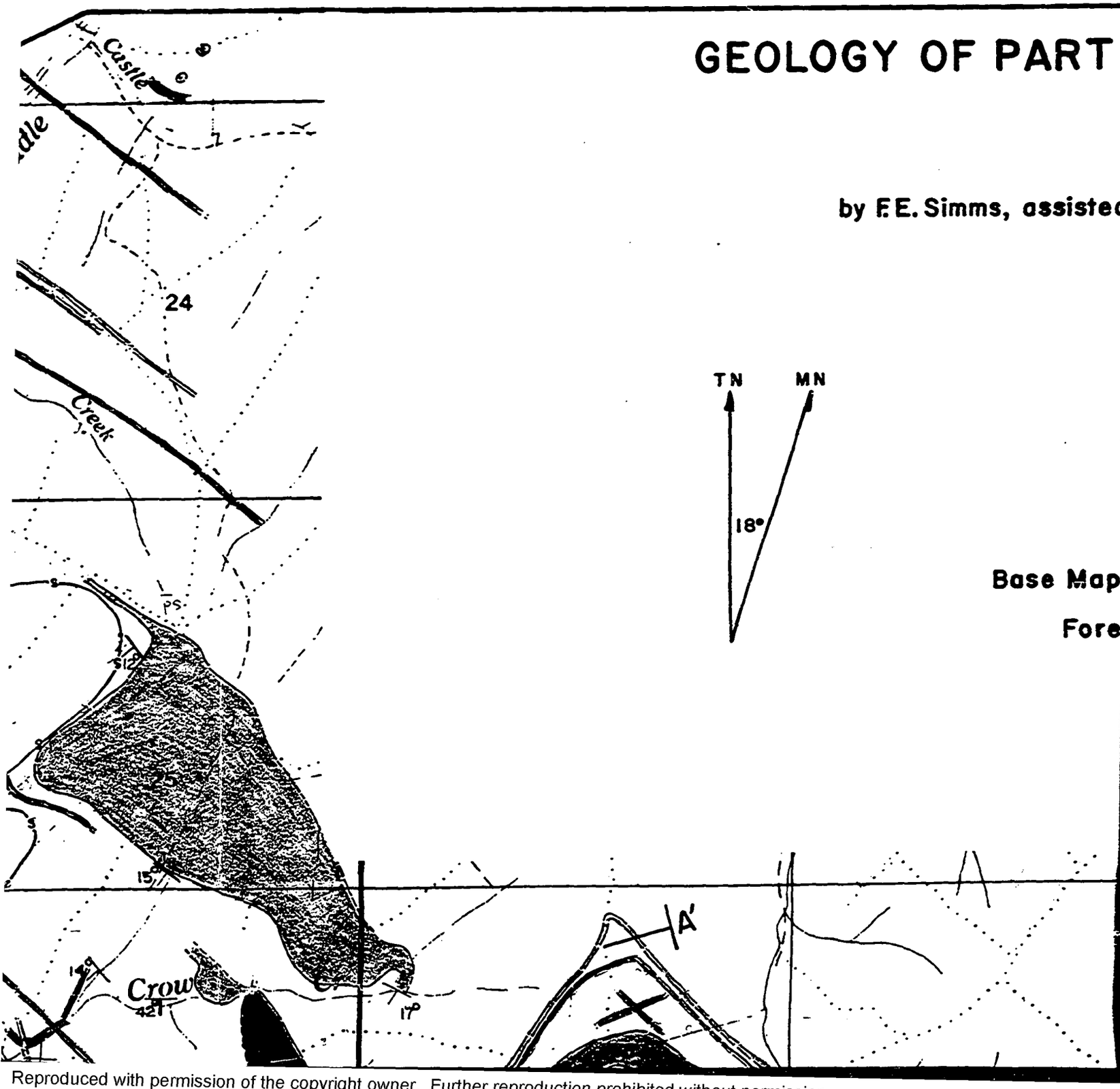

Base Map

Fore

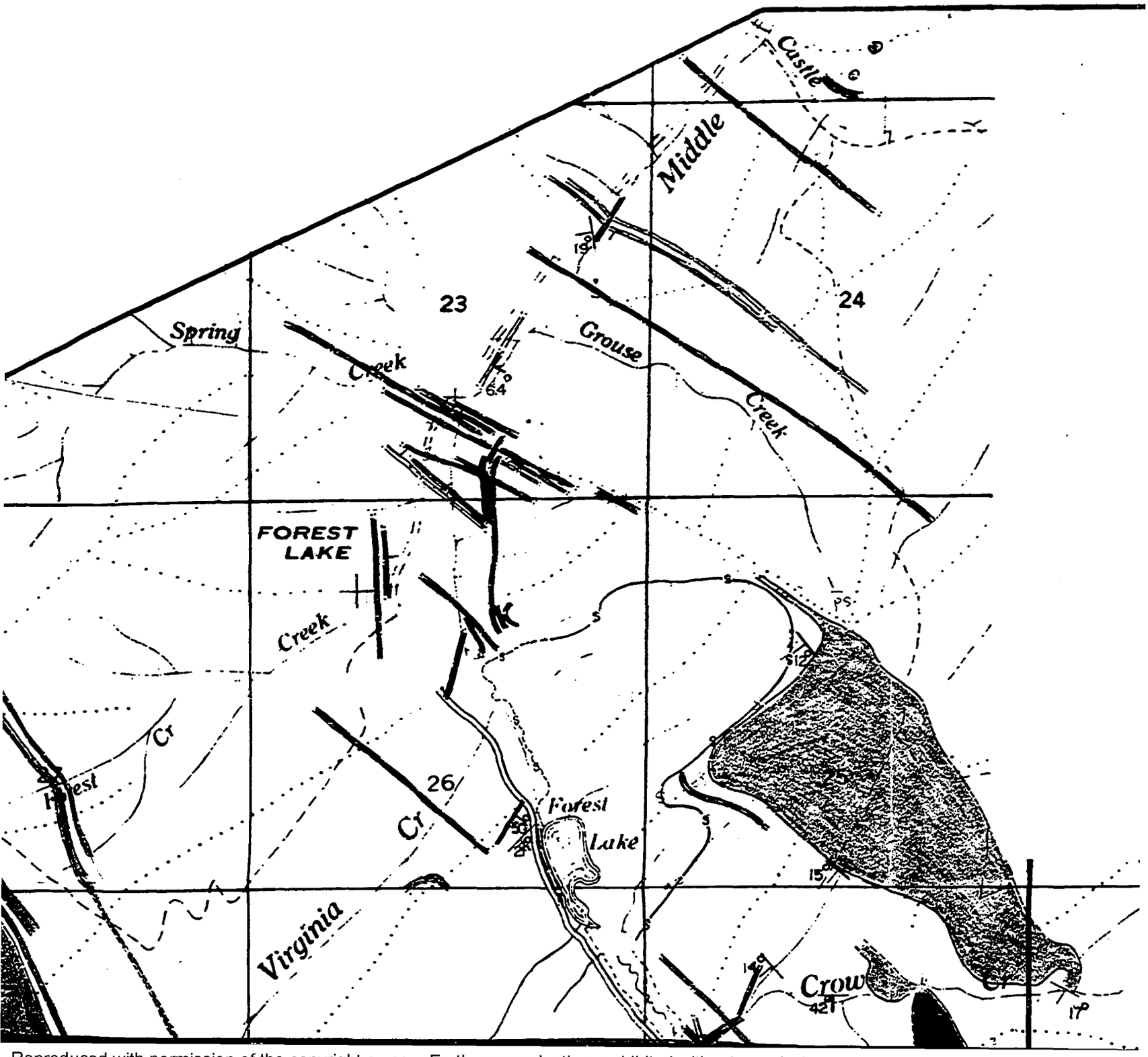

GEOLOGY OF PART OF THE NORTHERN
MONTANA

by F.E. Simms, assisted by J.Sims, R.Eigenberger, R.Sch

Scale approximately 1:20,000

ONE MILE

1965

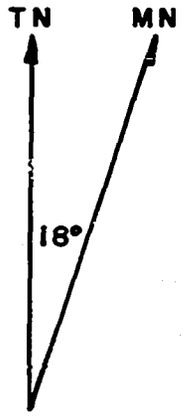

Base Map is United States Department of
Forest Service Planimetric Map Class

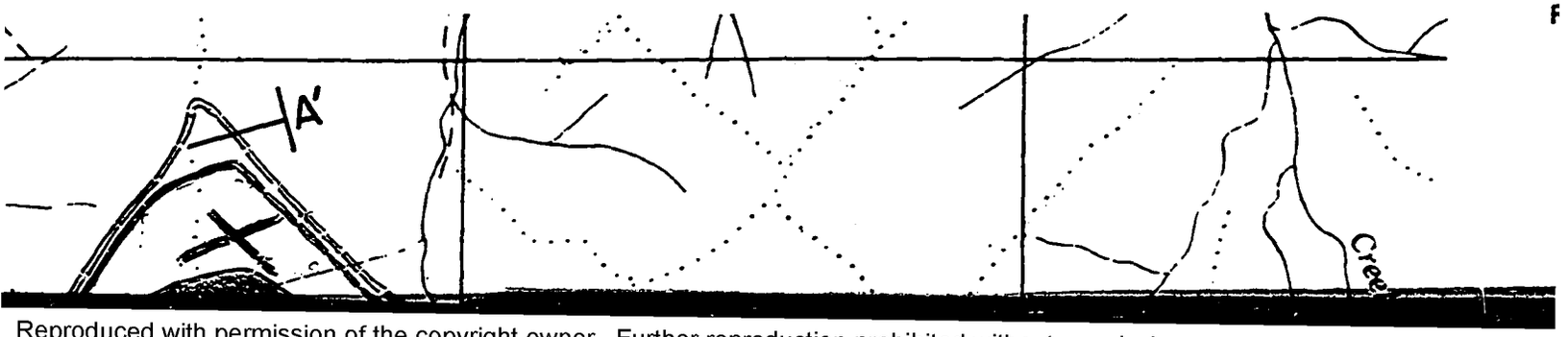

CRAZY MOUNTAINS,

Plate 1

pper, and H.Bloemer

H

griculture

, 1961

Map Area
Location

eistocene

cent

[r] Rockslide deposits

Unconsolidated alluvial gravel, sand and silt deposits; terrace deposits are Pliocene?

[d] Andesite porphyry

Basalt

Quartz latites, rhyolite porphyries

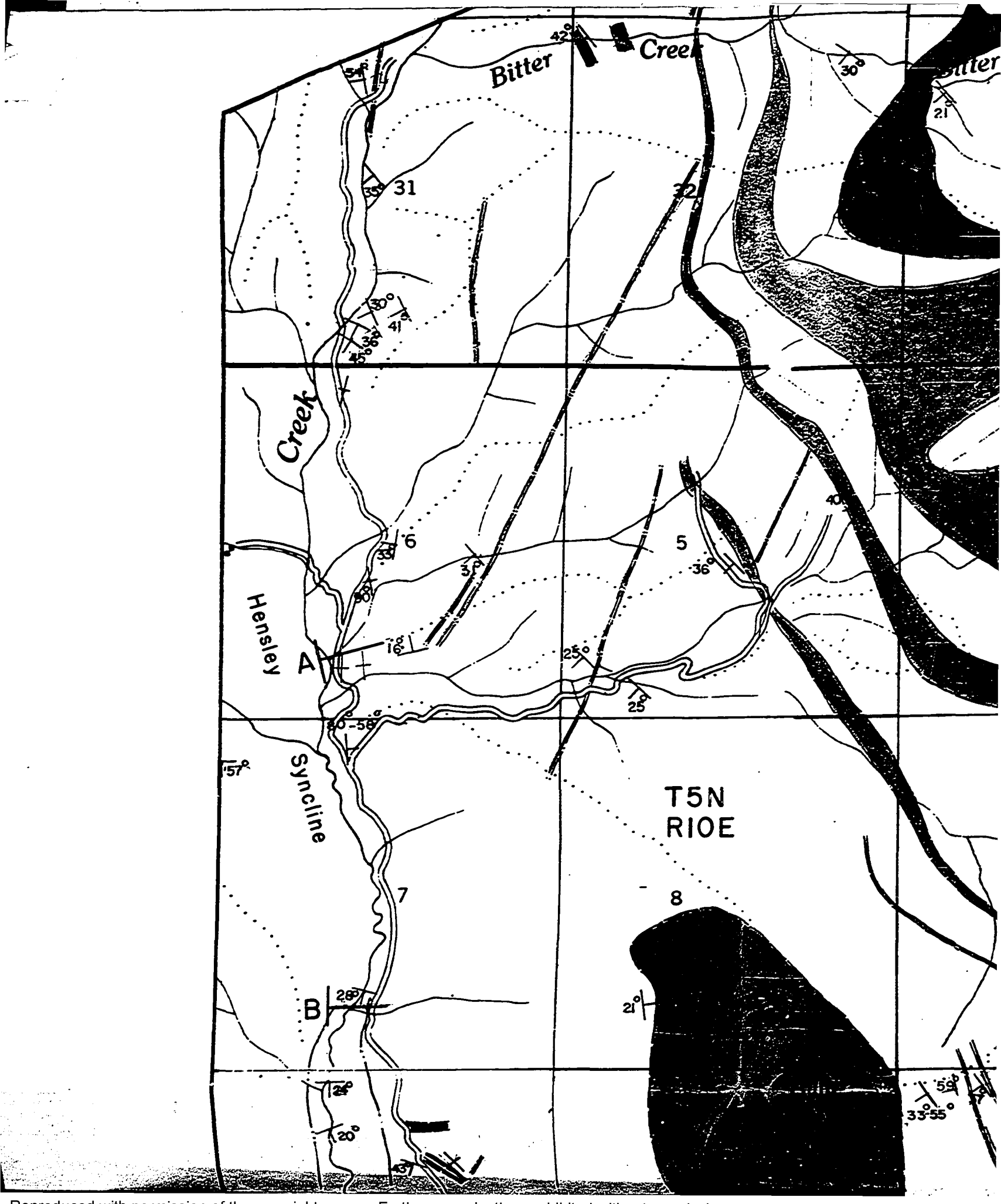

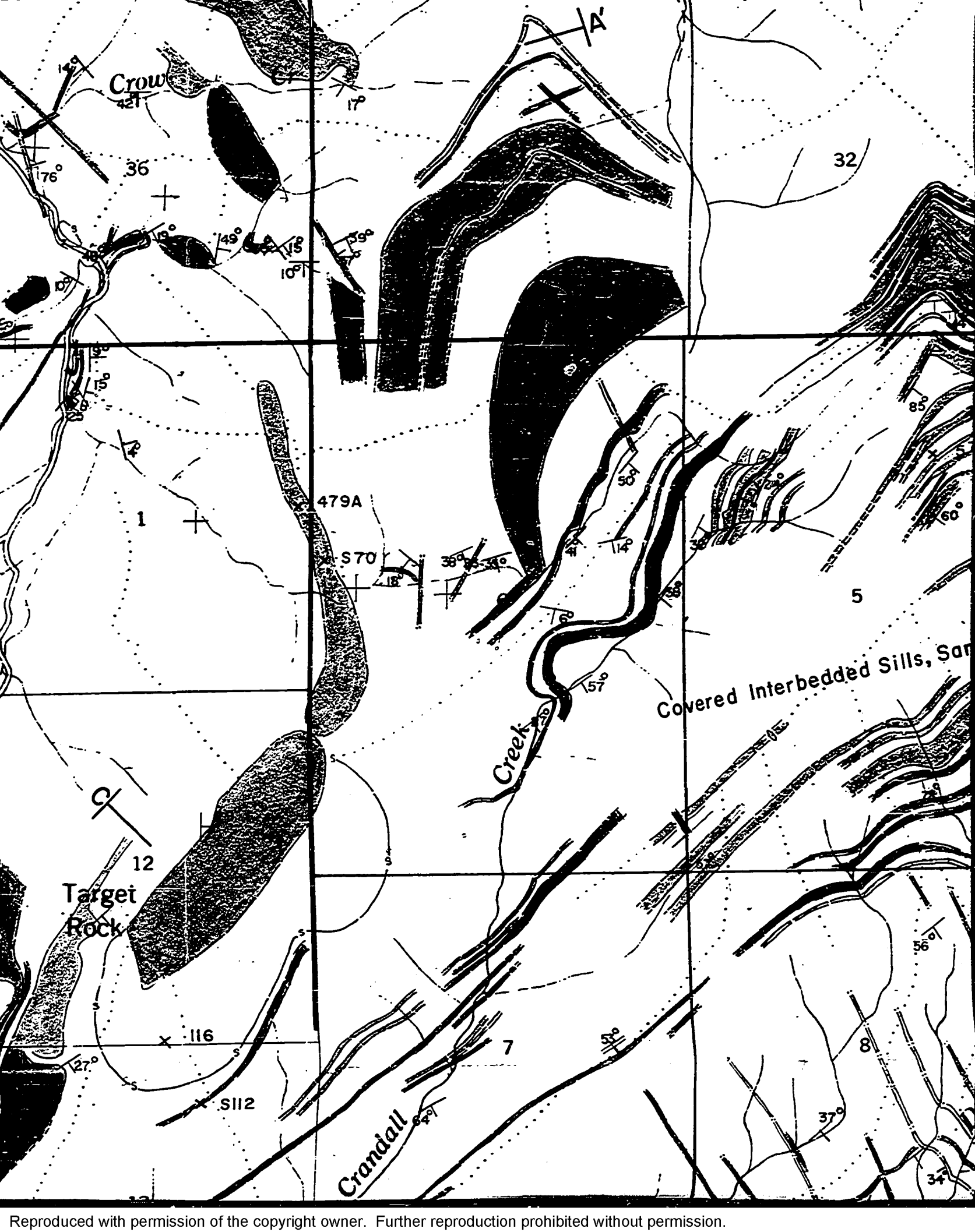

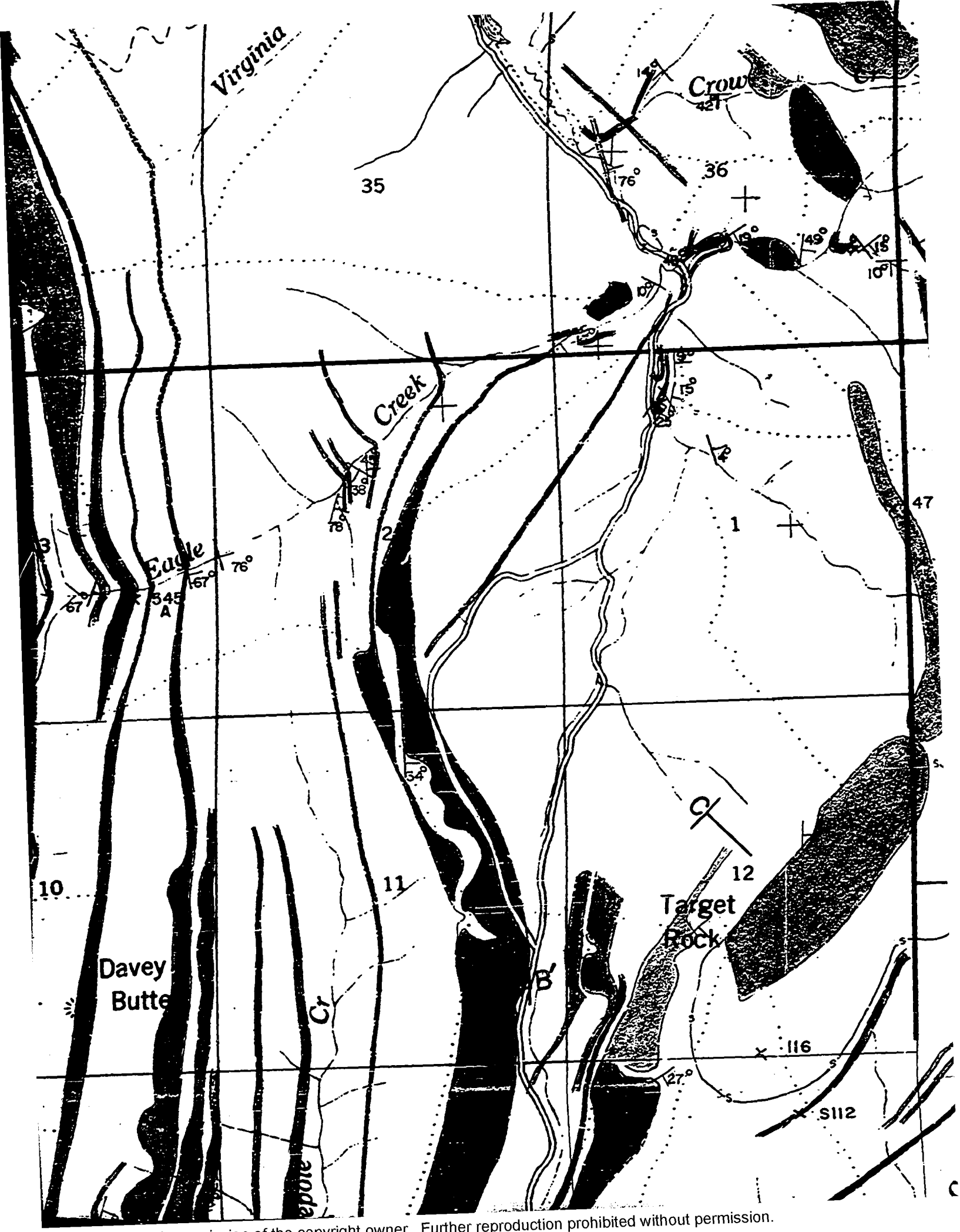

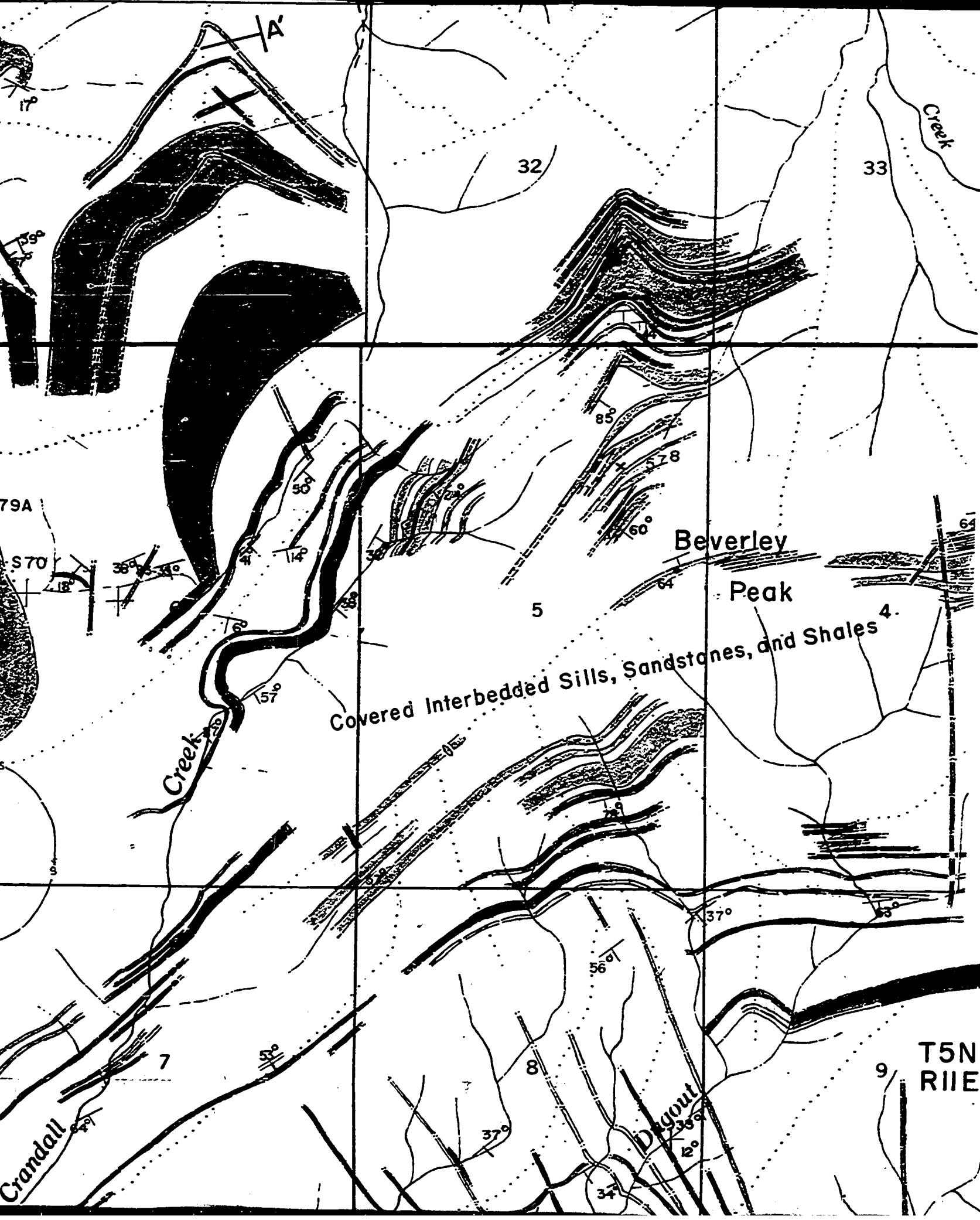

		[d] Andesite porphyry
		Basalt
		Quartz latites, rhyolite porphyries
Oligocene? and Eocene	Hypabyssal igneous intrusives	Alkeritic rocks including mafic trachytes and latites
		Feldspathoidal syenites, trachytes, and variants
		Biotite lamprophyres
		Malignites (mafic nepheline syenites)
Paleocene		Fort Union (silty sandstones and shales)

Drainage divide

20 Strike and dip of beds

Alluvium approximate contact

Length of contact lines indicate relative accuracy of contact

S S Rockslide

f U/D f Possible fault

58° Dip of dike

Mountain peak

X112 Sample location

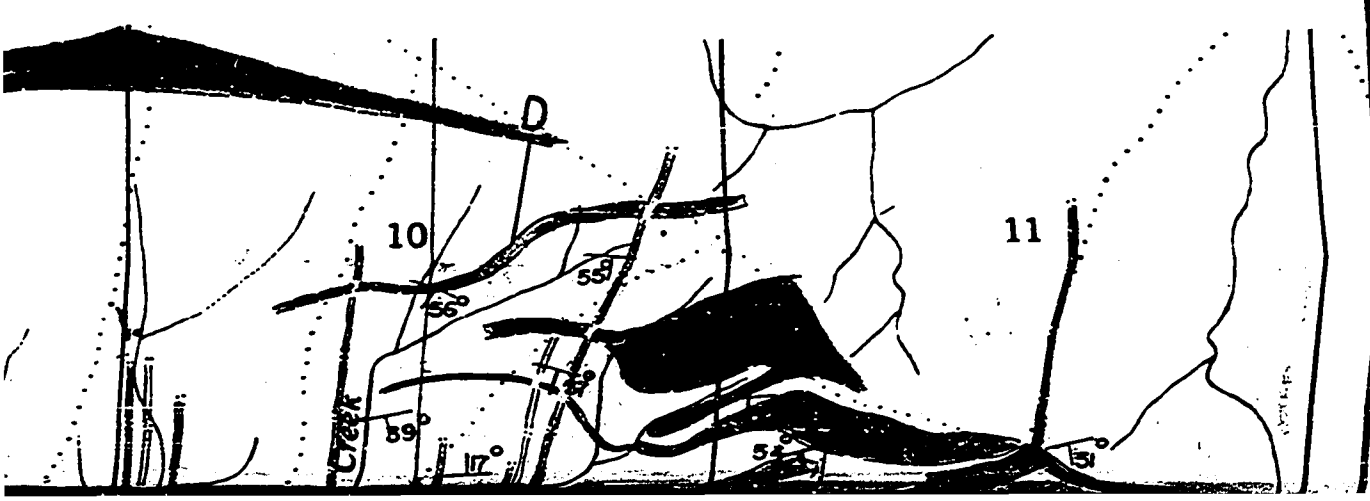

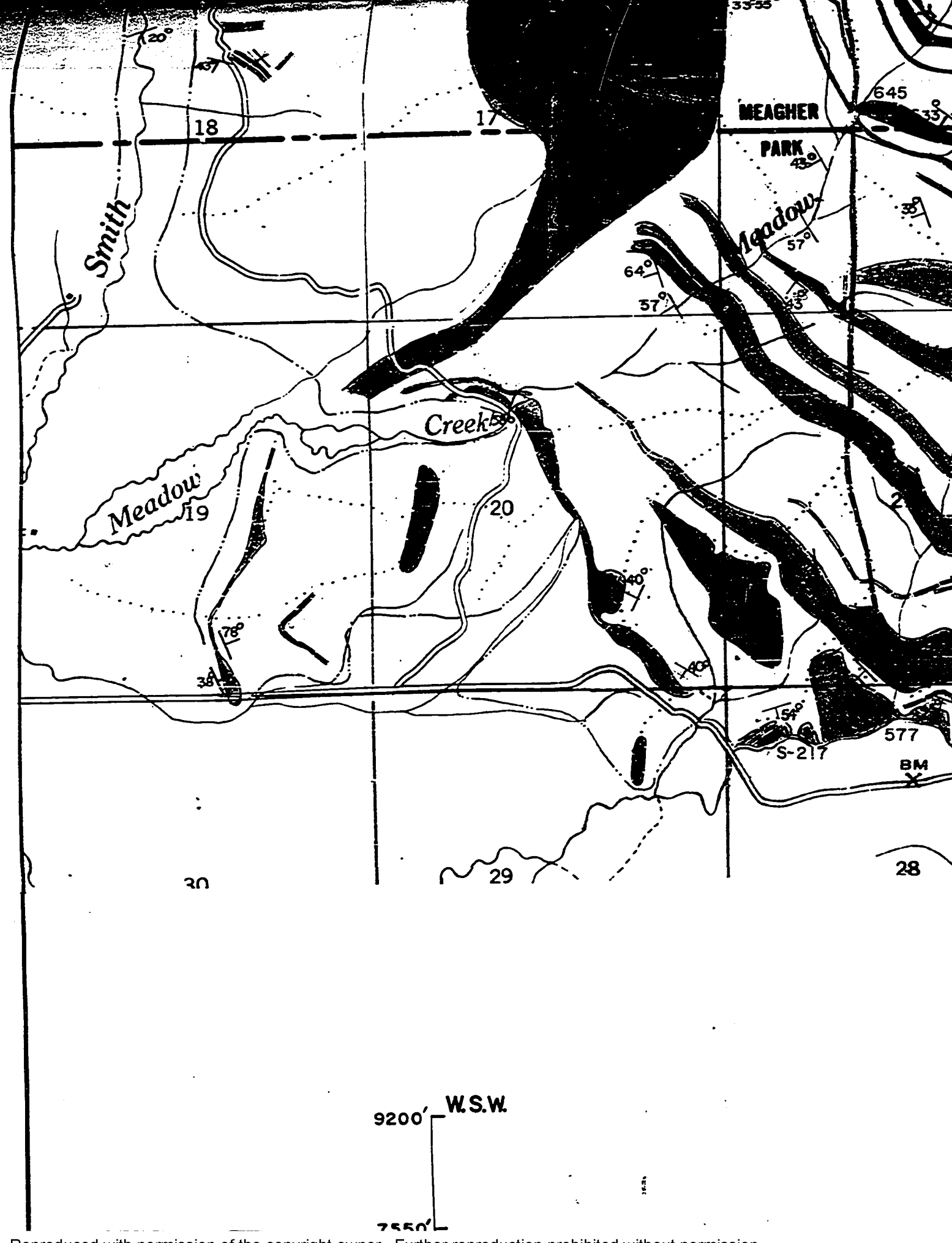

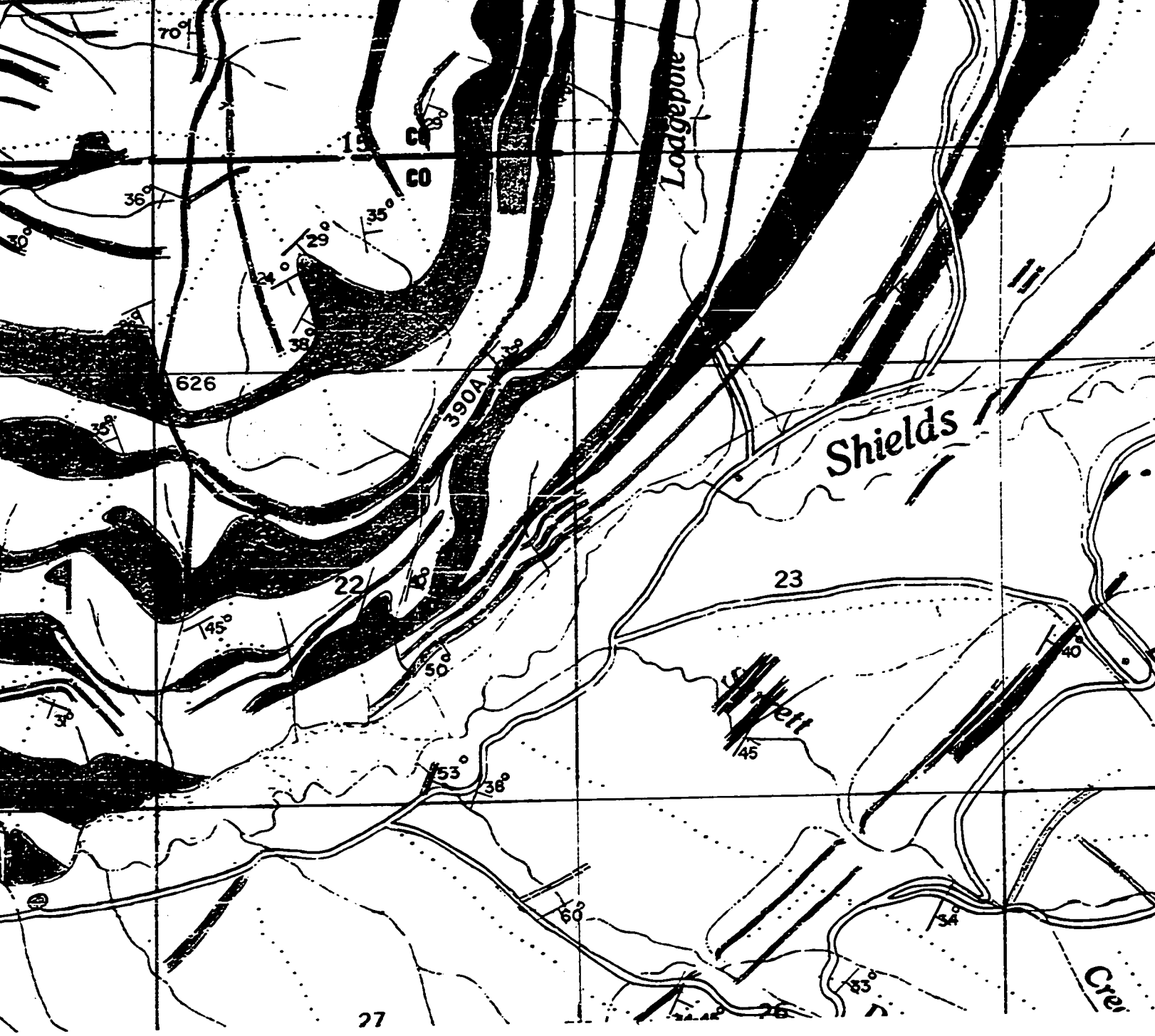

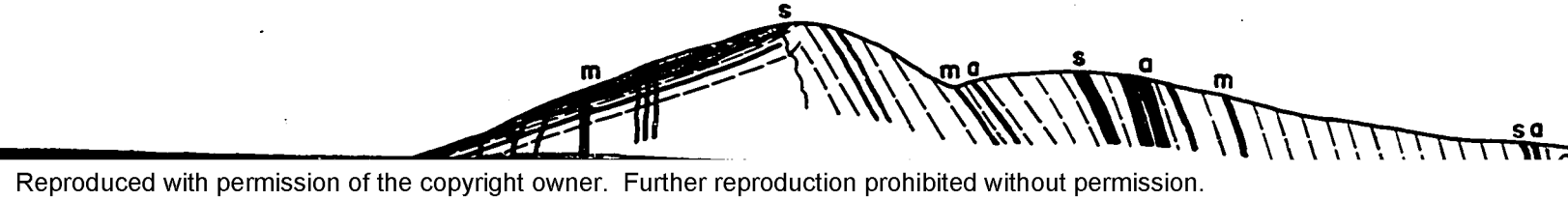

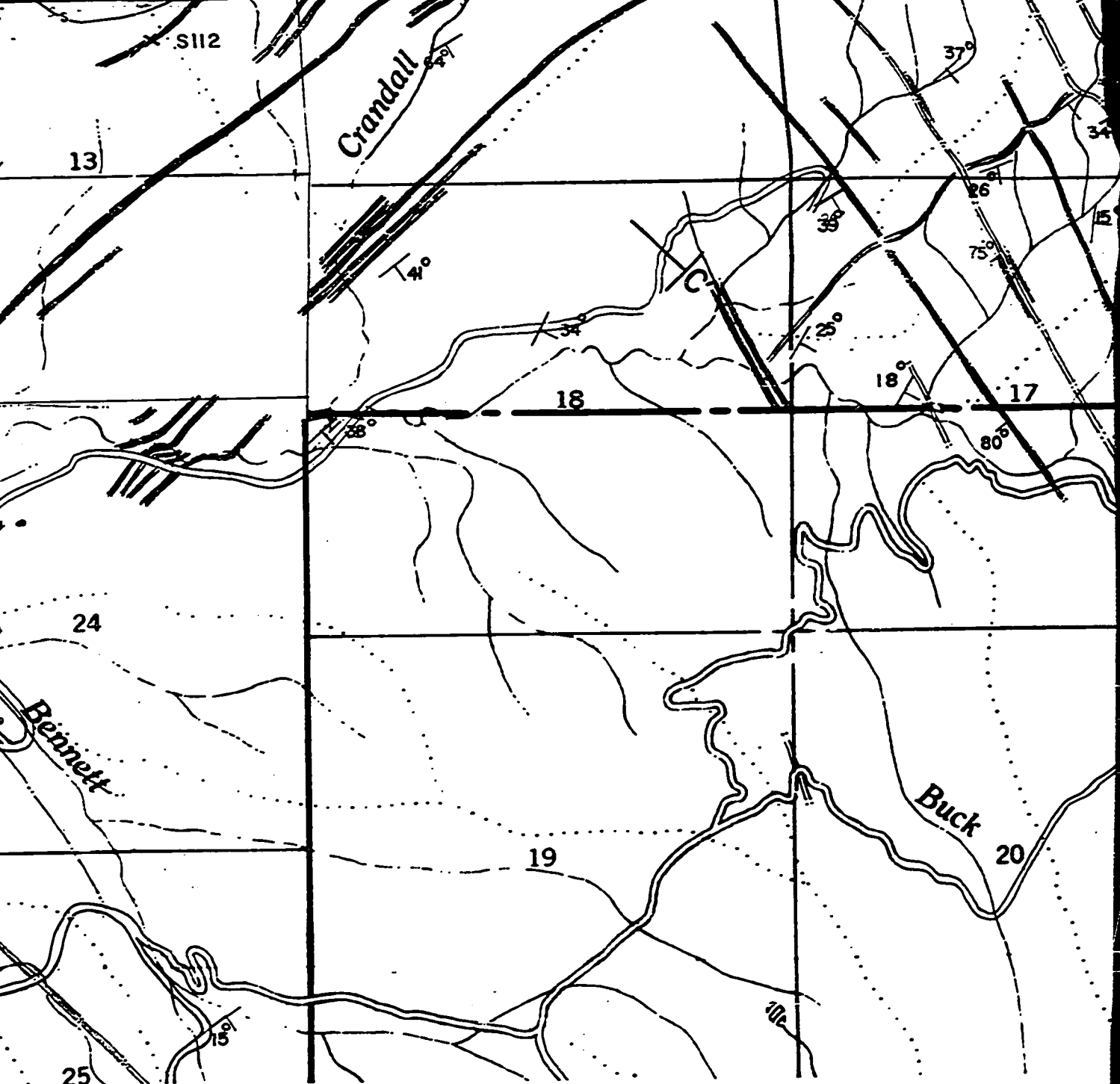

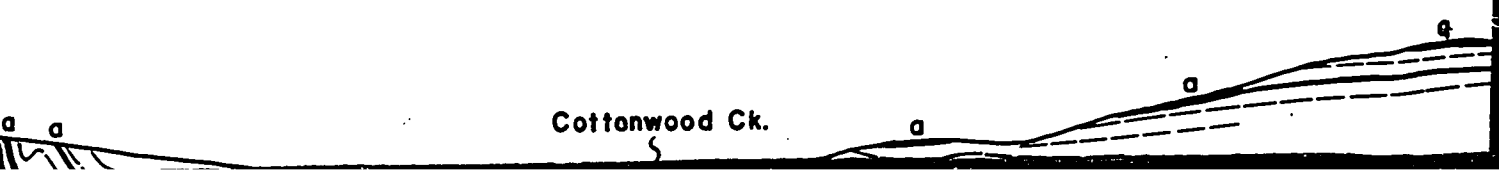

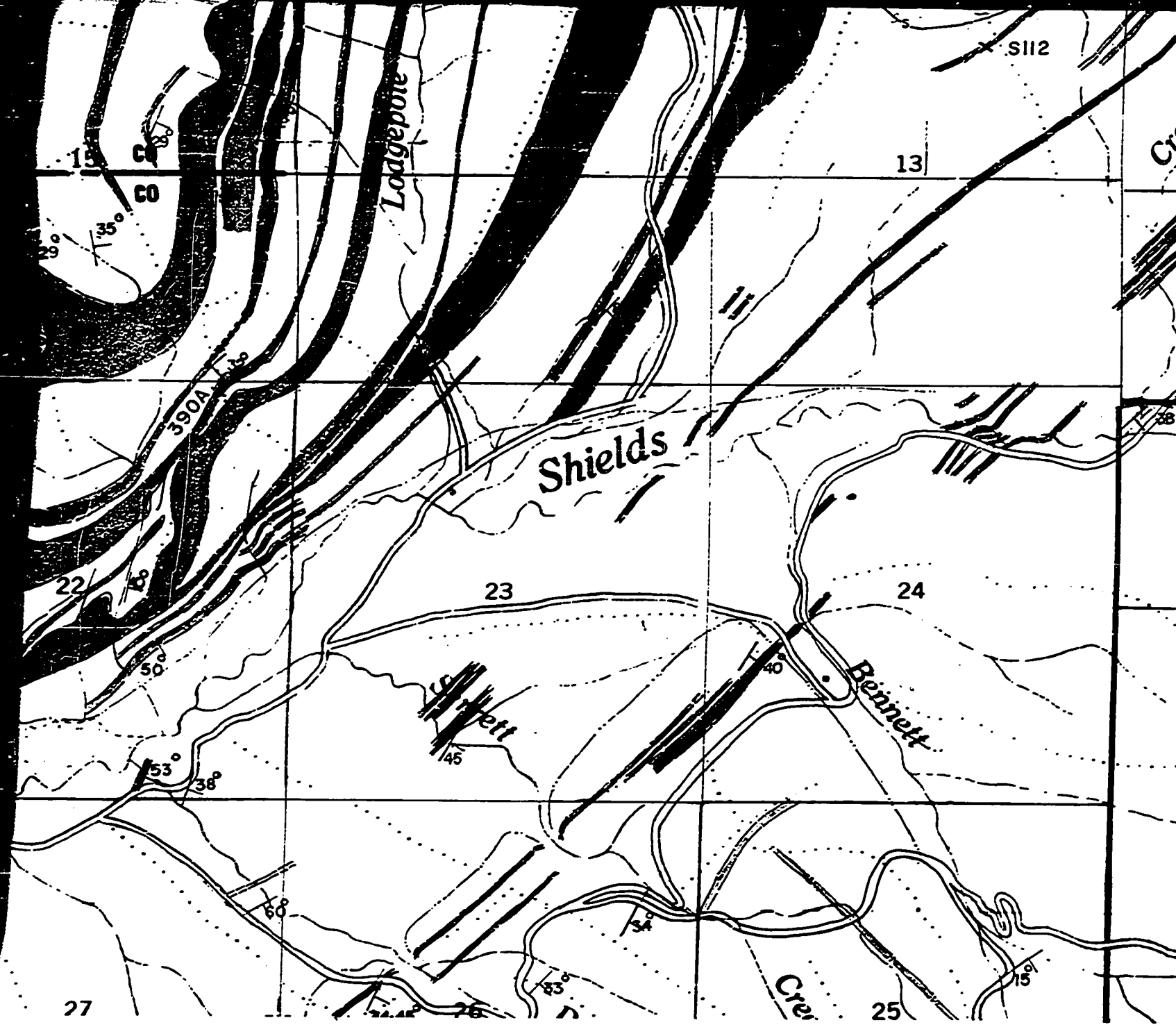

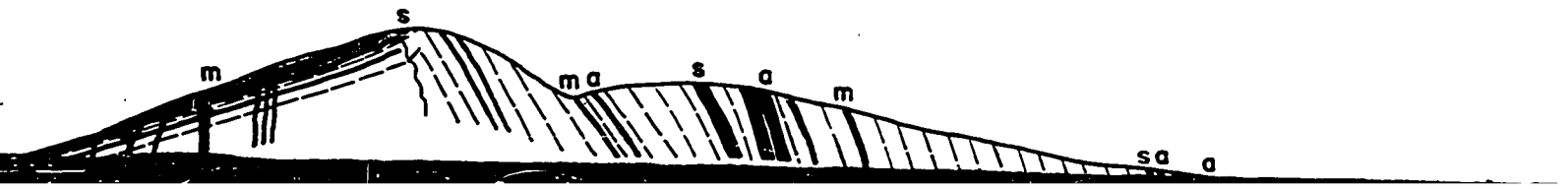

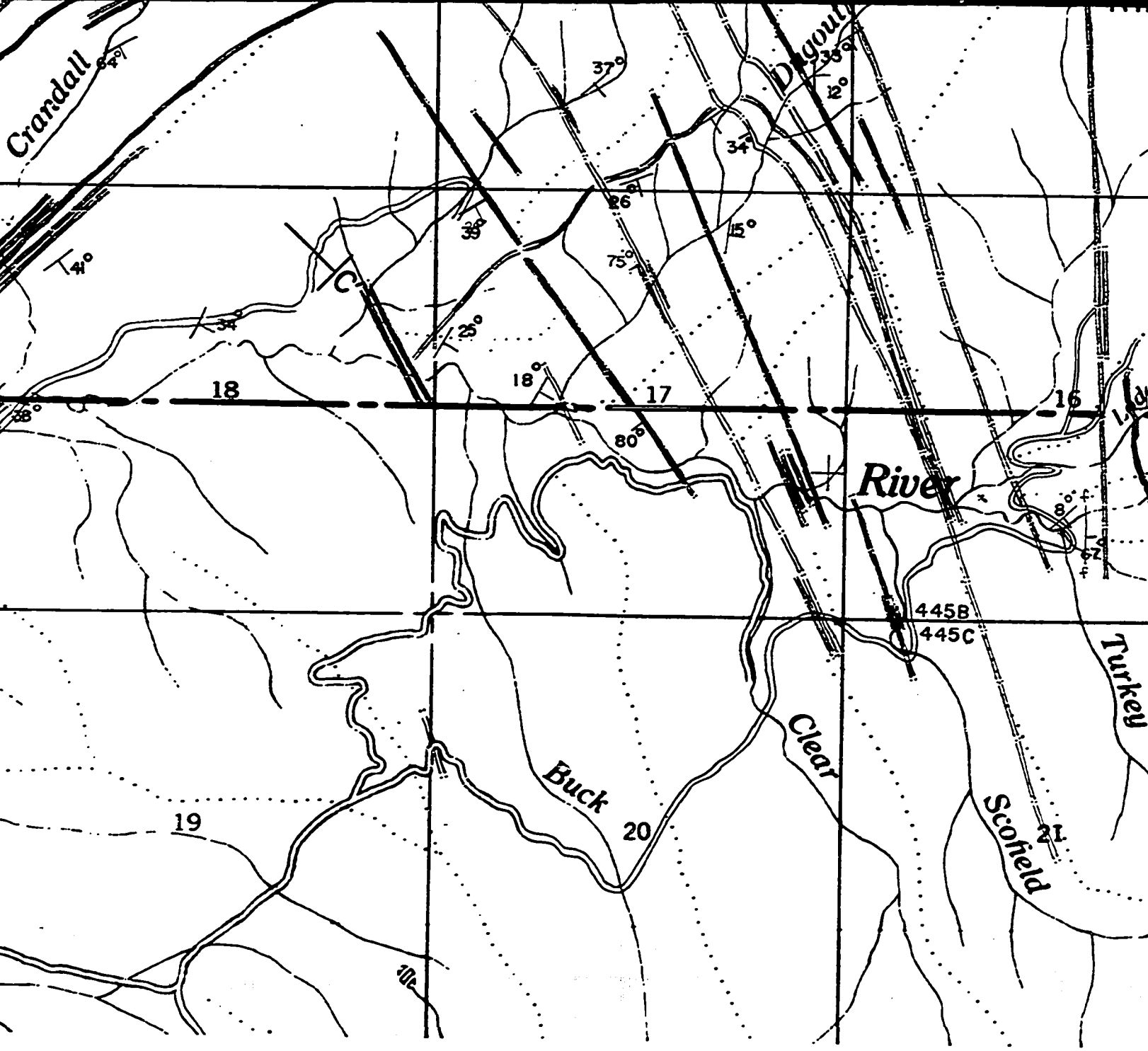

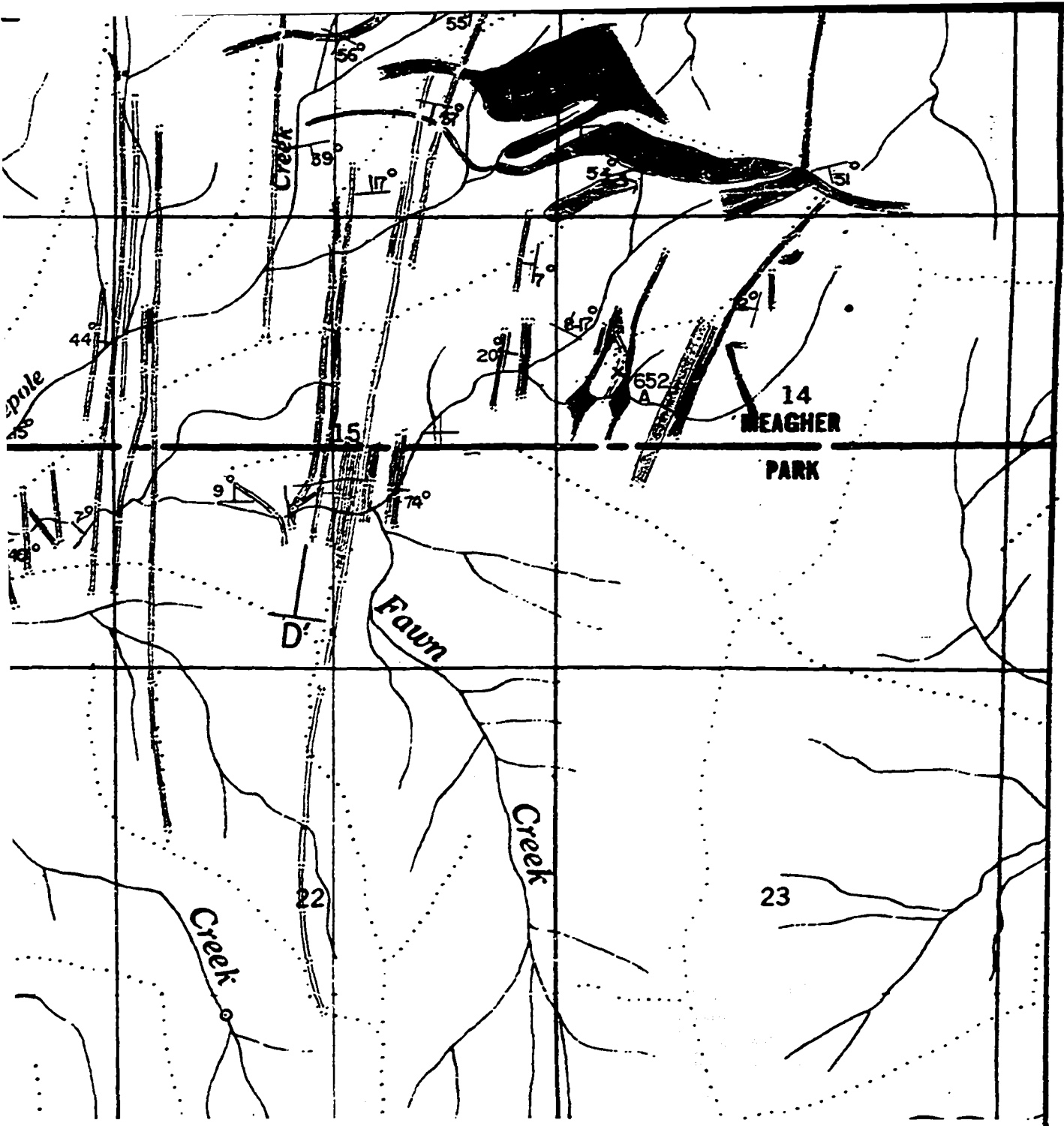

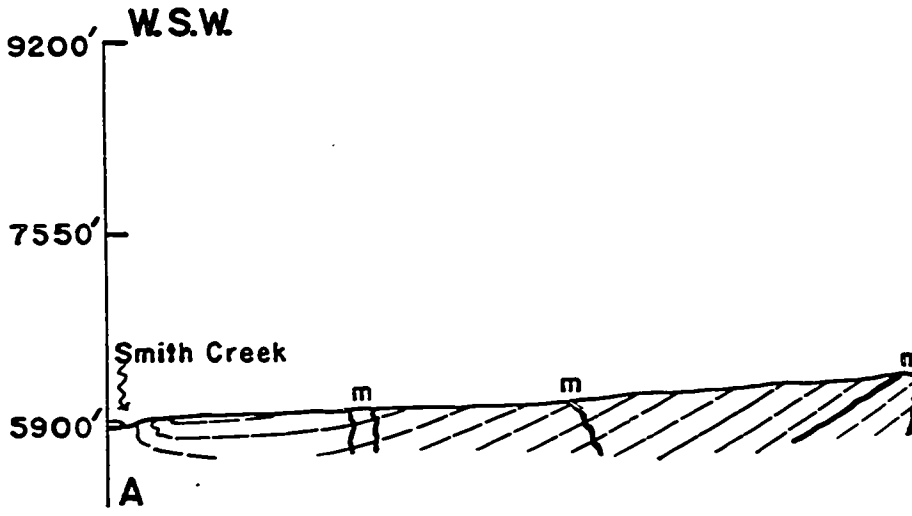

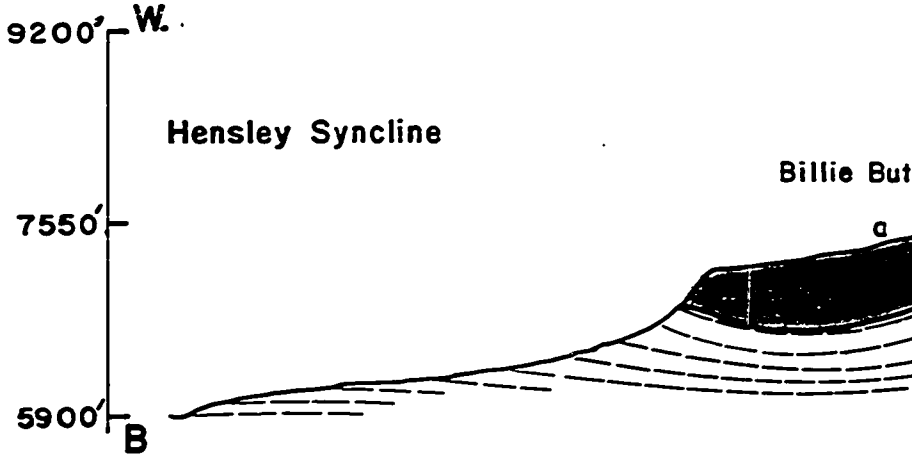

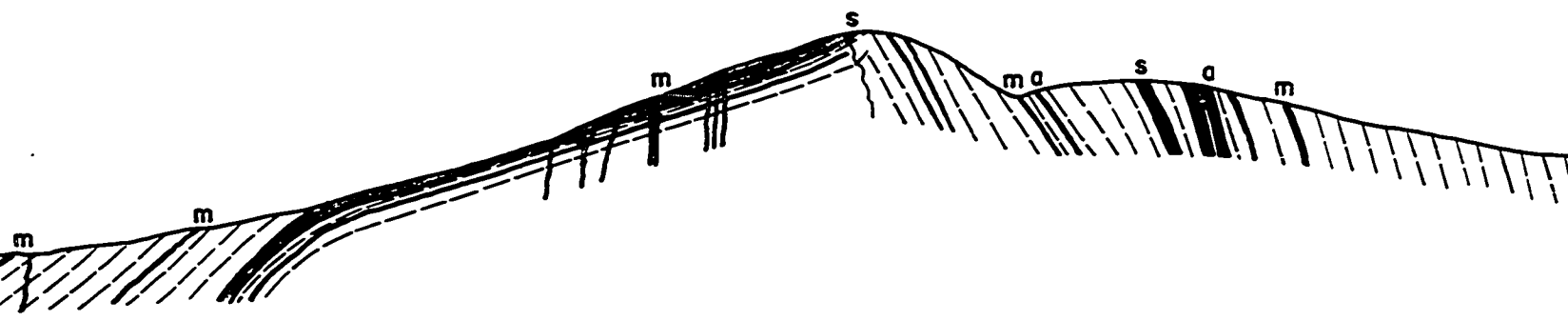

Robinson Anticline

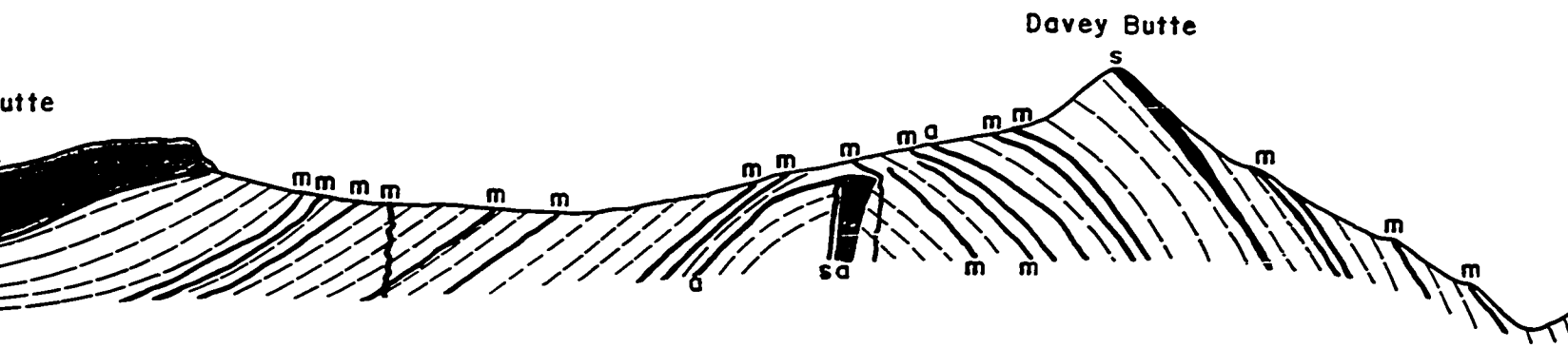

Geologic

No v

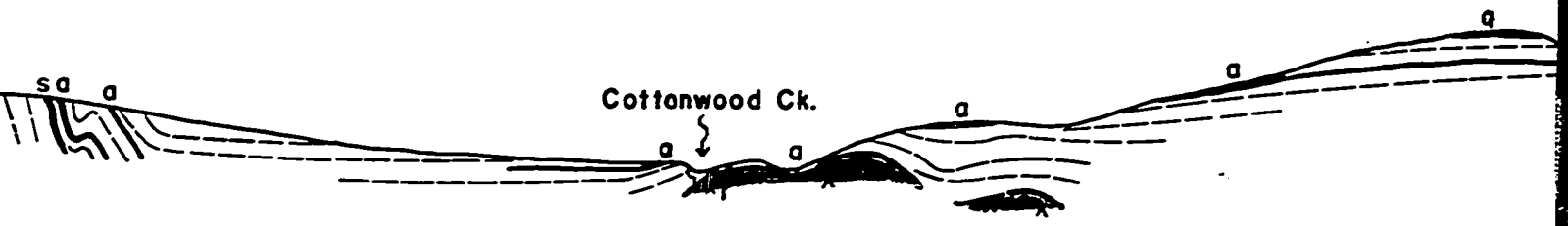

E. N.W.

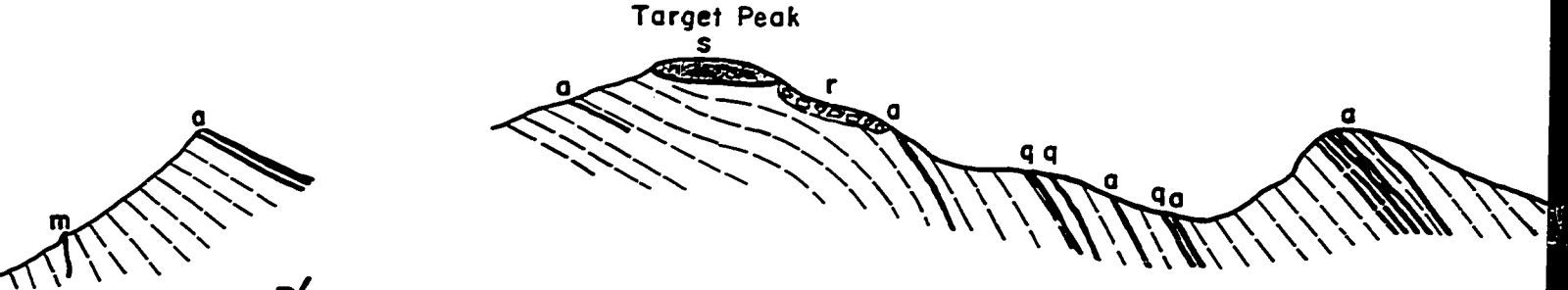

B′ C

cal Cross Sections

vertical exaggeration

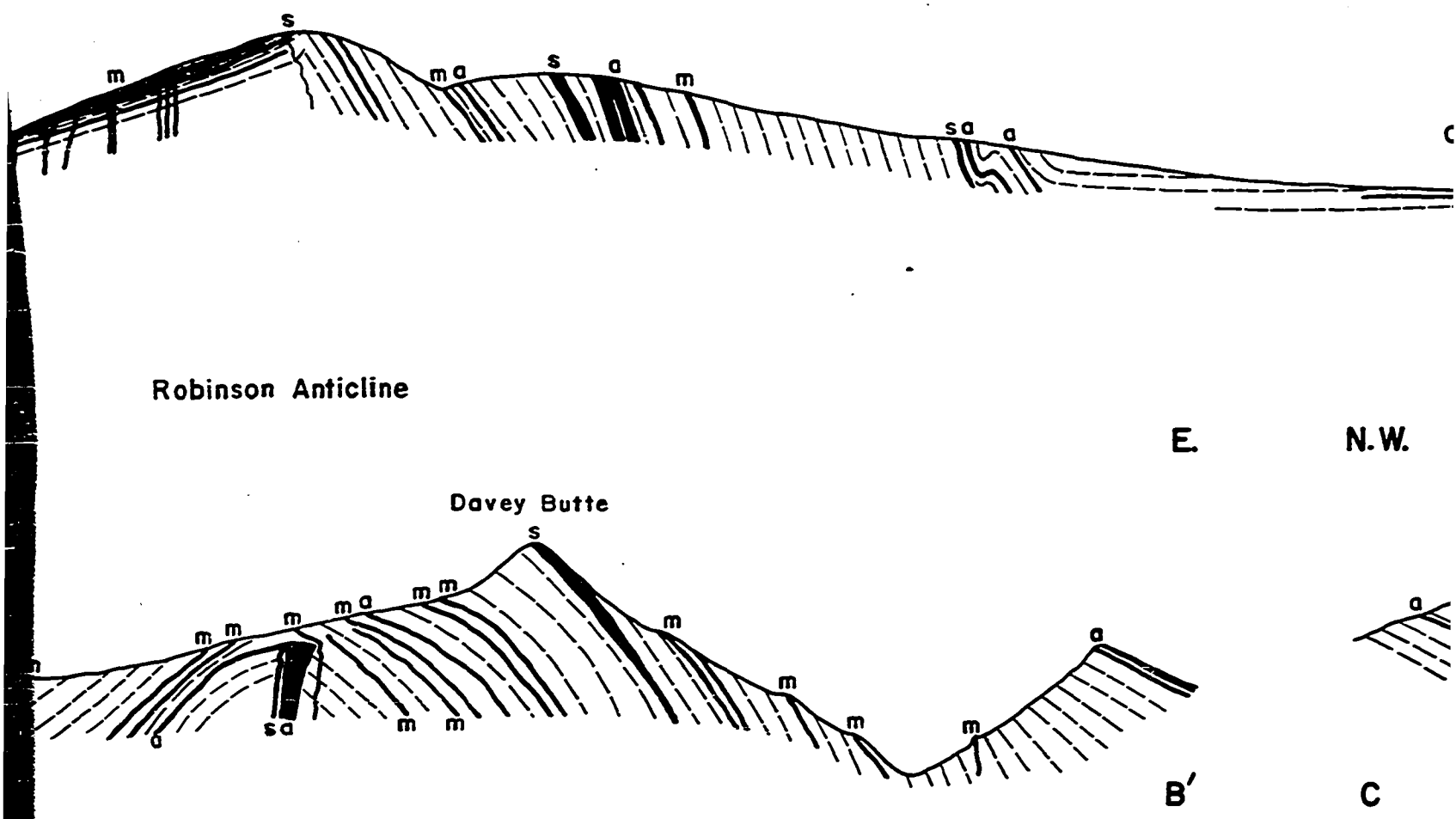

Geological Cross Sections

No vertical exaggeration